University of Strathclyde

Strathclyde Institute of Pharmacy and Biomedical Science

Development of a Method for the Detection and Quantification of the Reaction Products Formed Between Aldehydes and Proteins Using High Resolution Mass Spectrometry

By

Ahmed S. Ahmed

A thesis presented in fulfilment of the
degree requirement for the degree of

Doctor of Philosophy

2010

Singed: *Date:*

ACKNOWLEDGEMENTS

I would like to thank all people who have helped and inspired me during my PhD study.

First and foremost, I would like to express my sincere gratitude to my supervisor Dr. David G. Watson, whose contributions where key to the success of my study. Without his invaluable support, direction, funding and encouragement, I could not have finished this work. Part of my study was sponsored by my supervisor Dr. David G. Watson and Control Therapeutics (Scotland) Ltd.

I owe thanks to Dr. RuAngelie Edrada-Ebel for her continued help and support in the interpretation of NMR and mass spectrometry data. I extend my appreciation to Dr. Ruth Andrew from the Queen's Medical Research Institute (University of Edinburgh) for providing plasma samples required for this research project.

I also wish to thank the technical staff in lab SIPBS 307, in particular Mrs. Lorraine Allan and Mrs. Loraine Wood, for their help and assistance, as well as to all my friends and colleagues in the University of Strathclyde for being the surrogate family during the many years I studied there.

I am grateful for my wife, Anfal, for her invaluable support, devotion, patience, and help throughout the course. I also like to mention my two beloved sons, Anas and Ameen, who had accompanied me throughout my journey.

Last but not least, I would like to dedicate this thesis to my father (Mr. Saadi Ahmed), and my mother (Mrs. Fadia A. Hussian) to whom I shall forever be indebted to.

Ahmed Saadi Ahmed
University of Strathclyde
September, 2010

CONTENTS

List of Figures

List of Tables

Abstract

Detection of endogenous biomarkers is essential for the identification of certain abnormalities within biological systems which may result from different physiological or pathological conditions. Abnormalities within a biological system can result in excessive lipid peroxidation which can lead to the formation of certain lipo-peroxidation by-products, such as 2-alkenals, 4-hydroxy-2-alkenals and malondialdehyde (MDA). Such endogenous aldehydes can induce protein modifications and the formation of a set of biomarkers known as advanced lipo-peroxidation end products (ALEs). Previous detection methods which used for the detection of the modified proteins include immunohistochemical analysis, western blot analysis, 2D-gel electrophoresis, GC-MS, LC-MS, UV-visible and fluorescence detection. Most of these methods require pre-purification and off-line extraction and derivatisation steps prior to analysis [3]. Proteomics and immuno-assays have been used as a diagnostic tool for such biomarkers; however these techniques are not specific. In the case of immunohistochemical methods, cross reactivity can result in a non-specific signal. With proteomics approaches it is impossible to control the fragmentation processes for the protein molecule and multi-stage fragmentation is required to predict the site of modification.

In this research project two different methods were developed for the qualitative and quantitative analysis of biomarkers resulting from the modification of proteins by aldehydes. The first method involved the analysis of amino acids within serum albumin (human or bovine) which had been modified by reaction with a series of different 2-alkenals or 4-hydroxy-2-nonenal (HNE). The protein sample was reacted with these aldehydes and the reaction products were subjected to reductive stabilisation with $NaBH_4$, and were then hydrolysed with 6N HCl for 4 hrs at 145°C. The hydrolysis products were extracted and derivatised with propylchloroformate and then analysed by reversed phase liquid chromatography–mass spectrometry (RPLC–MS). The derivatisation method for the analysis of the reaction products between endogenous aldehydes (2-alkenal and HNE) and proteins was successful, but was complicated by the fact that partial derivatisation was possible.

The second method of analysis was based on the recently developed separation technology of hydrophilic interaction liquid chromatography (HILIC) which enabled retention of the aldehyde adducts, without the need for a derivatisation step. This method involved the same initial procedure as the first one, with the exception that the hydrolysis products were extracted using a protein crash plate filter (PPT filter) and then analysed by HILIC in combination with Fourier Transform mass spectrometry (HILIC-FTMS). The retention of the un-derivatised adducts on the HILIC column was efficient, and a combination of high organic solvent content in the chromatographic mobile phase and a free positively charged amine group in these adducts allowed sensitive detection.

High resolution mass spectrometry using an LTQ-Orbitrap instrument was able to characterise a wide range of aldehyde adducts with high sensitivity and minimum deviation of the observed masses from those of the theoretical masses. The fragmentation pattern of these adducts obtained using collision induced dissociation (CID) to enable structure elucidation for these compounds. Finally, limit of detection (LOD) and limit of quantification (LOQ) for amino acids and the related aldehyde adducts was determined.

The aim of this project was to implement a mass spectrometry detection protocol for these biomarkers in hospitals and other clinical research centres. Examination of human plasma from normal subjects revealed that a number of 2-alkenal adducts were present.

GLOSSARY

±STDEV	Standard Deviation
°C	Degree Celsius. Temperature Unit
^{13}C	Carbon Isotope with 13 electron
µl	Micro-litter
µM	Micro-molar. Concentration Unit= 1 x 10^{-6} M
2,4 -DNP	2,4 - Dinitrophenylhydrazine
Å	Angstrom. Length Unit= 1 x 10^{-10} meter
Acidified STD Stock	Standard Amino Acids Mixture Acidified with 0.1% (w/v) HCl.
Solution	Consists of 20 nmol of each amino acid
ACN	Acetonitrile
Acr	Acrolein
AGEs	Advanced Glycation End Products
ALEs	Advanced Lipo peroxidation End Products
amu	Atomic Mass Unit
Arg	Arginine Amino Acid
ATP	Adenosine Tri-Phosphate
BSA	Bovine Serum Albumin
C-18	Octadecysilane (ODS)
ca.	In approximately
CID	Collision Induced Dissociation
Cro	Crotanaldehyde
Cys	Cysteine
Da	Dalton. Mass unit used with...
DDA	Data-dependent acquisition
EI	Electron Impact
2-Alkenal	2-Alkenal
ESI	Electro-Spray Ionisation
FDP	N^{ε}-(3-Formyl-3,4-dehydropiperidino) lysine Adduct
FTMS	Fourier Transform Mass Spectrometry
H^+	Proton or Hydrogen ion

$H^{\bullet}$	Hydrogen Radical
H_2O	Water
HARG	Homo-Arginine. Internal Standard Amino Acid
HCl	Hydrochloric Acid
HILIC	Hydrophilic Interaction Liquid Chromatography
His	Histidine Amino Acid
HNE	4-Hydroxy-2-Nonenal
Hpe	t-2-Heptenal
HPHE	Homo-Phenylalanine. Internal Standard Amino Acid
HPLC	High Pressure Liquid Chromatography
hrs	Hours
HSA	Human Serum Albumin
Hxe	t-2-Hexenal
IDL	Instrumental Detection Limit
kV	Kilovolt
LC-MS	Liquid Chromatography-Mass Spectrometry
LLE	Liquid-liquid Extraction
LOD	Limit of Detection
LOQ	Limit of Quantification
LTQ	Linear iontrap quadrupole
Lys	Lysine Amino Acid
Lys-pyr	Lysine-2-alkenal-pyridinium Adduct
M	Michael Adduct
M	Molar
m/z	Mass/Charge Ratio
MD	Minimum Detectability
MDA	Malondialdehyde
MDL	Method Detection Limit
MeOH	Methanol
Met-d3	Methionine-d3. Internal Standard Amino Acid
ml	Millilitre. Volume Unit= 1×10^{-3} L
mM	Milli-molar. Concentration Unit= 1×10^{-3} M

mmu	Milli-Mass Unit= 1 x 10^{-3} amu
MS	Mass Spectrometry
MS/MS, MS^2	Fragmentation Mass Spectrometry within Ion-trap Quadrapole
N	Nitrogen
N	Normality Unit
Na_2CO_3	Sodium Carbonate
$NaBH_4$	Sodium Borohydride
NaOH	Sodium Hydroxide
ng	Nano-gram. Weight Unit=1 x 10^{-9} g
nM	Nano-molar. Concentration Unit= 1 x 10^{-9} M
nmol	Nano-mole. Amount Unit= 1 x 10^{-9} mol
Nne	t-2-Nonenal
O	Oxygen
oc	On column injection
$OH^{\bullet}$	Hydroxyl Radical
PBS	Phosphate Buffered Saline (pH= 7.2)
PDA	Photo Diode Array
Pne	t-2-Pentenal
Ppm	Part Per Million
PPT	Protein Precipitation Technique
Psi	Pounds per Sequare Inches
Pyr	Pyridinium Adduct
RDB	Rings Plus Double Bond
ROS	Reactive Oxygen Species
RPLC	Reversed Phase Liquid Chromatography
R_t	Retention time
S	Schiff Base
S	Sulfur
SAX	Strong Anion-Exchange
SCX	Strong Cation-Exchange
SPE	Solid-Phase Extraction
STD	Standard

STD Stock Solution	Standard Amino Acids Mixture. Consisting of 20nmol of each amino acid
UV	Ultra-Violet
V	Volt
v/v	volume/ volume
ZIC-HILIC	Silica Based HILIC Column from Sequant

1 CHAPTER ONE: Introduction

1.1 Introduction

Mitochondria are responsible for cellular energy production in the form of adenosine tri-phosphate (ATP), which is used as a source of chemical energy required for normal cellular functions. Mitochondria play an important role in cell signalling, cellular differentiation and apoptosis, in addition to the control of the cell cycle and cell growth [4]. However, mitochondria also represent the major source of reactive oxygen species (ROS) inside the biological system through the normal respiration process. Although ROS may be essential for the biological system and may participate in signalling within the cells, at the same time ROS may be considered as highly toxic substances and may have a harmful effect on the cells and tissues within the body. Additionally, ROS are considered as the main causative factor for DNA damage and mutation, and in some cases they may be responsible for cell death in several cell types through what is known as the apoptosis process. The concentration of ROS under normal physiological conditions is controlled by several cellular antioxidant defence mechanisms such as glutathione which plays a major role in the reduction of ROS to non-harmful products. However, imbalance between oxidant and antioxidant system may be the causative factor for complications associated with many diseases such as diabetes mellitus and heart disease [2].

Physiologically, there is an equilibrium state between the generation of oxygen free radicals and the anti-oxidant system of the normal healthy individuals. The anti-oxidant system protects the body against free radical induced damage, while a defect in this system may lead to an excessive production of oxygen free radicals that result in a general oxidative stress state inside the biological system [1]. It has been established by a number of studies [1, 5] that chronic hyperglycaemia provokes oxygen free radical production through glucose autoxidation and non-enzymatic glycation of proteins and a general oxidative stress situation can develop. A general oxidative stress situation inside the biological system would increase the production of oxygen free radicals which accelerates the lipid peroxidation process and the formation of lipid-peroxidation by-

products such as the 2-alkenal series, 4-hydroxy-2-alkenal series, and malondialdehyde [6]. These cytotoxic aldehydes may be used as a good markers for oxidative stress in diabetic and non diabetic patients [1]. Lipid peroxidation products that result from oxidative stress during hyperglycaemia are correlated to a number of diseases which may be due to their ability to damage proteins, lipids, and DNA by modifying or inactivating of these bio-molecules [7-9].

The α,β-unsaturated aldehydes, such as 2-alkenal and HNE, are chemically reactive compounds and can form a variety of products (known as advanced lipo-peroxidation end-products or ALEs) when they react with biomolecules [10, 11]; such reaction may produce covalent modifications that lead to a variety of biological effects including: inhibition of protein and DNA synthesis, inactivation and stimulation of enzymes, resistance to proteolytic degradation and a tendency towards aggregation [11]. These effects may initiate immune response, fibrosis, gene transcription or apoptosis [11]. Various types of protein damage are an indicator of aging [12] and are characteristic of some chronic diseases such as arteriosclerosis [13-15], diabetes [16-18], cancer [19], rheumatoid arthritis, cataract [20, 21] and neurodegenerative diseases [22-27]. Various types of 2-alkenal adducts have been described including pyridinium adducts [28, 29] FDP adducts [30] and Michael adducts [31, 32].

The current project will focus on studying the methods of production and detection of ALEs which may results from protein modification with 2-alkenal aldehydes or 4-hydroxy-nonenal (HNE) using HPLC connected to high resolution mass spectrometry. Acid hydrolysis with HCl will be used to get individual amino acids together with the modified amino acids ready for MS analysis rather than the detection of intact protein molecules.

1.2 Advanced Lipo-Peroxidation End Products (ALEs)

The 2-alkenals are considered to be highly reactive aldehydes (Figure 6.1, appendix chapter) as they contain two electrophilic centres that are located at the partially positive carbon atom at positions 1 and 3 in the aldehyde chain. These two carbon centres can undergo nucleophilic addition with the amine group of the amino acids residues when reacting with proteins. It has been found that the 2-alkenals, 4-hydroxy-2-alkenals, and malondialdehyde (MDA), can react with the amine groups in the side chains of lysine and arginine, the imidazole group of histidine, or with the sulfhydryl group of cysteine. The reactions between these aldehydes and amino acid residues occur through Schiff base [33] or Michael addition reactions [31, 32] which lead to the formation of different types of 2-alkenal adducts such as Schiff base, Michael-like adduct, FDP and pyridinium adducts [30, 34].

Acrolein is an important environmental contaminant since it is present in cigarette smoke [35, 36]; acrolein is also a breakdown product of endogenous lipids and it has been implicated in the pathophysiology of spinal cord injury [37], in the development of Alzheimer's disease [38] and has been found to inhibit T-cell response [39]. Reaction products formed between acrolein and proteins have been found to be a good marker for an increased risk of stroke [40], whereas reaction of acrolein with insulin hormone was found to reduce the effectiveness of the hormone [41].

The reactions of α,β-unsaturated aldehydes with proteins range from simple Schiff base formation and Michael-like addition to the formation of heterocyclic rings such as pyridines, piperidines and pyrroles. It has been established that the degree of modification via Schiff base formation and Michael-like addition varies from protein to protein. For example, the imidazole group of histidine is the predominant residue modified in haemoglobin [42], apomyoglobin [43] and β-lactoglobulin [42, 44]. On the contrary, the ε-amine group of lysine is the most reactive amine group in glucose-6-phosphatase [45]. In cytochrome C, different adducts formed between aldehydes and histidine, lysine and arginine residues [46]. Following from the initial formation of a

Schiff base it is possible that generation of a wide range of heterocyclic compounds can occur [28, 47-49]. There is evidence that such cyclic adducts are highly persistent and are not repairable [50]. The mechanism for the formation of these adducts has been extensively studied [29, 30, 51-53].

1.2.1 Reaction of 2-Alkenals with Amino Acids Residues within a Protein Molecule

Reactions of the 2-alkenal aldehydes with different amino acids follow two types of nucleophilic addition reactions, which are highly dependent on the electrophilicity of the carbon atom of the carbonyl group (Schiff base addition) and the β-carbon atom (Michael-like addition). Michael-like addition reaction occurs to a greater extent than Schiff base formation due to the decreased electrophilicity of the carbonyl group as a result of electron enriching properties of the attached alkene group [54].

The reactivity of the carbonyl containing compounds depends on the electron withdrawing properties of the oxygen atom which decreases the electron density around carbonyl carbon leading to the formation of partially positive carbon atom. This partially positive carbon atom can react as Lewis acid that can accept a pair of electrons from Lewis bases such as amine group through Schiff base reaction. In α,β- unsaturated aldehydes, electron contribution from the α,β- double bond can reduce the electron deficiency at carbonyl carbon and result in the formation of partially positive carbon atom at β position. In this case, partially positive β-carbon atom behaves like Lewis acid and can react with Lewis bases through Michael-like addition reaction [55].

1.2.1.1 Schiff Base Formation

The Schiff base reaction consists of nucleophilic addition of the amine group in the amino acid to an electron deficient carbonyl containing aldehydes (e.g. Figure 1.1). The nitrogen atom in the amine group becomes attached to carbon to form imine or Schiff base. Schiff base is known as “aldimine” when the nitrogen atom reacts with aldehyde, while it is known as “ketimine” when it reacts with ketone [56]. Schiff base

formation requires the availability of primary amine and carbonyl groups in the reacting molecules. Both primary and secondary amines can form Michael adducts. Schiff base formation may occur over a few hours during incubation of aldehyde containing molecules with protein until it reaches equilibrium [57, 58]; however Schiff bases can readily dissociate back to reform the original reacting molecules [54, 56].

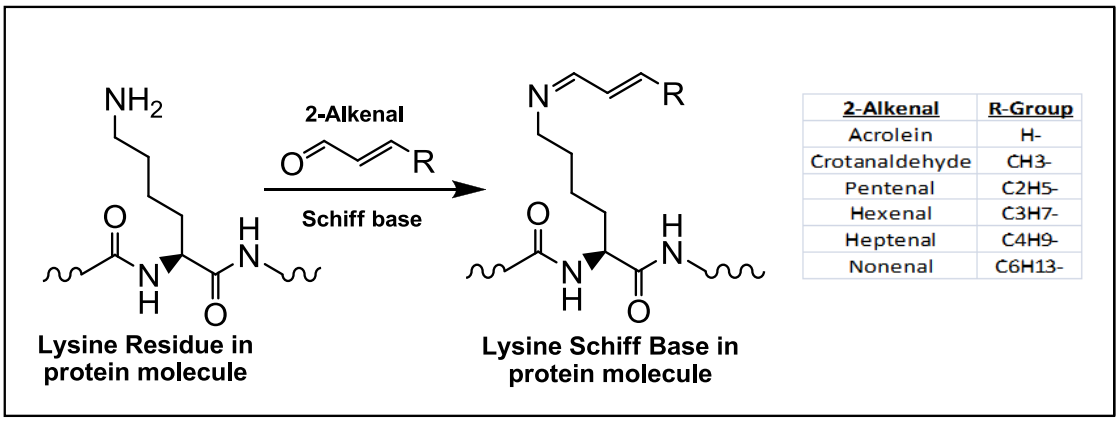

2-Alkenal	R-Group
Acrolein	H-
Crotanaldehyde	CH3-
Pentenal	C2H5-
Hexenal	C3H7-
Heptenal	C4H9-
Nonenal	C6H13-

Figure 1.1: Schiff base formation between 2-alkenal reactive aldehydes and lysine amino acids. Adapted from reference number [56].

1.2.1.2 Michael-Like Addition Reaction

The Michael addition reaction involves the reaction of nucleophilic groups (also known as Michael donors) with unsaturated electrophilic groups (also known as Michael acceptors). Michael donors consist of a wide range of functional groups with enough nucleophilicity to perform Michael addition reactions, such as amines & thiols. Whereas, Michael acceptors should have electron withdrawing groups attached [59] such as carbonyl group in aldehydes. In this research project, Michael addition reactions of the α,β- unsaturated double bond in the 2-alkenal series with the amine groups of lysine or arginine, the imidazole group of histidine, or the sulfhydryl group of cysteine will be studied (Figure 1.2).

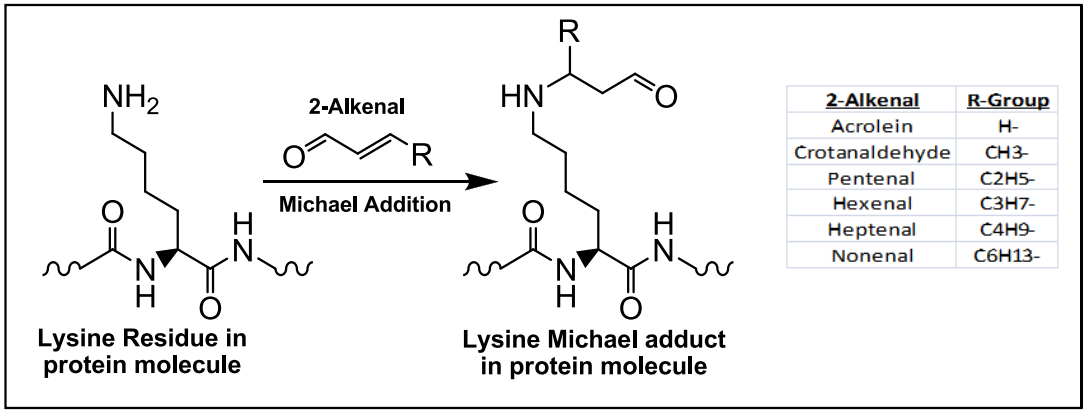

Figure 1.2: Michael addition reaction between a 2-alkenal reactive aldehyde and lysine amino acid.

1.2.1.3 Pyridinium Adducts Formation

Reaction between aldehydes and amino acids usually continues beyond the Schiff base or Michael addition stages leading to the formation of more complex compounds such as pyridinium or FDP adducts. Ichihashi *et al.* [30] suggest that pyridinium adduct formation consists of two consecutive reactions; starting with Schiff base addition followed by Michael addition with some re-arrangement (Figure 1.3). However, Baker *et al.* [28] proposed another mechanism for pyridinium adduct formation through lysine residue modification in the presence of 2-hexenal (Figure 1.4). The lysyl-pyridinium adduct III proposed by Baker *et al.* (Figure 1.4) has the same chemical formula as the lysyl-pyridinium adduct suggested by Ichihashi *et al.* (Figure 1.3), but a different structural arrangement. Lysyl-pyridinium adducts I & II (Figure 1.4) have the same chemical formula but different structural arrangements (skeletal isomers), and could be considered as a dehydrogenated form of lysyl-pyridinium adduct III (losing of H_2 molecule from its structure with double bond formation). For mass spectrometry detection of lysyl-pyridinium adducts, all these isomer possibilities should be considered. For the purposes of discussion, lysyl-pyridinium adducts I & II are assigned as lysyl-pyr (-2H), and lysyl-pyridinium adduct III is assigned as lysyl-pyr. Both lysyl-pyr and lysyl-pyr (-2H) should be present in non-reduced modified protein samples. It

should be noted that lysyl-pyridinium adducts I & II do not apply in case of acrolein aldehyde modification.

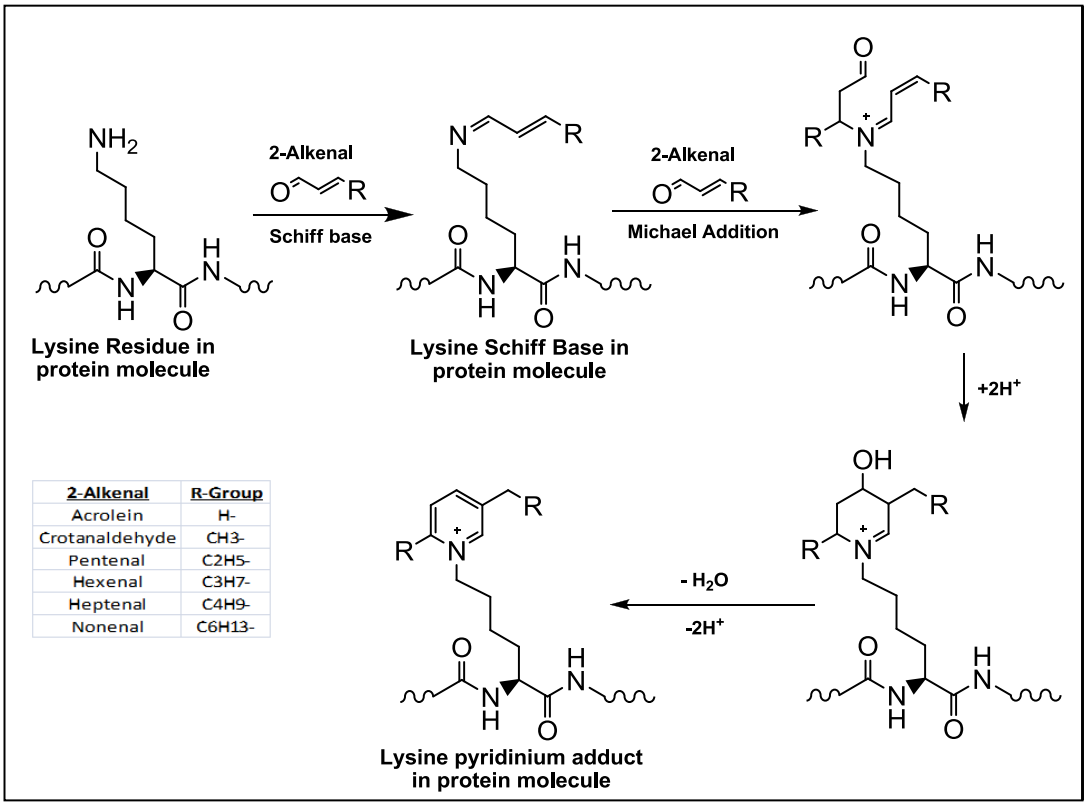

2-Alkenal	R-Group
Acrolein	H-
Crotanaldehyde	CH3-
Pentenal	C2H5-
Hexenal	C3H7-
Heptenal	C4H9-
Nonenal	C6H13-

Figure 1.3: Pyridinium adduct formation as suggested by Ichihashi *et al.* (2001) [30].

Lysine pyridinium adducts with different reduction status carry one single positive charge on the nitrogen atom inside the pyridinium ring. So, the pyridinium adducts are already ionised and do not acquire positive charge during ionization process prior to mass spectrometry detection, as confirmed by Shao *et al.* (2005) [34] and Zhu *et al.* (2009) [60].

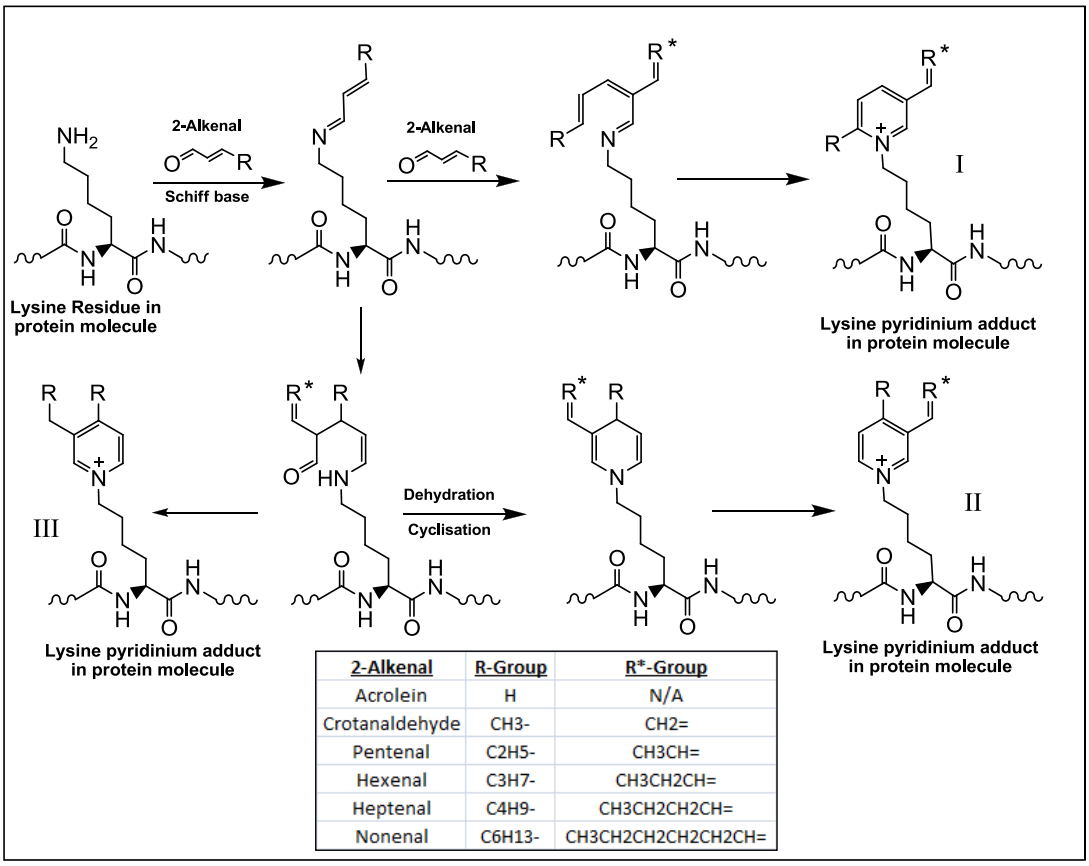

2-Alkenal	R-Group	R*-Group
Acrolein	H	N/A
Crotanaldehyde	CH3-	CH2=
Pentenal	C2H5-	CH3CH=
Hexenal	C3H7-	CH3CH2CH=
Heptenal	C4H9-	CH3CH2CH2CH=
Nonenal	C6H13-	CH3CH2CH2CH2CH=

Figure 1.4: Proposed mechanism for pyridinium adduct formation as suggested by Baker *et al.* [28].

1.2.1.4 N^{ε} (3-Formyl-3,4-Dehydro-Piperidino) Lysine Adducts (FDP) Formation

Similarly to the pyridinium adduct formation, FDP adduct represents another complex molecule that results from 2 consecutive Michael addition reactions (Figure 1.5). This involves nucleophilic addition of a 2-alkenal molecule through Michael addition to the terminal amine group of lysine followed by further attachment of another 2-alkenal molecule through another Michael addition reaction to the modified lysine; the resulting intermediate adduct undergoes a cyclisation and a condensation reaction leading to FDP-lysine adduct formation [30, 61]. In contrast to pyridinium adducts, FDP adducts contain no permanent positive charge, and will acquire a positive charge during the ESI step in the mass spectrometer, as stated by Shao *et al.* (2005) [34].

Uchida *et al.* (1998) suggests that FDP-lysine adduct is stable to acid hydrolysis [61]; such stability arises from the enal-dienol tautomerism stabilisation of the FDP-lysine adduct (Figure 6.2).

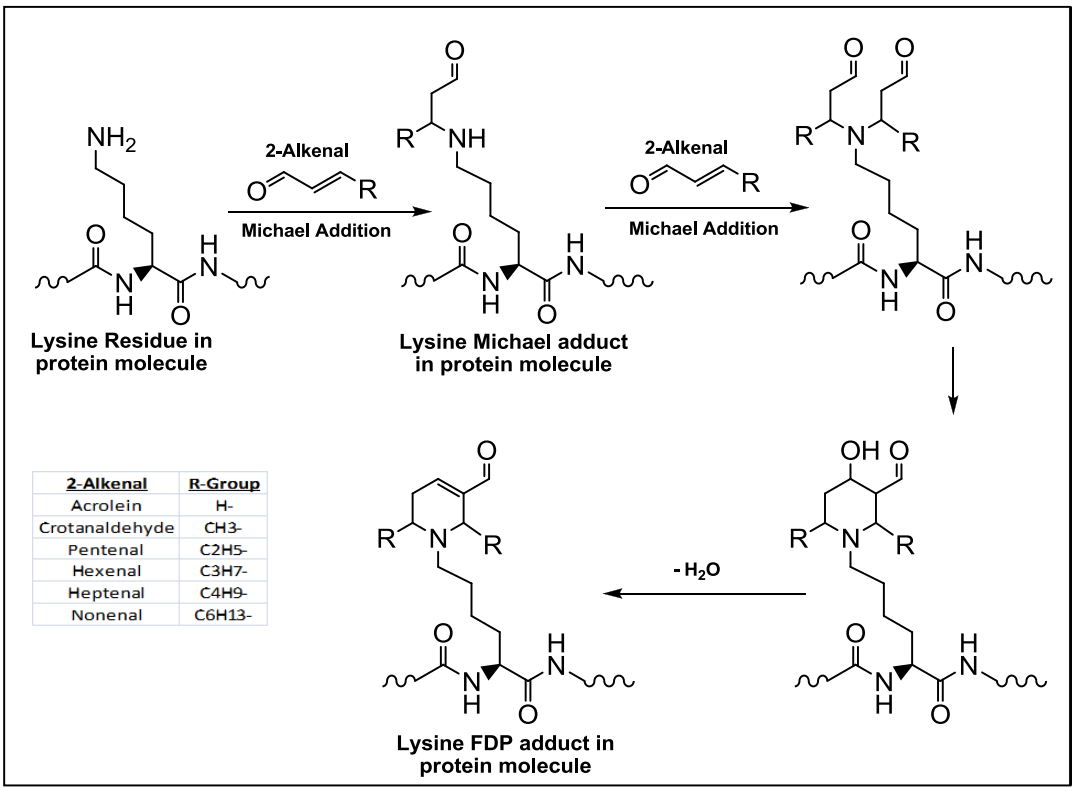

Figure 1.5 FDP-lysine adduct formation between 2-alkenal reactive aldehydes and lysine as suggested by Ichihashi *et al.* (2001) [30].

1.2.2 Reactions of 4-Hydroxynonenal (HNE) with Amino Acid Residues within a Protein Molecule

HNE is a highly reactive and toxic member of the 4-hydroxy-2-alkenal series [62] that results from the peroxidation of omega 6 polyunsaturated fatty acids such as linoleic and arachidonic fatty acids, two fatty acids which are abundant in the human body [8]. Oxidative stress is a main cause for HNE generation through the lipid peroxidation process [63]. Furthermore, HNE is considered as a potent cellular damage inducing compound due to its ability to modify amino acids in proteins such as lysine, histidine, and cysteine through Michael addition or Schiff base formation [8]. As a consequence of

amino acid modifications, HNE toxicity may be reflected in a number of biological effects such as the lysis of erythrocytes, deactivation of enzymes and inhibition of DNA and protein synthesis [33, 64]. The adducts of 4-hydroxynonenal (HNE), one of the major secondary products of lipid peroxidation process [46] have been detected in various human tissue samples such as atherosclerotic lesions, Lewy bodies, the neurons of the substantia nigra in Parkinson's disease, renal cell carcinoma and samples of tissue from Alzheimer patients [65, 66].

Under normal physiological conditions, the concentration of HNE may range from 1-3 μM; nevertheless it may increase up to 5mM under oxidative stress situation. HNE's potency results from its stability and high lipid/water solubility. The retina can contain HNE in an abundant amount due to its high metabolic activity, oxygen tension, and the availability of omega 6 polyunsaturated fatty acids which play a role in the production of HNE [67].

1.2.2.1 Reaction of HNE with Lysine Residue

Lysine can undergo chemical modification upon reaction with HNE either through Schiff base formation or Michael addition [46] to form adducts that are responsible for the biological toxicity of HNE (Figure 1.6) [33]. Furthermore, formation of hemiacetal compounds is expected by cyclisation of HNE-Michael adducts by the reaction of C-4 hydroxyl group of HNE with the aldehyde group of same HNE molecule [68]. Hemiacetal compound has the same chemical formula and mass for the correspondent Michael adduct. The only detection method by which we can differentiate between Michael and hemiacetal adducts is by the reaction of Michael adduct with 2,4-dinitrophenylhydrazine (2,4-DNP) to form protein-hydrazone derivatives which can easily be detected by a fluorescence method since the protein-dinitro-phenylhydrazone derivative absorbs radiation at 370 nm. The Michael adducts that result from the reaction between 2-nonenal and protein yield a free aldehyde group that can react with 2,4-DNP to form a hydrazone derivative that can be detected by the fluorescence at 370 nm. While in the case of HNE, the possible hemiacetal formation (by the interaction between

C-4 hydroxyl group of HNE with the aldehyde group of the same HNE molecule) may prevent the reaction of 2,4-DNP with the free aldehyde group of the HNE molecule, and this may explain the failure to determine the carbonyl content of protein samples after incubation with HNE. Furthermore, the reaction of 2,4-DNP with protein sample would provide an approximate value for the carbonyl content of the protein sample, which in turn would refer to the Michael adduct content [64].

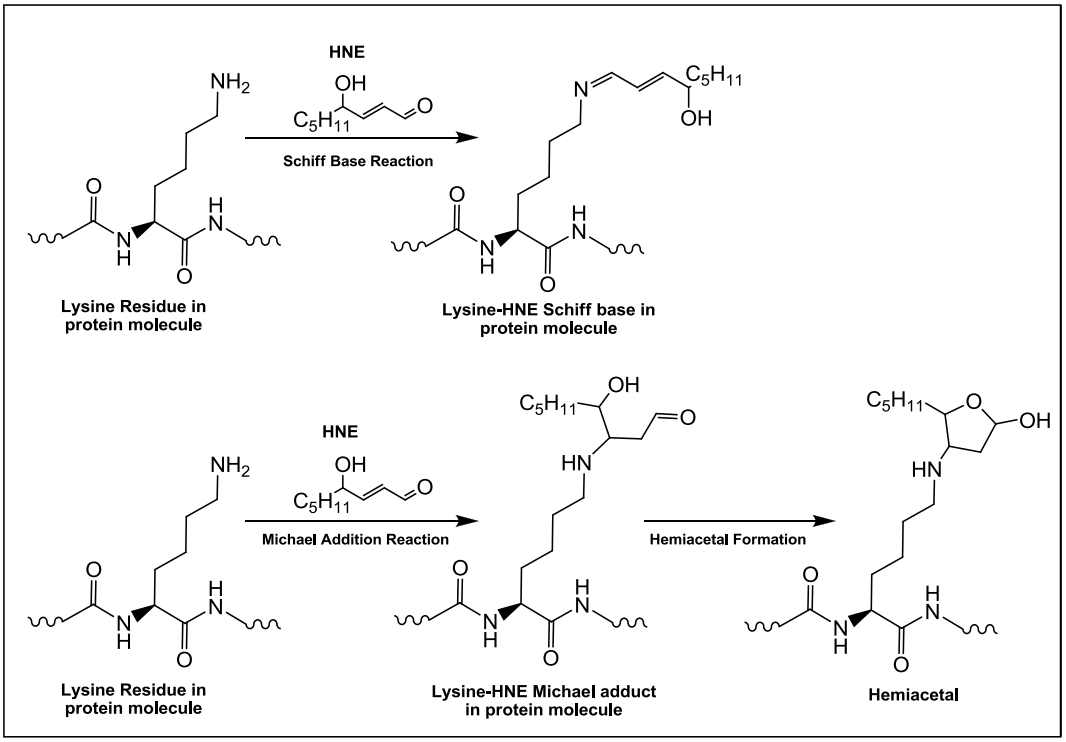

Figure 1.6: Reaction of HNE with a lysine residue through Schiff base formation, Michael addition, and hemiacetal formation [68].

1.2.2.2 Reaction of HNE with Histidine Residues

The reaction of HNE with histidine in a protein molecule, represents one of the primary targets for the reaction with HNE and is carried out through Michael addition reaction [46] which consists of nucleophilic addition of the imidazole nitrogen atom to the α,β- unsaturated double bond in HNE (Figure 1.7). The reaction usually continues to

involve the reaction between the C-4 hydroxyl group of HNE with the aldehyde group of the same HNE molecule resulting in the formation of a stable hemiacetal [64, 68].

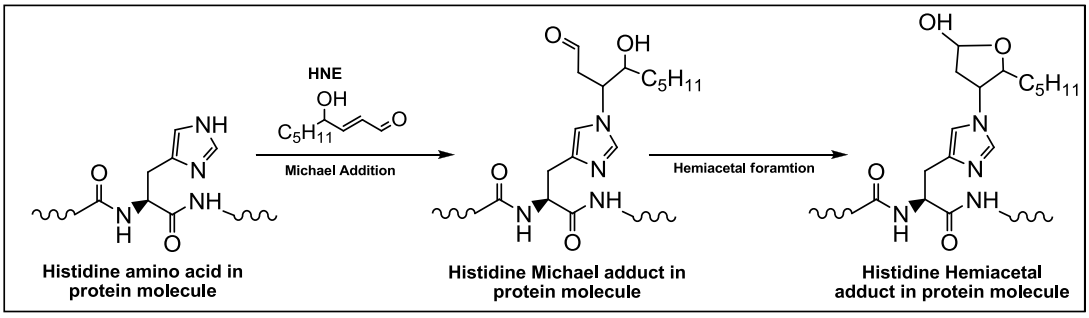

Figure 1.7: Reaction of HNE with a histidine residue through Michael addition, and hemiacetal formation [68].

1.2.2.3 Reaction of HNE with Arginine Residues

Arginine can provide an amine group that can react with HNE through Schiff base or Michael addition to form different adducts (Figure 1.8). Different studies proposed the ability of the arginine to react with 4-oxo-2-nonenal, in a model peptide, through Schiff base and Michael addition reaction; however arginine amino acid failed to show any adduction when incubated with HNE [63, 69]. On the other hand, Isom *et al.* confirmed the ability of arginine to react with HNE through 2-pentapyrrole formation, when cytochrome C had been incubated with HNE [46]. In accordance with the reaction of lysine with HNE, hemiacetal formation might be expected for arginine Michael adducts.

Obviously, arginine can provide more than one nitrogen atom that can react with the aldehyde group of HNE through Michael addition (Figure 6.3), since any amino acid that is expected to be modified by Michael addition should contain either a primary or secondary amine group, while Schiff base formation requires only a primary amine group.

Servetnick *et al.* demonstrated the ability of the arginine in reducing the level of AGEs formation in protein samples incubated with high glucose levels, due to the reaction of

arginine with carbonyl containing compounds which in turn reduce the level of protein modification [70].

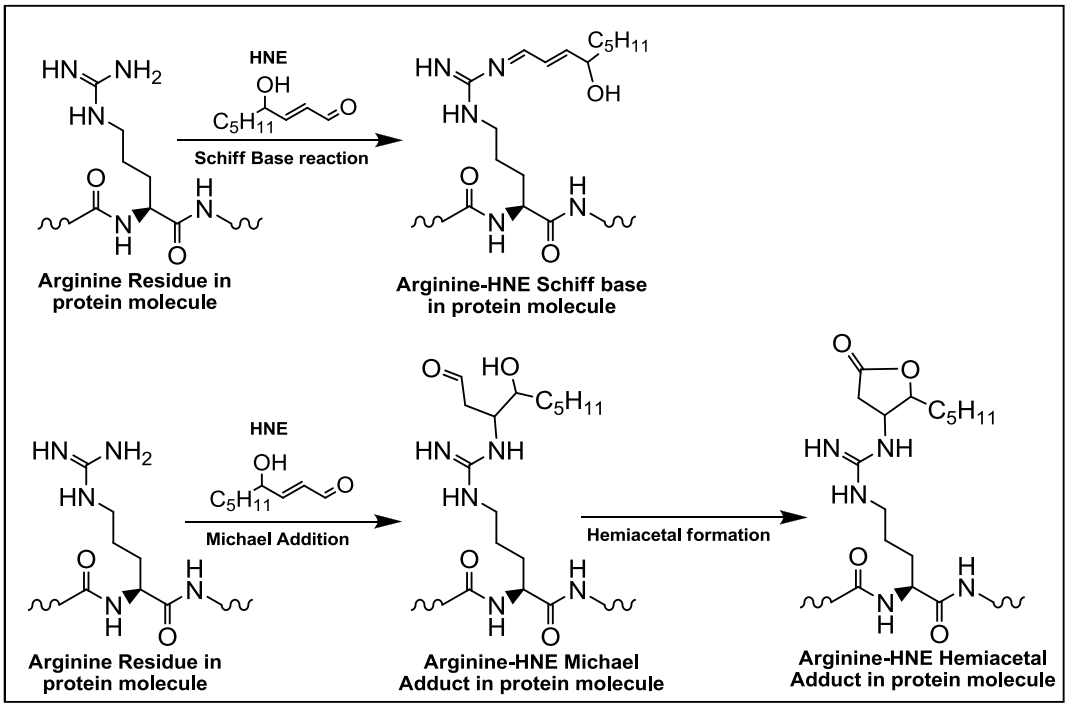

Figure 1.8: Reaction of HNE with arginine amino acid through Schiff base formation and Michael addition.

1.2.2.4 Reaction of HNE with Cysteine Residues

The sulfhydryl group of cysteine amino acid residues may undergo modification with HNE through the Michael addition reaction to form a stable thio-ether derivative (Figure 1.9), while the Schiff base reaction is not possible in this case [68]. The thio-ether derivative that is formed due to Michael addition of HNE to cysteine, could not be detected by the reaction with 2,4-DNP, although a free carbonyl group is available. Again, the failure to give a positive result with 2,4-DNP may support formation of the hemiacetal, but this is still unconfirmed [64, 68].

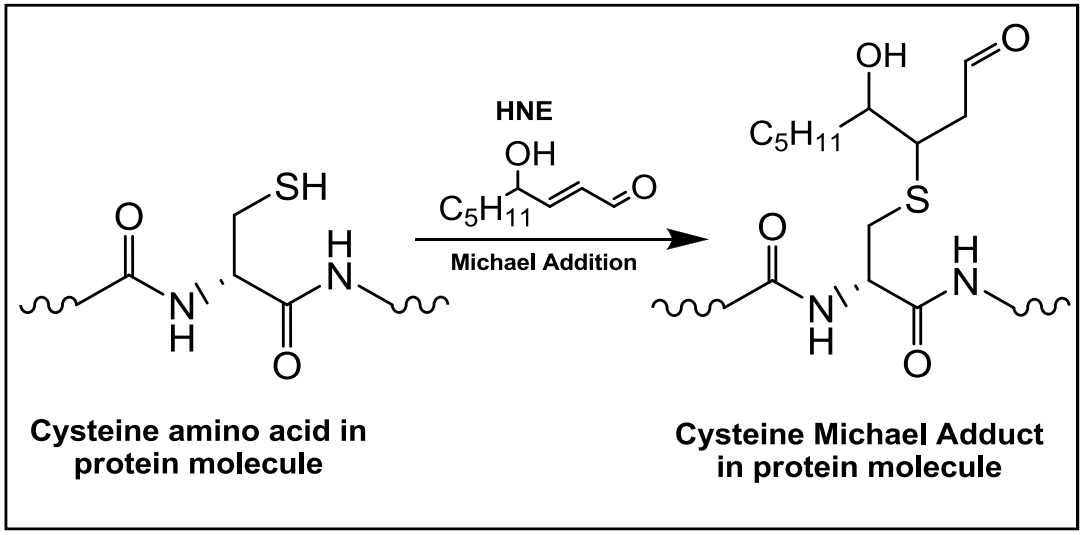

Figure 1.9: The expected reaction of HNE with cysteine amino acid that would occur through Michael addition reaction to form a thio-ether adduct.

1.2.2.5 Reaction of HNE with 2 Amino Acids Residues within a Single Protein Molecule

A few studies have described the reaction between HNE and 2 amino acids, but no significant data were recorded from these studies. An initial Michael addition of HNE to an amino acid can leave a free aldehyde group which can then cross-link to another amino acid through Schiff base formation. For example, the reaction of 2 lysine amino acids with HNE can occur through an initial Michael addition followed by Schiff base reaction to form a new adduct that is a 2:1 (lysine: HNE) adduct (Figure 1.10) [71].

Another case that can show a reaction between HNE and 2 amino acids is the reaction of HNE with histidine and lysine. An initial Michael addition of HNE to histidine leaves a free aldehyde group which in turn can react with another amino acid through Schiff base formation as in the case of the reaction of a histidine-HNE-Michael adduct with lysine (Figure 1.11) resulting in 1:1:1 (His:HNE:Lys) adduct [68].

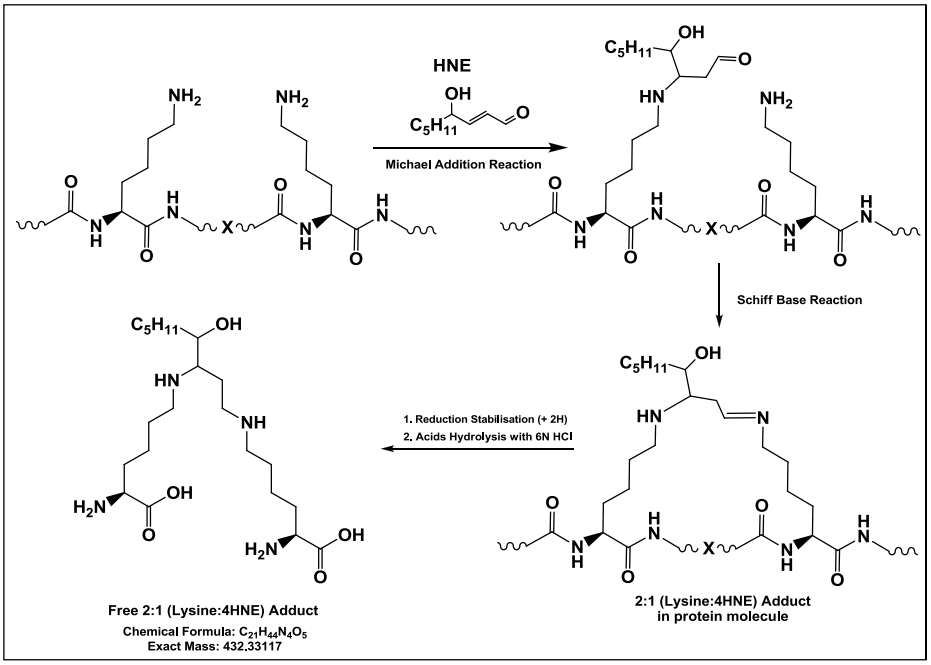

Figure 1.10: Reaction of HNE with two lysine amino acids through initial Michael addition followed by Schiff base adducts formation. X represents a specific number of amino acids residues.

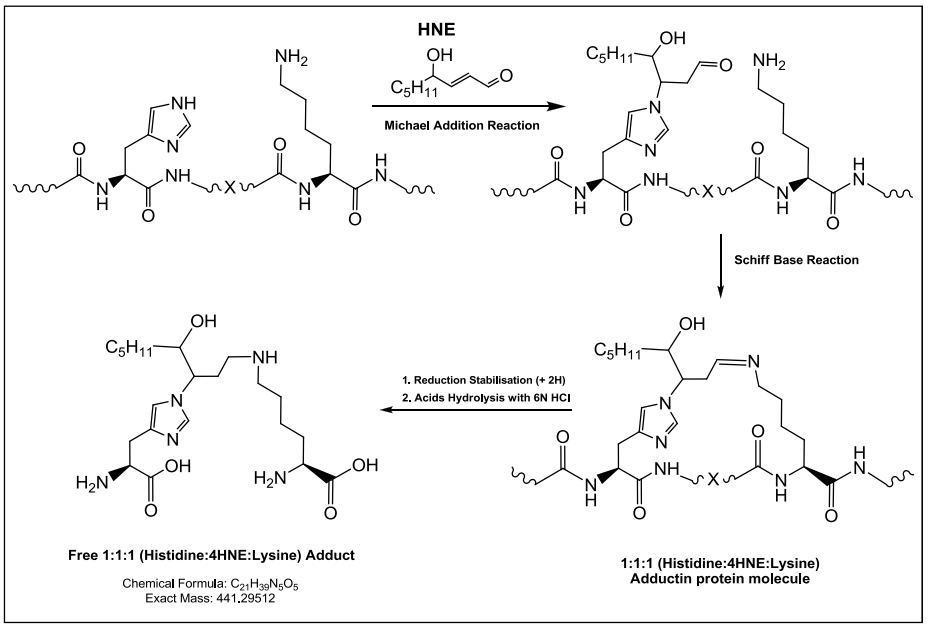

Figure 1.11: Reaction of histidine-4HNE-Michael adduct with a lysine amino acid residue through Schiff base to form His-HNE-lysine adduct [68]. X represents a specific number of amino acids residues.

1.3 Preparation of Protein Samples for Acid Hydrolysis

1.3.1 Extraction of Proteins from Biological Samples

Isolation and purification of proteins in a protein mixture is an essential step in the amino acids (free and modified amino acids) composition determination in a particular protein before the hydrolysis method. The purification method depends on some physical characteristics of the protein such as solubility, polarity, molecular size, charge, and specific interactions.

Table 1-1 shows different extraction and purification techniques which enable us to separate a particular protein from a protein mixture, depending on some of the physical and chemical properties of the required protein [72].

Table 1-1: Physico-chemical properties of protein exploited by the different separation techniques [72].

Technique	Properties of protein
Centrifugation	**Solubility**
Gel filtration	**Size**
Ion exchange chromatography	**Charge, with some influence of polarity**
Paper electrophoresis	**Charge and size**
Paper chromatography	**Polarity**
Thin layer electrophoresis	**Charge and size**
Thin layer chromatography	**Polarity**
Polyacrylamide gel electrophoresis	**Charge and size**
HPLC	**Polarity**
Gas chromatography	**Volatility of derivatives**
Counter current extraction	**Polarity; some specific interactions**
Affinity chromatography	**Specific interactions**
Covalent chromatography or irreversible binding	**Disulfide bond; reactivity of homoserine lactone**

1.3.2 Reduction with Sodium Borohydride ($NaBH_4$)

Reduction of non-enzymatic modification products such as Schiff bases is an essential step for ALEs analysis prior to acid hydrolysis, since these adducts are liable to acid hydrolysis. The reduction step is carried out by addition of an enough molar excess of $NaBH_4$ (preferably of an alkaline pH) to the protein sample, by dissolving a certain amount of $NaBH_4$ in dilute NaOH (0.01N) or sodium bicarbonate, whereas neutral phosphate buffer is used as solvent for protein samples. The reaction between the protein samples and $NaBH_4$ is allowed to continue for 1-4 hours at room temperature[16]. A

fresh solution of 5M $NaBH_4$ is prepared by dissolving 378.5 mg of $NaBH_4$ in 2 ml of HPLC grade water. A protein sample should be incubated with 0.42 M solution of $NaBH_4$ by the addition of 37.5 µl of 5M $NaBH_4$ solution to 400 µl of protein sample which had been incubated with 11 µl of the modifying aldehyde.

1.3.3 Hydrolysis of Normal and Modified Proteins

Hydrolysis of a protein is an essential step in a protein and peptide identification. An accurate and precise hydrolysis procedure is required in order to determine amino acid composition for proteins, peptides, and other proteinaceous compounds [73, 74]. Different hydrolysis protocols had been reported such as enzymatic digestion [75, 76], alkaline hydrolysis using 5M NaOH [77], and acid hydrolysis with HCl [74, 78-81].

The acid hydrolysis protocol (described by Macpherson, Moore and Stein) with 6N HCl for 24-72 hrs at 110°C is the most widely used hydrolysis method for proteins analysis over the last few decades [79]. Strong acidic conditions (6N HCl) at such a high temperature (110°C) are enough to break down the peptide linkage in proteins and peptides (Figure 6.4) resulting in a smaller peptide segments which are then subject to further degradation into free amino acid residues. However, there are some problems with this method such as valine and isoleucine being incompletely hydrolyzed and threonine and serine being subject to a higher destruction rate during acid hydrolysis [74]. Furthermore, sulfur containing amino acids (methionine and cysteine) are partially destroyed [82] or oxidized to methionine sulfone and cysteic acid; tryptophan is totally destroyed [78], and tyrosine is heat sensitive and partially destroyed [79]. Aspargine and glutamine are recovered as aspartic acid and glutamic acid due to deamination. Cysteine and cystine usually determined as one unit (cysteine-cystine content) due to partial destruction of cystine to cysteine or oxidation to cysteic acid [73].

Acid hydrolysis with 6N HCl at 110°C for 24-72 hours is time consuming, and hence another hydrolysis method was suggested by Roach and Gehrke (1970) where protein

hydrolysis is done under vacuum using 6N HCl at 145°C for 4 hrs [78] according to the following procedures:

a) Weigh about 10 mg of protein sample in to 25 *200 mm Pyrex glass screw –top culture tubes.
b) 10 ml of 6N HCl is added to the sample.
c) Dissolved air in the protein sample should be removed using a glass "T" arrangement (attached with one arm to vacuum pumping and to the other arm to nitrogen supply) with a rubber stopper was fastened into the tube. Additionally, a Whitney valve is placed in the vacuum line so that the vacuum and nitrogen gas pressure can be controlled. The pressure inside the sample tube is reduced to about 0.2 mmHg via vacuum pumping. The sample tube then held in an ultrasonic bath for about 10 sec to remove the dissolved air from the solution. Finally, the tube was purged with nitrogen gas (slight flow) to remove any source of oxygen that is responsible for oxidation process during acid hydrolysis process. Sonication was used to remove dissolved air before placing the hydrolysis vessel in the oven [78].
d) In order ensure that all dissolved air in the sample was removed, the previous step (pressure reduction, sonication, and N_2 purging) should be repeated 3 to 5 times.
e) The Whitney valve is partially closed so that a slight nitrogen stream would flow through. On the other hand, the nitrogen valve is slowly turned on so that a slight nitrogen gas pressure would be formed inside the sample tube.
f) The sample tube was tightened with PTFE-lined screw cap after the removal of the "T".
g) The sample tube is then placed in an oven at 145 ± 2°C for 4 hrs ± 5 min. The sample is then removed from the oven and allowed to cool to room temperature and the sample is ready now to be analyzed for individual free and modified amino acids detection.

1.3.4 Solid Phase Extraction (SPE) Methods

SPE can be used in two different ways for sample clean up prior to analysis: (a) scavenger SPE, and (b) catch and release SPE. Scavenger SPE is based on retaining impurities which carry a net electric charge opposite to that of the desired compounds. Retention of the impurities by the SPE sorbent bed allows for the desired compounds to pass through [83]. For example, removing of the negatively charged impurities from the positively charged amino acids mixture is done by using strong anion exchange (SAX) SPE cartridges for this purpose. Isolute-SAX SPE cartridge from Biotage Company is composed of silica based quaternary ammonium ion [-Si-$(CH_2)_3$ -N^+- $(CH_3)_3$ Cl^-] with an average pore diameter of 60 Å [84]. Negatively charged molecules will be retained on the SAX sorbent bed by interaction with the positively charged quaternary ammonium ion backbone of the SAX sorbent bed and by chloride exchange. It should be mentioned that SAX SPE will only retain negatively charged molecules, while neutral and positively charged molecules can pass through the sorbent bed.

Catch & release SPE is based on removing impurities by retaining the compounds of interest, which carry a specific charge, to be eluted in a different step. The catch & release SPE method can be carried out using strong cation exchange (SCX) cartridges from different manufacturer (Figure 1.12) to separate positively charged amino acids from neutral and negatively charged impurities in amino acids mixture. Strata-SCX cartridge from Phenomenex Inc company is composed of silica bonded benzene sulfonic acid with an average pore size of 70 Å; Isolute-SCX-2 cartridge from Biotage company is composed of silica based propyl-sulfonic acid with an average pore size of 60 Å [83, 84].

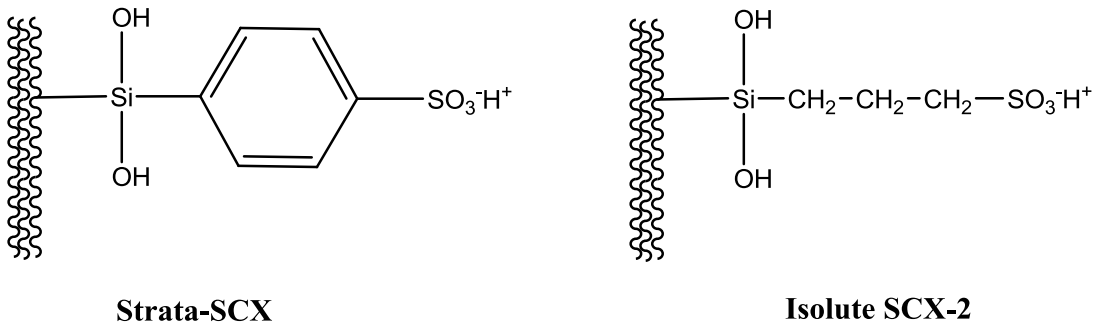

Strata-SCX **Isolute SCX-2**

Figure 1.12: SPE-SCX structures for different type from different sources.

1.3.5 Protein Precipitation Filtration (PPT+)

Protein precipitation can be carried out using a 96-well plate from the Biotage Company which represents a new era in the high throughput sample preparation technique. The principle of this technique depends on protein removal from the biological samples using filtration technique, which totally displaced the routine centrifugation technique, with no off-line steps. PPT technique is a non-selective method suitable for acidic, basic, and neutral compound extraction [84].

Isolute PPT+ filtration cartridges used with a 96-well plate consists of a single frit which is composed of sintered polyethylene matrix with an average porosity size of 20 µm. The thickness of the frit is more than 1 mm and pores run in multidirectional pathways leading to high retention percentage for the particles < 20 µm [83, 84]. So, dissolved and un-dissolved particles which have an average diameter less than 20 µm can pass through the filtration system by in-depth filtration, whereas larger particles and precipitated protein molecules are retained by the frit without complete blockage of the filtration array.

Protein precipitation protocol (Figure 1.13) includes spiking 300 µl of protein sample or amino acids standard solution into Isolute PPT+ array filled with 1 ml acetonitrile (crashing solvent) to remove any protein material by precipitation without off-line vortex. Allow for the mixture to stand for 10 min, then the filtration process

accomplished by using 96-well plate vacuum manifold operating at 10 mmHg [85]. The filtrate should be collected in a dry and clean 4 ml vial and subject to evaporation under slight nitrogen stream at 50°C till dryness, and then re-dissolve in 400 µl of HPLC grade water, and the samples are ready to be analysed by LC-MS.

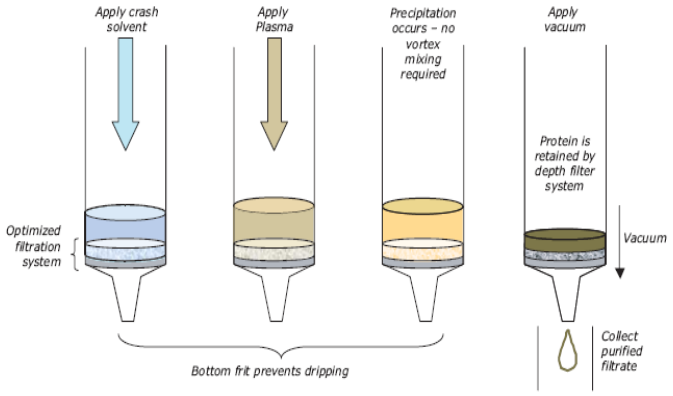

Figure 1.13: Protein precipitation protocol [84]

Acetonitrile has been recommended by Biotage Company as the best crashing solvent for protein precipitation in the biological samples [84]. Different studies confirm the suitability of acetonitrile for protein precipitation from biological samples [86-88].

A neutralisation step with 1 M solution of Na_2CO_3 in a volume of 2:1 (Na_2CO_3 solution: protein-hydrolysate solution) after HCl hydrolysis step is essential to keep the pH of the hydrolysed samples around 3-5. At such pH range most of the amino acids will be in the zwitterionic form which is suitable for both negative and positive ion mass spectrometry detection. Accurate adjustment for the mobile phase pH (within acceptable acidic range) is essential to retain a net positive charge on the terminal amine group of the amino acids. A net positive or negative charge is required for perfect separation of these compounds on HILIC column.

Extra precautions should be considered when adjusting the pH of the sample and the mobile phase as the stability of the silica may be affected by strong acidic or basic conditions. So, the pH of the samples and the mobile phases should be kept within this

limit, as acidic conditions may affect the stability of the ZIC-HILIC matrix (a pH range of 2-10 is recommended for the polymeric based ZIC-*p*HILIC column while a pH range 3-8 is recommended for silica based ZIC-HILIC column) [89].

1.4 Chromatographic Separation Techniques

1.4.1 Reversed-Phase Liquid Chromatography (RP-LC)

RP-LC is the most common separation technique [90] and it is highly compatible with ESI source of a mass spectrometer [91]. The retention of the analytes on a RP-LC column depends on the lipophilic interaction of the non-polar parts of analyte molecules with the lipophilic stationary phase of the column. Hence, it is recommended for the separation of lipophilic compounds [92]. However, other mechanisms have been suggested for RP-LC phenyl phase stationary phase such as hydrogen bonding, ion-exchange and π-π interaction [93]. Polar compounds need derivatisation step prior to RP-LC in order to be retained on a lipophilic stationary phase. Derivatisation will improve retention of polar compounds by the RP-LC, in addition to the improving in the ESI response for these compounds [94].

The stationary phase of the analytical columns used for RP-LC is mainly composed of a silica base modified with hydrocarbon chain. The retention of the non-polar compounds on the RP-LC column depends on the carbon load of each stationary phase; the retention time for non-polar compounds increases as the carbon load on silica particles increases. The stationary phase of a C-18 (octadecylsilane) column contains the highest carbon load followed by C-8> C-4>phenyl> and cyanopropyl column [95].

Acetonitrile and methanol are recommended as mobile phases for RP-LC coupled to mass spectrometry [96]. Replacement of methanol with acetonitrile in a mobile phase would decreases the retention time for non-polar compounds on RP-LC columns due to higher solubility of the lipophilic compounds in acetonitrile than methanol [95].

Different factors can affect the chromatographic retention and resolution of the analytes in RP-LC such as particle size, column internal diameter (column id), column length, pore size [97], type of column modifier (C-18, C-8, C-4, or aminopropyl) [95, 97], temperature [98], flow rate [99], type of buffer system, pH [90, 100, 101], and the mobile phase content (aqueous to non-aqueous percentages) [102].

1.4.2 Hydrophilic Interaction Liquid Chromatography (HILIC)

HILIC is a high-performance liquid chromatographic technique used for the separation of polar and hydrophilic compounds [103]. The principle of HILIC is similar to that of normal phase chromatography (NP-LC), but the eluent solvent system consists of water and a water miscible organic solvent instead of the non aqueous mobile phase used in NP-LC. A typical HILIC applications use acetonitrile at a concentration between 50-95% in water or volatile buffer such as aqueous ammonium formate, ammonium acetate or their acids, which have high solubility in organic solvents [104]. The ZIC-HILIC column (150 x 4.6 mm with a particle size of 5 μm and a pore size of 200 Å) manufactured by Merck SeQuant AB (Sweden) is an example of column used for HILIC separation. It is composed of a sulfonalkylbetaine zwitterionic functional group covalently bonded onto a silica backbone with a net charge of zero [104] (Figure 1.14). Separation of polar molecules can be achieved with high efficiency using a ZIC-HILIC column due to the zwitterionic nature of the column [105]. The mechanism of compound retention on a ZIC-HILIC column is based on the partitioning of the polar analyte between the water-rich layer at the surface of the stationary phase and the high organic content of the mobile phase [106]. The second mechanism involves electrostatic interaction of the charged molecules (positive or negative) with the negative charge of the sulfonate or positive charge of the ammonium ion on the stationary phase of the ZIC-HILIC column [89]. However, hydrogen bonding and dipole-dipole interactions have also been suggested as factors producing retention on the ZIC-HILIC column [107].

Different factors can affect the retention of polar analytes by the ZIC-HILIC column including: the concentration of the buffer, pH of the mobile phase, in addition to the percentage of the organic solvent used in the mobile phase [106].

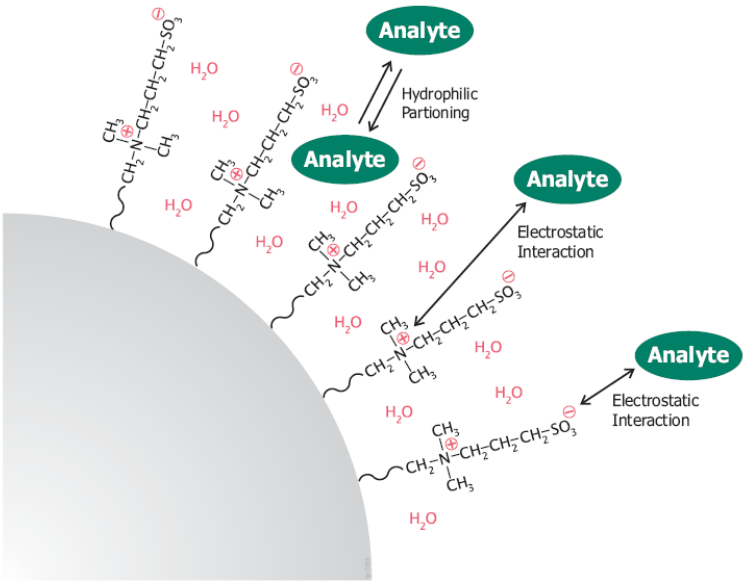

Figure 1.14: Sulfonalkybetaine zwetterionic functional group of the HILIC column bonded to the silica backbone of the HILIC column [89].

1.5 Mass Spectrometry

Mass spectrometry has been applied extensively in the study of protein modification by reactive aldehydes [20, 21, 29, 42, 43, 45, 46, 108-111]. The tendency has been to focus on the study of aldehyde modified peptides released from modified proteins by enzymatic digestion. Orbitrap mass spectrometers are considered perfect qualitative and quantitative analysis tool for low molecular weight compounds and macromolecules [112, 113] and can be readily applied in the study of protein modification.

1.5.1 Electrospray Ionisation (ESI)

ESI is a pneumatically assisted electrospray process which consists of nebulising a solution through stainless steel or a fused silica capillary with the help of the coaxial nebulising gas, usually nitrogen (N_2), at atmospheric pressure (Figure 1.15). ESI involves production of a fine spray, with the assistance of a strong field potential (e.g. 4.5 kV). The charged droplets formed will be subject to subdivision due to internal Coulombic repulsion until the generation of individual gas phase ions occurs. Use of heat can accelerate the process of droplet evaporation [112].

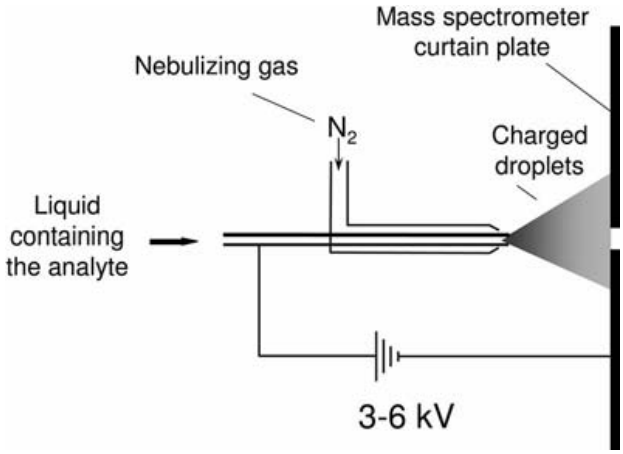

Figure 1.15: Electrospray ion source of the mass spectrometry [112].

Different theories have been proposed to explain the formation of gas phase ions from the nebulised charged droplets, but all of them still in their early stage and further investigations are required. However, two mechanisms have been accepted to explain the formation of gas phase ions from the subdivided droplets: the ion evaporation model (IEM) and the charge residue model (CRM) [114]. The IEM model is a direct implementation of "Coulomb droplet fission" concept, and it proposes that gas-phase ions will be evolved from the subdivided droplets as the droplets radius reaches a critical point at which the surface potential is large enough to help the desorption of the solvated ions. The CRM suggests that electrosprayed droplets undergo evaporation and splitting apart (fission cycle) up to the point where droplets contain an average of one analyte ion or more and no more splitting is possible. The formation of gas-phase ions, according to

CRM theory, will occur after complete evaporation of the remaining solvent molecules. IEM is most applicable to small molecules while CRM applies to proteins and big molecules [112, 114-116].

A critical requirement for the ESI process is that the pH of the mobile phase should be adjusted into a specific range that can help ionisable group either to acquire a proton (positive mode) or eject a proton (negative mode). For example; an amine group requires a slightly acidic condition to be ionised to ammonium ion which is positively charged group and easily detected by LC-MS. Detection of neutral molecules is also possible through adduct formation with other molecules such as: ammonia, potassium, calcium, sodium, formate or acetate [112].

1.5.2 Mass Analyzer

In the mass analyser, gas phase ions are physically separated according to their mass to charge ratio (m/z) rather than by mass only [113]. Ions separation by mass analysers depends on different physical properties such as their velocity, momentum or the kinetic energy [113, 117]. Different mass analysers have different operating principles, but all of them use magnetic and/or electric fields (static or dynamic) to separate ions according to their physical properties [113]. The efficiency and accuracy of mass spectrometry largely depends on the performance of the mass analyser and its resolving power. Mass analysers work on dispersing ions according to their m/z ratio, and then focus them to be passed through a specific lens to the detectors [112].

Different mass analysers have different operating parameters and have different characteristics related to their performance such as: mass range limit, accuracy, resolution and resolving power, transmission, and analysis speed (scan speed) [113].

The Orbitrap mass analyser has advantages of high mass resolving power that can exceed 100,000 calculated according to the full width at half maximum (FWHM) [112], high mass accuracy (below 5 ppm), wide dynamic range, good duty cycle [118], good

sensitivity and high mass range (up to 6000 amu) [92, 117]. However, the Orbitrap mass spectrometry mass range is usually limited by mass range for linear ion trap (LTQ) which is usually 50-2000 or 200-4000 mass unit [113]. Mass Resolution in an FT-ICR analyser is inversely proportional to the m/z value, while the case is different with Orbitrap as the resolution is inversely proportional to $(m/z)^{1/2}$ value which results in a stable resolution over a wide range of m/z values [119].

1.5.2.1 Orbitrap

Makarov proposed a novel type of mass analyser, known as the Orbitrap which was commercially introduced onto the market by the Thermo Electron Corporation in 2005. The idea of Orbitrap based on the trapping the orbiting ions around a central axial electrode with an electrostatic field [112, 113, 117]. In 1923 Kingdon was the first who described the principles of an Orbitrap where an electrostatic field is used to trap ions orbiting around a central electrode, but he used this device for ion capturing rather than mass analyser [112, 117]. The modern Orbitrap consists of an outer barrel shape electrode (cut into two exact halves) and a coaxial inner spindle-like electrode [112, 113, 117]. The outer electrode consists of two exact halves with a small distance between both of them. Ions can be injected into the Orbitrap through small channel between the two halves [113, 117]. The electrostatic field generated by the two electrodes permits the trapping, rotating and oscillating of ions around a central spindle like electrode [118]. The m/z values of the trapped ions are related to the frequencies of the oscillating ions along the z-axis of the Orbitrap [112, 117]. The frequencies of the trapped ions oscillating around the inner electrode can be detected by using image current detection that can detect the current induced between the two halves of the outer electrode. Fast Fourier transformation correlates the currents induced in the two halves and converts these currents into mass spectra [112, 117, 120].

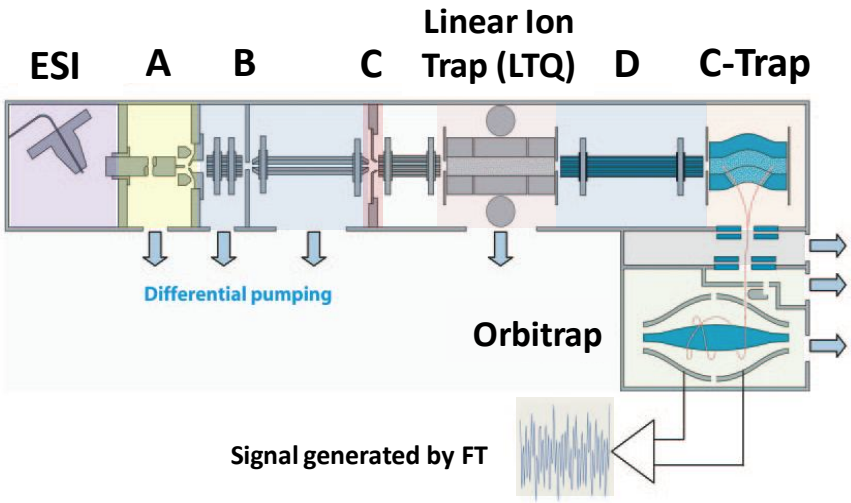

Figure 1.16: Schematic draw for the linear ion trap (LTQ)–Orbitrap (LTQ Orbitrap, Thermo). Adapted from reference [121].

Orbitrap mass spectrometer presented by Thermo Electron Corporation (Figure 1.16) consists of: ESI ionisation source, heated capillary (A) followed by multi-pole focusing devices (B), a gating lens (C) followed by a focusing octapole, linear ion trap (LTQ) followed by focusing multi-pole (D) which leads to new bent quadrupole (C-trap), and finally the Orbitrap mass analyser [113]. In order to achieve high performance, a very high vacuum (~10^{-10} torr) is applied to Orbitrap mass analyser [120].

Thermo Electron Corporation fitted a linear ion trap (LTQ) to the Orbitrap which can perform various MS or MS^n experiments [112]. During a 1 second cycle in Orbitrap mass spectrometry, the LTQ can produce ions in MS^n mode which are then injected into Orbitrap. Meanwhile, LTQ can perform another MS or MS^n while the ions are being detected by the Orbitrap. Because high resolution acquisition requires more time than low resolution acquisition, therefore it is possible to have 2 low resolution acquisitions from the LTQ and 1 high resolution acquisition from Orbitrap at the same time [113]. MS^n spectra generated by LTQ for a specific precursor ion can be detected in low resolution (at 15000) either by LTQ [122] or Orbitrap mass analyser [121]. However, Orbitrap can provide much cleaner MS/MS spectra as compared to that one obtained by LTQ [121].

Ions generated by ESI will be guided though different multi-pole focusing devices leading to LTQ which is coupled to Orbitrap through C-trap. The C-trap acts as trapping and focusing device allowing storage of ions, with the help of nitrogen gas to quench their energy, until ejection toward Orbitrap [113]. Additionally, C-trap can store background ions of known composition and use them as lock masses (internal calibrants) in the real time domain to correct any mass deviation through a simple mathematical correlation. Calibrant ions will be injected into C-trap followed by sample ions, then injected together into Orbitrap allowing for real time correction for analyte masses [119]. Short pulses of high voltage will eject ions from C-trap into Orbitrap. In order to avoid space charge effect or over filling of LTQ or Orbitrap above the specified values, a gating lens (C), known as automatic Gain Control (AGC), will control the number of ions injected into the LTQ and hence number of ions being injected into Orbitrap [112, 113]. A pre-scan event for the total ion charge before injection into LTQ will help AGC to control ion injection time required for each mass scan [118]. For example, if the target value for the LTQ was specified as a maximum of 30,000 charges per scan to fill the LTQ with ions, and the pre-scan in AGC has detected 10,000 charges per 1 ms, that means LTQ needs 3 ms to be filled with requested number of ions [123]. The Orbitrap scan time is proportional to the required resolution; the Orbitrap scan time would be 0.1 sec with a resolution of 7500, 0.4 sec with a resolution of 30,000, and 1.9 sec with a resolution of 100,000 [124].

1.6 Limit of Detection (LOD), Quantification (LOQ) and Minimum Detectability (MD)

LOD can be defined as the minimum amount of a specific compound that can be detected by a specific detector such as a UV detector or mass spectrometry detector, which gives a reasonable indication of the presence of that compound. LOD has a specific indication for each analytical procedure and can be different from one procedure to another. The LOD usually refers to a sample prepared by the complete analytical procedure including extraction and dilution steps. While minimum detectability (MD) can be defined as the minimum concentration or amount of the analyte (in a solvent) that produces enough signal to be distinguished from other noise. In most cases, MD can be recognized as the signal/noise ratio (S/N) which is a readable value from the software program used for data processing e.g. the Xcalibur program for mass spectrometry analysis, and generally this value would be equal to 3 or more. Chromatographer may be confused between LOD and MD because of their similarity [125].

Nevertheless, the LOD refers to complete analytical conditions such as extraction conditions, temperature, column length and width, mobile phase and type of detector being used, while MD cannot include these conditions and it refers specifically to the sensitivity of the detector [125]. Since 2-alkenal adduct detection consists of a number of operations, LOD expression will be used instead of MD.

Sometimes, LOD can be subdivided to instrumental detection limit (IDL) and method detection limit (MDL). IDL refers to the minimum amount of the analyte that can be detected with a certain level of confidence using a specific instrument (sensitivity of the detector to detect a specific analyte), whereas MDL refers to the minimum amount of the analyte that can be detected with a certain level of confidence using specific method such as extraction and analysis method for a specific analyte in a matrix [126].

Three different methods for LOD and LOQ determination have been proposed by ICH guidelines; these include: (1) signal to noise method, (2) visual determination of LOD and LOQ [127-129] , and finally (3) standard deviation and slope method [130].

1.7 SIEVE v1.2 Software

SIEVE software (Vast Scientific, Inc. Cambridge, MA and Thermo Fisher Scientific, San Jose, CA, USA) is rigorous automated LC/MS differential analysis software used to compare between different LC/MS data according to their intensity and retention time [131]. It has two main processes: a chromatographic alignment process and a framing process. Chromatographic alignment is done using a chromatographic alignment algorithm to compare between similar chromatographic surfaces using the full information obtained in each raw file. The framing process starts by classifying the mass spectra from each raw file into a 3D plane [retention time (R_t) *vs* mass/charge ratio (m/z) *vs* mass intensity]. Another framing algorithm is applied to sort the mass spectra for all raw files, above a specific threshold, according to their intensity. The process of frame creation is based upon the most intense spectrum, and continues until all the mass spectra have been defined. Finally, the SIEVE results generated are divided into m/z *vs* retention time plane at 0.02 amu intervals. SIEVE v1.2 software performs a t-test to look for the statistically significant differences in the extracted ion chromatograms between the 2 sets of samples assigned as control *vs* treated samples. Extracted ion chromatograms which show a significant difference are sent to the SEQUEST and Chemspider databases for peptide and small molecule identification respectively. The Frames provide useful information about the quality of the results: the p-value, ratio, standard deviation for the ratio, number of MS^2 scans, MS/MS correlation, ratio and total ion chromatogram (TIC) normalized ratio [131].

2 CHAPTER TWO: Experimental

2.1 Chemicals

All chemicals used were of analytical reagent grade or better. The following materials were obtained from SIGMA® (Sigma-Aldrich Poole, Dorset, UK): ammonium bicarbonate, bovine serum albumin, human serum albumin, hydrochloric acid solution (constant boiling). The following materials were obtained from Sigma-Aldrich Chemical Co., Gillingham, Dorset, UK): hydrochloric acid solution (constant boiling), phosphate buffered saline (PBS) tablets, $NaBH_4$, acrolein (Acr), crotonaldehyde (Cro), t-2-pentenal (Pne), t-2-hexenal (Hxe), t-2-heptenal (Hpe), t-2-nonenal (Nne). The following materials were obtained from BDH Merck Laboratory Supplies, Lutterworth, UK: ammonium formate, sodium hydroxide, HyperSolv® HPLC grade acetonitrile, ammonia, ethyl acetate, formic acid, methanol and water. The EZ:faast kit for amino acids extraction and derivatisation was obtained from Phenomenex® (Macclesfield, U.K.) 4-hydroxynonenal (HNE) was obtained as liquid solution in hexane (5 mg) from Axxora Ltd (Nottingham, U.K.).

2.2 Preparation of the Amino Acids Standard Solutions

A standard amino acid mixture was prepared by diluting 100 µl of amino acid standard reagent from the EZ:faast kit (consists of 200 nmol/ml of each amino acid) with 800 µl of HPLC grade water. An aliquot of 100 µl of internal standard from the EZ:faast kit was added to the diluted amino acids mixture in a total volume of 1000 µl. The internal standard consisted of 200 nmol/ml of homoarginine (HARG), methionine-d3 (MET-d3), and homophenyalanine (HPHE). This sample was labelled as **STD stock solution** which consists of 20 nmol/ml of each amino acid in a total volume of 1000 µl.

An acidified amino acids mixture was prepared by the same procedure described earlier, with the exception of diluting 100 µl of amino acids standard reagent from the EZ:faast kit with 750 µl of HPLC grade water instead of 800 µl. This followed by the addition of 50 µl of 0.1% HCl to the standard amino acid mixture to lower the pH of the solution to

the acidic range (pH range 3 to 5). This sample was labelled as **acidified STD stock solution** which consists of 20 nmol/ml of each amino acid in a total volume of 1000 µl. The STD stock solution was used to validate LLE and PPT methods, whereas acidified STD stock solution was used to validate the SPE method.

2.3 Production of Advanced Lipo-peroxidation End products (ALEs)

The production of different ALEs will be explained in detail in this section. The subsequent reduction step with $NaBH_4$ and acid hydrolysis step with 6N HCl, which are essential to prepare these adducts for LC-MS detection, will also be discussed.

2.3.1 Production of 2-Alkenal Adducts

This method involved the incubation of proteins with different aldehydes (acrolein, crotonaldehyde, 2-pentenal, 2-hexenal, 2-octenal and 2-nonenal) as follows: A 2.5 mg/ml solution of HSA or BSA (ca 0.04 mM) was prepared in PBS and an aliquot (400 µl) was mixed with a 9 mM solution of aldehyde [by addition of 11 µl of 338 mM solution of the aldehyde in acetonitrile] and overnight incubated at 37ºC [132].

2.3.1.1 Production of HNE Adducts

Preparation of HNE adducts consists the same process for ALEs production with the exception that, 2.5 mg/ml solution of HSA or BSA (ca 0.04 mM) was prepared in PBS and an aliquot (400 µl) was mixed with a 6 mM solution of HNE solution [by addition of 11µl of 229 mM solution of the HNE in acetonitrile] and overnight incubated at 37ºC. A solution of 229 mM HNE in acetonitrile was prepared by totally evaporating n-hexane from the original packing [5mg HNE solution in n-hexane] which had been bought from Axxora Ltd, Nottingham U.K. under slight nitrogen stream, and then re-dissolve it 140 µl of HPLC grade acetonitrile solution [132].

2.3.2 Preparation of ALEs Compounds for LC-MS Detection: Acid Hydrolysis Step

Different ALEs can be produced by incubating protein sample (HSA or BSA) with different members of 2-alkenal series according to the procedure mentioned in section 2.3. Reduction with $NaBH_4$ is an essential step to stabilise these adduct against harsh conditions during acid hydrolysis with 6N HCl. Acid hydrolysis was carried out using the Roach and Gehrke method mentioned in section 1.3.3, in order to get individual free and modified amino acids. Briefly, 400 µl of a 2.5 mg/ml of protein sample (HSA, BSA) was overnight incubated with 11 µl of 338 mM solution of aldehyde in a 10 ml test tube at 37°C in a constant temperature room. A reduction step carried out by adding 37.5 µl of a freshly prepared 5M $NaBH_4$ solution to the protein sample in a test tube. The sample was mixed for 10 sec then incubated for 1 hr at 37°C in a constant temperature room. This step is essential to stabilise ALEs against acid hydrolysis and to remove any reactive aldehydes by reducing them to their equivalent alcohol molecules. Acid hydrolysis with 6N HCl was carried out by adding 400 µl of 6M HCl to the protein sample in a test tube; the samples were sonicated for about 5 min, using water bath sonicator, and then were purged for 0.5 min under a slight nitrogen stream. The temperature of a GC-oven set at 145°C, and then the test tubes were placed inside the GC-oven at that temperature for 4 hrs ±5 min. Such harsh conditions (temperature and acidity) for 4 hrs are enough to breakdown all the protein and peptide bonds (amide linkage) to get individual amino acids. The test tubes were removed from the GC-oven after 4hrs and left it for about 10 min to cool down before starting the extraction process [132].

For method validation process, samples should be compared with standards or a blank sample. A blank sample can be prepared by the same procedure mentioned above with one exception; the protein samples will be incubated with 11 µl of acetonitrile instead of acetonitrile containing 2-alkenal aldehydes. Extraction of free and modified amino acids was carried out by using either the EZ:faast method, solid phase extraction (SPE), liquid-liquid extraction (LLE), or protein precipitation technique (PPT).

2.4 Extraction of Amino Acids & ALEs Compounds: Preparation for RPLC-MS Injection

Extraction of the hydrolysate was carried out by using two methods in order to prepare these compounds for mass spectrometry detection. The first method involved the extraction and derivatisation of these compounds with propylchloroformate using the EZ:faast method. The derivatised compounds are then separated on C-18 column using RP-LC interfaced with ESI-FTMS. The second method involved the extraction of the compounds of interest without derivatisation from the protein hydrolysate using either a protein crash plate method (PPT), liquid-liquid extraction method (LLE), or solid phase extraction method (SPE) to remove the proteinaceous material from the hydrolysate. The second method is mainly applicable for the extraction and separation of the hydrophilic compounds on HILIC column which will be discussed in section 2.5.

2.4.1 EZ:faast Method

In order to extract reduced aldehyde-modified amino acids from acidic aqueous solutions, EZ:faast kit (Phenomenex®, Macclesfield, U.K.) was used. The EZ:faast method is a recently developed method for amino acid analysis from protein hydrolysate using liquid chromatography-mass spectrometry as a detection method. The EZ:faast kit for analysis of protein hydrolysate contained solid phase extraction SCX packed tips, reagents, and solvents used for derivatisation and extraction [133].

2.4.1.1 The EZ:faast Kit

The EZ:faast kit consists of 5 reagents (Table 6-1). The eluting medium is prepared by mixing 3 parts of reagent 3A with 2 parts of reagent 3B in a capped vial; the eluting solvent for the EZ:faast method should be freshly prepared each day. At the end of the day, all remaining eluting medium should be discarded [133].

2.4.1.2 Sample Preparation

Reagent 2 (1M Na_2CO_3) was added in a drop-wise manner to 100 µl of protein hydrolysate (always keeping the ratio of 1:2 of protein hydrolysate to reagent 2), and the sample was mixed for about 5 seconds. The pH of the solution was then adjusted to between 1.5 and 5. The pH was checked using a Hydrion plastic pH meter strip (Micro Essential Laboratories, New York, USA). Then about 50 µl of the mixture was pipetted into an EZ:faast vial and 100 µl of reagent 1 was added and the mixture vortexed for 5 seconds [133].

2.4.1.3 Solid Phase Extraction (SPE)

Solid phase extraction was performed using the sorbent tips that were provided with the EZ:faast kit (Figure 2.1). The sorbent tip will extract amino acids from protein hydrolysate based on the cation exchange interaction between amino acids and the sorbent substance in the tip. Other substances and contamination will pass thorough without retardation by the sorbent tip [133].

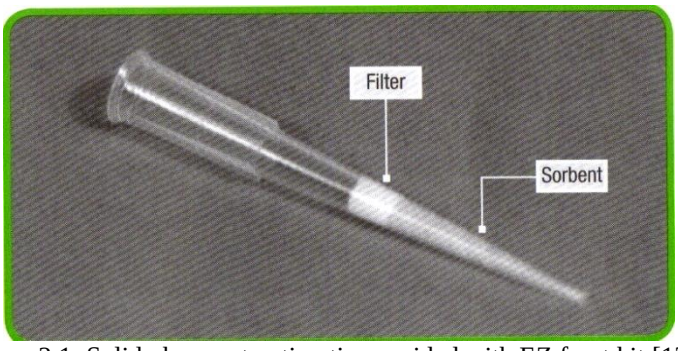

Figure 2.1: Solid phase extraction tip provided with EZ:faast kit [133].

A syringe (1.5 ml) was attached to a sorbent tip, and the plunger was slowly pulled back until all the solution in the vial has been withdrawn. After this point, all positively charged amino acids will be retained by the solid phase particles. Water soluble impurities were removed by addition of 200 µl of HPLC water which was pulled into the syringe until air was pulled into the syringe to dry the solid phase. Syringe was then detached and the liquid accumulated in the syringe was discarded. In order to drain the

solid phase particles from the sorbent tip, 200 µl of elution medium (freshly prepared by mixing 3 parts of reagent 3A with 2 part of reagent 3B) was added. A syringe (0.6 ml) halfway pulled back was attached to sorbent tip, and the piston was pulled back to wet the sorbent tip with elution solvent up to the filter, then directly ejected it with the sorbent particles. The process was repeated until all sorbent particles were in the sample tube [133].

2.4.1.4 Derivatisation Step

The second step in this method was the derivatisation of amino acids using propylchloroformate to esterify the carboxylic acid groups of the amino acids to their propyl ester form; the amine group of the amino acids will be modified to their propyl carbamate (Figure 2.2). The process of derivatisation makes the amino acids more lipophilic and more suitable for the next extraction step. Using a glass-tipped micro dispenser, 50 µl of reagent 4 (propyl chloroformate in chloroform) was added, and the resultant emulsion was vortexed for 8 seconds and left for 1 min. The sample was vortexed again for another 8 sec and left for another 1 min [133].

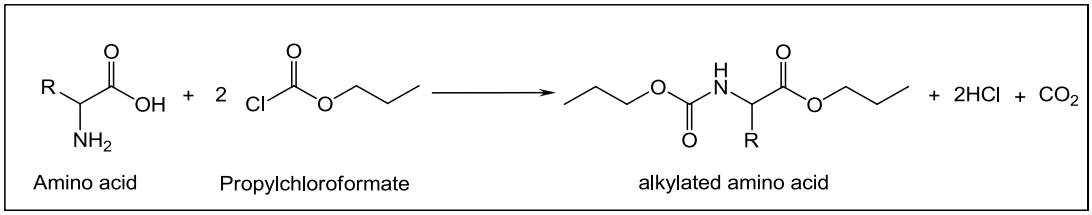

Figure 2.2: Derivatisation methods for amino acids by the EZ:faast method.

2.4.1.5 Liquid-liquid Extraction

The last step in this method was liquid-liquid extraction by the addition of organic solvent (chloroform and iso-octane) to the sample, allowing for the derivatised amino acids to migrate to the organic layer. At the end, all the derivatised amino acids will be in the organic layer. LLE step was done according to the following protocol: a micro-dispenser was used to add 100 µl of reagent 5 and sample was vortexed for 5 seconds and then left for a further 2 min. A pipette was used to transfer 50 µl of the organic layer

which was then evaporated under a slight stream of nitrogen. The sample was re-dissolved in 100 µl of HPLC mobile phase, and the sample was transferred to HPLC auto-sampler inserts to be analyzed by LC-MS [133].

2.4.1.6 Mobile Phase Preparation

A mobile phase of 10mM ammonium formate in water and 10mM ammonium formate in methanol was prepared. An exact amount (160.87 mg) of ammonium formate (purity 98%, Mw 63.06 g/mole) was weighed and transferred to two 250 ml beakers and dissolved in about 200 ml of solvent, which was either a water or methanol. Using a pH meter, formic acid was gradually added to the solution with stirring till the pH had been adjusted to about 4.5, and the solution was then transferred to a 250 ml volumetric flask and made up to the volume [133]. The mobile phase gradient used is shown in Table 2-1.

Table 2-1: Chromatographic eluting program. A: 10 mM ammonium formate in water; B: 10mM ammonium formate in methanol.

Time	***A%***	***B%***	***Flow rate***
0.00	30	70	0.25 ml/min
15.00	5	95	0.25 ml/min
20.00	5	95	0.25 ml/min
20.01	30	70	0.25 ml/min
29.00	30	70	0.25 ml/min

2.4.1.7 Instrumentation: Analysis of Derivatised Amino Acids Using RP-LC Chromatography and an LTQ Orbitrap Mass Spectrometer

A Finnigan™ LTQ™ linear ion trap instrument (Thermo Electron Corporation, San Jose, CA, USA) coupled with a Fourier transform LTQ Orbitrap™ mass spectrometer (Thermo Electron Corporation, San Jose, CA, USA) was used in order to determine the masses and elemental compositions of the derivatised adducts. The system was equipped with a surveyor HPLC system (Thermo Electron Corporation, San Jose, CA, USA) consisting of a Surveyor MS pump, a Surveyor as auto sampler, and a Surveyor PDA

UV-detector. Xcalibur™ software version 2.0 (Thermo Electron Corporation, San Jose, CA, USA) was used for the acquisition of data. Full scan mass spectrometry was operating at positive polarity with the following parameters: a mass resolution set at 60,000 (FWHM), capillary temperature 350°C, injection time 100 ms, and mass range: 50-1000 amu. The ionization was generated in positive mode and the spray voltage set at 4kV; sheath and auxiliary nitrogen gas were applied to help the evaporation of the solvent at a flow rate of 60 and 20 arbitrary units, respectively. All MS/MS scan were performed with an isolation window of 1 amu and collision induced dissociation (CID) set at 35% as fragmentation energy. Helium gas was used as collision gas to help trapping the ions in the LTQ quadrupole during MS/MS fragmentation process. Separation of the analytes was carried out on a Phenomenex® the EZ:faast AAA-MS column (250×2.0mm, 4µm particle size). The column oven temperature was set at 40°C. The mobile phase conditions are shown in Table 2-1.

2.5 Extraction of Amino Acids & ALEs Compounds: Preparation for HILIC-MS Injection

The second method used for analysis involved the extraction of the compounds of interest without derivatisation from the protein hydrolysate. Three methods for removal of proteinaceous material from the hydrolysate were compared in this step: solid phase extraction method (SPE), liquid-liquid extraction method (LLE), and protein crash plate method (PPT).

2.5.1 SPE methods

Different SPE methods (mentioned in section 1.3.4) were examined to compare their efficiency for the analysis of the protein hydrolysate. These include examination of SAX-SPE method (Scavenger SPE method) and SCX-SPE method (Catch and release SPE method).

Scavenger SPE protocol involves column solvation (Isolute-SAX SPE cartridge from Biotage Company) with 1 ml of methanol, followed by column equilibration with 1 ml of 0.1% HCl to maximise the retention of impurities by the sorbent particles during sample loading step. Finally, 300 µl of acidified STD stock solution (amino acid mixture prepared according to the procedure described in section 2.2) was loaded on the SAX sorbent bed. The filtration process accomplished by using vacuum manifold operating at 10 mmHg to ensure a maximum flow rate of 1 ml/min. The filtrate which contains the desires compounds (neutral and positively charged amino acids) should be collected for detection (Figure 6.5).

Catch & release SPE protocol involves column solvation (either Strata-SCX cartridge from Phenomenex Inc company or Isolute-SCX-2 cartridge from Biotage company) with 1 ml of methanol, followed by column equilibration with 1 ml of 0.1% HCl solution to maximise the interaction between the positively charged molecules and the SCX sorbent particles of Strata-SCX or Isolute SCX-2 cartridges. A volume of 300 µl of acidified STD stock solution was loaded on the SCX sorbent bed. On contrast to the scavenger

SPE method, the compounds of interest (positively charged amino acids) being retained on the SCX bed , due to the interaction with the negatively charged sulfonium ion group of the sorbent bed. Furthermore, column washing step with 1 ml of 1:1 (0.1% HCl in water: 0.1% HCl in methanol) is required to remove any remaining impurities (neutral and negatively charged molecules).

Finally, the retained compounds of interest could be eluted from the SCX sorbent bed by using 2 ml of (5%) NH_4OH/methanol solution (Figure 6.6). During this step, ammonium ion will displace the positively charged amino acids from the sorbent bed, leading to the elution of the positively charged amino acids with the filtrate. Collect the filtrate in clean and dry 4 ml vial as it contains the desired compounds [83]. Vacuum manifold operating at 10 mmHg was used in any single step of catch & release SPE method to ensure a maximum flow rate of 1 ml/min.

The collected filtrates from scavenger or catch & release SPE subject to complete evaporation till dryness under slight nitrogen stream at 50°C, and then re-dissolved in 400 µl of HPLC grade water, to avoid sample to sample fluctuation in amino acids concentrations.

2.5.2 Liquid-Liquid Extraction Methods (LLE)

LLE is a very common and versatile technique, whereby 2 immiscible solutions (aqueous and organic) brought into contact allowing free movement of the compounds between these 2 immiscible layers according to their partition coefficient (log P). For compounds to be soluble in the aqueous layer, it is essential for these compounds to contain some polar or ionisable groups to dissolve in the aqueous layer rather than organic layer.

Extraction of amino acids using LLE was examined using 2 types of organic solvents: heptane and chloroform. Both organic solvents can dissolve lipophilic compounds from protein samples. So, free amino acids should have higher solubility in the aqueous layer

rather than organic layer due to low partition coefficient (log P); such low partition coefficient for amino acids can be attributed to the availability of ionisable groups (carboxyl and amine group) in the structure of the amino acids.

The LLE protocol consisted of mixing 300 µl of STD amino acid stock solution (prepared according to the procedure described in section 2.2) with 600 µl of the organic solvent (heptane or chloroform). Vortex the liquids mixture for 1 min, then leave for 5 min. Pipette the aqueous layer using 1 ml syringe into clean and dry 4 ml vial. Evaporate the aqueous layer till dryness under slight nitrogen stream at 50°C, and re-dissolve in 400 µl of HPLC grade water. On the contrary to the case where chloroform is used as organic solvent, the aqueous layer will be the lower layer in the case where heptane is used as organic solvent.

2.5.3 Protein Precipitation (PPT+) Filtration Technique

In order to prepare protein hydrolysate samples for PPT extraction, the next step was to bring the pH of the protein hydrolysate within the acceptable range (3-5); a volume of 1.697 ml aliquot of 1M Na_2CO_3 was required to neutralise the acidity of the protein hydrolysate [prepared according to the procedure described in section 2.3] and elevate the pH within the range 3-5.

The concentration of the albumin protein samples before starting the PPT method is about 0.39285 mg/ml, according to the calculations done in Table 2-2. An initial volume of 0.4 ml of 2.5 mg/ml protein sample was diluted to a final volume of 0.8485 ml by the addition of 0.011, 0.0375, and 0.4 ml of 2-alkenal aldehydes, $NaBH_4$, and HCl, respectively. A neutralisation step is done by addition of 1.697 ml of Na_2CO_3. The concentration of the protein sample till the point of PPT extraction step would be about 0.3929 mg/ml in a total volume of 2.5455 ml.

Extraction with PPT cartridges was carried according to the following procedure: add 1 ml of ACN to the cartridges, leave for 1 min then spike 300 µl of protein sample or

amino acids standard solution (STD stock solution, prepared according to the procedure described in section 2.2, is used for PPT method validation). An aliquot of 100 µl of I.S (reagent 1 from the EZ:faast kit) should be added in the case of protein hydrolysate validation. The sample should be left over for 10 min to make sure that all proteinaceous compounds from the hydrolysed sample had been precipitated. The filtration process is accomplished by using 96-well plate vacuum manifold operating at 10 mmHg [85]. The samples were collected in 4 ml vials and the evaporated to dryness using a dry-block at 50°C and nitrogen stream, and then re-dissolve in 400 µl HPLC water. However, carry over tests for amino acids separation and detection from protein hydrolysate samples which had been extracted using PPT method show a minimum amount of amino acids after the 3 runs. So, it is recommended to re-dissolve the evaporated hydrolysate samples after filtration with PPT cartridges with 600 µl instead of 400 µl HPLC grade water.

Table 2-2: Concentration of albumin protein sample till PPT extraction step.

Steps	Volume (ml)	Concentration (mg/ml)
HSA	0.400	2.5
2-Alkenal aldehyde	0.011	
Reduction step with 5M $NaBH_4$	0.0375	
Acid hydrolysis step with 6 N HCl	0.400	
Final volume	0.8485	
Protein conc. after acid hydrolysis step		1.1786
Neutralisation step with Na_2CO_3	1.6970	
Final volume	2.5455	
Final protein concentration before PPT extraction		0.3929

2.5.4 Instrumentation: Analysis of Un-derivatised Amino Acids and their Adducts Using HILIC Chromatography and an LTQ Orbitrap Mass Spectrometer

Finnigan LTQ iontrap mass spectrometry (Thermo Electron Corporation) coupled with Fourier transform LTQ-Orbitrap hybrid mass spectrometer equipped with an electrospray ionization (ESI) source for accurate mass detection. The mass spectrometry system connected to a Finnigan Surveyor Plus HPLC System consists of Finnigan Surveyor Autosampler Plus and a Finnigan Surveyor MS Pump Plus fitted with an ZIC®-HILIC column (5µm, 200 Å, 150×4.6mm; HICHROM, UK). A ZIC®-HILIC column was used for chromatographic separation of hydrolysed protein samples. Full

scan mass spectrometry was operating at positive polarity with the following parameters: a mass resolution set at 60,000 (FWHM), capillary temperature 250°C, injection time 100 ms, and mass range: 50-1000 amu. The ionization was generated in positive mode and the spray voltage set at 4kV. Sheath and auxiliary nitrogen gas were applied to help the evaporation of the solvent at a flow rate of 40 and 10 arbitrary units, respectively. The mobile phase used in this case was 0.1% (v/v) formic acid in water (A) and 0.1% (v/v) formic acid in acetonitrile (B) in a percentage of 10 (A): 90 (B) with a follow rate of 500 µl per min. The elution program started at 10% A: 90% B. The percentage of A increased from 10% to 60% over 20 min, followed by Isocratic elution for another 20 min (60% A: 40% B). The washing period was over 2 stages: stage one started with the gradual decrease in the percentage of the mobile phase (A) from 60% to 10% over 5 min and the second stage continue as isocratic elution (10% A: 90% B) for another 5 min; the overall run time of the sample was 50 min.

2.5.4.1 Data Dependent Acquisition (DDA) Fragmentation

Data dependent acquisition (DDA) represents a new development in handling huge data generated be mass spectrometry, as it has increased the capability of the mass spectrometer to perform more than one scan even in the same time. Normally, a full scan event would be coupled with tandem mass event(s) to be performed in the same time. The selection of precursor ions from the first mass scan event (usually full MS scan) that would subject to tandem mass based on previously specified parameters in the DDA method; different mass spectrometry experiments can be initiated once the incoming data coincides with previously specified parameters.. DDA criteria can be manipulated in order to: (1) determine the range and threshold for precursor ion selection, (2) specify the type of tandem mass scan (product-ion scan, SRM or MRM), and (3) to exclude and background ions or any interfering ions [112, 122]. One requirement for DDA is that the threshold for the precursor ion should be set at or slightly below the noise level for optimum results. Setting the threshold higher than the noise level can decrease the

number of the acquired spectra, while setting it below the noise level can result in false results.

For example, parameters for mass spectrometry can be set to initiate data dependent fragmentation for lysine amino acid (m/z=147.1128) once lysine was detected in sufficient intensity in the previous scan time. So that a total scan and a MS2 scan for lysine can be performed in the same run. Usually, the data dependent scan will consider the most abundant ion from the previous scan, but parameters can be changed to set a list of parent ions that can be subject to MS2 fragmentation once these parent ions could be detected in sufficient intensity [134]. All DDA scan were performed with an isolation window of 1 amu and collision induced dissociation (CID) set at 35% as fragmentation energy. Helium gas was used as collision gas to help trapping the ions in the LTQ quadrupole during MS/MS fragmentation process.

2.6 Plasma Samples of Diabetic and Obese Patients

Plasma samples from diabetic and obese patients were used to screen for different types of modified proteins such as advanced glycation end-products (AGEs), advanced lipo-peroxidation end-products (ALEs), 4-hydroxy-nonenal (HNE) adducts, and malondialdehyde (MDA) adducts. Plasma samples were obtained from the Queen's Medical Research Institute, University of Edinburgh with full ethical approval from volunteers who had enrolled in another study. The plasma samples were stored a -80ºC until being analysed. The samples were allowed to thaw at room temperature and then immediately processed.

The process of protein extraction from plasma included the addition of 1 part of plasma to 5 parts of acetonitrile in a 1.5 ml Eppendorf tube. Acetonitrile (1 ml) was pipetted into 1.5 ml Eppendorf tube and then plasma (200 µl) was spiked into the centrifuge vial. The sample was centrifuged for 12 min at 4000 rpm. The supernatant was then removed out of the centrifuge vial into a separate vial labelled as "supernatant layer". The centrifuge vial was then placed under a stream of nitrogen for 3 min in order to remove the

remaining acetonitrile. PBS (1 ml, pH 7.4) was then added to the centrifuge vial in order to dissolve protein precipitate; pellet pestle was used to disrupt large protein aggregation. The samples were left for 5 min and then 800 µl of the solution was pipetted into 4 ml vial, labelled as "PPT layer vial". The protein precipitate was mixed for 2 min (using pellet pestle), followed by the addition of another 1 ml of PBS (pH 7.4). The samples were vortexed again for 1 min, then all the remaining volume was transferred into the "PPT layer vial". An additional 1 ml of PBS (pH 7.4) was added before starting the filtration process in order to ease the process of filtration. The filtration process was carried out by using a Millipore filter (0.22 µm); usually 2 filters were required for 3-4 ml protein solution by switching from one filter to another clean one when flow blockage occurred in the first one.

Evaporation process was used to concentrate the protein content in 1 ml of PBS using a slight nitrogen stream at 50°C. The concentration of protein in the sample after precipitation, re-dissolving and filtering was estimated to be 7-11 mg/ml. Finally, an aliquot of filtered sample (400 µl) was subjected to the standard acid hydrolysis procedure with 6N HCl at 145°C for 4hrs.

The supernatant layer left after precipitation of the plasma proteins was also examined for the presence of the modified adducts. The supernatant in the supernatant layer vial which contained acetonitrile was evaporated under a slight stream of nitrogen gas till dryness. Then 600 µl of PBS (pH 7.4) was added in order to dissolve the remaining protein and amino acids. An aliquot of supernatant (400 µl) was subjected to the standard acid hydrolysis procedure with 6N HCl at 145°C for 4 hrs. Finally, the protein samples are ready for analysis with LC-FTMS. Non-hydrolysed samples from the supernatant were also examined for the presence of free adducts (non protein attached adducts).

3 CHAPTER THREE: Results and Discussions for the Analysis of 2-Alkenal Adducts using Reversed Phase Chromatography (RP-LC) and Mass Spectrometry

3.1 Introduction

All the samples in this chapter were prepared and detected according to the standard procedure described in section 2.3 & section 2.4 unless otherwise specified.

Using ESI as ion generating source in mass spectrometry results in the addition of 1 H^+ ion (with a mass of 1.00728 Thomson) for the total mass of the detected molecule. The position of this H^+ ion will either be delocalized over the whole molecule, or be localized over one of the highly electronegative atom such as N, O, or S. So, wherever a molecule is detected by mass spectrometry, we should expect the addition of 1 H^+ to the chemical formula of the expected molecule. The acid hydrolysis of a protein molecule and the formation of free lysine with the chemical formula $C_6H_{14}N_2O_2$ and an exact mass of 146.10553 Da were shown in Figure 3.1. Mass spectrometry detection using ESI as ionization source will result in the addition of 1 H^+ ion to the whole lysine molecule which results in the formation of an ionized lysine with a chemical formula of $C_6H_{15}N_2O_2^+$ and monoisotopic mass of 147.11280 m/z.

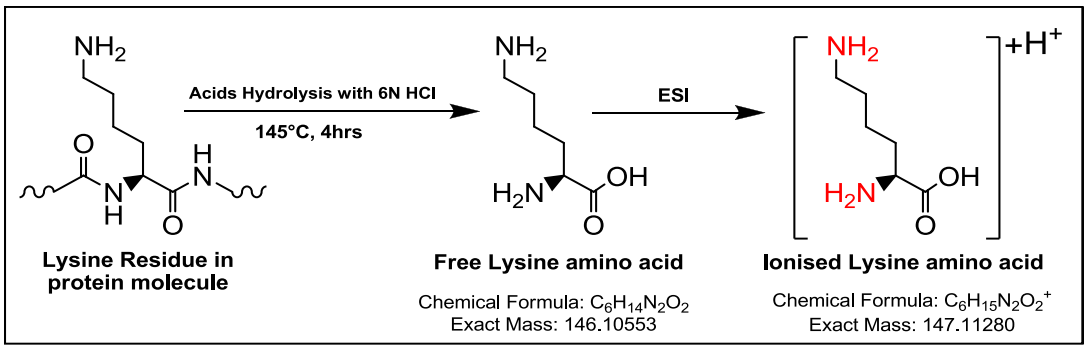

Figure 3.1: Ionisation process in ESI mass spectrometry.

Compound identity was assigned by low mass deviation (less than 3ppm) with regard to a proposed chemical formula, and by comparing the intensity of the ^{13}C peak for each proposed compound which should be *ca* 1.1% multiplied by the total number of carbon atoms for the base peak for the same compound with ^{12}C structure (Figure 3.2).

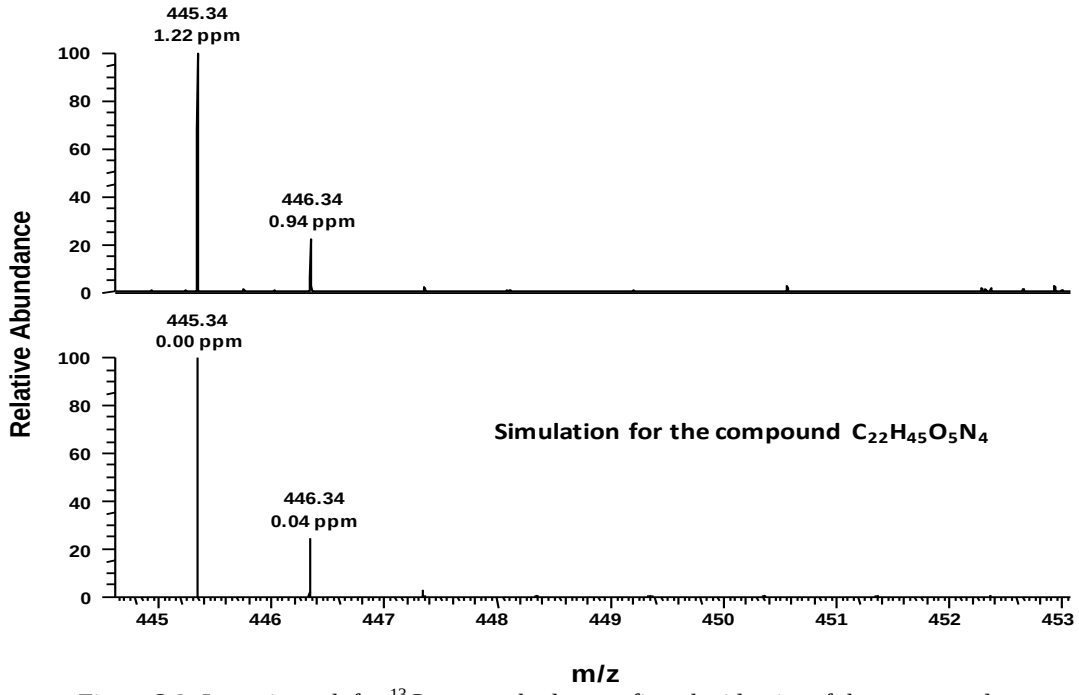

Figure 3.2: Isotopic peak for ^{13}C as a method to confirm the identity of the compound.

The free 2-alkenal adducts could be extracted and derivatised with propylchloroformate using the EZ:faast method, described in section 2.4.1, for perfect RPLC-FTMS separation and detection. Derivatisation of the 2-alkenal adducts with propylchloroformate occurs only at the free α-amine group and α-carboxyl group liberated during the hydrolysis of the protein, as the terminal amine group is already protected by the modifying 2-alkenal group. Derivatisation of the α-amine group and α-carboxyl group of the amino acid will add 128 amu (equivalent to $C_7H_{12}O_2$) to the total mass of the amino acid. Derivatisation process will add an extra lipophilicity to the amino acid molecules; it is essential for RP-LC retention and separation of hydrophilic compound on lipophilic C-18 column. Ionisation process with ESI may add 1 H^+ ion (1.00728 amu) to the total mass of the amino acid, or may not depending on the ionisation status of the molecule.

3.2 Reactions of 2-Alkenals with Lysine Residues with the Analysis of the Modified Residues Using the EZ:faast Method

In vitro non-enzymatic modification of the lysine residue in protein molecule with 2-alkenal series consists of the nucleophilic reaction between the ε-amine group of lysine with aldehyde group or the unsaturated double bond of the 2-alkenal molecule resulting in a different variety of lysine-2-alkenal adducts such as Schiff base, Michael adduct, pyridinium and FDP adducts [30, 51, 60]. Amino acids modification with 2-alkenal aldehydes through Schiff base or Michael addition will add some stereochemistry to the molecule resulting in different isomer for each compound.

3.2.1 Schiff base and Michael-Like Addition Reactions

The nucleophilic reaction between ε-amine group of lysine with 2-alkenal aldehyde results in a set of compounds known as Schiff base and Michael adducts.

Figure **3.3** shows the general scheme for lysine Schiff base & Michael adduct formation, followed by the reduction step, acid hydrolysis, extraction and derivatisation with the EZ:faast method as described previously [sections 2.3 & 2.4]. Table 3-1 & Table 3-2 show the expected elemental formula for the ionised lysine-2-alkenal Schiff bases & Michael adducts after reduction, acid hydrolysis and derivatisation steps. Also, they show MS results for these adducts using full MS scan operating in the positive mode; all the observed masses closely match the expected elemental composition for the derivatised adducts. It is noticeable from these tables that the retention time for Michael adducts on RP-LC is less than the retention time for the correspondent Schiff base adducts; this can be attributed to fact that Michael adducts are less lipophilic than Schiff base due to the availability of the peripheral aldehyde group. The retention times, as would be expected in reverse phase mode, gradually increase with the lipophilic chain of the 2-alkenals.

A single chromatographic peak could be detected for lysine adducts (Schiff base or Michael adducts) which had been modified with short chain 2-alkenal aldehydes such as

Acrolein and 2-hexenal; multiple peaks could be detected for lysine adducts which had been modified with long chain 2-alkenal aldehyde such as 2-heptenal and 2-nonenal.

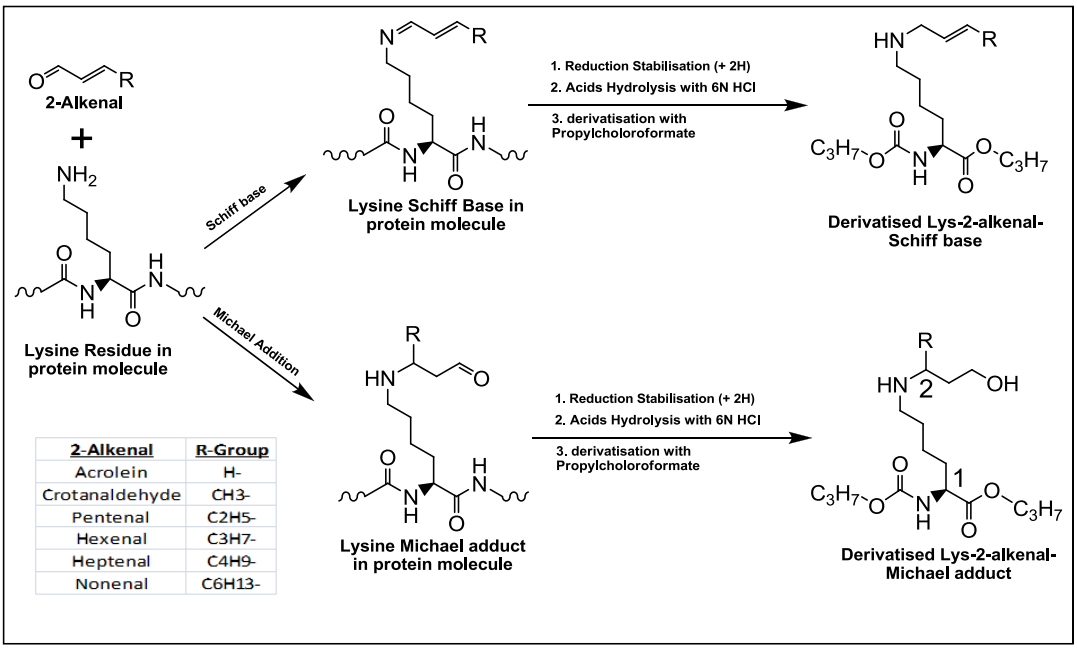

Figure 3.3: Reaction of 2-alkenal aldehydes with a lysine residue within a protein molecule through Schiff base and Michael addition reactions. Acid hydrolysis with 6N HCl results in the formation of free form for these adducts.

Table 3-1: Mass spectrometric results for derivatised Lys-Schiff bases modified with different 2-alkenals using RPLC coupled toESI-FTMS.

Adduct	*Elemental formula*	*RDB*	*R_t (min)*	*Observed m/z*	*Delta ppm*
Acr-Lys-S	$C_{16}H_{31}N_2O_4$	**2.5**	**2.36 min**	**315.22818**	**1.098**
	$C_{16}H_{29}N_2O_4$ **(-2H)**	**2.5**	**2.30 min**	**313.21182**	**-1.163**
Cro-Lys-S	$C_{17}H_{33}N_2O_4$	**2.5**	**3.20 min**	**329.24359**	**0.321**
Pne-Lys-S	$C_{18}H_{35}N_2O_4$	**2.5**	**3.49 min**	**343.25888**	**-0.741**
Hxe-Lys-S	$C_{19}H_{37}N_2O_4$	**2.5**	**4.01 min**	**357.27408**	**-1.972**
Hpe-Lys-S	$C_{20}H_{39}N_2O_4$	**2.5**	**4.75/5.12 min**	**371.29019**	**-0.659**
Nne-Lys-S	$C_{22}H_{43}N_2O_4$	**2.5**	**7.42/8.36 min**	**399.32089**	**-1.89**

Table 3-2: Mass spectrometric results for derivatised Lys-Michael adduct modified with different 2-alkenals using RPLC coupled to ESI-FTMS.

Adduct	*Elemental formula*	*RDB*	*R_t (min)*	*Observed m/z*	*Delta ppm*
Acr-Lys-M	$C_{16}H_{33}N_2O_5$	**1.5**	**2.67 min**	**333.23862**	**0.664**
Cro-Lys-M	$C_{17}H_{35}N_2O_5$	**1.5**	**2.91 min**	**347.255**	**2.738**
Pne-Lys-M	$C_{18}H_{37}N_2O_5$	**1.5**	**3.00 min**	**361.26929**	**-1.133**
Hxe-Lys-M	$C_{19}H_{39}N_2O_5$	**1.5**	**3.17 min**	**375.285**	**-0.931**
Hpe-Lys-M	$C_{20}H_{41}N_2O_5$	**1.5**	**3.19/3.55/3.83/4.45**	**389.30069**	**-0.795**
Nne-Lys-M	$C_{22}H_{45}N_2O_5$	**1.5**	**5.68/6.29 min**	**417.33148**	**-1.964**

Multiple peaks pattern for lysine adducts can be explain by the availability of the different isomers for each adducts; lysine Schiff base adducts show a diastereoisomers as a result of the peripheral double bond. Whereas, lysine Michael adducts contain more than one chiral centre (position 1 & 2 in Figure 3.3) which can result in different stereoisomers for the same compound. Theoretically, all lysine adducts which are modified with 2-alkenal should show the same peak multiplicity, however enough retention and separation time of such compounds on C-18 column is required to show such peak multiplicity. Surprisingly, non-reduced Acr-lysine Schiff base adducts could be detected with this method with a significant intensity.

3.2.2 Lysine-Pyridinium Adduct Formation

Pyridinium adducts are another type of adduct that can be detected as a result of non-enzymatic modification of lysine residues in a protein sample with the 2-alkenal series [135]. By considering the mechanistic pathway for pyridinium adduct formation which has been suggested by Baker *et al.* [28] in section 1.2.1.3, Figure 6.7 shows the different isomers for the lysyl-pyr adducts which result from different levels of reduction with $NaBH_4$. Pyridinium adducts will accept 2, 4, 6 & 8 hydrogen atoms from the reduction step with $NaBH_4$.

Figure 3.4 shows the general structure for the different pyridinium adducts after reduction, hydrolysis, and derivatisation with propylchloroformate. The pyridinium adducts do not require protonation under the ESI conditions since they carry a permanent charge, so Table 3-3 summarizes the expected m/z ratios for the different pyridinium adducts formed with different 2-alkenal moieties.

Table 3-3: Expected masses for the derivatised lysine-2-alkenal-pyridinium adduct when RPLC coupled to ESI-FTMS is used for detection

2-ALKENAL	Lys-Pyr (-2H)	Lys-Pyr	Lys-Pyr (+2H)	Lys-Pyr (+4H)	Lys-Pyr (+6H)
Acrolein	**N/A**	**351**	**353**	**355**	**357**
Crotanaldehyde	**377**	**379**	**381**	**383**	**385**
t-2-pentenal	**405**	**407**	**409**	**411**	**413**
t-2-hexenal	**433**	**435**	**437**	**439**	**441**
t-2-heptenal	**461**	**463**	**465**	**467**	**469**
t-2-nonenal	**517**	**519**	**521**	**523**	**525**

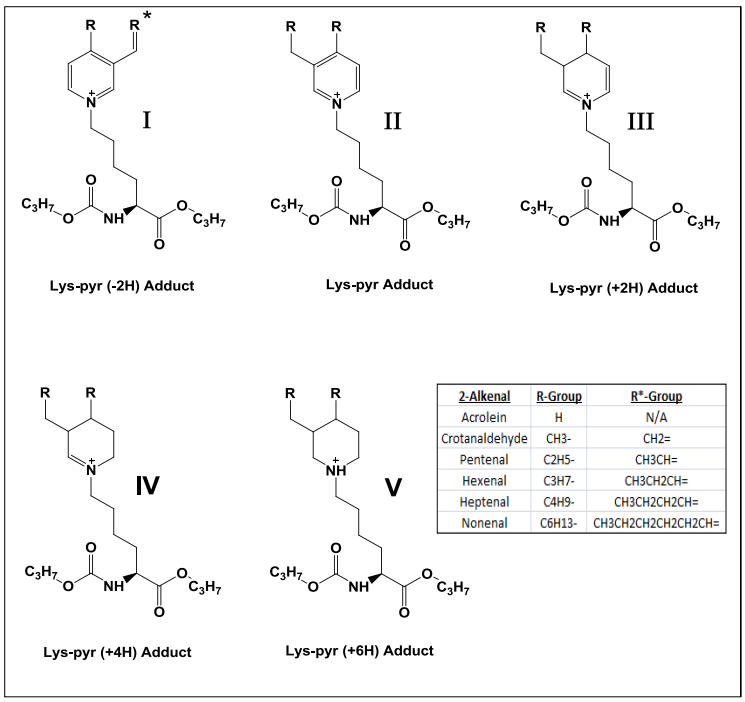

2-Alkenal	R-Group	R*-Group
Acrolein	H	N/A
Crotanaldehyde	CH3-	CH2=
Pentenal	C2H5-	CH3CH=
Hexenal	C3H7-	CH3CH2CH=
Heptenal	C4H9-	CH3CH2CH2CH=
Nonenal	C6H13-	CH3CH2CH2CH2CH2CH=

Figure 3.4: Possible chemical structures and formulae for different free forms of Lys-pyridinium adducts derivatised with propylchloroformate.

The complexity of the pyridinium adducts due to the varying degrees of reduction means that each Lys-pyridinium adduct has different reduced form; these forms are assigned as Lys-pyr (-2H) adduct (I), Lys-pyr adduct (II), Lys-pyr (+2H) adduct (III), Lys-pyr (+4H) adduct (IV), and Lys-pyr (+6H) adduct (V). Since the ring is being reduced at different positions, different isomers could be detected for each individual adduct after reduction step with $NaBH_4$. It is also possible that diastereoisomers can be formed as a result of 3 chiral centres: one chiral centre at the amino acid portion of the molecule and two chiral centres within pyridinium ring. The mass spectrometry results for pyridinium adducts which results from the reaction of 2-alkenals with different amino acids are summarized in Table 6-2 to Table 6-7. It is quite obvious from these tables that the retention time of the Lys-pyr adducts on C-18 column increases as the side chain of the 2-alkenal aldehyde increases. However, all the derivatised Lys-pyr adducts have less retention time as compared to the derivatised lysine, with the exception of the derivatised Hpn-pyr and Nne-pyr adducts which have a comparable retention time for derivatised lysine or even more. This can be justified as follow:

derivatised lysine consists of 3 attached derivatising moieties whereas reaction of the 2-alkenal with lysine in protein molecule will leave lysine with 2 available sites for derivatisation. Long chain 2-alkenal aldehyde will have enough lipophilicity comparable to the lipophilicity of the derivatising moiety or even more. Multiple chromatographic peaks could be detected for each Lys-pyr adduct, as reflected by multiple retention time, and could be justified by the multiple isomers; these isomers may result from different reduction site during reduction step with $NaBH_4$. Stereoisomers are available also due to the availability of the double bond inside the ring or in the side chain of the pyridinium adduct.

In order to investigate Baker's assumption [discussed in section 1.2.1.3] for pyridinium adduct formation, protein samples were incubated with 2-alkenal series and then subjected to acid hydrolysis without reduction with $NaBH_4$ (Table 6-8). In non-reduced protein samples, only the Lys-pyr (-2H) adduct (I) and the Lys-pyr adduct (II) could be detected with mass spectrometry, whereas other adducts could be detected with reduced protein samples only. A single reduction step can reduce any double bond inside the pyridinium adduct or the double bond in the alkyl side chain. It wa noticeable that the multiple peaks pattern disappeared with non-reduced samples which confirmed that the multiple peaks pattern was a result of different reduction sites for each Lys-pyr adduct.

3.2.3 Formyl-Dehydro-Piperidino (FDP) Adducts Formation

Formyl-dehydropiperidino adducts (FDP) represent another form of adduct that could be detected as a result of lysine residue modification. Figure 3.5 shows different reduction steps for the Lys-FDP adduct, which were suggested by Ichihashi *et al.* [section 1.2.1.4]. Different forms of the Lys-FDP adduct are expected as a result of different reduction level with $NaBH_4$, such as Lys-FDP (non-reduced form), Lys-FDP (+2H), and finally Lys-FDP (+4H) adduct. Furthermore, it should be noticed that the non-reduced Lys-FDP adduct contains a peripheral aldehyde group that is reduced to the corresponding primary alcohol group during reduction with $NaBH_4$. Reduction step with

$NaBH_4$ can result in the formation of different isomers and this explains the multiple peaks that appear in the chromatograms in some cases.

Different forms of Lys-FDP could be extracted from the protein hydrolysate and derivatised with propylchloroformate using the EZ:faast method, described previously, to get the derivatised Lys-FDP adducts (Figure 3.6). Table 3-4 summarizes the expected m/z for different ionised and reduced Lys-FDP adducts, whereas Table 3-5 & Table 3-6 show the mass spectrometry results for the derivatised and ionised Lys-FDP (+2H) and Lys-FDP (+4H) adducts, respectively. Although Lys-FDP (+4H) could be detected in protein samples incubated with 2-alkenals, these adducts showed a very low intensity as compared to Lys-FDP (+2H) and were undetectable in other cases.

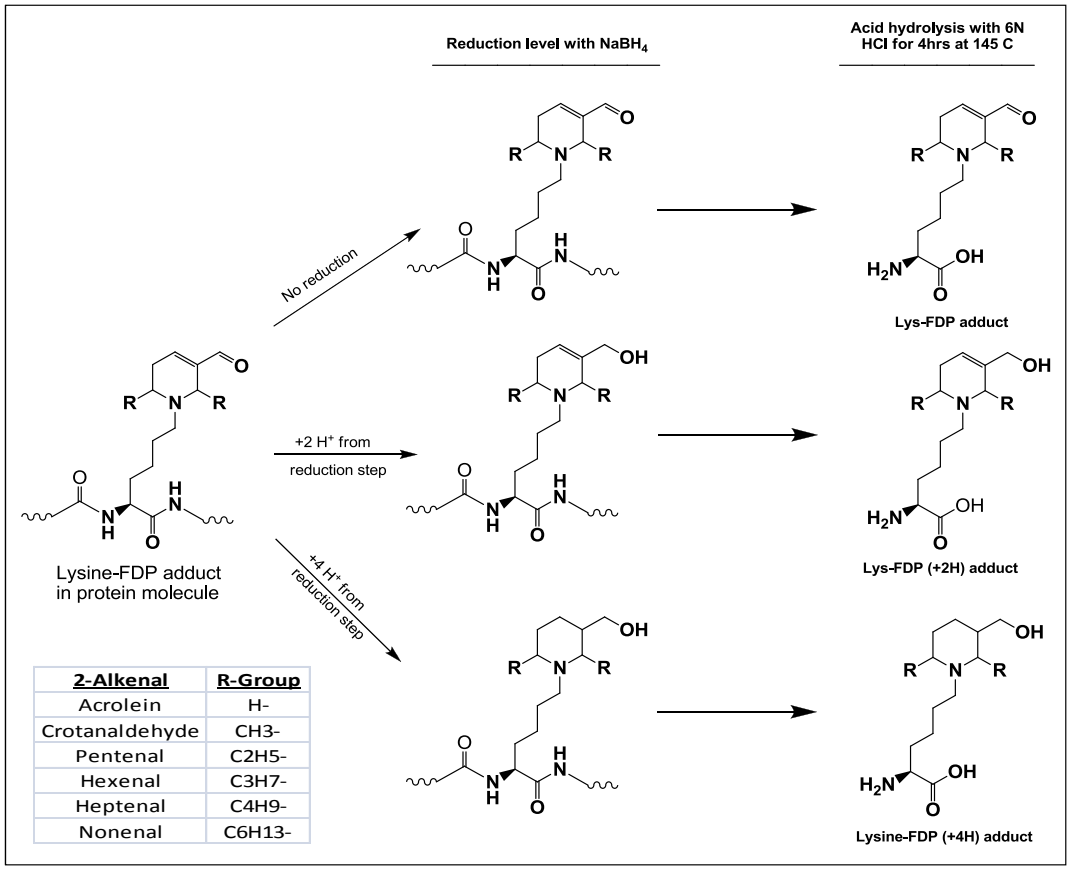

2-Alkenal	R-Group
Acrolein	H-
Crotanaldehyde	CH3-
Pentenal	C2H5-
Hexenal	C3H7-
Heptenal	C4H9-
Nonenal	C6H13-

Figure 3.5: Different reduction steps for lysine-FDP adduc; acid hydrolysis with 6N HCl lead to the formation of the free form of these adducts.

2-Alkenal	R-Group
Acrolein	H-
Crotanaldehyde	CH3-
Pentenal	C2H5-
Hexenal	C3H7-
Heptenal	C4H9-
Nonenal	C6H13-

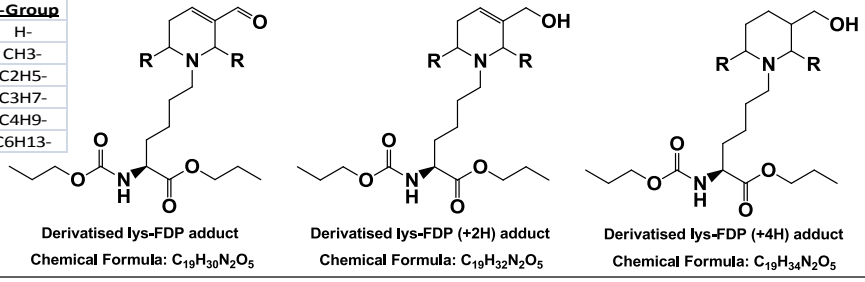

Figure 3.6: Proposed chemical structures for Lys-FDP adducts derivatised with propylchloroformate using the EZ:faast method.

Table 3-4: Expected masses for the derivatised free Lys-FDP adducts which result by incubating protein samples with different 2-alkenals when RPLC coupled to ESI-FTMS is used for detection.

2-ALKENAL	*Ionised Lys-FDP adduct*	*Ionised Lys-FDP (+2H) Adduct*	*Ionised Lys-FDP (+4H) Adduct*
ACROLEIN	**369**	**371**	**373**
CROTANALDEHYDE	**397**	**399**	**401**
2-PENTENAL	**325**	**427**	**429**
2-HEXENAL	**453**	**455**	**457**
2-HEPTENAL	**481**	**483**	**485**
2-NONENAL	**537**	**539**	**541**

Table 3-5: Mass spectrometry results for ionised lysine-FDP (+2H) adduct which have been incubated with different 2-alkenal aldehydes (using RPLC coupled to ESI-FTMS).

Adduct	*Type of Adduct*	*Elemental formula*	*RDB*	*R_t (min)*	*m/z*	*Delta ppm*
Lysine	***Lysine a.a.***	**$C_{17}H_{33}O_6N_2$**	**2.5**	**7.89 min**	**361.2324**	**-1.557**
Acr-FDP-371	***Lys-FDP (+2H)***	**$C_{19}H_{35}O_5N_2$**	**3.5**	**2.76 min**	**371.25339**	**-1.775**
Cro-FDP-399	***Lys-FDP (+2H)***	**$C_{21}H_{39}O_5N_2$**	**3.5**	**2.98 min**	**399.2847**	**-1.625**
Pne-FDP-427	***Lys-FDP (+2H)***	**$C_{23}H_{43}O_5N_2$**	**3.5**	**3.14 min**	**427.31653**	**-0.278**
Hxe-FDP-455	***Lys-FDP (+2H)***	**$C_{25}H47O_5N_2$**	**3.5**	**4.05, 4.61 min**	**455.34772**	**-0.505**
Hpe-FDP-483	***Lys-FDP (+2H)***	**$C_{27}H_{51}O_5N_2$**	**3.5**	**5.24, 6.36, 7.26, 9.32min**	**483.37881**	**-1.159**
Non-FDP-539	***Lys-FDP (+2H)***	**$C_{31}H_{59}O_5N_2$**	**3.5**	**11.19, 11.50, 12.18, 13.29min**	**539.44177**	**-0.548**

Table 3-6: Mass spectrometry results for ionised lysine-FDP (+4H) adduct which have been incubated with different 2-alkenal aldehydes (using RPLC coupled to ESI-FTMS).

Adduct	*Type of Adduct*	*Elemental formula*	*RDB*	*R_t (min)*	*m/z*	*Delta ppm*
Lysine	***Lysine a.a.***	**$C_{17}H_{33}O_6N_2$**	**2.5**	**7.89 min**	**361.2324**	**-1.557**
Acr-FDP-373	***Lys-FDP (+4H)***	**$C_{19}H_{37}O_5N_2$**	**3.5**	**2.84 min**	**373.26974**	**0.110**
Cro-FDP-401	***Lys-FDP (+4H)***	**$C_{21}H_{41}O_5N_2$**	**3.5**	**3.05, 3.25 min**	**401.30188**	**0.451**
Pne-FDP-429	***Lys-FDP (+4H)***	**$C_{23}H_{45}O_5N_2$**	**3.5**	**3.61, 4.14 min**	**429.36224**	**-0.137**
Hxe-FDP-457	***Lys-FDP (+4H)***	**$C_{25}H_{49}O_5N_2$**	**3.5**	**3.97, 4.55, 5.49 min**	**457.36279**	**-1.771**
Hpe-FDP-485	***Lys-FDP (+4H)***	**$C_{27}H_{53}O_5N_2$**	**3.5**	**5.75, 6.42, 7.62, 8.1 min**	**485.39456**	**-0.700**
Non-FDP-541	***Lys-FDP (+4H)***	**$C_{31}H_{61}O_5N_2$**	**3.5**	**11.83, 12.28, 12.95, 13.45, 14.48, 15.32 min**	**541.45813**	**1.164**

The Lys-FDP adducts could be detected in hydrolysed protein samples without reduction, furthermore Lys-FDP adducts -2H, -4H, and -6H could also be detected. In order to confirm the presence of these adducts, HSA was reacted with 2-alkenals and then hydrolysis was carried out without the reduction step with sodium borohydride, as Lys-FDP and Lys-pyridinium adducts are stable to hydrolysis. The result for these samples confirmed that normal FDP adducts and FDP adducts (-2H, -4H, and -6H) were present in these samples. This gives an indication that FDP adducts might be converted to a pyridinium ring (Figure 6.8).

3.3 Reaction of 2-Alkenals with Arginine Residues

Although Baker *et al.* (1999) [29] could not report any modification for arginine residues when a protein sample was incubated with 2-hexenal, our research results contradict his findings. Logically, arginine residue in protein molecule should be more reactive than lysine residues towards the aldehyde group of the 2-alkenal series, and more complex modifications should be expected than that for lysine amino acid. The guanidine group in the arginine residue consists of 2 reactive amine groups: primary and secondary amines. The primary amine group could be the target for Schiff base and Michael addition reactions with 2-alkenals, whereas the secondary amine group in the arginine residue can provide a reactive site for Michael addition reaction only. Nevertheless, only 2 types of arginine adducts (Schiff base and Michael adduct) could be detected by *in vitro* modification of arginine residues with the 2-alkenal series by overnight incubation (Figure 3.7). Figure 3.8 shows the expected chemical structure for the derivatised arginine Schiff base and Michael adduct after being reduced and hydrolysed with 6N HCl.

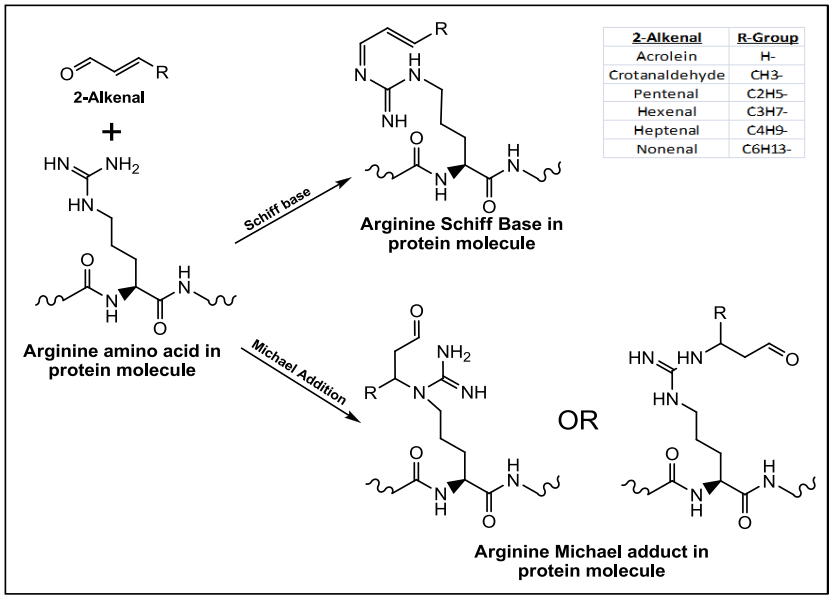

2-Alkenal	R-Group
Acrolein	H-
Crotanaldehyde	CH3-
Pentenal	C2H5-
Hexenal	C3H7-
Heptenal	C4H9-
Nonenal	C6H13-

Figure 3.7: Mechanism for Schiff base and Michael adduct formation as a result of arginine residue modification with the 2-alkenal series in a protein molecule.

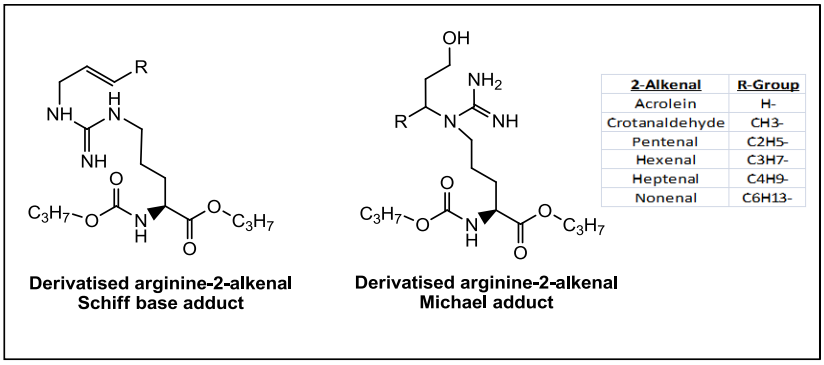

2-Alkenal	R-Group
Acrolein	H-
Crotanaldehyde	CH3-
Pentenal	C2H5-
Hexenal	C3H7-
Heptenal	C4H9-
Nonenal	C6H13-

Figure 3.8: Derivatised arginine Schiff base and Michael adducts after reduction, acid hydrolysis and derivatisation steps.

The possibility of imine group reduction during the reduction step with $NaBH_4$ had been investigated. Therefore, the possibility of arginine reduction with 4 H atoms instead of 2 H atoms being acquired during reduction step had been examined. None of the arginine or any of its adduct (Schiff base or Michael adduct) which had been fully reduced could be detected; this indicates that imine group is not susceptible for reduction during $NaBH_4$ reduction step. The mass spectrometry results for the expected chemical formula, the observed masses and retention time for derivatised arginine Schiff base adducts and Michael adducts are summarized in Table 3-7 & Table 3-8, respectively.

Table 3-7: Chemical formulae and mass spectrometry results for the derivatised 2-alkenal-arginine-Schiff bases using RPLC coupled to ESI-FTMS. The retention time for the derivatised arginine is 2.71 min on C-18 column.

Adduct	*Type of Adduct*	*Elemental formula*	*RDB*	*R_t (min)*	*m/z*	*Delta ppm*
Acr-Arg	**Arg-Schiff base**	**$C_{16}H_{31}N_4O_4$**	**3.5**	**2.8 min**	**343.23389**	**-0.268**
Cro-Arg	**Arg-Schiff base**	**$C_{17}H_{33}N_4O_4$**	**3.5**	**3.12 min**	**357.24973**	**0.273**
Pne-Arg	**Arg-Schiff base**	**$C_{18}H_{35}N_4O_4$**	**3.5**	**3.33 min**	**371.26486**	**-1.138**
Hxe-Arg	**Arg-Schiff base**	**$C_{19}H_{37}N_4O_4$**	**3.5**	**3.70 min**	**385.28055**	**-0.993**
Hpe-Arg	**Arg-Schiff base**	**$C_{20}H_{39}N_4O_4$**	**3.5**	**4.64 min**	**399.29602**	**-1.409**
Nne-Arg	**Arg-Schiff base**	**$C_{22}H_{43}N_4O_4$**	**3.5**	**7.34, 7.70 min**	**427.32663**	**-2.932**

Table 3-8: Chemical formulae and mass spectrometry results for the derivatised 2-alkenal-arginine-Michael adducts using RPLC coupled to ESI-FTMS. The retention time for the derivatised arginine is 2.71 min on C-18 column.

Adduct	*Type of Adduct*	*Elemental formula*	*RDB*	*R_t (min)*	*m/z*	*Delta ppm*
Acr-Arg	**Arg-Michael adduct**	**$C_{16}H_{33}N_4O_5$**	**2.5**	**2.67 min**	**361.24405**	**-1.375**
Cro-Arg	**Arg-Michael adduct**	**$C_{17}H_{35}N_4O_5$**	**2.5**	**2.78 min**	**375.26065**	**1.207**
Pne-Arg	**Arg-Michael adduct**	**$C_{18}H_{37}N_4O_5$**	**2.5**	**3.24 min**	**389.276**	**0.393**
Hxe-Arg	**Arg-Michael adduct**	**$C_{19}H_{39}N_4O_5$**	**2.5**	**3.44 min**	**403.2912**	**-0.737**
Hpe-Arg	**Arg-Michael adduct**	**$C_{20}H_{41}N_4O_5$**	**2.5**	**4.03 min**	**417.30713**	**-0.042**
Nne-Arg	**Arg-Michael adduct**	**$C_{22}H_{45}N_4O_5$**	**2.5**	**6.52 min**	**445.33865**	**0.455**

The retention times for arginine Schiff base and Michael adducts range between 2.78 and 7.7 min which is as expected for RPLC separation on the C-18 column, and the deviation of the observed mass was less than 3ppm which was close enough to confirm the identity of the compounds. Although it has been reported by many studies [65, 136, 137] that acrolein aldehyde is the most reactive 2-alkenal, the acrolein adducts for arginine amino acids could not be detected in some samples. The high reactivity of acrolein aldehyde may result in the formation of more complex modifications with arginine residue, or between arginine residues and other amino acid residues of the protein molecules. Insufficient information about the nature of these modifications represents the biggest obstacle in the detection of such complex adducts. It is noticeable that the 2-nonenal Schiff base adduct with arginine has two peaks which gives some evidence for the formation of different isomers for the Nne-Arg Schiff base (Figure 3.9). The identity of the first peak at R_t= 7.34 min was confirmed by the mass deviation (less than 3ppm) and the ^{13}C peaks were identical for the simulated mass (Figure 3.10).

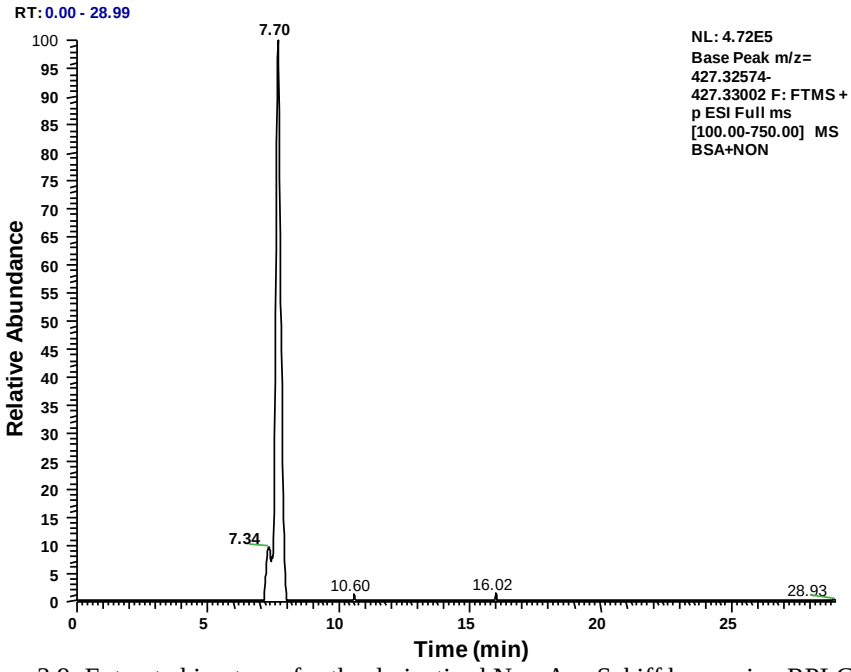

Figure 3.9: Extracted ion trace for the derivatised Nne-Arg-Schiff base using RPLC coupled to ESI-FTMS.

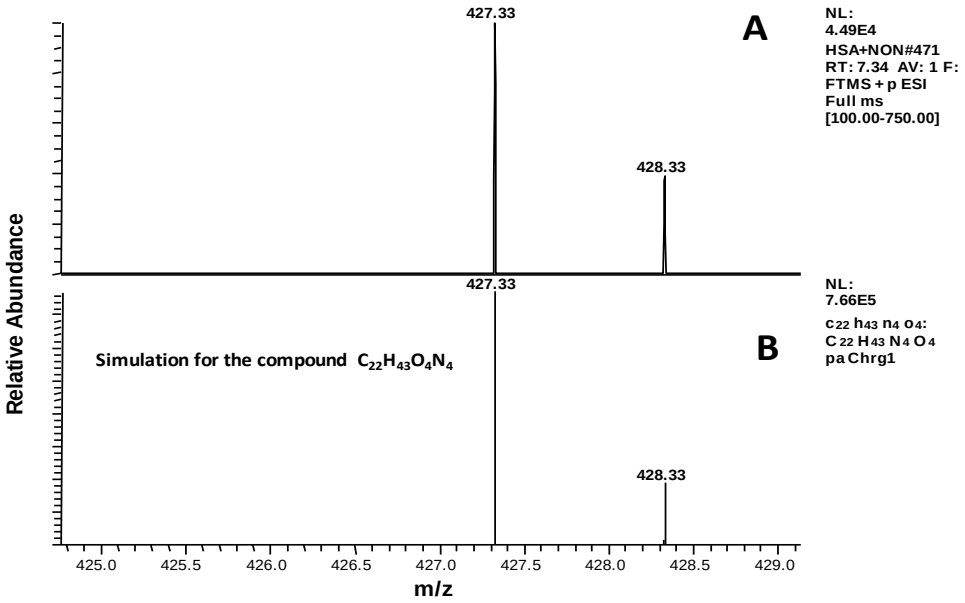

Figure 3.10: High resolution mass spectra for the derivatised Nne-Arg Schiff base using RPLC coupled to ESI-FTMS. The upper figure (A) represents the mass spectra from the first peak at 7.34 min, while the lower figure (B) represents the simulation for the compound Nne-Arg Schiff base with ^{13}C peak.

A cyclisation process can be proposed in order to justify the second peak appearing in the analysis of the Nne-Arg Schiff base (Figure 6.9). The proposed cyclisation process involves conversion of the Schiff base to another cyclic adduct by a further Michael addition reaction, whereas arginine Michael adduct would convert to the cyclic adduct by a further Schiff base reaction. Reduction step with $NaBH_4$ can reduce the double bond inside the tetra-hydropyrimidine ring of the cyclic adduct. Acid hydrolysis of the protein samples followed by derivatisation with propylchloroformate can result in the formation of 2 isomers (cyclic adduct I and II) with the same chemical formula as the Nne-Arg Schiff base. Ionization of these cyclic adducts by ESI of mass spectrometry can generate a second peak for Nne-Arg Schiff base with very low intensity. The same principle can be applied for other arginine-2-alkenal adducts, but due to poor separation by C-18 column, both Schiff base and cyclic adducts may elute in the same time.

3.4 Reaction of 2-Alkenal with Histidine Residues

Histidine residues in protein molecules represents another amino acid that can undergo modification by reactive aldehydes such as 2-alkenals. Figure 3.11 shows the chemical structure for a His-2-alkenal Michael adduct after being reduced, acid hydrolysed, and derivatised with propylchloroformate using the EZ:faast method described in section 2.4.1. ESI of the mass spectrometry will add 1 H^+ ion to the structure of the histidine Michael adducts so that they are detectable by MS. Table 3-9 shows the expected chemical formula and the retention time for different histidine Michael adducts, after derivatisation with propylchloroformate. Also it shows the deviation of the observed masses from the actual expected masses in ppm (all His-adducts could be detected with less than 1.4 ppm). Again, the retention time range for such adducts was 2.61-6.66 min, and the increase in the retention time was consistent with the increase in the lipophilicity of adducts as the hydrocarbon moiety of the 2-alkenal increases from acrolein to nonenal.

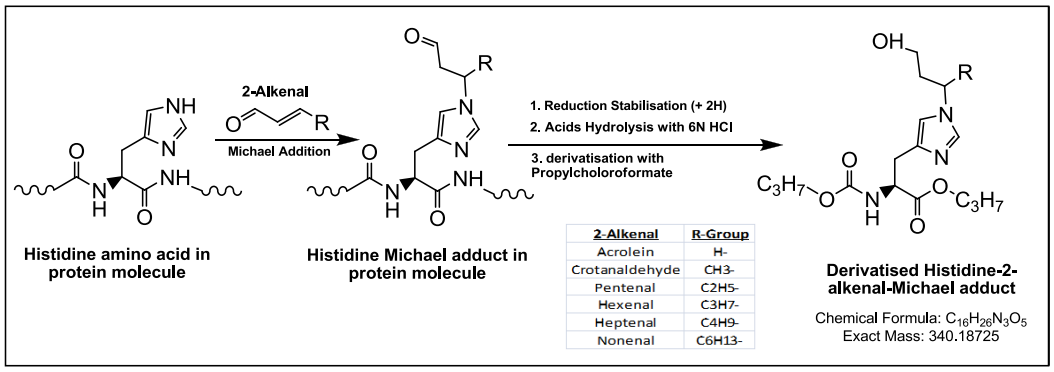

Figure 3.11: Reaction of highly reactive aldehydes from 2-alkenal series with histidine amino acid residue through Michael addition reaction. Reduction stabilisation, acid hydrolysis and derivatisation process can result in the formation of the derivatised His-2-alkenal Michale adduct.

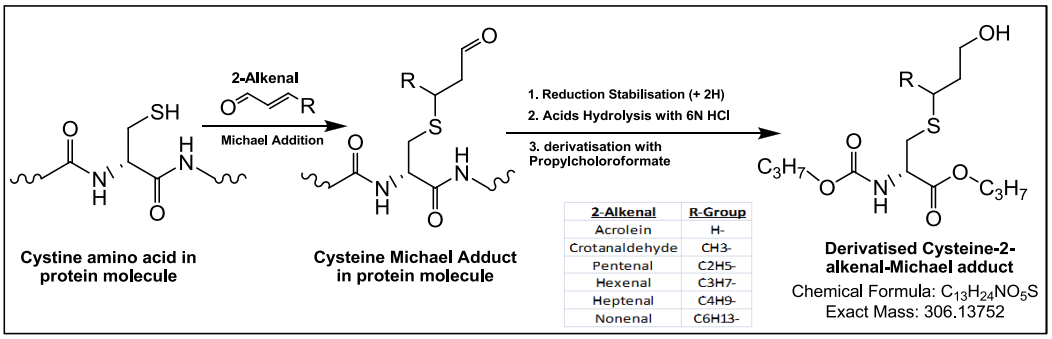

Figure 3.12: Reaction of highly reactive aldehydes from 2-alkenal series with cysteine amino acid residue through Michael addition reaction. Reduction stabilisation, acid hydrolysis and derivatisation process can result in the formation of the derivatised Cys-2-alkenal Michale adduct.

Table 3-9: Chemical formulae and mass spectrometry results for the derivatised 2-alkenal-His-Michael adducts using RPLC coupled to ESI-FTMS. The retention time for the derivatised histidine is 7.01 and 9.01 min on C-18 column.

Adduct	*Type of Adduct*	*Elemental formula*	*RDB*	*R_t (min)*	*m/z*	*Delta ppm*
Acr-His	**His-Michael adduct**	**$C_{16}H_{28}N_3O_5$**	**4.5**	**2.61 min**	**342.20187**	**-1.396**
Cro-His	**His-Michael adduct**	**$C_{17}H_{30}N_3O_5$**	**4.5**	**3.83 min**	**356.21777**	**-0.64**
Pne-His	**His-Michael adduct**	**$C_{18}H_{32}N_3O_5$**	**4.5**	**3.03 min**	**370.2338**	**0.411**
Hxe-His	**His-Michael adduct**	**$C_{19}H_{34}N_3O_5$**	**4.5**	**3.12 min**	**384.24918**	**-0.307**
Hpe-His	**His-Michael adduct**	**$C_{20}H_{36}N_3O_5$**	**4.5**	**3.58 min**	**398.26465**	**-0.749**
Nne-His	**His-Michael adduct**	**$C_{22}H_{40}N_3O_5$**	**4.5**	**6.66 min**	**426.29617**	**-0.184**

Table 3-10: The expected chemical formulas and masses for the derivatised 2-alkenal-Cys-Michael adducts when RPLC is coupled to ESI-FTMS.

Adduct	*Type of Adduct*	*Expected Elemental formula*	*Expected m/z*
Acr-Cys	**His-Michael adduct**	**$C_{13}H_{26}N_1O_5S_1$**	**308.15262**
Cro-Cys	**His-Michael adduct**	**$C_{14}H_{28}N_1O_5S_1$**	**322.16827**
Pne-Cys	**His-Michael adduct**	**$C_{15}H_{30}N_1O_5S_1$**	**336.18392**
Hxe-Cys	**His-Michael adduct**	**$C_{16}H_{32}N_1O_5S_1$**	**350.19957**
Hpe-Cys	**His-Michael adduct**	**$C_{17}H_{34}N_1O_5S_1$**	**364.21522**
Nne-Cys	**His-Michael adduct**	**$C_{19}H_{38}N_1O_5S_1$**	**392.24652**

3.5 Reaction of 2-Alkenals with Cysteine Residues

Cysteine amino acid was also examined as a possible target for modification with 2-alkenals, as it contains sulfhydryl group within its structure which can behave in the same way as secondary amine group. The sulfhydryl group of the cysteine residue can undergo a Michael addition reaction when the protein samples incubated with 2-alkenals. Figure 3.12 shows the chemical structure for cysteine Michael adducts modified with different 2-alkenals after reduction, acid hydrolysis and then derivatisation with propylchloroformate. Table 3-10 shows the expected chemical formula and masses for derivatised cysteine Michael adducts after ionization in the MS source. None of the expected cysteine adducts could be detected in the hydrolysate of the protein samples, and this can be attributed to the harsh condition of the acid hydrolysis process with 6N HCl that leads to the distraction of the cysteine amino acids or due to conversion to cystic acid during acid hydrolysis [section 1.3.3].

3.6 Analysis of the Reaction Products between 4-Hydroxy-2-Nonenal (HNE) and Amino Acids Residues Using EZ:faast Method in Combination with RPLC-FTMS

The lipid peroxidation process can result in the formation of a variety of endogenously toxic aldehydes such as 2-alkenals [138] and 4-hydroxy-2-alkenals [33, 139, 140]. Due to its high availability as compared to other 4-hydroxy-2-alkenals, HNE is considered as the most toxic member of this group [140-142]. Sample preparation was carried out according to the procedure described in section 2.3. Reactions of HNE with different amino acids such as lysine, arginine, histidine, and cysteine have been discussed in detail in section 1.2.2. A reduction step with $NaBH_4$ prior to acid hydrolysis of protein samples is expected to reduce one double bond in the Schiff base, while conversion of the aldehyde group in the Michael and hemiacetal adduct to the corresponding alcohol group is also expected. Figure 3.13 shows the expected chemical structures, formulae and theoretical masses for different HNE adducts after reduction, hydrolysis, derivatisation with propylchloroformate, and finally ionization by ESI.

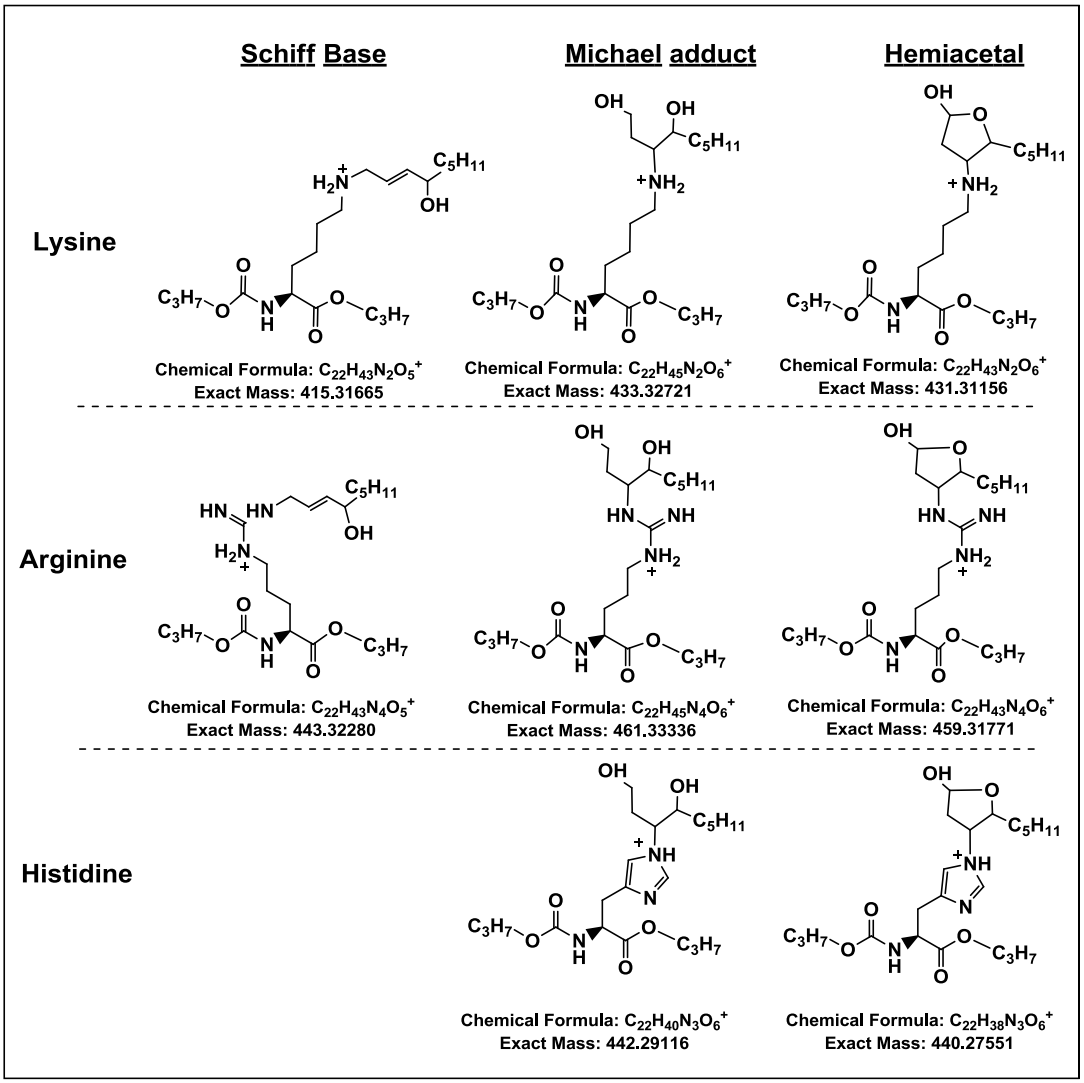

Figure 3.13: The expected chemical structure, formula, and theoretical mass for the derivatised HNE adducts for lysine, arginine, and histidine amino acids after reduction, acid hydrolysis and derivatisation processes.

Table 3-11 shows the mass spectrometry results for the derivatised HNE adducts for lysine, arginine, and histidine amino acids, respectively. All adducts matched the expected elemental composition within 3 ppm. The cysteine adduct could not be detected. The retention time for HNE adducts ranged between 4 min and 6 min, irrespective of the retention time of the corresponding amino acid.

Table 3-11: Mass spectrometry results for different HNE adducts which had been derivatised with propylchloroformate reagent and detected by using RPLC coupled to ESI-FTMS. N=3.

Adduct	*Type of adduct*	*Elemental formula*	*R_t (min)*	*Observed mass (m/z)*	*Delta ppm*	*Intensity*
Lysine	**Amino Acid**	$C_{17}H_{33}O_6N_2$	**7.04 min**	**361.234**	**1.844**	**2.71E+07**
Lys-HNE	**Schiff base**	$C_{22}H_{43}N_2O_5$	**4.67 min**	**415.3176**	**2.146**	**4.14E+06**
			5.06 min	**415.3176**	**2.362**	
	Michael addition	$C_{22}H_{45}N_2O_6$	**4.30 min**	**433.3282**	**2.252**	**1.77E+05**
	Hemiacetal	$C_{22}H_{43}N_2O_6$	**N/A**	**N/A**	**N/A**	**N/A**
Adduct	***Type of adduct***	***Elemental formula***	***R_t (min)***	***Observed mass (m/z)***	***Delta ppm***	***Intensity***
Arginine	**Amino Acid**	$C_{13}H_{27}O_4N_4$	**2.71 min**	**303.2035**	**2.698**	**2.66E+06**
Arginine-HNE	**Schiff base**	$C_{22}H_{43}N_4O_5$	**4.92 min**	**443.3238**	**2.240**	**1.64E+05**
			5.15 min	**443.32382**	**2.308**	
			5.42 min	**443.324**	**2.646**	
	Michael addition	$C_{22}H_{45}N_4O_6$	**N/A**	**N/A**	**N/A**	**N/A**
	Hemiacetal	$C_{22}H_{43}N_4O_6$	**N/A**	**N/A**	**N/A**	**N/A**
Adduct	***Type of adduct***	***Elemental formula***	***R_t (min)***	***Observed mass (m/z)***	***Delta ppm***	***Intensity***
Histidine	**Amino Acid**	$C_{17}H_{28}O_6N_3$	**7.01, 9.01 min**	**370.198**	**1.994**	**4.75E+05**
His-HNE	**Michael addition**	$C_{22}H_{40}N_3O_6$	**4.19 min**	**442.2921**	**2.005**	**3.36E+06**
	Hemiacetal	$C_{22}H_{38}N_3O_6$	**N/A**	**N/A**	**N/A**	**N/A**

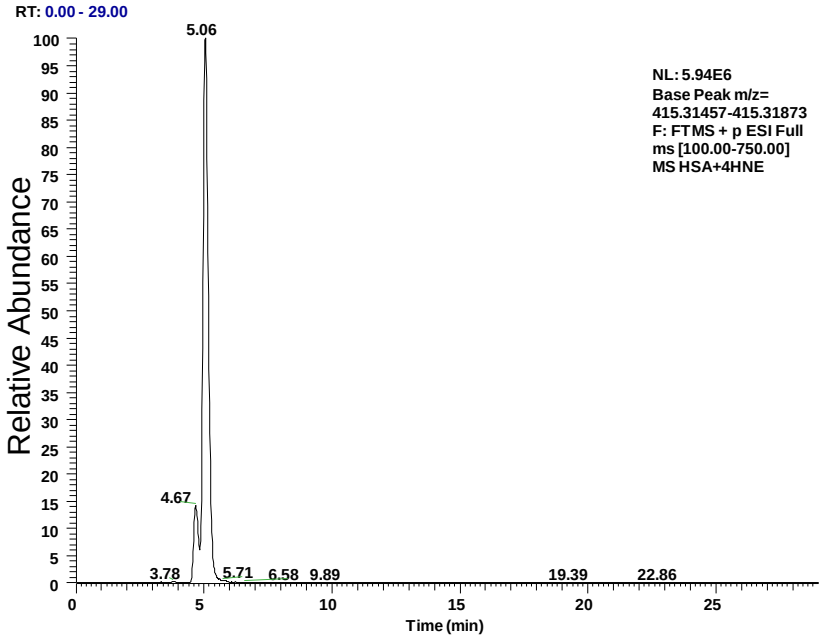

Figure 3.14: Extracted ion chromatogram for the derivatised lysine-HNE Schiff base adduct (m/z=415) using RPLC coupled to ESI-FTMS.

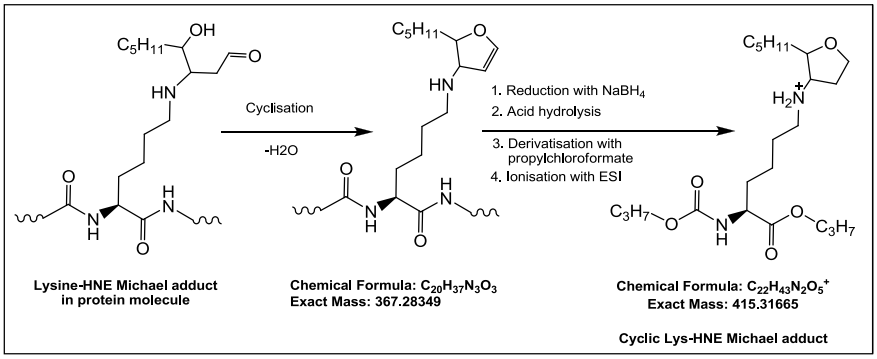

Figure 3.15: Proposed mechanism for the formation of cyclic compound from Lys-HNE Michael adduct which match the chemical formula for Lys-HNE Schiff base.

Mass spectrometry results for the derivatised HNE-lysine and HNE-arginine Schiff bases indicate multiple peaks; the HNE moiety contains a chiral centre, thus at least 2 diastereoisomers are expected due to the availability of 2 chiral centres in the HNE-Arg-Schiff base molecule. Figure 3.14 shows two peaks for the derivatised Lys-HNE Schiff base, one peak at R_t=4.67 and the other at 5.06 min. Both peaks match the theoretical formula for the Lys-HNE Schiff base with little deviation (less than 2.3ppm).

Another mechanism for the formation of the cyclic compounds from Michael adduct has been suggested by Sayre *et al.* (Figure 3.15) [143]. According to this mechanism, the Michael adducts undergo a cyclisation process by losing a water molecule, and the new compound will have the same chemical formula as the derivatised Lys-HNE Schiff base ($C_{22}H_{43}N_2O_5$=415 m/z) after reduction stabilisation of the protein sample with $NaBH_4$, acid hydrolysis and derivatisation with propylchloroformate.

MS^2 fragmentation was carried out to confirm the identity of the 2 peaks; Figure 3.16 shows the MS^2 spectrum for the Lys-HNE Schiff base. The fragmentation of Lys-HNE Schiff base follows the same pattern for the 2 peaks, with the exception of the fragment at m/z 385 at the first peak (R_t =4.88 min from the chromatogram of the MS^2). This peak can be explained by tetrahydrofuran ring opening of the cyclic compound and losing of CH_2O molecule from the tetrahydrofuran ring, and this supports the proposed mechanism for the conversion of the Michael adduct to the cyclic compound through water molecule loss rather than hemiacetal formation, or hemiacetal formation could be

considered as a transitional state for the formation of the cyclic compound. Other fragments will be explained in detail in section 3.6.1.

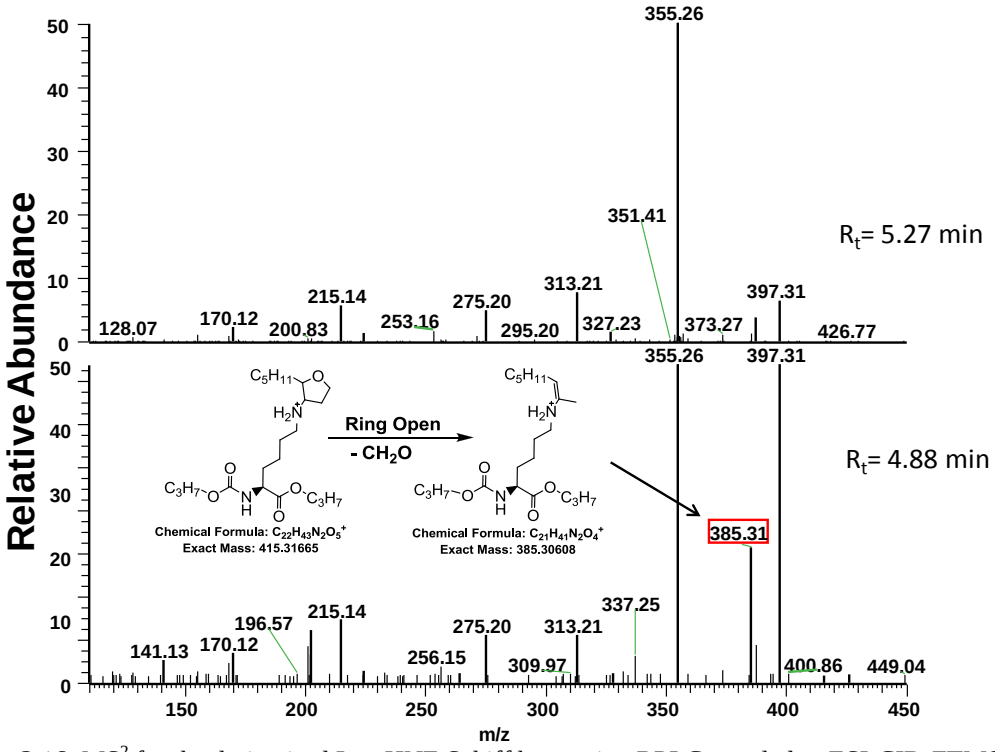

Figure 3.16: MS^2 for the derivatised Lys-HNE Schiff base using RPLC coupled to ESI-CID-FTMS/MS.

The same proposition can be made for the 3 peaks for arginine-HNE Schiff base, 2 peaks belong to the cyclic compounds as there are 2 possible sites for Michael addition reactions with arginine amino acid; the third peak belongs to Schiff base. The complete disappearance of the Arg-HNE Michael adduct and the appearance of 3 peaks for the Schiff base support cyclisation with the proposed mechanism.

The reaction between 2 amino acids and HNE was detected by high resolution mass spectrometry. Table 3-18 shows the chemical formulae and the expected theoretical masses for the HNE attached to 2 molecules of lysine amino acids, and the HNE attached to histidine and lysine amino acids [section 1.2.2.5]. The observed masses match the theoretical proposed masses with only a small deviation, of around 2 ppm. Low intensity for such adducts suggests the low possibility of the formation of such

adducts. The identity of these adducts was examined using MS^2 fragmentation, as will be discussed in section 3.6.1. Finally, none of the HNE-arginine 2-pentapyrrol adducts suggested by Isom *et al.* [46] could be detected throughout this research project, as well as none of the hemiacetal adducts could be detected.

Table 3-12: Accurate masses for derivatised HNE adducts formed between 2 amino acid residues using RPLC coupled to ESI-FTMS. N=3.

Adduct	*Type of adduct*	*Elemental formula*	*R_t (min)*	*m/z*	*Delta ppm*	*Intensity*
Lys-HNE-Lys	**Lys+4HNE+Lys**	**$C_{35}H_{69}N_4O_9$**	**5.93 min**	**689.5075**	**2.238**	**7.88E+04**
His-HNE-Lys	**His+4HNE+Lys**	**$C_{35}H_{64}N_5O_9$**	**6.02 min**	**698.4713**	**1.996**	**8.08E+04**
			6.24 min	**698.4708**	**1.394**	**1.34E+05**

3.6.1 Structure Elucidation for HNE Adducts Using Mass Spectrometry

The structures of the HNE adducts with lysine, histidine and arginine were further characterized by carrying out fragmentation using ESI-FTMS/MS. MS^2 analysis for the derivatised HNE adducts was performed in the positive polarity using CID (35%) as fragmentation energy. The mass range was set between 110 m/z and 450 m/z in order to identify the possible fragments in this range, and an isolation width window for the precursor ion set at 1 amu (±0.5 amu).

MS^2 analysis for the derivatised arginine-HNE Schiff base with a mass of m/z 443.23 was performed in the positive polarity. Figure 3.17 shows the MS/MS chromatogram for the analysis of the derivatised arginine-HNE Schiff base, and it shows 2 peaks for the extracted adduct in the MS^2 analysis which have the same retention time as the precursor adducts. Figure 3.18 shows the corresponding MS^2 spectrum generated from Arg-HNE Schiff base precursor ion and both peaks show the same fragments. Repeated samples show the same fragmentation pattern for the same precursor ion as most fragments could be detected at m/z 425, 401, 383, 355, 341 and 285.

Scheme 3-1 is proposed to explain the different pathways for the formation of the product ions from the derivatised Arg-HNE Schiff base precursor ion, and it consists of 2 pathways. Pathway (I) consists of 3 subsequent steps. The first step starts by the loss

of a H_2O molecule (18 amu), whereas the second and third steps consist of losing a propylene molecule (CH_3-CH=CH_2, 42 amu) each. The three steps in the pathway (I) result in the formation of the product ions at m/z 425, 383, and 341 respectively. Obviously, formation of the product ion at m/z 383 by subsequent loss of water and propylene molecules is more abundant than other fragments (m/z 425 & 341) of this pathway (Figure 3.18).

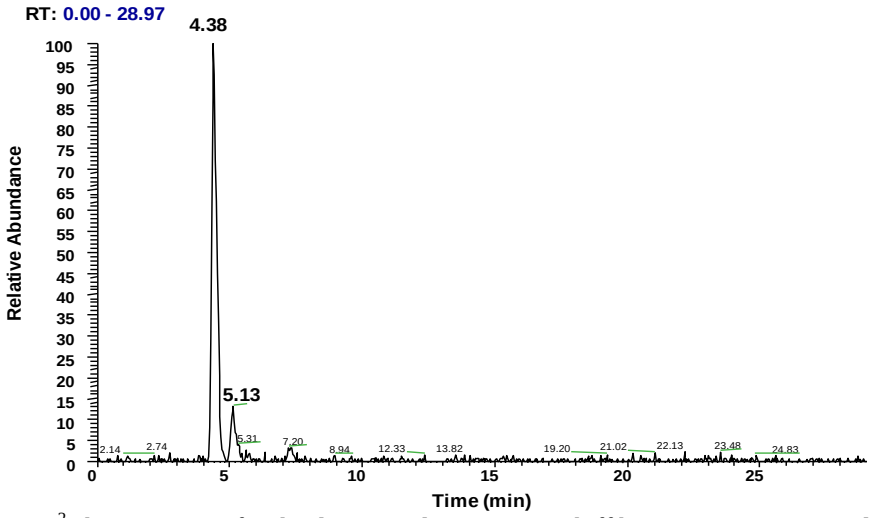

Figure 3.17: MS^2 chromatogram for the derivatised Arg-HNE Schiff base using RPLC coupled to ESI-CID-FTMS/MS.

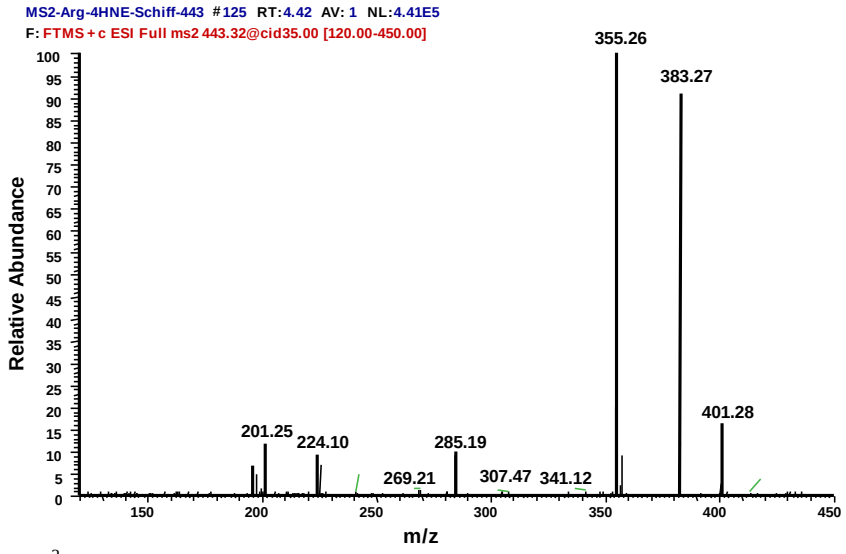

Figure 3.18: MS^2 spectrum for the derivatised Arg-HNE Schiff base using RPLC coupled to ESI-CID-FTMS/MS.

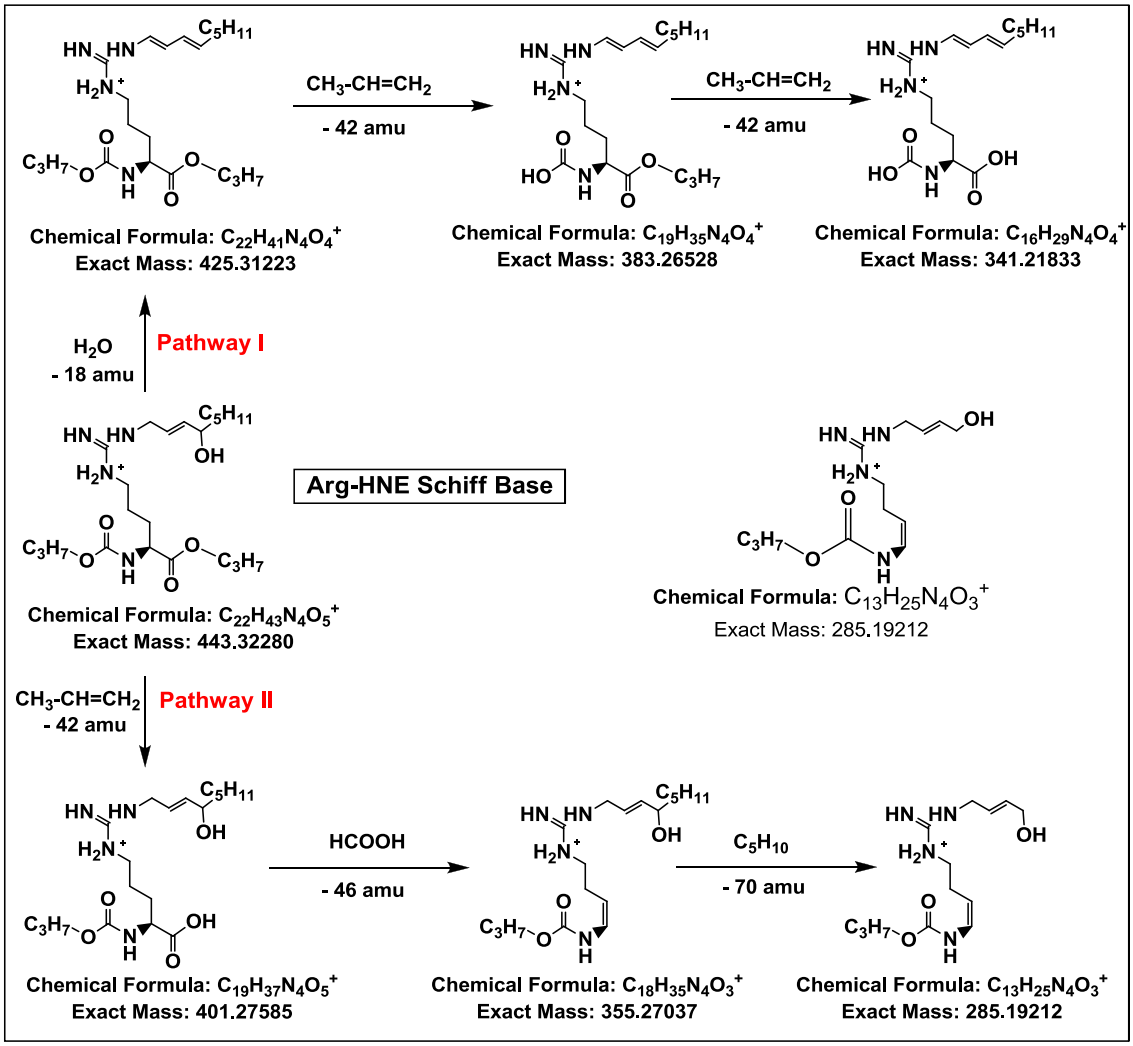

Scheme 3-1: Fragmentation pathways for the derivatised Arg-HNE Schiff base using RPLC coupled to ESI-CID-FTMS/MS.

Pathway (II) proposed in Scheme 3-1 consists of 3 subsequent steps. The first step in the pathway results in the formation of the product ion at m/z 401 by the loss of a propylene molecule (CH_3-CH=CH_2, 42 amu) from the derivatised Arg-HNE Schiff base precursor ion. The second step results in the formation of the product ion at m/z 355 with a dominant peak in the MS^2 spectra by the loss of a HCOOH molecule (46 amu) from the product ion generated at the first step of the same pathway. Low abundance product ion at m/z 285 will be generated in step 3 of the same pathway by further fragmentation of the product ion m/z 355 by the loss of pent-1-ene from the 4-HNE moiety.

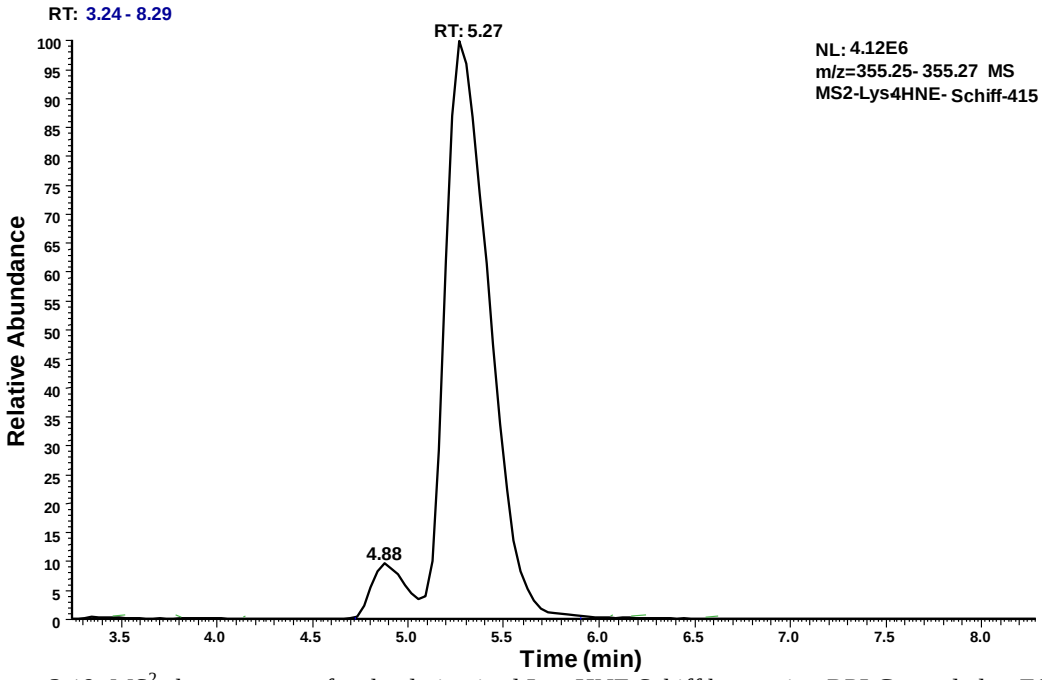

Figure 3.19: MS^2 chromatogram for the derivatised Lys-HNE Schiff base using RPLC coupled to ESI-CID-FTMS/MS.

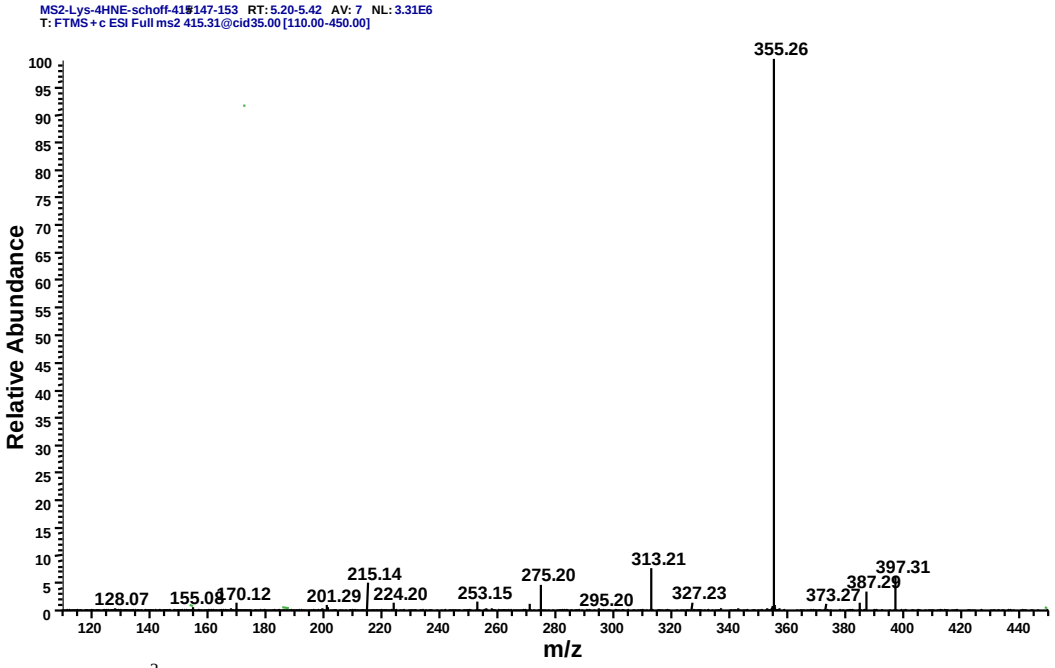

Figure 3.20: MS^2 spectrum for the derivatised Lys-HNE Schiff base using RPLC coupled to ESI-CID-FTMS/MS.

MS^2 analysis for the derivatised Lys-HNE Schiff base with a molecular ion at m/z 415.31 was performed in the positive polarity. The MS^2 chromatogram for the derivatised Lys-HNE Schiff base peak still showed the splitting pattern into 2 peaks (Figure 3.19). Figure 3.20 shows the corresponding MS^2 spectrum generated from the Lys-HNE Schiff base precursor ion. The same Fragments could be detected for both peaks at m/z 397, 387, 373, 355, 327, 313, 275, 224, 215, 170, and 128. Repeated samples shows the same fragmentation pattern.

Lys-HNE Schiff base adducts show the same fragmentation pattern as that which was proposed for Arg-HNE Schiff base. Most of the fragments result from the combination loss of water (H_2O, 18 amu), propylene (CH_3-CH=CH_2, 42 amu), formic acid (HCOOH, 46 amu), or HNE ($C_9H_{16}O_1$, 140 amu) molecule. A schematic pathway (Scheme 3-2) is proposed to explain different pathways for the formation of the product ions from the derivatised Lys-HNE Schiff base precursor ion, and it consists of 4 pathways.

Pathway (I & II) is quite similar to the pathways proposed in Scheme 3-1 for the derivatised Arg-HNE Schiff base, as pathway (I) consists of 3 consecutive steps starting by loss of a water molecule followed by loss of a propylene molecule over the following 2 steps. Product ions at m/z 397, 355 and 313 could be detected in the MS^2 spectrum of the derivatised Lys-HNE Schiff base can be explained by this pathway. Pathway (I) is the preferred fragmentation route for the Lys-HNE Schiff base; all the product ions generated by this route are the most dominant fragments (Figure 3.20).

Products ions at m/z 373, 327, and 224 may be generated through pathway (II) of the fragmentation pathway of HNE Schiff base with lysine. Loss of the propylene molecule followed by a formic acid molecule and finally loss of the propyl carbamate could lead to the product ions at m/z 373, 327, and 224 respectively.

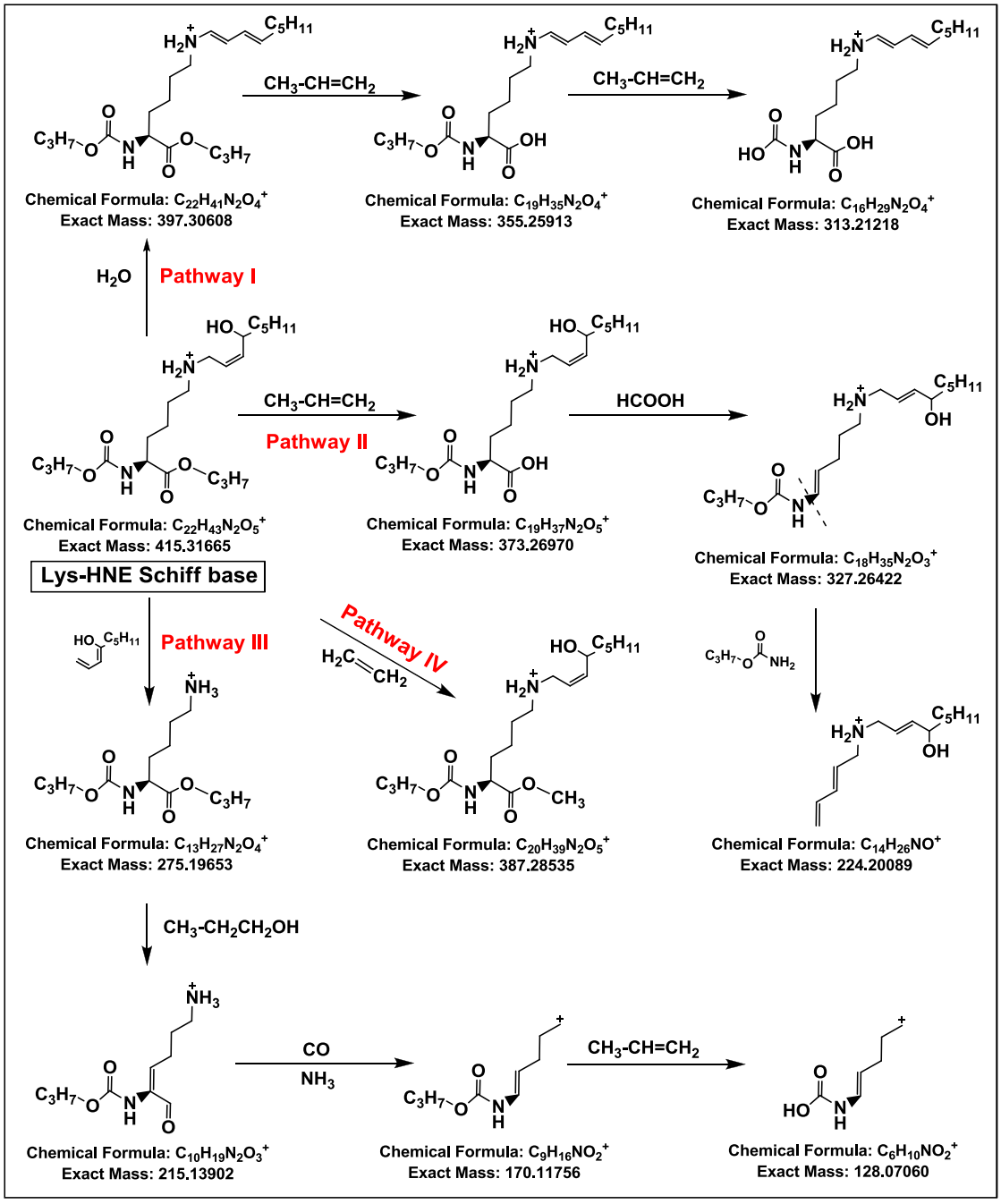

Scheme 3-2: Fragmentation pathways for the derivatised Lys-HNE Schiff base using RPLC coupled to ESI-CID-FTMS/MS.

Pathway (III) consists of 4 steps; the first step starts by losing HNE moiety from the Lys-HNE Schiff base and the products ions are related to derivatised lysine amino acid. Formation of the relatively high abundance product ions at m/z 275 & 215 could be a result of the loss of the HNE moiety followed by the loss of a propanol moiety in a two

consecutive steps. The formation of the relatively low abundance product ions at m/z 170 and 128 could be generated by further fragmentation of the product ion 215 m/z through step 3 and 4 of the pathway (III); step 3 includes loss of ammonia and carbon monoxide while step 4 involves loss of another propylene moiety.

Loss of CO from a molecule during ESI-CID-FTMS/MS is not unusual for a molecule during MS^2 fragmentation; loss of CO had been reported by Fenaille *et al.* (2003) [111], Sasaki *et al.* (1997) [144], and Baker *et al.* (1999)[29]. Joyce *et al.* (2004) [145] and Smyth *et al.* (2004) [146] reported a wide variety of product ions in ESI-MS/MS fragmentation; these include loss of water (H_2O, 18 amu), propylene (CH_3-CH=CH_2, 42 amu), carbon monoxide (CO, 28 amu), carbon dioxide (CO_2, 44 amu) and ammonia (NH_3, 17 amu) which supports the current research findings for the MS^2 behaviour for HNE adducts.

A question is raised about the final chemical structure of the product ions at m/z 170 & 128, whether it is a matter of carbocation formation or it is a matter of positive charge translocated to the α-amine group? A mechanism for the positive charge movement from the terminal carbocation to α- amine group has been proposed in Figure 3.21. So, it is possible that both structures can be available in MS^2 spectra, and either of these proposed structures is correct.

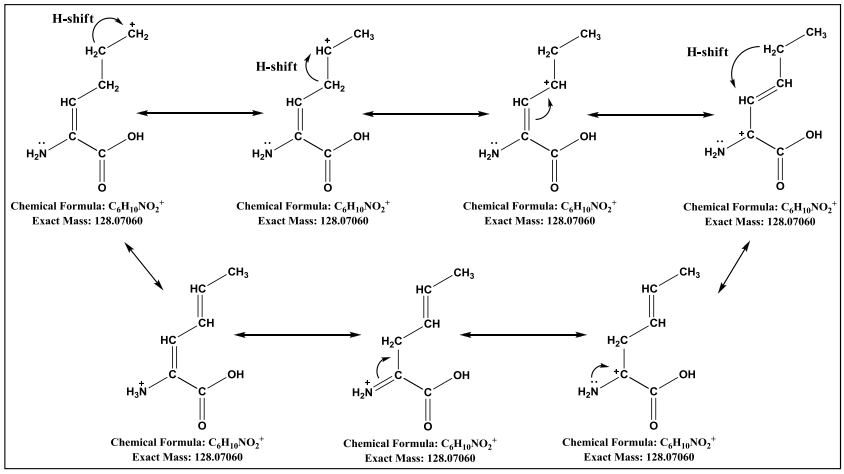

Figure 3.21: Translocation of the positive charge from the carbocation to the α-amine group.

It has been reported by many studies that $CH_2=CH_2$ could be easily lost by EI [147-149] and FAB [150, 151] mass spectrometry; however, pathway (IV) shows that loss of an ethylene group ($CH_2=CH_2$) by ESI-MS/MS mass spectrometry, as proposed by Joyce *et al.* (2004) [145].

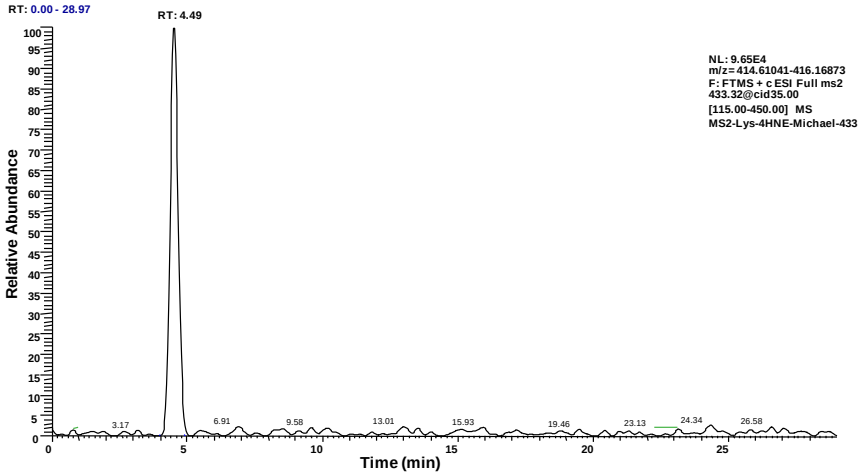

Figure 3.22: MS^2 chromatogram for the derivatised Lys-HNE Michael adduct using RPLC coupled to ESI-CID-FTMS/MS.

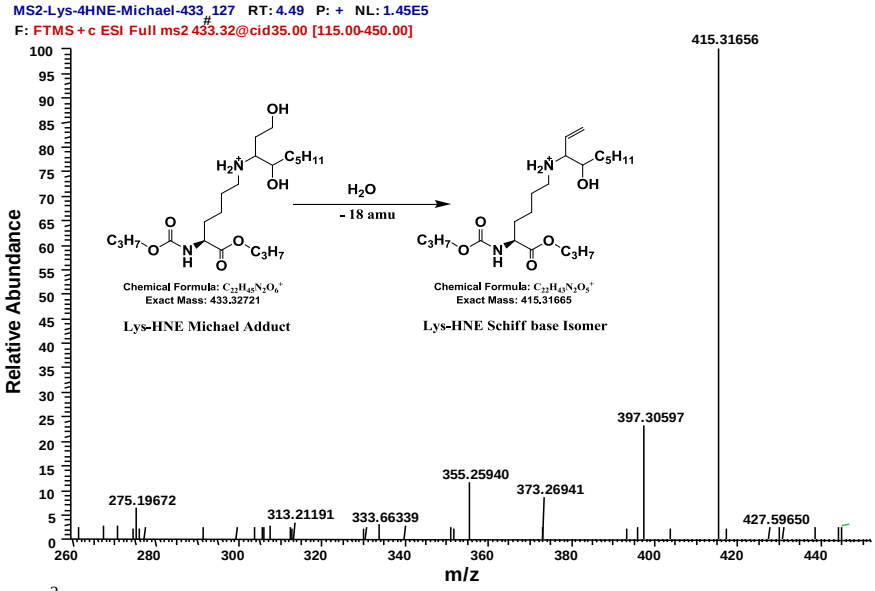

Figure 3.23: MS^2 spectra for the derivatised Lys-HNE Michael adduct using RPLC coupled to ESI-CID-FTMS/MS.

MS^2 analysis for the derivatised Lys-HNE Michael adduct with a molecular ion at m/z 433.23 was carried out. Figure 3.22 shows the MS^2 chromatogram the derivatised Lys-

HNE-Michael adduct; Figure 3.23 shows the mass spectrum for the same adduct.

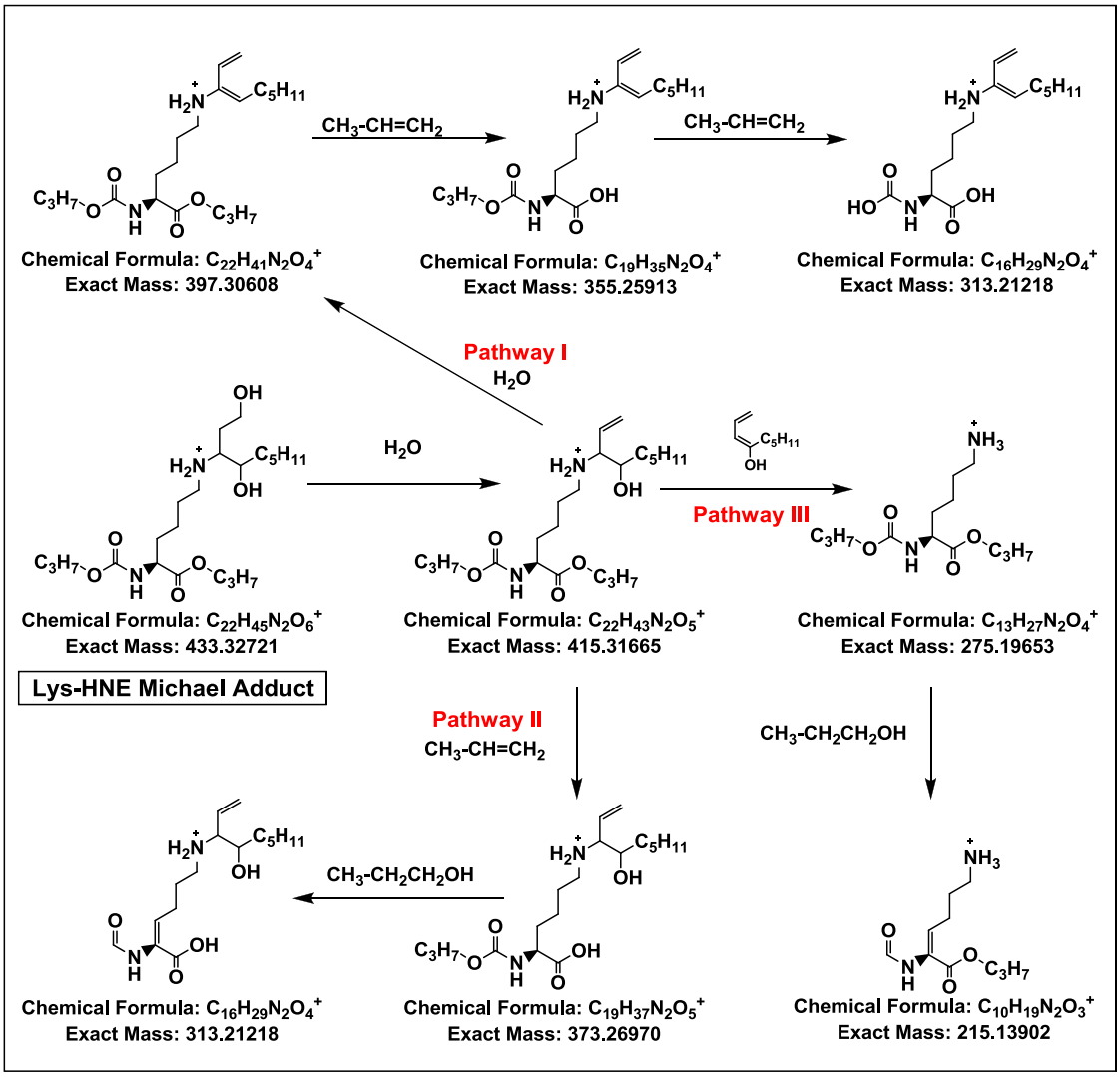

Scheme 3-3: Fragmentation pathways for the derivatised Lys-HNE Michael adduct using RPLC coupled to ESI-CID-FTMS/MS.

The dominant product ion for the Lys-HNE (Michael adduct) has the exact mass and chemical formula for the Lys-HNE (Schiff base); this product ion is the result of loss of a water molecule resulting in an isomer that has the same chemical formula as Lys-HNE Schiff base (Figure 3.23). The Lys-HNE Michael adduct fragmentation then follows the same fragmentation pathways proposed for the Schiff base, and results in the same product ions (Scheme 3-3).

The HNE double adducts Lys-HNE-Lys and His-HNE-Lys show few fragments due to their low abundance in the mixture. In general, a product ion at m/z 415 is dominant which represents the derivatised lysine portion of the molecule. All the MS^2 data: retention time, exact mass of the precursor ion, mass loss, and deviation from the theoretical mass (around 2 ppm) is listed in Table 3-13.

Table 3-13: MS^2 results for the derivatised HNE adducts detected using RPLC coupled to ESI-CID-FTMS/MS.

Adduct	*Elemental formula*	*R_t control (min)*	*R_t (min) for MS^2*	*Precursor ion*	*Mass Loss*	*Product ion*	*chemical formula*	*Delta ppm*
ARG-HNE-Schiff base	$C_{22}H_{43}N_4O_5$	4.97, 5.42	4.42, 5.13	443.3228	-18	425	$C_{22}H_{41}N_4O_4$	1.499
					-42	401	$C_{19}H_{37}N_4O_5$	1.678
					-60	383	$C_{19}H_{35}N_4O_4$	1.457
					-88	355	$C_{18}H_{35}N_4O_3$	1.865
					-102	341	$C_{14}H_{26}N_3O_1$	1.000
					-158	285	$C_{13}H_{25}N_4O_3$	-0.561
LYS-HNE-Schiff base	$C_{22}H_{43}N_2O_5$	4.88, 5.27	4.74, 5.16	415.3177	-18	397	$C_{22}H_{41}N_2O_4$	1.171
					-42	373	$C_{19}H_{37}N_2O_5$	0.298
					-60	355	$C_{19}H_{35}N_2O_4$	1.341
					-88	327	$C_{17}H_{31}N_2O_4$	-0.783
					-102	313	$C_{16}H_{29}N_2O_4$	1.872
					-140	275	$C_{13}H_{27}N_2O_4$	-2.033
					-191	224	$C_{14}H_{26}NO$	1.513
					-200	215	$C_{10}H_{19}N_2O_3$	-2.140
					-245	170	$C_9H_{16}O_2N_1$	1.324
					-287	128	$C_6H_{10}O_2N_1$	1.055
LYS-HNE-Michael adduct	$C_{22}H_{45}N_2O_6$	4.42	4.32	433.3284	-18	415	$C_{22}H_{43}N_2O_5$	1.400
					-36	397	$C_{22}H_{41}N_2O_4$	-0.343
					-60	373	$C_{19}H_{37}N_2O_5$	2.335
					-78	355	$C_{19}H_{35}N_2O_4$	1.594
					-120	313	$C_{16}H_{29}N_2O_4$	2.160
					-158	275	$C_{13}H_{27}N_2O_4$	2.462
					-218	215	$C_{10}H_{19}N_2O_3$	1.102
LYS-HNE-LYS	$C_{35}H_{69}N_4O_9$	6.01	5.98	689.5074	-18	671	$C_{35}H_{67}N_4O_8$	1.115
					-274	415	$C_{22}H_{43}N_2O_5$	1.328
					-292	397	$C_{22}H_{41}N_2O_4$	1.474
HIS-HNE-LYS	$C_{35}H_{64}N_5O_9$	6.17, 6.42	6.14, 6.40	698.471	-60	638	$C_{32}H_{56}N_5O_8$	0.782
					-283	415	$C_{22}H_{43}N_2O_5$	1.472
					-301	397	$C_{22}H_{41}N_2O_4$	0.542

3.7 Structure Elucidation for ALEs Using RPLC-FTMS/MS and the EZ:faast method

MS^2 has been applied extensively to obtain the fragmentation patterns for the derivatised 2-alkenal adducts, especially for the Lys-pyridinium and Lys-FDP adducts. The MS/MS analysis for these samples was repeated 6 times to confirm the fragmentation patterns.

3.7.1 MS^2 Fragmentation Pattern for Lysine-Pyridinium Adducts

As has been proposed in section 3.2.2, a reduction step with $NaBH_4$ prior to acid hydrolysis step results in the formation of different Lys-2-alkenal-pyridinium adducts which may result from different reduction levels for these adducts. Although the detection of these different adducts was confirmed using high resolution mass spectrometry which could confirm the identity of each individual peak within 2 ppm deviation of the observed mass from that of the expected chemical formula, MS^2 was carried in order to observe the fragmentation behaviour of these adducts.

The product ions observed for the derivatised Lys-pyr adducts are listed in Table 3-14. All the observed product ions are reported with less than 3ppm mass deviation from the theoretical expected mass. The data in this table have been arranged in a specific manner where there is a specific mass loss (-42, -60, -86, -102, -128, -174, -191, and -257 amu) from the precursor ion, or according to the appearance of a common ion at m/z 258, 216, 172, 170, and 128 in all types of 2-alkenal-pyr adducts. Initiation of the data dependent fragmentation process in MS^2 spectrometry requires the compound to be available at a specific intensity, below which it would be excluded with other background ions. Therefore, MS^2 results for some adducts have not been reported because the intensity of these adducts fall below the instrument's intensity requirement to trigger the fragmentation process.

Table 3-14: MS^2 results for the series of derivatised Lys-2-alkenal pyr adducts using RPLC coupled to ESI-CID-FTMS/MS. Number of samples for each adduct N=6. (A) refers to the availability of the common ion fragment in the MS/MS spectra. Mass deviation is less than 3ppm for all adducts.

		Product ions by fixed mass loss from the precursor ion								Common Ion Fragments				
Adduct	***Type of Adduct***	***-42***	***-60***	***-86***	***-102***	***-128***	***-174***	***-191***	***-257***	***258***	***216***	***172***	***170***	***128***
Acr-pyr-351	***Lys-pyr***													
Acr-pyr-353	***Lys-pyr (+2H)***	**311**	**293**											
Acr-pyr-355	***Lys-pyr (+4H)***	**313**	**295**	**269**	**253**	**227**		**164**		**A**	**A**	**A**	**A**	**A**
Acr-pyr-357	***Lys-pyr (+6H)***													
Adduct	***Type of Adduct***	***-42***	***-60***	***-86***	***-102***	***-128***	***-174***	***-191***	***-257***	***258***	***216***	***172***	***170***	***128***
Cro-pyr-377	***Lys-pyr (-2H)***													
Cro-pyr-379	***Lys-pyr***	**337**												
Cro-pyr-381	***Lys-pyr (+2H)***	**339**	**321**	**295**									**A**	
Cro-pyr-383	***Lys-pyr (+4H)***	**341**	**323**										**A**	**A**
Cro-pyr-385	***Lys-pyr (+6H)***													
Adduct	***Type of Adduct***	***-42***	***-60***	***-86***	***-102***	***-128***	***-174***	***-191***	***-257***	***258***	***216***	***172***	***170***	***128***
Pne-pyr-405	***Lys-pyr (-2H)***	**363**												
Pne-pyr-407	***Lys-pyr***	**365**	**347**	**321**					**150**			**A**	**A**	**A**
Pne-pyr-409	***Lys-pyr (+2H)***	**367**	**349**	**323**	**307**			**218**	**152**				**A**	**A**
Pne-pyr-411	***Lys-pyr (+4H)***	**369**	**351**			**283**							**A**	**A**
Pne-pyr-413	***Lys-pyr (+6H)***	**371**	**353**										**A**	**A**
Adduct	***Type of Adduct***	***-42***	***-60***	***-86***	***-102***	***-128***	***-174***	***-191***	***-257***	***258***	***216***	***172***	***170***	***128***
Hxe-pyr-433	***Lys-pyr (-2H)***	**391**	**373**						**176**				**A**	**A**
Hxe-pyr-435	***Lys-pyr***	**393**	**375**	**349**	**333**	**307**			**178**		**A**		**A**	**A**
Hxe-pyr-437	***Lys-pyr (+2H)***	**395**	**377**	**351**	**335**	**309**	**263**	**246**	**180**				**A**	**A**
Hxe-pyr-439	***Lys-pyr (+4H)***	**397**	**379**	**353**				**248**	**182**				**A**	**A**
Hxe-pyr-441	***Lys-pyr (+6H)***													
Adduct	***Type of Adduct***	***-42***	***-60***	***-86***	***-102***	***-128***	***-174***	***-191***	***-257***	***258***	***216***	***172***	***170***	***128***
Hpe-pyr-461	***Lys-pyr (-2H)***	**419**	**401**			**333**			**204**				**A**	**A**
Hpe-pyr-463	***Lys-pyr***	**421**	**403**	**377**	**361**	**335**	**289**		**206**	**A**		**A**	**A**	**A**
Hpe-pyr-465	***Lys-pyr (+2H)***	**423**	**405**	**379**	**363**	**337**	**291**	**274**	**208**			**A**	**A**	**A**
Hpe-pyr-467	***Lys-pyr (+4H)***	**425**	**407**	**381**				**276**	**210**				**A**	**A**
Hpe-pyr-469	***Lys-pyr (+6H)***	**427**	**409**											
Adduct	***Type of Adduct***	***-42***	***-60***	***-86***	***-102***	***-128***	***-174***	***-191***	***-257***	***258***	***216***	***172***	***170***	***128***
Nne-pyr-517	***Lys-pyr (-2H)***	**475**												
Nne-pyr-519	***Lys-pyr***	**477**	**459**	**433**	**417**	**391**	**345**		**262**	**A**			**A**	**A**
Nne-pyr-521	***Lys-pyr (+2H)***	**479**	**461**	**435**	**419**	**393**	**347**	**330**	**264**				**A**	**A**
Nne-pyr-523	***Lys-pyr (+4H)***	**481**	**463**	**437**		**395**			**266**				**A**	**A**
Nne-pyr-525	***Lys-pyr (+6H)***	**483**	**465**	**439**				**334**	**268**				**A**	**A**

The fragmentation process for the derivatised lysine pyridinium adduct will be discussed according to the general structure suggested by Baker *et al.* [28] for lysine pyridinium adducts (Figure 3.24). The lysine pyridinium adducts show 2 types of fragment: fixed mass losses fragments and common ion fragments.

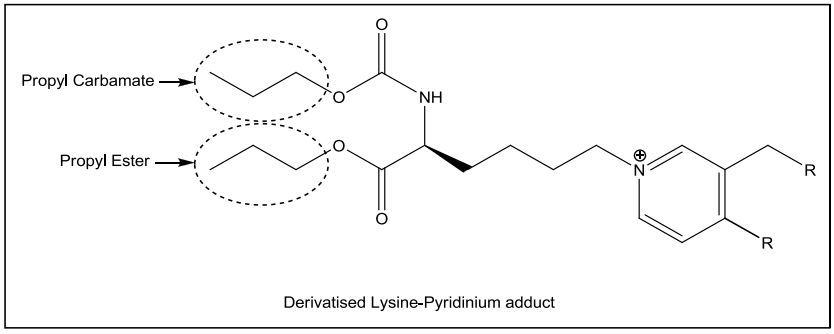

Figure 3.24: Propyl carbamate and propyl ester moieties of derivatised lysine-pyridinium adduct (as suggested by Baker *et al.* [28]) that are subject to fragmentation process using ESI-CID-FTMS/MS.

3.7.1.1 Fixed Mass Loss Fragments for Different Lys-Pyr Adducts

The first type of lysine pyridinium fragment (fixed mass loss fragments) appears as a result of the loss of a specific mass from the precursor ion; all lysine pyridinium adducts will show the same mass loss. For example, lysine Pne-pyr adduct (m/z 409) loses 42 amu to give a fragment at m/z 367, while the lysine Hxe-pyr adduct at m/z 437 loses 42 amu to give a fragment at m/z 395.

Figure 3.25 shows the extracted ion chromatogram and the fragmentation pattern for the lysine Hxe-pyr adduct (m/z 437) after being derivatised with propylchloroformate. Most of these fragments are generated by losing specific masses from the precursor ion.

MS^2 results for different lysine pyridinium adducts show the same fragmentation pattern where most of the commonly observed fragments are related to the loss of the derivatising groups in the form of propylene molecule (CH_3-CH=CH_2, 42 amu) or propanol molecule (CH_3-CH_2-CH_2-OH, 60 amu). However, loss of formic acid molecule (HCOOH, 46 amu), carbon dioxide (CO_2, 44 amu) and ammonia (NH_3, 17 amu) is also possible. Generally, the pyridinium adduct can lose a single moiety or a combination of different moieties; for example loss of the propylene moiety (42 amu) followed by the loss of CO_2 molecule (44 amu) can occur to produce a fragment formed by a total loss of 86 amu.

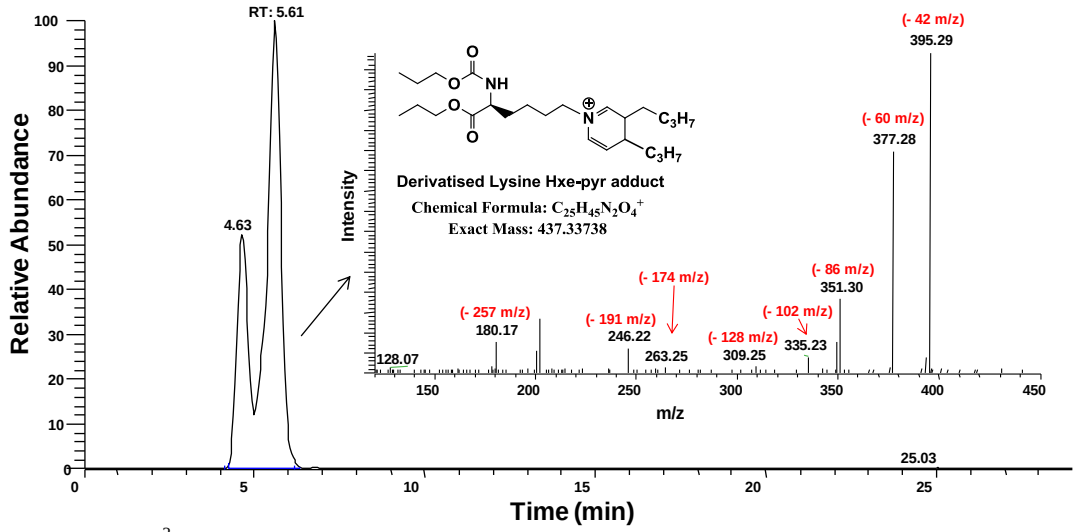

Figure 3.25: MS^2 chromatogram and spectra for the derivatised lysine Hxe-pyr adduct (m/z 437) using RPLC coupled to ESI-CID-FTMS/MS.

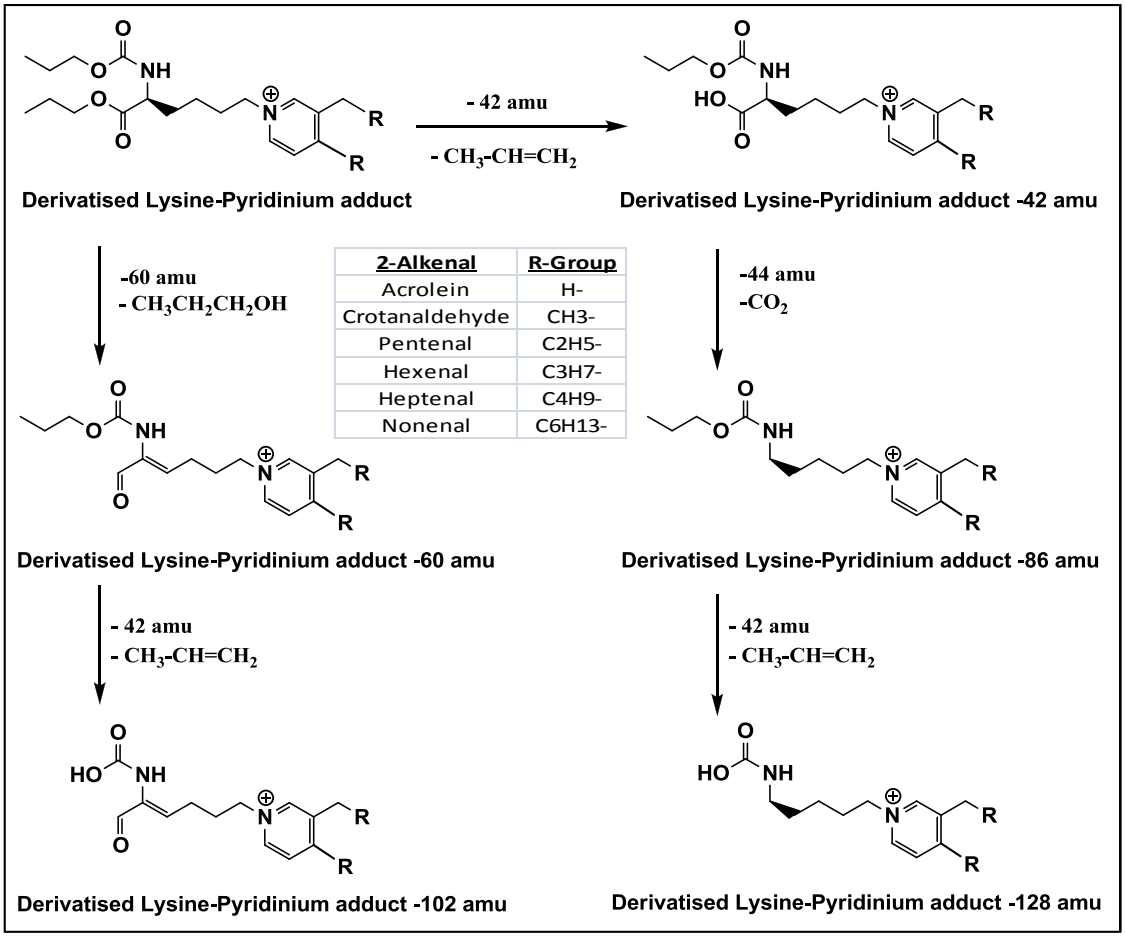

2-Alkenal	R-Group
Acrolein	H-
Crotanaldehyde	CH3-
Pentenal	C2H5-
Hexenal	C3H7-
Heptenal	C4H9-
Nonenal	C6H13-

Scheme 3-4: MS^2 fragmentation pattern of derivatised lysine-pyridinium adducts formed by losing specific masses: 42, 60, 86, 102, and 128 amu (using RPLC coupled to ESI-CID-FTMS/MS).

Different pathways can be proposed to explain the mass losses from the molecular ion. Losses of 42, 60, 86, 102, and 128 amu from the precursor ion are explained in Scheme 3-4, whereas losses of 88, 130, 174, and 191 amu from the precursor ion are explained in Scheme 3-5.

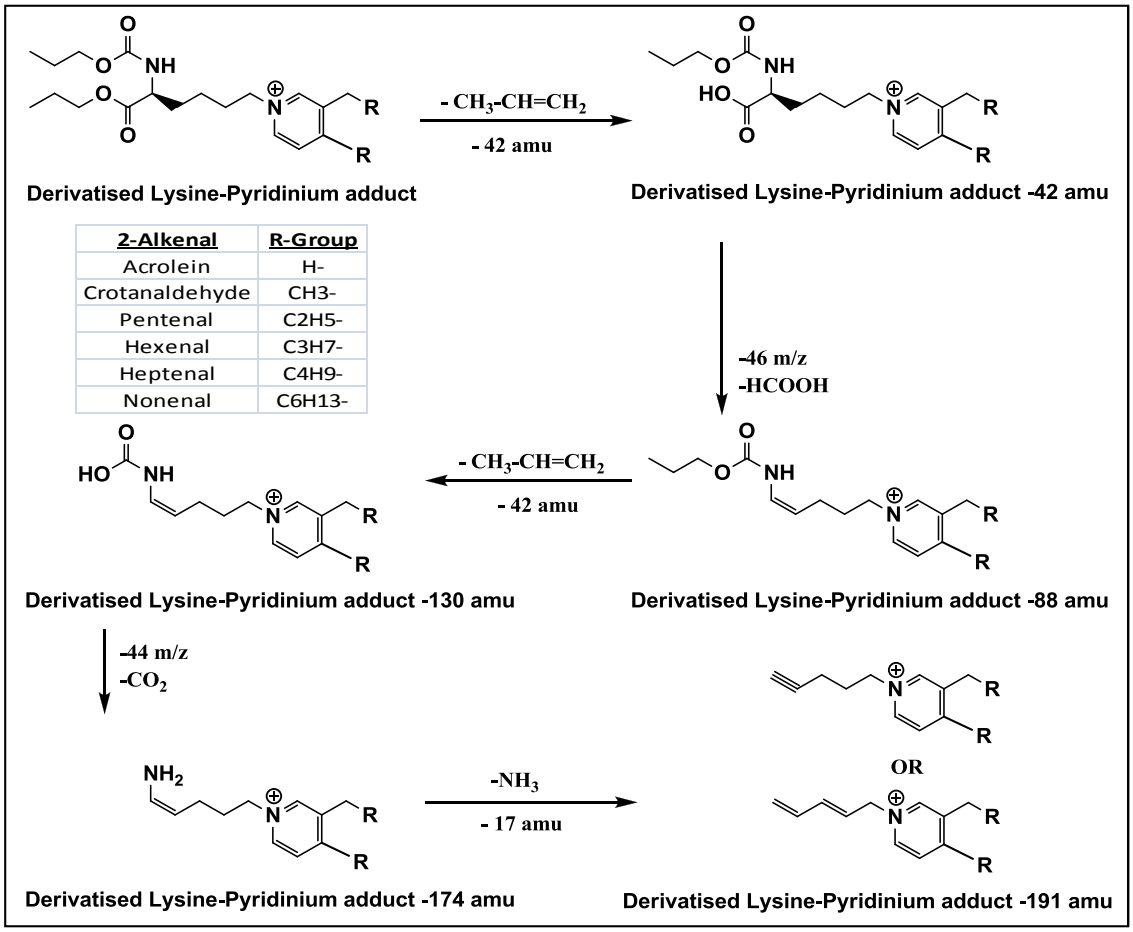

Scheme 3-5: MS^2 fragmentation pattern of derivatised lysine-pyridinium adduct formed by loss of specific masses: 42, 88, 130, 174, and 191 amu (using RPLC coupled to ESI-CID-FTMS/MS).

However, low abundance fragment ions have been reported for different lysine pyridinium adducts which can be explained by the loss of the lysine moiety; these fragments consist of the pyridinium part of the molecule with the attached alkyl groups which are related to the 2-alkenals used in the modification of the protein samples, as shown in Scheme 3-6.

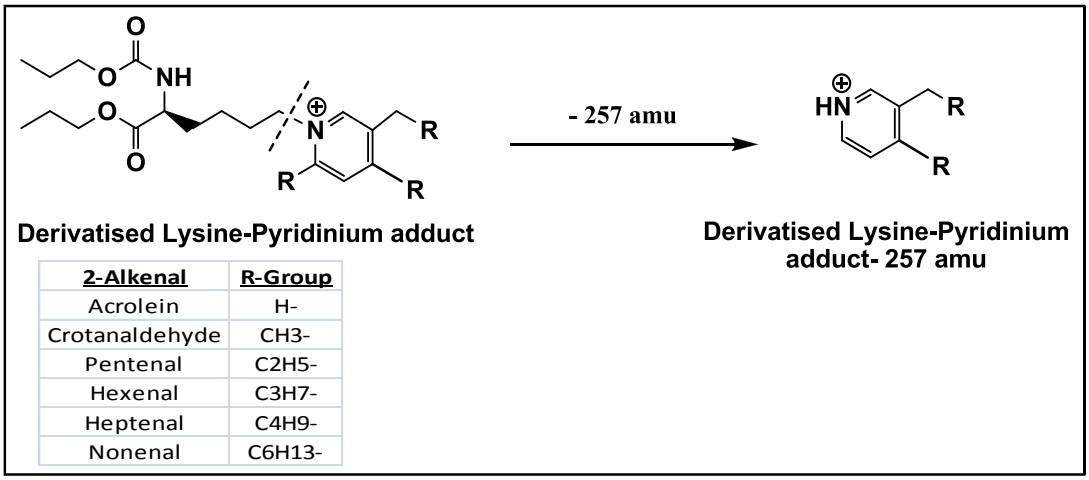

2-Alkenal	R-Group
Acrolein	H-
Crotanaldehyde	CH3-
Pentenal	C2H5-
Hexenal	C3H7-
Heptenal	C4H9-
Nonenal	C6H13-

Scheme 3-6: MS^2 fragmentation pattern of derivatised lysine-pyridinium adduct formed by the loss of lysine moiety (using RPLC coupled to ESI-CID-FTMS/MS).

The mass losses which may be observed from the lysine pyridinium adducts under MS^2 conditions are summarized in Table 3-15, with possible explanation for the nature of the losses according to the chemical formula for the fragments as compared to the precursor ion. Lysine-HNE adducts show the same pattern of mass losses as shown earlier (Scheme 3-2) by losing propylene (CH_3-CH-CH_2), propanol (CH_3-CH_2-CH_2-OH), formic acid (HCOOH), carbon dioxide (CO_2), and amine (NH_3) moieties from the precursor ion.

Table 3-15: MS^2 neutral fragments which will be lost from the molecular ions of the derivatised Lys-2-alkenal-pyridinium adducts using RPLC coupled to ESI-CID-FTMS/MS.

Mass loss	***Represent***	***Availability***
-42	CH_3-CH=CH_2	Dominant
-60	42 + H_2O (18 amu)	Dominant
-86	42 + CO_2 (44 amu)	Dominant
-102	60 + 42	Low abundance
-128	86 + 42	Low abundance
-174	42 + HCOOH (46 amu)+ 86	Low abundance
-191	174 + NH_3 (17 amu)	Low abundance
-257	Losing of derivatised lysine moiety	Very low abundance

3.7.1.2 Common Ion Fragments for Different Lys-Pyr Adducts

The second type of lysine pyridinium fragment ions (common ion fragments) represents a set of product ions with fixed m/z which appear in different type of the pyridinium adducts as a result of pyridine ring elimination with its attached alkyl groups which are related to the 2-alkenal used in the modification of the protein samples. For example, product ions at m/z 258, 170, and 128 appear in the MS^2 of the lysine Acr-pyr adduct (m/z 355) and Nne-pyr adduct (m/z 519), as both adducts lose the pyridine ring with its attached alkyl groups and the fragment ions relate to the lysine portion of the molecules which is common for both adducts.

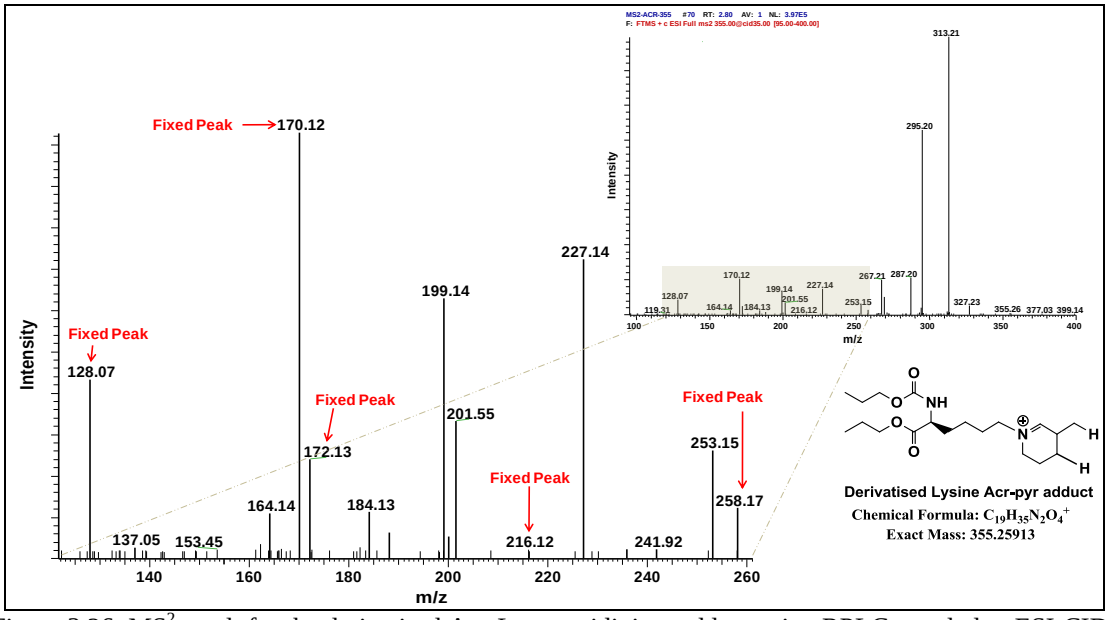

Figure 3.26: MS^2 result for the derivatised Acr-Lys--pyridinium adduct using RPLC coupled to ESI-CID-FTMS/MS.

From the MS^2 results for all lysine pyridinium adducts, these common ion fragments could be detected with very low intensity as compared to the fragments produced via fixed mass loss pathways discussed earlier. Figure 3.26 shows different common ion fragments in the MS^2 results of derivatised lysine Acr-pyr adduct (355 m/z); these common ion fragments have low intensity as compared to other fragments produced by loss of the derivatising moiety rather than the pyridine ring.

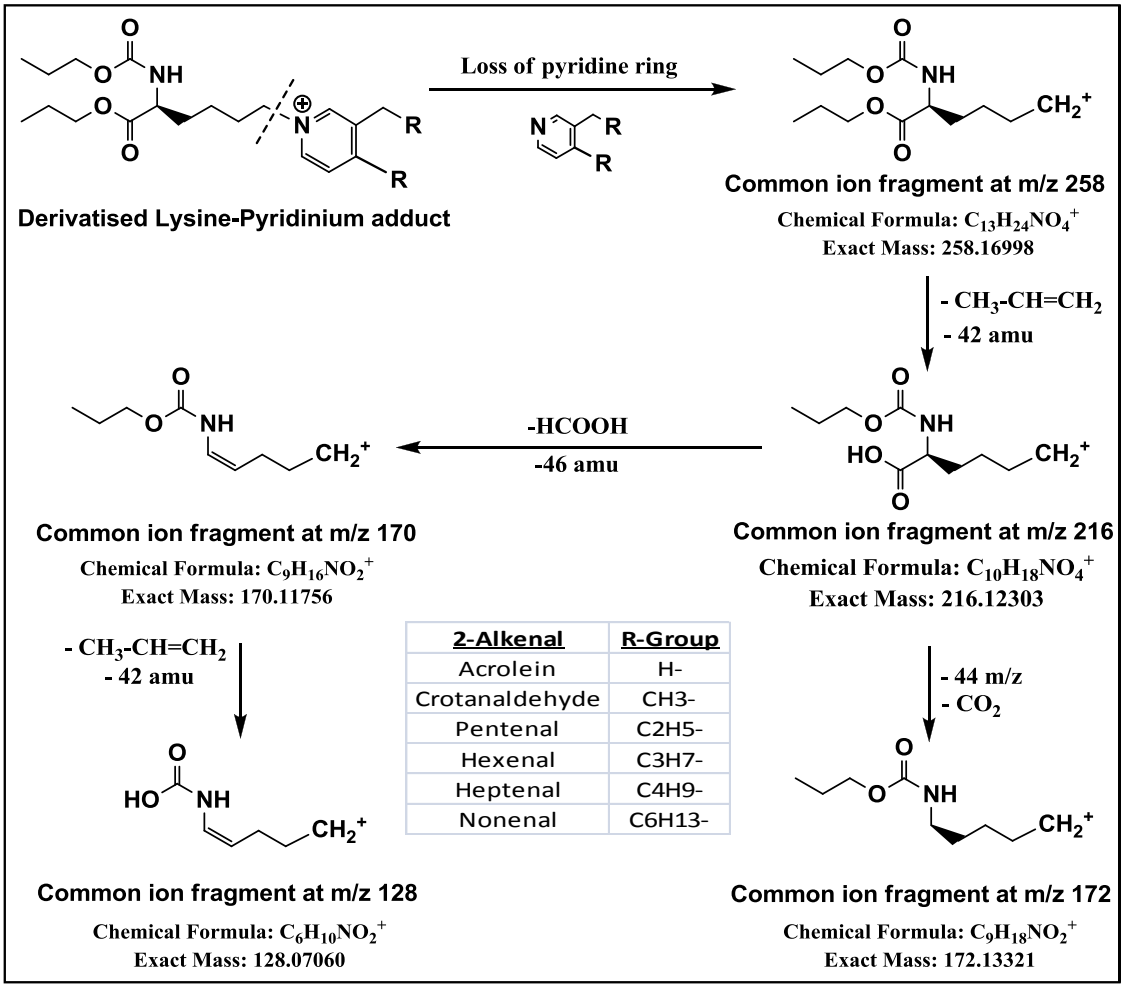

2-Alkenal	R-Group
Acrolein	H-
Crotanaldehyde	CH3-
Pentenal	C2H5-
Hexenal	C3H7-
Heptenal	C4H9-
Nonenal	C6H13-

Scheme 3-7: MS^2 fragmentation pattern of derivatised lysine-pyridinium adduct (using RPLC coupled to ESI-CID-FTMS/MS) which leads to common ions at m/z 128, 170, 172, 216, and 257.

Table 3-16: Common ion fragments that could be detected with different 2-alkenal-pyridinium adducts using RPLC coupled to ESI-CID-FTMS/MS.

Common ion	*Formula*	*Represent*	*Availability*
258	$C_{13}H_{24}O_4N_1$	Alkylated lysine without pyridine ring	Rare
216	$C_{10}H_{18}O_4N_1$	258 - 42 amu (CH3-CH=CH2)	Rare
172	$C_9H_{18}O_2N_1$	216- 44 amu (CO_2)	Low availability
170	$C_9H_{16}O_2N_1$	216 – 46 amu (HCOOH)	Available
128	$C_6H_{10}O_2N_1$	170 - 42 amu (CH3-CH=CH2)	available

There are two possibilities for the formation of these common ion fragments. The first possibility could be loss of specific masses from the derivatising moiety such as propylene (CH_3-CH=CH_2, 42 amu), formic acid (HCOOH, 46 amu), and carbon dioxide (CO_2, 44 amu) followed by the loss of the pyridine ring. For example, loss of the

propylene moiety from the derivatised lysine Acr-pyr adduct with mass of m/z 355 followed by loss of the pyridine ring will result in the formation of the common ion at m/z 216. The second possibility for the formation of the common ion fragments could be loss of the pyridine ring from the pyridinium adduct followed by loss of specific mass unit from the derivatising moiety as explained in Scheme 3-7. Table 3-16 shows the chemical formulae and the abundance of the common ion fragments in different pyridinium adducts.

The common ion fragment ions with m/z 258 represents loss of the pyridine ring from the Alkylated lysine pyridinium adduct; this fragment could be reported in a limited number of pyridinium adducts. Together with the low intensity for all common ion fragments, this gives an indication that pyridinium adducts have more tendency towards the loss of specific masses from the derivatising moieties rather than losing pyridine ring. The HNE adduct shows the same type of fragmentation having common ions at m/z 170 and 128, as discussed earlier in Scheme 3-2.

3.7.2 Fragmentation Pattern for Lysine-FDP Adducts

MS^2 fragmentation of FDP adducts is based on the structures proposed by Ichihashi *et al.* [section 1.2.1.4], and this includes 2 levels of reduction. The first reduction step involves the reduction of the peripheral aldehyde group to the corresponding alcohol group with 2 H atoms acquired during the reduction step with $NaBH_4$. The second level includes reduction of the double bond within the piperdine ring with the addition of two H atoms during the same reduction step. The observed product ions of the derivatised Lys-FDP adduct modified with different 2-alkenals are listed in Table 3-17, where all fragments are reported with less than 3 ppm deviation of the observed mass from that of the expected chemical formula. Again, the fragments in this table have been arranged according to a fixed mass loss from the precursor ion (-18, -42, -60, -86, -88, -102, and -257 amu), or according to the appearance of a common ion fragment at m/z 170. Little fragmentation information could be deduced for lysine-FDP adducts as a result of their low intensity as compared Lys-Pyr adducts.

Table 3-17: MS^2 fragmentation pattern for the derivatised lysine-FDP adducts using RPLC coupled to ESI-CID-FTMS/MS. (A) refers to the availability of the common ion fragment at m/z 170.

		Product ions by fixed mass loss from the precursor ion							Common Ion Fragment
Adduct	*Type of adduct*	*-18*	*-42*	*-60*	*-86*	*-88*	*-102*	*-257*	*170*
Acr-Lys-FDP-371	*Lys-FDP (+2H)*								
Acr-Lys-FDP-373	*Lys-FDP (+4H)*								
Cro-Lys-FDP-399	*Lys-FDP (+2H)*	381							
Cro-Lys-FDP-401	*Lys-FDP (+4H)*	383							
Pne-Lys-FDP-427	*Lys-FDP (+2H)*	409	385	367					
Pne-Lys-FDP-429	*Lys-FDP (+4H)*	411	387						
Hxe-Lys-FDP-455	*Lys-FDP (+2H)*	437	413	395					
Hxe-Lys-FDP-457	*Lys-FDP (+4H)*	439	415						
Hpe-Lys-FDP-483	*Lys-FDP (+2H)*	465	441	423		395	381	226	A
Hpe-Lys-FDP-485	*Lys-FDP (+4H)*	467	443						
Nne-Lys-FDP-539	*Lys-FDP (+2H)*	521	497	479	453	451	437	282	A
Nne-Lys-FDP-541	*Lys-FDP (+4H)*	523	499		455				

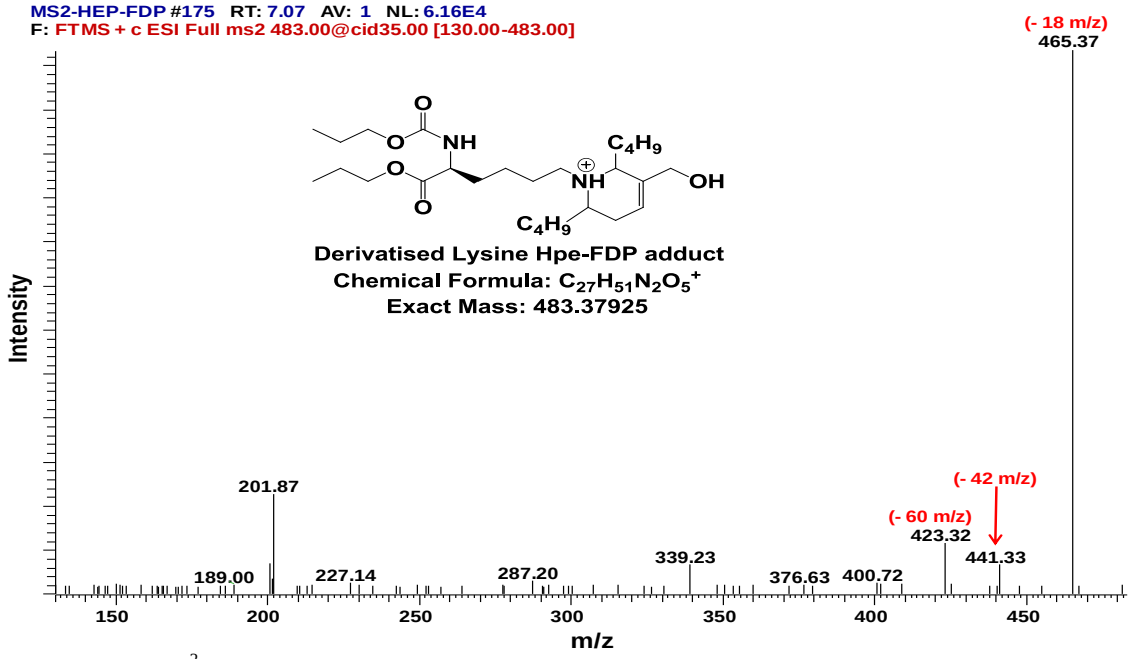

Figure 3.27: MS^2 spectra for the derivatised lysine Hpe-FDP adduct using RPLC coupled to ESI-CID-FTMS/MS. The fragment at m/z 465 (-18 amu) is dominant over other fragments.

The fragmentation pattern for lysine-FDP adducts is variable, where fragment ions produced by loss of a water molecule (- 18 amu) from the precursor ion are dominant in some MS^2 spectra, while fragments produced by losing water and a propylene molecule (- 60 amu) are dominant in other MS^2 spectra. For example, fragment ion at m/z 465 generated by loss of a water molecule is dominant in the MS^2 spectra for the derivatised lysine Hpe-FDP adduct which has a monoisotopic peak at m/z 483 (Figure 3.27). Figure

3.28 shows the MS^2 spectrum of the derivatised lysine Nne-FDP adduct which has a monoisotopic peak at m/z 539 where the fragment ion at m/z 479 generated by loss of 60 amu is dominant over other fragment ions.

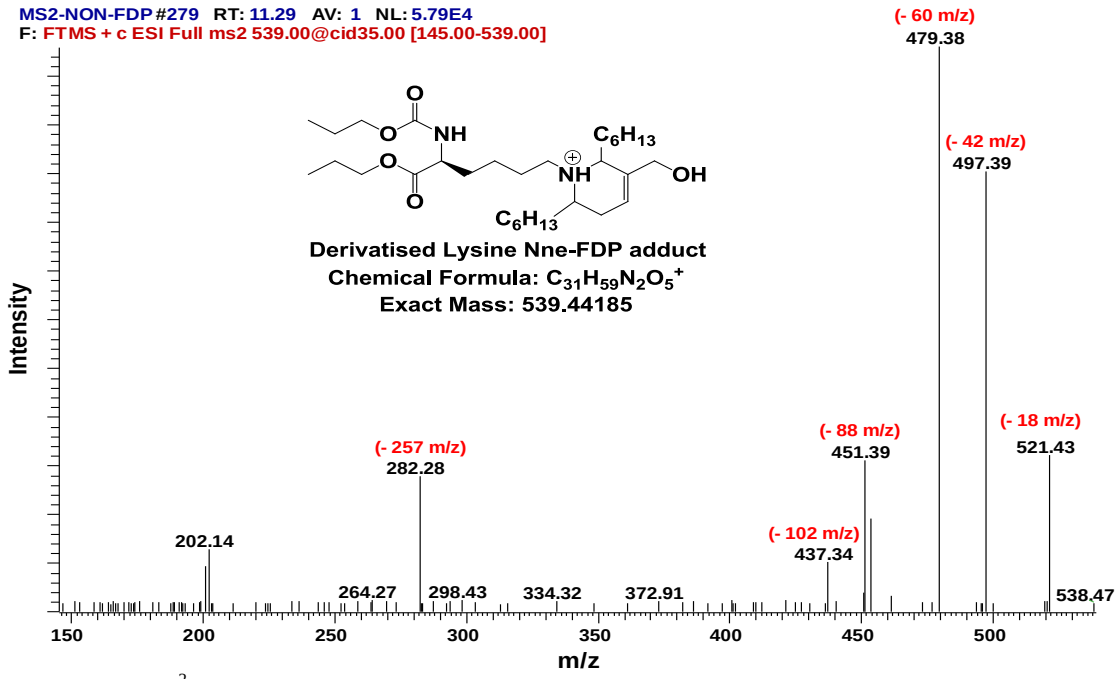

Figure 3.28: MS^2 spectrum for the derivatised lysine Nne-FDP adduct using RPLC coupled to ESI-CID-FTMS/MS. The fragment at m/z 479 (-60 amu) is dominant over other fragments.

Scheme 3-8 shows the possible fragmentation pathways for the derivatised lysine-FDP adducts that could lead to the formation of fixed mass loss fragments or common ion fragments. The derivatised lysine-FDP adducts show the same fragmentation pattern as lysine pyridinium adducts where most of the fragments are generated by losing specific fragments from the derivatising group. These fixed mass loss are represented by loss of propylene (CH_3-CH=CH_2, 42 amu), propanol (CH_3-CH_2-CH_2-OH, 60 amu), formic acid (HCOOH, 46 amu), carbon dioxide (CO_2, 44 amu), or any combination of these losses. However, the derivatised lysine-FDP adduct may lose water molecule (H_2O, 18 amu) due to the availability of peripheral alcohol group in its structure. The only noticeable common fragment ion for FDP adducts is seen at m/z 170 due to the lysine side chain of the lysine-FDP adduct. Loss of 60 amu from the precursor ion should be the feasible

pathway for the fragment generation and should have abundant intensity in the MS^2 spectra as there are two possible ways for the formation of such fragment.

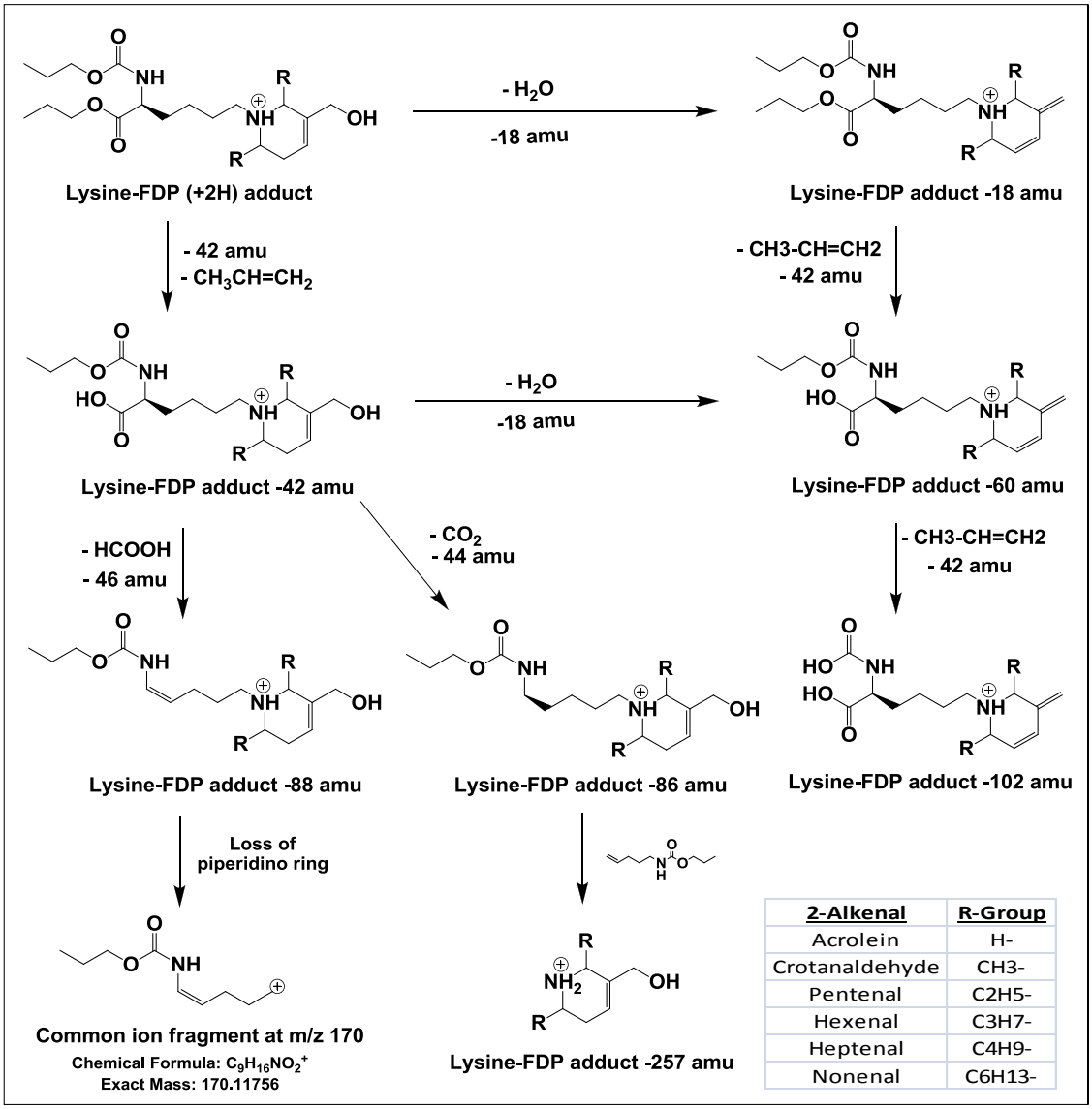

Scheme 3-8: MS^2 fragmentation pattern of a derivatised lysine-FDP adduct using RPLC coupled to ESI-CID-FTMS/MS.

The first way is by losing water molecule from the peripheral alcohol group followed by loss of a propylene molecule from the derivatising group in a total of 60 amu; the second way could be a result of losing propylene followed by losing water molecule from the same derivatising group moiety in a total of 60 amu. Table 3-18 shows the fixed mass losses which may be observed from the lysine-FDP adducts under MS^2 conditions, with

a possible explanation for the nature of the losses according to the chemical formula for the fragments as compared to the precursor ion.

Table 3-18: Neutral fragments that will be lost from the parent Lys-2-alkenal-FDP adducts when subject to fragmentation by ESI-CID-FTMS/MS resulting in the production of different fragments.

Mass loss	*Represent*	*Availability*
-18	H_2O (18 amu)	Dominant
-42	CH_3-CH=CH_2 (42 amu)	Dominant
-60	42 + 18	Dominant
-86	42 + 44 amu (CO_2)	Low abundance
-88	42 + 46 amu (HCOOH)	Available
-102	60 + 42	Low abundance
-257	Leaving piperidino ring only	Rare
-275	257+18	Very rare

3.8 Defining a Limit of Aldehyde Concentration Required for 2-Alkenal Adducts Formation and Detection by RPLC-FTMS

The total protein concentration in the normal biological systems ranges between 6.3-8.2 g/100ml [152]. Only the aldehyde concentration inside the biological system varies from time to time depending on the biological and pathological condition of the system under study; Alhamdani *et al.* [153] reported a very low level for different aldehydes: alkanals, 2-alkenals and 4-hydroxy-2-alkenals in normal individuals as compared to uremic patients. The levels of such aldehydes were within the nM level; most of these aldehydes were reported with a P- value less than 0.001, for example 2-hexenal was reported at 225±66.9 nM, 2-heptenal reported at 158±47.6 nM, 2-nonenal at 132±36.9 nM, and 4-hydroxy-2-nonenal at 105±57.6 nM. In this experiment, an attempt was made to predict the concentration of the aldehyde at which the formation of 2-alkenal adducts will cease or fail to produce significant modification to proteins in tissue and organs. The production and detection of different adducts was performed according to the procedure described in section 2.3 & 2.4. Full mass spectrometry operating in the positive mode was used as the detection method.

Table 3-19, Table 3-20 and Table 3-21 show the lowest aldehyde concentrations required for the formation of different adducts in an amount sufficient to produce a significant peak in mass spectrometry. The concentrations indicated refer to the initial

aldehyde concentration in mM, while the numbers in brackets refer to the aldehyde concentration after incubation of an 11µl aliquot of different aldehyde concentration with protein sample. Incubating 400 µl of human serum albumin (2.5 mg/ml) with an 11 µl aliquot of an initial aldehyde concentration of 338, 200, 100, 50, 25, 10 and 5 mM will result in a final aldehyde concentration of 9.05, 5.35, 2.68, 1.34, 0.67, 0.27, 0.13 mM respectively. For example, incubating 400 µl of HSA with 11 µl of 5 mM 2-nonenal will result in a final concentration of 0.134 mM (or 134 µM) of 2-nonenal after dilution, which was not enough to mimic the level for 2-nonenal in human body which was about 132 ± 36.9 nM as indicated by Alhamdani *et al.* [153]. Below such aldehydes concentrations (134 µM) all protein samples failed to show any sign of 2-Nonenal adducts as a result of the dilution series occurs during extraction and derivatisation process with EZ:faast method.

Table 3-19: Concentration limits for aldehyde used in incubations below which different lysine-2-alkenal adducts cannot be detected. M= Michael, S=Schiff. The aldehyde limits represent the initial aldehyde concentration used, while the number in the brackets represents the aldehyde concentration after dilution. N=3

Lysine Adducts					
Type of adduct	**limit of aldehyde (mM)**	**Type of adduct**	**limit of aldehyde (mM)**	**Type of adduct**	**limit of aldehyde (mM)**
Acr-Lys-M	**10 (0.267)**	**Pne-Lys-M**	**10 (0.267)**	**Hpe-Lys-M**	**10 (0.267)**
Acr-Lys-S	**N/A**	**Pne-Lys-S**	**25 (0.669)**	**Hpe-Lys-S**	**25 (0.669)**
Acr-pyr-349	**N/A**	**Pne-pyr-405**	**338 (9.046)**	**Hpe-pyr-461**	**N/A**
Acr-pyr-351	**10 (0.267)**	**Pne-pyr-407**	**25 (0.669)**	**Hpe-pyr-463**	**10 (0.267)**
Acr-pyr-353	**25 (0.669)**	**Pne-pyr-409**	**50 (1.338)**	**Hpe-pyr-465**	**25 (0.669)**
Acr-pyr-355	**5 (0.134)**	**Pne-pyr-411**	**10 (0.267)**	**Hpe-pyr-467**	**50 (1.338)**
Acr-pyr-357	**5 (0.134)**	**Pne-pyr-413**	**25 (0.669)**	**Hpe-pyr-469**	**100 (2.677)**
Acr-FDP-371	**10 (0.267)**	**Pne-FDP-427**	**25 (0.669)**	**Hpe-FDP-483**	**50 (1.338)**
Type of adduct	**limit of aldehyde (mM)**	**Type of adduct**	**limit of aldehyde (mM)**	**Type of adduct**	**limit of aldehyde (mM)**
Cro-Lys-M	**10 (0.267)**	**Hxe-Lys-M**	**10 (0.267)**	**Nne-Lys-M**	**10 (0.267)**
Cro-Lys-S	**50 (1.338)**	**Hxe-Lys-S**	**50 (1.338)**	**Nne-Lys-S**	**10 (0.267)**
Cro-pyr-377	**N/A**	**Hxe-pyr-433**	**N/A**	**Nne-pyr-517**	**200 (5.353)**
Cro-pyr-379	**50 (1.338)**	**Hxe-pyr-435**	**10 (0.267)**	**Nne-pyr-519**	**25 (0.669)**
Cro-pyr-381	**25 (0.669)**	**Hxe-pyr-437**	**50 (1.338)**	**Nne-pyr-521**	**200 (5.353)**
Cro-pyr-383	**5 (0.134)**	**Hxe-pyr-439**	**25 (0.669)**	**Nne-pyr-523**	**25 (0.669)**
Cro-pyr-385	**5 (0.134)**	**Hxe-pyr-441**	**50 (1.338)**	**Nne-pyr-525**	**200 (5.353)**
Cro-FDP-399	**200 (5.353)**	**Hxe-FDP-455**	**100 (2.677)**	**Nne-FDP-539**	**50 (1.338)**

Table 3-20: Concentration limits for aldehydes used in incubations below which different arginine-2-alkenal adducts cannot be detected. M= Michael, S=Schiff. The aldehyde limits represent the initial aldehyde concentration used, while the number in the brackets represents the aldehyde concentration after dilution. N=3

ARGININE ADDUCTS			
Type of adduct	**limit of aldehyde (mM)**	**Type of adduct**	**limit of aldehyde (mM)**
Acr-Arg-M	**N/A**	**Hxe-Arg-M**	**5 (0.134)**
Acr-Arg-S	**N/A**	**Hxe-Arg-S**	**50 (1.338)**
Cro-Arg-M	**10 (0.267)**	**Hpe-Arg-M**	**5 (0.134)**
Cro-Arg-S	**5 (0.134)**	**Hpe-Arg-S**	**25 (0.669)**
Pne-Arg -M	**25 (0.669)**	**Nne-Arg-M**	**5 (0.134)**
Pne-Arg-S	**25 (0.669)**	**Nne-Arg-S**	**5 (0.134)**

Table 3-21: Concentration limits for aldehydes used in incubations below which different histidine-2-alkenal adducts cannot be detected. M= Michael. The aldehyde limits represent the initial aldehyde concentration used, while the number in the brackets represents the aldehyde concentration after dilution. N=3

HISTIDINE ADDUCTS			
Type of adduct	**limit of aldehyde (mM)**	**Type of adduct**	**limit of aldehyde (mM)**
Acr-His-M	**5 (0.134)**	**Hxe-His-M**	**5 (0.134)**
Cro-His-M	**5 (0.134)**	**Hpe-His-M**	**5 (0.134)**
Pne-His-M	**5 (0.134)**	**Nne-His-M**	**5 (0.134)**

Table 3-19 shows the aldehyde concentration limits for the detection of different lysine 2-alkenal adducts in mM concentration. The lysine pyridinium adducts were the dominant adducts as they could be detected when the protein samples were incubated with a very low aldehyde concentrations down to 5 mM. In general, Michael adducts for lysine amino acids could be detected at lower aldehyde concentrations than those required for Schiff bases formation. The Schiff base can be dissociated back to the aldehyde group and primary amine group. The non-reduced form of lysine pyridinium adducts (Lys-pyr -2H) could only be detected at very high concentrations of aldehydes, 200-338 mM. Other lysine pyridinium adducts required between 5mM and 338mM of aldehyde for their formation.

Figure 3.29 shows the distribution of different Lys-Pne adducts over a range of 2-pentenal aldehyde concentrations. It is noticeable that Lys-FDP and Pne-pyr adducts (mainly Lys-pyr & Lys-pyr +4 H) are dominant over other adducts while Pne-pyr-2H (Pne-Pyr-405) is only detectable high aldehyde concentrations. Shao *et al.* (2005) [34] referred to the dominance of FDP and pyridinium adducts when acrolein aldehyde was incubated with a synthetic peptide; while other studies [28, 29, 53] confirm the

dominance of the pyridinium adduct over other adducts. Our results for the incubation of 2-alkenals with protein (Figure 3.29 for 2-pentenal results) confirm the earlier observation where FDP and pyridinium adducts are dominant over other adducts. However, all Pne-Lys adducts disappeared at 5mM aldehyde concentration.

Arginine modifications are limited to Schiff base and Michael adducts; Table 3-20 shows the aldehyde concentration limits for different arginine 2-alkenal adducts. In comparison to the corresponding adducts for lysine, there is no significant difference in the aldehyde concentration required for the formation of the Schiff base and Michael adducts for arginine. Some of the arginine Michael adducts have a lower aldehyde concentration limit than Schiff base limit (e.g. Hxe-Arg-M), while others have higher aldehyde concentration limit than Schiff base limit (e.g. Cro-Arg-M). In comparison to lysine and arginine Michael-adducts, histidine-Michael adducts seem to be more readily formed at a lower aldehyde concentration (*ca*. 5mM) than those required for the formation of lysine and arginine adducts (Table 3-21).

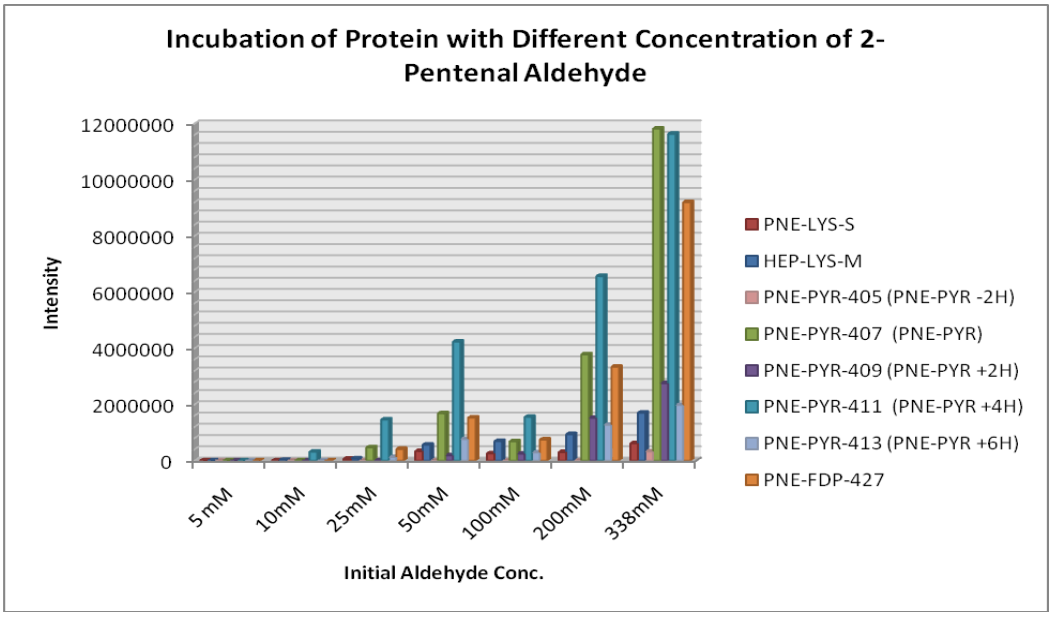

Figure 3.29: Comparison between the average intensity of different Pne-Lys adducts which results from the incubation of protein samples (2.5 mg/ml) with 2-pentenal aldehyde by the addition of 11 µl of 2-pentenal at different initial concentrations of 5, 10, 25, 50, 100, 200, and 338mM.

The specified concentration limits for the production and detection of different 2-alkenal adducts could be a reasonable justification for the inability to detect these adducts in plasma samples from normal individuals or from diabetic patients with slightly elevated aldehyde levels. By considering the assigned limit for the different aldehydes, all adducts required greater aldehyde concentrations than that which may be available in the biological system to produce a significant amount of 2-alkenal adducts for RPLC-FTMS detection, with the exception of the histidine adducts. However, histidine is present in a relatively low amount in the HSA molecule, 2.6% as specified by Swiss Institute of Bioinformatics [154], which may be the possible reason for the lack of a sufficient amount of adduct to produce a signal in the mass spectrometer. In general, Schiff base and Michael adducts of different amino acids that are modified with acrolein aldehyde could not be detected in some samples, as discussed previously, due to the possibility of the further modification to a more complex form. Figure 3.30 shows the disappearance of the lysine amino acid peak in the total ion chromatograms when a protein sample was incubated with increasing acrolein concentrations.

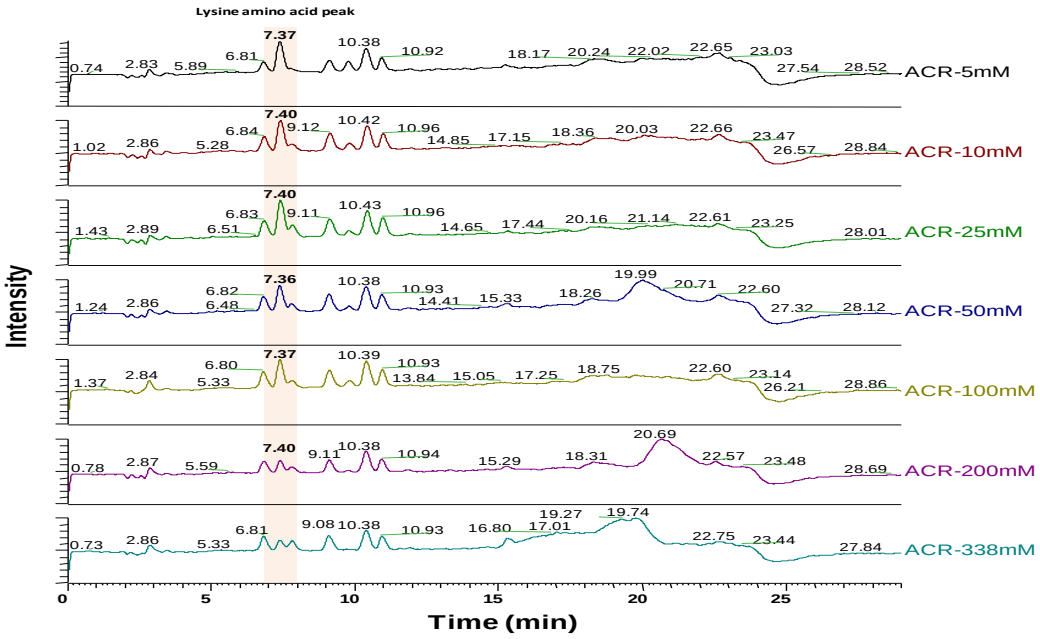

Figure 3.30: The response for the lysine peak over different acrolein concentrations using EZ:faast method and RPLC-ESI-FTMS.

3.9 Percentages of 2-Alkenal Adducts in HSA Hydrolysate Samples

Calculating the percentage of different 2-alkenals adducts according to mass spectrometry detection is based on 3 assumptions. Firstly, equal response factors for 2-alkenal adducts and the parent amino acid has been assumed for the mass spectrometry detection process. Secondly, amino acids (lysine, arginine, and histidine) residues in a protein molecule are assumed to undergo specific types of modifications when incubated with different 2-alkenals; these modifications may include: Schiff base, Michael adduct, pyridinium and FDP adducts. Finally, all the chemical reactions of 2-alkenals with amino acid residues in the protein sample, and the subsequent extraction and derivatisation protocol were reproducible. These assumptions enabled the calculation of the modification percentages for each basic amino acid residue within a protein molecule. Certainly this represents only a very rough approximation but it does allow for some insight into the degree of modification occurring.

In each protein sample which had been modified with 2-alkenals, the detected free amino acid (lysine, arginine, and histidine) is considered as the remaining amount after modification and formation of 2-alkenal adducts related to that amino acid. For example, incubation of the protein sample with 2-hexenal aldehyde returned the results shown in (Table 3-22) for lysine amino acid together with its related adducts.

The percentage of each compound was calculated according to the peak area of that compound, for example: the percentage for the remaining lysine could be calculated by dividing the peak area for the observed lysine (in each injection) by the total peak area for lysine and its related adducts (in each injection) multiplied by 100%. Each sample has been injected twice to minimise the errors; Mean 1 (%) = [Peak Area 1A (%) + Peak Area 1A (%)]/2. Then the average (%) for remaining lysine was calculated from the mean of the 2 samples; Average (%) = [Mean 1(%) + Mean 2 (%)]/2. The same calculations were carried out for all lysine, arginine, and histidine adducts.

It is quite obvious from Table 3-22 that there is a fluctuation in the percentage of the amino acid and its related adducts from one injection to another, or from one sample to another. This can be explained by different chemical conditions in different samples that may favour the formation of certain adducts over other types in different samples, or could results from instrument fluctuation in different injections. Table 3-23 shows the average percentage for each 2-alkenal adduct in comparison to the parent amino acid (lysine, arginine and histidine) as calculated according to the procedures described in Table 3-22 for 2-hexenal adducts.

Table 3-22: Method used for calculating the average % for 2-alkenal adducts using 2 repeated injections for sample #1 and #2. **Peak area (%)** = 100% * (Peak Area/Total Peak Area). **Mean (%)** = [Peak Area 1A (%) + Peak Area 1B (%)]/2. **Average (%)** = [Mean 1 (%) + Mean 2 (%)]/2. **SE Mean** = STDEV/√N N=2

	Sample #1					*Sample #2*				
Type of adduct	***Peak Area 1A***	***Peak Area 1A (%)***	***Peak Area 1B***	***Peak Area 1B (%)***	***Mean 1 (%)***	***Peak Area 2A***	***Peak Area 2A (%)***	***Peak Area 2B***	***Peak Area 2B (%)***	***Mean 2 (%)***
Remaining Lysine	1.93E+09	90.04	1.97E+09	89.95	90.00	1.95E+09	90.62	1.99E+09	90.34	90.48
Hxe-Lys-M	2.11E+07	0.98	2.24E+07	1.02	1.00	1.72E+07	0.80	1.82E+07	0.83	0.81
Hxe-Lys-S	5.51E+06	0.26	6.34E+06	0.29	0.27	6.08E+06	0.28	7.00E+06	0.32	0.30
Hxe-pyr-433	4.15E+05	0.02	3.98E+05	0.02	0.02	1.12E+05	0.01	1.08E+05	0.00	0.01
Hxe-pyr-435	4.74E+07	2.21	4.29E+07	1.96	2.09	3.48E+07	1.61	3.15E+07	1.43	1.52
Hxe-pyr-437	4.16E+07	1.94	4.88E+07	2.23	2.08	6.25E+07	2.90	7.33E+07	3.32	3.11
Hxe-pyr-439	6.77E+07	3.16	6.91E+07	3.15	3.16	6.30E+07	2.92	6.43E+07	2.91	2.92
Hxe-pyr-441	6.20E+06	0.29	6.08E+06	0.28	0.28	3.89E+06	0.18	3.81E+06	0.17	0.18
Hxe-FDP-455	2.36E+07	1.10	2.41E+07	1.10	1.10	1.46E+07	0.68	1.49E+07	0.68	0.68
Total =	2.14E+09	100.00	2.19E+09	100.00	100.00	2.16E+09	100.00	2.21E+09	100.00	100.00

Type of adduct	***Average (%)***	***STDEV***	***SE mean***
Remaining Lysine	**90.24**	**0.24**	**0.17**
Hxe-Lys-M	**0.91**	**0.10**	**0.07**
Hxe-Lys-S	**0.29**	**0.01**	**0.01**
Hxe-pyr-433	**0.01**	**0.01**	**0.00**
Hxe-pyr-435	**1.80**	**0.28**	**0.20**
Hxe-pyr-437	**2.60**	**0.51**	**0.36**
Hxe-pyr-439	**3.04**	**0.12**	**0.08**
Hxe-pyr-441	**0.23**	**0.05**	**0.04**
Hxe-FDP-455	**0.89**	**0.21**	**0.15**
Total =	**100.00**		

Schiff base adducts for lysine show the lowest percentages as compared to Michael, pyridinium and FDP adducts. In contrast, pyridinium adducts as a total (reduced and non reduced forms) constitute the highest percentages amongst different lysine adducts. This supports the idea that Schiff base reaction is a transitional step in the reaction leading to the formation of other adducts [60]. Nevertheless, lysine and arginine amino acids show less modification as compared to histidine amino acids (less than 10%), with the exception of protein samples which had been incubated with acrolein and 2-heptenal aldehydes where lysine shows a high percentage of modification, as high as *ca.* 35% and 18%, respectively. Uchida *et al.* (1998) [136] reports high reactivity for acrolein aldehyde, using an immuno-assay test, as compared to other biological aldehydes; our research results shown in Table 3-23 confirm the high reactivity of acrolein aldehyde when incubated with protein samples as compared to other aldehydes.

Histidine shows the highest level of modification as compared to lysine and arginine amino acids. The percentages of the histidine adducts range between 36% and 88%, compared with histidine amino acid from the HSA hydrolysate in most of the cases where protein incubated with 2-alkenals (with the exception of 2-pentenal samples which showed 19% modification only). However, the low availability of histidine in tissues throughout the body [139] is a reasonable justification for the inability to detect histidine adducts in biological samples, despite its high reactivity, as indicated by our research results in Table 3-23. Tang *et al.* (2007) [139] suggest using a histidine analogue as a scavenger for toxic aldehydes such as HNE, due to the ability of the histidine analogues to react with these aldehydes preventing their harmful effects.

Table 3-23: Percentage of the derivatised 2-Alkenal Adducts in relation to the remaining amino acid in HSA. N=4

Type of adduct	Average %	*Type of adduct*	Average %	*Type of adduct*	Average %
Remaining Lysine	64.434	*Remaining Lysine*	93.118	*Remaining Lysine*	92.184
Acr-Lys-M	0.249	*Cro-Lys-M*	0.513	*Pne-Lys-M*	0.666
Acr-Lys-S	0.015	*Cro-Lys-S*	0.081	*Pne-Lys-S*	0.133
Acr-pyr-349	2.096	*Cro-pyr-377*	0.001	*Pne-pyr-405*	0.077
Acr-pyr-351	4.407	*Cro-pyr-379*	0.260	*Pne-pyr-407*	2.242
Acr-pyr-353	3.322	*Cro-pyr-381*	1.235	*Pne-pyr-409*	0.196
Acr-pyr-355	10.732	*Cro-pyr-383*	3.258	*Pne-pyr-411*	2.122
Acr-pyr-357	5.552	*Cro-pyr-385*	1.421	*Pne-pyr-413*	0.424
Acr-FDP-371	9.193	*Cro-FDP-399*	0.113	*Pne-FDP-427*	1.956
Type of adduct	Average %	*Type of adduct*	Average %	*Type of adduct*	Average %
Remaining Arginine	99.891	*Remaining Arginine*	95.967	*Remaining Arginine*	93.304
Acr-Arg-M	0.081	*Cro-Arg-M*	1.833	*Pne-Arg-M*	3.342
Acr-Arg-S	0.028	*Cro-Arg-S*	2.200	*Pne-Arg-S*	3.354
Type of adduct	Average %	*Type of adduct*	Average %	*Type of adduct*	Average %
Remaining Histidine	63.000	*Remaining Histidine*	80.580	*Remaining Histidine*	63.850
Acr-His-M	37.000	*Cro-His-M*	19.420	*Pne-His-M*	36.150

2-Hexenal		*2-Heptenal*		*2-Nonenal*	
Type of adduct	Average %	*Type of adduct*	Average %	*Type of adduct*	Average %
Remaining Lysine	90.240	*Remaining Lysine*	82.763	*Remaining Lysine*	93.324
Hxe-Lys-M	0.905	*Hpe-Lys-M*	0.874	*Nne-Lys-M*	0.480
Hxe-Lys-S	0.286	*Hpe-Lys-S*	0.172	*Nne-Lys-S*	0.099
Hxe-pyr-433	0.012	*Hpe-pyr-461*	0.239	*Nne-pyr-517*	0.121
Hxe-pyr-435	1.802	*Hpe-pyr-463*	6.222	*Nne-pyr-519*	2.577
Hxe-pyr-437	2.600	*Hpe-pyr-465*	1.851	*Nne-pyr-521*	0.806
Hxe-pyr-439	3.036	*Hpe-pyr-467*	3.902	*Nne-pyr-523*	1.003
Hxe-pyr-441	0.230	*Hpe-pyr-469*	0.558	*Nne-pyr-525*	0.164
Hxe-FDP-455	0.889	*Hpe-FDP-483*	3.419	*Nne-FDP-539*	1.426
Type of adduct	Average %	*Type of adduct*	Average %	*Type of adduct*	Average %
Remaining Arginine	91.358	*Remaining Arginine*	87.820	*Remaining Arginine*	90.410
Hxe-Arg-M	6.606	*Hpe-Arg-M*	12.179	*Nne-Arg-M*	8.000
Hxe-Arg-S	2.036	*Hpe-Arg-S*	0.001	*Nne-Arg-S*	1.590
Type of adduct	Average %	*Type of adduct*	Average %	*Type of adduct*	Average %
Remaining Histidine	56.142	*Remaining Histidine*	12.000	*Remaining Histidine*	46.000
Hxe-His-M	43.858	*Hpe-His-M*	88.000	*Nne-His-M*	54.000

3.10 Determination of Limit of Detection (LOD) and Limit of Quantification (LOQ) for 2-Alkenals Adducts Using the RPLC-FTMS

An exact expression should be used to define LOD and LOQ for the Orbitrap instrument, since it is difficult to define LOD and LOQ in a proper way in high resolution mass spectrometry LC-FTMS. Orbitrap parameters will discard background ions together with some of the analyte ions which fall below a certain threshold in order to avoid overfilling the trap with background ions. As a result, the LOD is defined as the last concentration which could be detected before the signal disappeared. A golden rule was set to differentiate between LOD and LOQ, where LOD was defined as the last concentration where the peak could be observed with 3 main criteria: (1) the observed mass should be within ±5ppm deviation from the theoretical mass, (2) with an average intensity more than 1.50 E+4, (3) and with at least 3 scans across the peak. This definition for LOQ allows enough confidence when quantifying a certain compound with the Orbitrap. If the observed peak failed to fulfil these requirements, the observed peak was considered as the LOD instead of the LOQ. Figure 3.31 explains the definition of LOD and LOQ for histidine in a serial dilution series of an amino acids mixture using HILIC-FTMS analysis. The peak on the right has been assigned as LOQ for histidine as it shows an average intensity of 1.63 E+4 with 4 scans cross the peak each of which fall within ±5ppm deviation from the theoretical mass for histidine. The peak on the left failed to fulfil the requirements and was assigned as the LOD for histidine.

A stock dilution method for the modified protein samples was designed to examine the LOD and LOQ for different 2-alkenal adducts. A stock solution consisting of 2.5 mg/ml human serum albumin (HSA) in phosphate buffer saline solution (PBS) at pH 7.4 was incubated with 11 μl of 338 mM solutions of the 2-alkenal series and processed in the usual way according to the procedure described in section 2.3.2. A hydrolysis process for the modified protein sample with 6N HCl will result in the formation of the protein hydrolysate with a protein content what is equivalent to 1.178 mg/ml; this protein

hydrolysate had been assigned as stock solution for the dilution series required for LOD and LOQ determination.

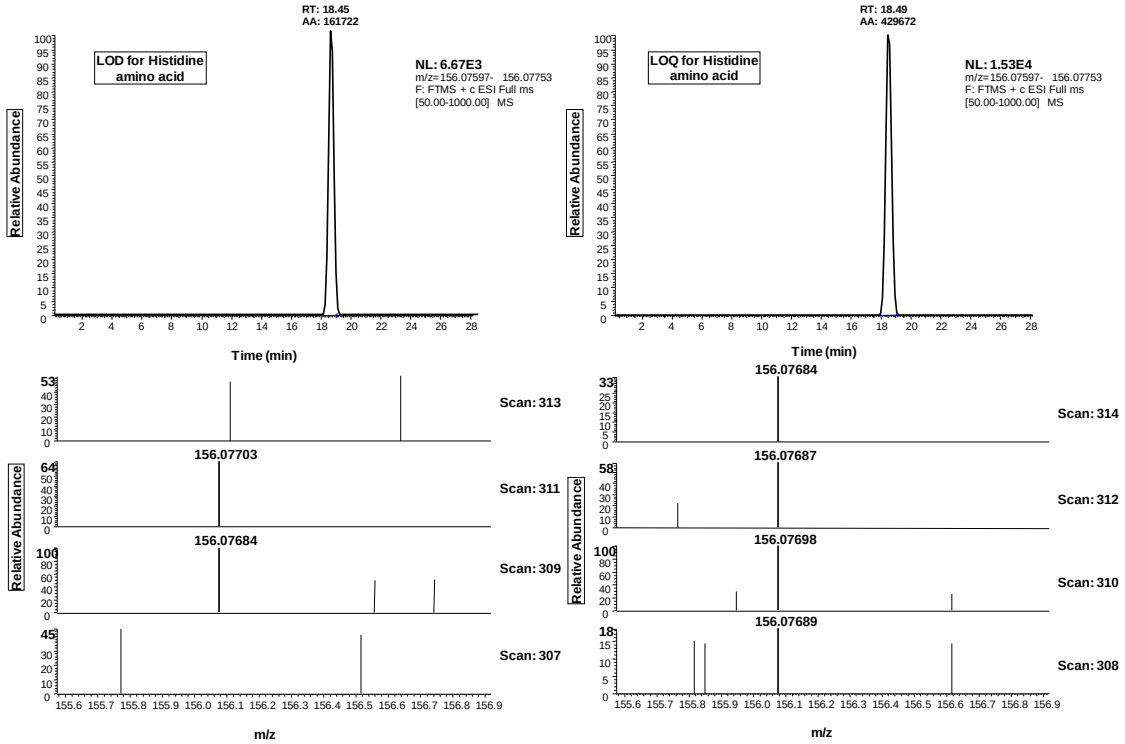

Figure 3.31: LOD and LOQ definition for non-derivatised histidine using ESI-FTMS analysis.

Before starting with the EZ:faast method, a dilution steps for the stock solution was carried out in order to prepare a series of diluted solutions for the protein hydrolysate at 0.943, 0.471, 0.236, 0.118, 0.047, and 0.024 mg/ml or what is equivalent to an initial protein concentration (without hydrolysis) of 2, 1, 0.5, 0.25, 0.1, and 0.05 mg/ml, respectively. Following the dilution law equation,

$$C1 * V1 = C2 * V2$$

Where C1 is the initial concentration of the stock solution, in this case it will be protein hydrolysate with a concentration of 1.178 mg/ml (equivalent to initial protein concentration of 2.5 mg/ml without hydrolysis), C2 is the required standard concentration, which is either 0.943 (2), 0.471 (1), 0.236 (0.5), 0.118 (0.25), 0.047 (0.01), and 0.024 (0.05) mg/ml; the numbers in the brackets represent the initial protein

concentration without hydrolysis. V2 is the volume for the required standard concentration, and V1 is the volume that should be pipetted from the stock solution and diluted to V2 with phosphate buffered saline solution (pH 7.4) in order to achieve the intended standard concentration, C2. The EZ:faast method is used as the main part of the analytical process for amino acids and 2-alkenal adducts detection according to the procedure in section 2.4.1. The EZ:faast method requires 100 µl from the dilution series (1.18, 0.94, 0.47, 0.24, 0.12, 0.05, and 0.02 mg/ml) to do extraction and derivatisation processes for amino acids and 2-alkenal adducts. As a result of that, V2 is assigned as 100 µl in the dilution law, which is the volume required for extraction and derivatisation processes with the EZ:faast method. The dilution table is shown in Table 3-24.

Table 3-24: Preparation of a dilution series from an original stock solution of protein hydrolysate. C refers to the concentration in mg/ml whereas V refers to the volume in µl. The numbers in the brackets represents the initial protein concentration without hydrolysis

C1 (mg/ml)	*C2 (mg/ml)*	*V2 (µl)*	*V1 (µl)*	*Required dilution volume of PBS in (µl)*
1.18 (2.5)	**0.94 (2)**	**100**	**80**	**20**
1.18 (2.5)	**0.42 (1)**	**100**	**40**	**60**
1.18 (2.5)	**0.24 (0.5)**	**100**	**20**	**80**
1.18 (2.5)	**0.12 (0.25)**	**100**	**10**	**90**
1.18 (2.5)	**0.05 (0.1)**	**100**	**4**	**96**
1.18 (2.5)	**0.02 (0.05)**	**100**	**2**	**98**

Finally, the standard solutions were ready for extraction and derivatisation with the EZ:faast method and analysis with LC-MS. Several steps are required in order to determine the LOD for each adduct; these are: determine the dilution factor for the EZ:faast method, determine the amount of protein injected in 10 µl to LC-MS, determine the percentage of each amino acid in the protein sample, and finally calculate LOD and LOQ using the percentage of each adduct [section 3.9] in relation to its inherent amino acid content.

3.10.1 Calculation of Dilution Factor for the EZ:faast Method and the Amount of Protein Injected on C-18 Column

The amount of protein in 10 µl of 2.5 mg/ml of protein sample (HSA or BSA) being injected into LC-MS should contain 655 ng of protein after being extracted and derivatised with the EZ:faast method according to the following steps. First, to make acid hydrolysis with 6N HCl, 0.4 ml of 2.5 mg/ml of protein solution being pipetted into 10ml test tube followed by the addition of 11 µl of aldehyde, 37.5 µl of $NaBH_4$, and 400 µl of 6N HCl to give a total volume of 0.8485 ml. so the final concentration will be:

2.5 mg/ml * 0.4 ml = Y * 0.8485 ml $\Longrightarrow$ Y = 1.1786 mg/ml

For the EZ:faast method, 0.1 ml of protein hydrolysate was diluted with 0.2 ml of reagent 2 from the EZ:faast kit, which consists of sodium carbonate solution. So, there will be a dilution to a total volume of 0.3 ml and the concentration of protein will

1.1786 mg/ml * 0.1 ml= Y * 0.3 ml $\Longrightarrow$ Y= 0.3928 mg/ml = 392.85 µg/ml

Pipette 0.05 ml of this solution to make the EZ:faast extraction with the EZ:faast tips. So, the amount of protein in this 0.05 ml will be:

392.85 µg/ml * 0.05 ml= 19.6425 µg in the 50 µl of the protein sample.

The process of the EZ:faast method includes: extraction, derivatisation and liquid-liquid extraction. In the liquid-liquid extraction step, the addition of 50 µl of reagent 4 and 100 µl of reagent 5 will constitute a total volume of 150 µl of organic layer. So, the total amount of protein (19.6 µg) would be dissolved in 150 µl of the upper layer (organic layer), based on the assumption that 100% recovery could be achieved by extraction and derivatisation step for the EZ:faast method. An aliquot (50 µl) from this upper layer was pipetted into a HPLC vial, which will contain protein hydrolysate equivalent to 6.5475 µg. The sample was then evaporated under a slight nitrogen gas stream until dry, and

then re-dissolved in 100 µl of mobile phase. So, the final concentration of protein before injection would be:

6.5 µg/ 0.1 ml= 65.5 µg/ml

So the final amount of protein that will be analysed by LC-MS will be (65.476 µg/ml * 0.01 ml = 0.65475 µg = 654.75 ng) of protein sample which will be injected onto C-18 for RPLC-FTMS detection.

C (mg/ml) * 26.19 = µg/ml the final concentration of before injection on C-18 column for RPLC-FTMS analysis

C is the initial concentration of protein (mg/ml) before acid hydrolysis and the EZ:faast method; while 26.19 represents a dilution factor for the whole process of protein samples treatment which starts by incubating 400 µl of the protein sample with 11 µl of aldehydes and finish by the last step before injecting the protein sample onto C-18 column for RPLC-FTMS detection, including reduction and acid hydrolysis steps.

Table 3-25: Amounts of protein in a 10 µl aliquot of the diluted protein solution series that are injected into the LC-MS.

Initial concentration (mg/ml)	Dilution factor for the EZ:faast	Final concentration (µg/ml)	Amount of protein in 10µl injected on C-18 Column (ng)
2.5	26.19	65.475	654.75
2	26.19	52.38	523.8
1	26.19	26.19	261.9
0.5	26.19	13.095	130.95
0.25	26.19	6.5475	65.475
0.1	26.19	2.619	26.19
0.05	26.19	1.3095	13.095

Table 3-25 shows the final amount of protein in ng that would be injected in 10 µl aliquot onto C-18 column, for different initial protein concentrations, whereas Table 6-9 shows the % of the amino acids in HSA molecule based on the information reported by the Swiss Institute of Bioinformatics [154]. Furthermore, side chain properties such as polarity, acidity or basicity are also shown in the same table.

3.10.2 LOD & LOQ

Depending on the information and results achieved in sections 3.9, 3.10, and 3.10.1, the LOD and LOQ for different 2-alkenal adducts in a dilution series could be determined using the rules for LOD and LOQ which have been discussed in section 1.6. Table 6-10 to Table 6-15 show the approximate LOD and LOQ values for lysine, arginine, and histidine together with their related adducts. LOD and LOQ for amino acids could be calculated by multiplying the amount of protein that would be injected in 10 µl on C-18 column by the percentage of the amino acid in the protein molecule, for example lysine amino acid LOD= 13.1ng* 9.85/100=1.289 ng. The LOD and LOQ for the amino acids were determined using a protein sample which had not been incubated with 2-alkenals, whereas LOD and LOQ for 2-alkenal adducts were determined using protein samples which had been incubated with 2-alkenals aldehydes. LOD or LOQ for 2-alkenal adducts were calculated by multiplying the percentage of adduct by the percentage of the related amino acid by the amount of protein injected on C-18 column, for example Acr-Lys-Michael LOD= 261ng * (9.85/100) * (0.249/100) = 274*9.85*0.249/10000=0.0640 ng. The LOD values for most of the 2-alkenal adducts have been estimated within sub-nanogram level, whereas the LOQ values for most of these adducts could be detected as 2 times the LOD for that adduct.

3.11 Detection of Adducts in Samples of Plasma Protein Using the EZ:faast Method

Plasma samples from the Queen's Medical Research Institute, University of Edinburgh were prepared according to the procedure described in section 2.6. Both the supernatant and the precipitate were examined for the 2-alkenal adducts. Full scan mass spectrometry for plasma samples revealed a number of 2-alkenal adducts listed in Table 3-26 and Table 3-27, for the precipitate and the supernatant layers, after hydrolysis and the derivatisation process. These plasma samples had been treated according to the procedure for protein extraction from plasma samples described in section 2.6.

Table 3-26: MS detection for the derivatised 2-alkenals adducts in plasma samples from obese patients usin RPLC-ESI-FTMS. These adducts had been recovered from the the precipitate layer for the plasma samples after reduction, acid hydrolysis and derivatisation steps.

Adduct	*R_t control (min)*	*R_t (min)*	*Observed m/z*	*Intensity*	*ppm*	*Sample I.D*	*Status*
Acr-ppy-351	**2.77**	**2.38**	**351.22845**	**2.69E+04**	**0.616**	**11BAS40**	**2 Spikes**
		2.37	**351.22769**	**1.44E+04**	**-0.144**	**8AAS40**	**2 Spikes**
Pne-pyr-407	**3.56**	**3.83**	**407.29065**	**3.28E+04**	**0.215**	**9BBS40**	**Significant**
		3.84	**407.29117**	**5.12E+04**	**0.735**	**10AAS40**	**Significant**
		3.83	**407.29117**	**2.67E+04**	**0.735**	**11BAS40**	**Significant**
		3.86	**407.29056**	**9.81E+04**	**0.125**	**12BAS40**	**Significant**
		3.84	**407.29086**	**4.20E+04**	**0.425**	**3ABS40**	**Significant**
		3.84	**407.29068**	**2.03E+04**	**0.245**	**4BBS40**	**Significant**
		3.83	**407.29077**	**5.70E+04**	**0.335**	**5ABS40**	**Significant**
		3.86	**407.29071**	**8.64E+04**	**0.275**	**6AAS40**	**Significant**
		3.86	**407.29144**	**2.39E+04**	**1.005**	**7ABS40**	**Significant**
		3.84	**407.29071**	**1.28E+05**	**0.275**	**8AAS40**	**Significant**
		3.87	**407.29123**	**2.46E+04**	**0.795**	**13BAS40**	**3 Spikes**
		3.86	**407.29141**	**2.01E+04**	**0.975**	**2BAS40**	**One Spike**
Hpe-Arg-S	**4.64**	**4.39**	**399.29611**	**1.78E+04**	**-0.473**	**3ABS40**	**One Spike**

Although some of these could not be quantified as they failed to fulfil the requirement of the golden rule for LOQ that "LOQ peaks should have a minimum intensity of 1.5 E+4 and a minimum of 3 scans across the peak and should be within 5 ppm deviation from the theoretical mass"; other peaks which fulfilled these requirements had been assigned as significant peaks. Other peaks could not fulfil the criterion of "3 scans across the peak" despite enough intensity and being within 5 ppm deviation; the number of scans across each peak has been listed in Table 3-26 & Table 3-27.

The identity of these adducts was confirmed by: (1) narrow mass window for the compound with less than 5ppm deviation, (2) retention time as compared to a standard, (3) comparing the mass spectra for the adduct with a simulation for the exact mass for that adduct, and finally (4) MS^2 fragmentation. Simulation can provide useful information about the isotopic distribution for the compounds, especially ^{13}C intensity expected for a particular adduct. Due to low intensity for 2-alkenal adducts in plasma samples, the ^{13}C isotope peak could not be detected in all of these adducts.

Table 3-27: MS detection for the derivatised 2-alkenals adducts in plasma samples from obese patients using the EZ:faast method and RPLC-ESI-FTMS. These adducts had been recovered from the the supernatant layer for the plasma samples after reduction, acid hydrolysis and derivatisation steps.

Adduct	*R_t control (min)*	*R_t (min)*	*Observed m/z*	*Intensity*	*ppm*	*Sample I.D*	*Status*
Acr-pyr-351	2.77	2.38	351.22815	3.55E+04	0.899	9BBS40	Significant
Cro-pyr-379	3.08	2.85	379.25925	1.85E+04	0.305	10AAS40	One Spike
		2.71	379.25943	2.16E+04	0.779	11BAS40	One Spike
		2.74	379.25995	2.03E+04	2.15	5ABS40	One Spike
		2.8	379.2601	2.04E+04	2.546	9BBS40	One Spike
Cro-pyr-383	3.56	3.89	383.29083	1.89E+04	1.032	11BAS40	One Spike
Pne-Arg-M	3.24	3.74	389.27576	1.86E+04	-0.224	7ABS40	One Spike
Pne-Arg-S	3.33	3.22	371.26553	2.02E+04	0.667	9BBS40	One Spike
		3.64	371.26529	1.69E+04	0.02	10AAS40	One Spike
		3.7	371.26547	1.82E+04	0.505	11BAS40	One Spike
		3.71	371.26535	2.20E+04	0.182	8AAS40	One Spike
Pne-pyr-407	3.56	3.84	407.29089	3.63E+05	1.118	9BBS40	Significant
		3.86	407.29047	3.31E+04	0.087	10AAS40	Significant
		3.85	407.29092	2.26E+05	1.192	11BAS40	Significant
		3.83	407.29089	3.41E+04	1.118	12BAS40	Significant
		3.85	407.29102	5.56E+04	1.437	13BBS40	Significant
		3.82	407.29074	5.36E+04	0.75	2BAS40	Significant
		3.85	407.2905	4.20E+04	0.161	3ABS40	Significant
		3.83	407.29099	1.06E+05	1.364	4BBS40	Significant
		3.83	407.29007	2.36E+04	-0.895	5ABS40	Significant
		3.8	407.29071	3.32E+04	0.676	6AAS40	Significant
		3.86	407.29065	1.65E+04	0.529	7ABS40	Significant
		3.86	407.28998	2.37E+04	-1.116	8AAS40	Significant
Pne-pyr-409	3.69	3.54	409.30542	1.65E+04	-1.624	4BBS40	One Spike
Hxe-His-M	3.12	2.75	384.25092	1.56E+04	4.221	9BBS40	One Spike
Hxe-pyr-439	5.43, 6.02, 6.60, 7.36	5.96, 6.24	439.35263	2.18E+04	-0.922	12BAS40	One Spike
Hpe-Arg-M	4.03	4.78	417.30676	1.67E+04	-0.928	13BBS40	One Spike
		4.57	417.3078	1.60E+04	1.564	3ABS40	One Spike
		4.76	417.30737	1.98E+04	0.534	7ABS40	One Spike
Hpe-Lys-S	4.75, 5.12	5.34	371.28983	1.78E+04	-1.628	2BAS40	One Spike
		4.72	371.28931	1.84E+04	-3.029	9BBS40	One Spike
Hpe-pyr-461	5.38, 6.19, 7.28, 8.06	6.18	461.33713	1.58E+04	-0.552	9BBS40	One Spike
		6.92	461.33838	2.22E+04	2.157	3ABS40	One Spike
Hpe-pyr-469	9.33, 10.09, 11.25	9.85, 10.96	469.39993	1.69E+04	-0.117	9BBS40	One Spike
		11.46	469.39853	1.88E+04	-3.1	13BBS40	One Spike
Nne-Lys-M	5.68/6.29	6.05	417.33249	1.92E+04	0.457	10AAS40	One Spike
		5.54/6.68	417.33228	1.90E+04	-0.047	4BBS40	2 Spikes
Nne-Lys-S	7.42/8.36	7.67	399.32129	1.69E+04	-1.114	2BAS40	One Spike
		8.57	399.32144	1.83E+04	-0.738	6AAS40	One Spike
Nne-pyr-519	14.14	14.76	519.41583	2.55E+04	0.375	11BAS40	One Spike
		14.79	519.41418	2.08E+04	-2.802	8AAS40	One Spike
		14.61	519.41351	2.52E+04	-4.092	9BBS40	One Spike
Nne-pyr-521	12.81, 14.00, 14.44, 15.80	15.55	521.43146	3.04E+04	0.335	9BBS40	One Spike
		15.6	521.43298	2.03E+04	3.25	4BBS40	One Spike
Nne-pyr-525	14.46, 15.57	15.49	525.46228	2.24E+04	-0.581	12BAS40	One Spike
Nne-Arg-M	6.52	6.49	445.3378	1.82E+04	-1.454	2BAS40	2 Spikes
Nne-Arg-S	7.34/7.70	7.83	427.32794	1.87E+04	0.134	13BBS40	One Spike

Nevertheless, Figure 3.32 shows the mass chromatograms and spectra for the ^{12}C monoisotopic peak for Pne-pyr-407 adduct in a plasma sample with the ID 12BAS40 from the precipitate layer. Also the identity of such peak was confirmed by the presence of similarity for the ^{13}C peak and spectra between the detected and the simulated one. However, the detection of ^{13}C isotope peak failed for the other peaks although there was enough intensity to have seen it. For example, Acr-pyr-351 adduct could be detected in enough intensity in the plasma sample with the ID#11BAS40 from the supernatant layer (Figure 3.33).

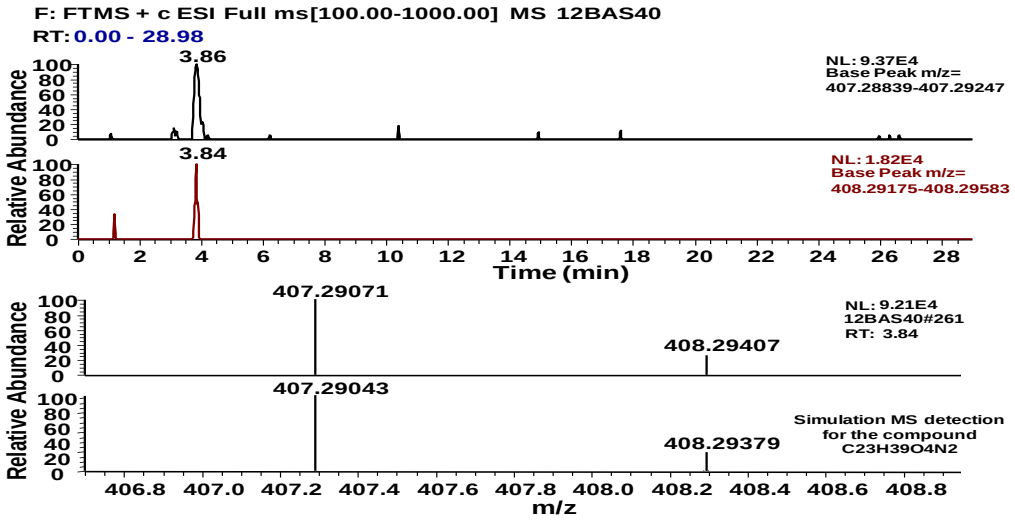

Figure 3.32: Full mass spectrometry detection for derivatised Pne-pyr-407 pyridinium adducts in plasma using the EZ:faast method and RPLC-ESI-FTMS. Upper chromatogram shows the peak for the monoisotopic peak for the ^{12}C adduct while the lower chromatogram shows the monoisotopic peak for the ^{13}C adduct. Upper spectra shows the real mass spectra at a retention time 3.84 min while the lower spectra shows the simulation for the mass spectra for Pne-pyr-407 adduct.

Additionally, MS^2 fragmentation was used as a method to confirm the identity of 2-alkenal adducts by comparing MS^2 results with the standard ones. Again, only adducts with high intensity could produce good MS^2 results. Figure 3.34 shows the MS^2 spectrum for pen the pyr adduct in plasma samples from obese patients. By comparing the product ions for this adduct with standard samples (the product ions for the Pne-pyr-407 which had been produced by incubating HSA with 2-pentenal), it is possible to see that both of them follow the same fragmentation pattern by losing propanol (-60 m/z) or propylene and CO_2 moieties (-86 m/z) from the molecular ion.

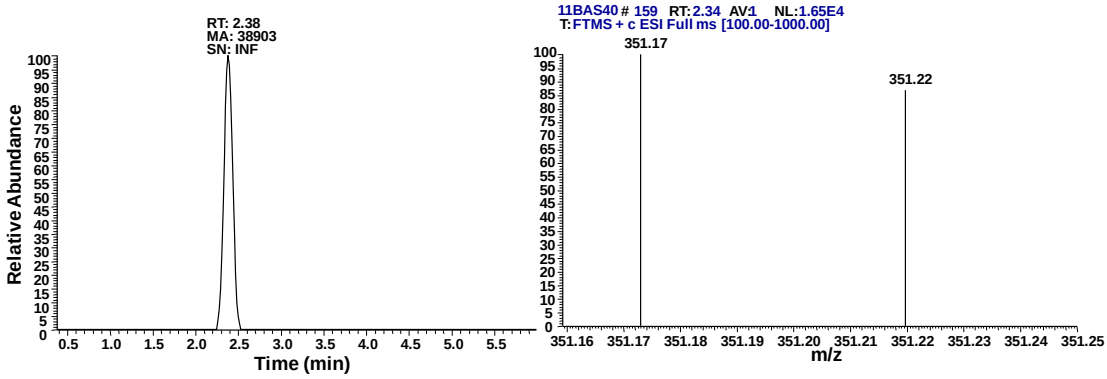

Figure 3.33: Full scan mass spectrometry detection for the derivatised Acr-pyr-351 adducts in plasma samples from obese patients using the EZ:faast method and RPLC-ESI-FTMS.

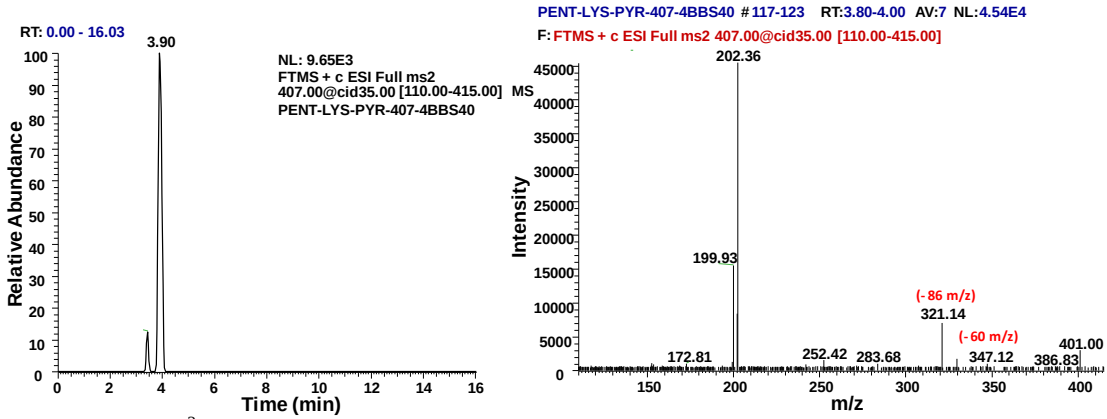

Figure 3.34: MS^2 result for Pne-pyr-407 in a plasma samples from an obese patient using the EZ:faast method and RPLC-ESI-FTMS/MS.

A high number of 2-alkenal adducts could be detected in the supernatant layer rather than the precipitate (protein pellet); this could be attributed to the high free amino acids [155, 156] and peptides [157, 158] content in the human blood samples which allows a high percentage of modification with biological aldehydes. Modification of the amino acid residues in proteins may be prevented by the steric hindrance due to the secondary structure of the protein. As many studies indicate that free amino acids are present in human blood and plasma samples [155, 156, 159-161], the formation of free 2-alkenal adducts that may result from free amino acid modification with biological aldehydes was examined in a non-hydrolysed solution from the supernatant layer. Table 3-28 shows the

results for mass spectrometry detection of 2-alkenal adducts in the supernatant layer in plasma samples from obese patients without a hydrolysis step. Figure 3.35 and Figure 3.36 show the MS detection for the derivatised 2-alkenal adducts (Cro-pyr-379 & Nne-Lys-M adducts) in the supernatant layer of the plasma samples from obese patients.

Table 3-28: MS results for the derivatised 2-alkenals adducts in plasma samples from obese patients using the EZ:faast method and RPLC-ESI-FTMS. These adducts had been recovered from the the supernantant layer for the plasma samples after reduction and derivatisation steps (without hydrolysis step).

Adduct	*R_t control (min)*	*R_t (min)*	*Observed m/z*	*Intensity*	*ppm*	*Sample I.D*	*Status*
Cro-pyr-379	3.08	2.66	379.25839	1.99E+04	-0.744	13BBS40	One Spike
		2.69	379.25864	1.96E+04	-0.494	12BAS40	One Spike
		2.69	379.259	2.51E+04	-1.134	5BAS40	2 Spikes
		2.66	379.25946	2.37E+04	0.326	6AAS40	3 Spikes
		2.68	379.25925	1.66E+04	0.116	7ABS40	Significant
Pne-pyr-407	3.56	3.76	407.28983	5.72E+04	-1.484	11BAS40	Significant
		3.76	407.29025	1.25E+05	-0.453	12BAS40	Significant
		3.73	407.29022	1.26E+05	-0.527	13BBS40	Significant
		3.74	407.29007	3.66E+04	-0.895	2BAS40	Significant
		3.73	407.29089	3.37E+04	1.118	3ABS40	Significant
		3.74	407.28958	5.84E+04	-2.098	4BBS40	Significant
		3.74	407.28958	8.41E+04	-2.098	5ABS40	Significant
		3.8	407.28995	6.72E+04	-1.19	6AAS40	Significant
		3.71	407.28964	8.31E+04	-1.951	7ABS40	Significant
		3.82	407.29019	3.73E+04	-0.601	8AAS40	Significant
		3.83	407.29083	2.24E+04	0.971	9BBS40	2 Spikes
Nne-Lys-M	5.68, 6.29	5.78, 6.11	417.33258	2.14E+04	0.672	10AAS40	One Spike
		5.78	417.33221	1.81E+04	-0.214	12BAS40	One Spike
		5.65	417.33289	1.63E+04	1.415	9BBS40	One Spike

Alhamdani *et al.* [153] reported a very low level for different aldehydes: alkanals, 2-alkenals and 4-hydroxy-2-alkenals in normal individuals as compared to uremic patients [section 3.8]. The levels of such aldehydes were within the nM level. However, the aldehyde levels indicated by Alhamdani *et al.* for control and uremic individuals are still insufficient to produce a significant modification in the protein molecule sufficient for detection by mass spectrometry. According to our research [section 3.8], full mass spectrometry in the positive mode failed to detect any protein modification when the

protein samples were incubated with 2-alkenals at a concentration below 5 mM. This could be a possible justification for the inability to detect widespread 2-alkenal adducts in the plasma samples from real patients. However, according to the current method it was possible to observe some adducts. The lowest aldehyde concentration at which some adducts could be detected by MS was still above the aldehyde level indicated by Alhamdani *et al.;* an aldehyde concentration of 134 µM (11 µl of 5M aldehyde diluted with 400 µl of protein solution) was the lowest aldehyde concentration, and below this level the aldehydes failed to produce protein modification sufficient for MS detection.

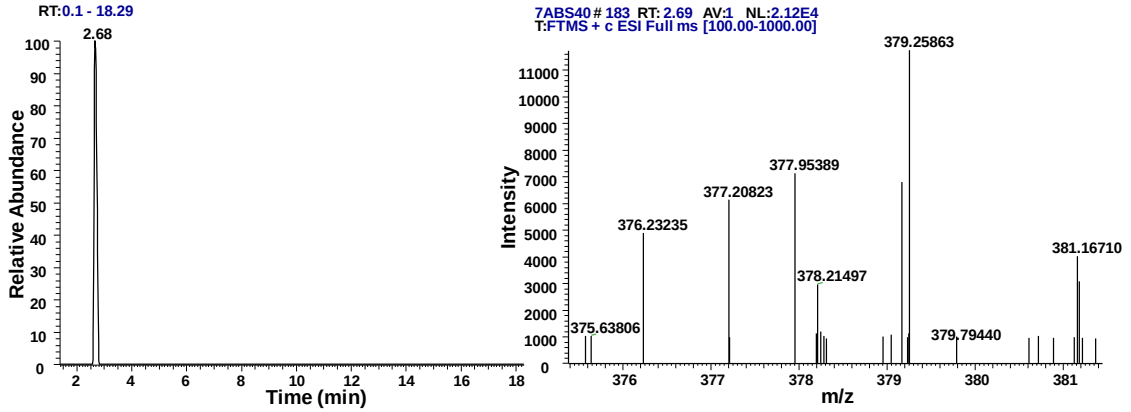

Figure 3.35: Full mass spectrometry in the positive mode for the derivatised Cro-pyr-379 lysine adduct in plasma sample from obese patient using the EZ:faast method and RPLC-ESI-FTMS.

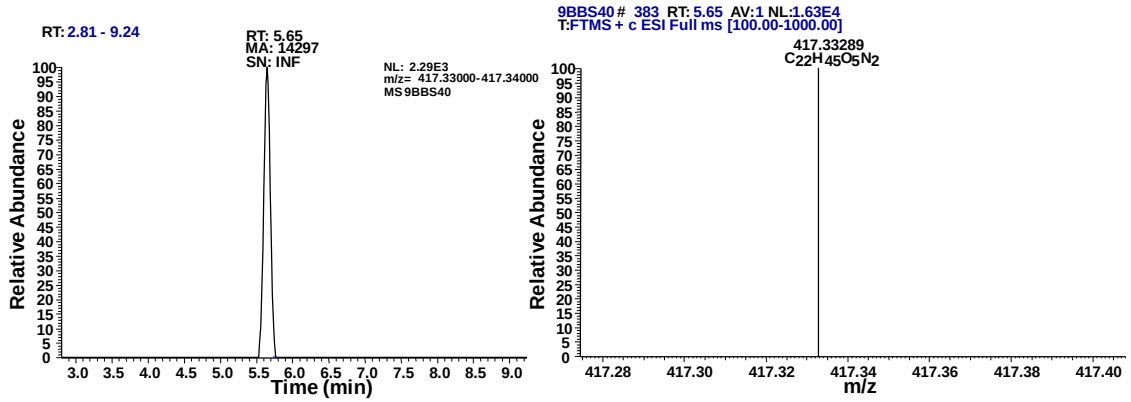

Figure 3.36: Full mass spectrometry in the positive mode for the derivatised Nne-Lys-M adduct in plasma sample from an obese patient using the EZ:faast method and RPLC-ESI-FTMS.

4 CHAPTER FOUR: Results and Discussions for the Analysis of 2-Alkenal Adducts using hydrophilic interaction chromatography (HILIC) and Mass Spectrometry

4.1 Introduction

The detection of 2-alkenal adducts was in the first instance carried out using the EZ:faast method extraction and derivatisation method. The derivatisation step complicates the analysis and can produce multiple products since the amine & carboxyle groups in these adducts were masked by derivatisation. Hence, new chromatographic method was developed where 2-alkenal adducts could be chromatographed and detected without the derivatisation process.

A new technology had been evolved during time based on using hydrophilic interaction liquid chromatography. The original technology was based on bare silica gel; recently a column based on the surface modification of silica gel with a zwitterionic moieties was produce (ZIC-HILIC column from SeQuant) [89]. This column allows retention of hydrophilic compounds without the need for the derivatisation step, which is required to retain hydrophilic compounds on C-18 columns.

4.2 Aims

In this chapter the best extraction, separation and detection methods for non-derivatised amino acids, as well as for non-derivatised 2-alkenal adducts were investigated. In addition, MS^2 fragmentation for non-derivatised amino acids and 2-alkenal adducts will be carried out. Limit of detection (LOD) and limit of quantification (LOQ) for 2-alkenal adducts will also be established.

4.3 Optimisation of the Best Extraction Method for 2-Alkenal Adducts

Exploring the best method for amino acids extraction was carried out by investigating the different extraction methods described in section 2.5, such as solid phase extraction (SPE), liquid-liquid extraction (LLE) and the protein precipitation technique (PPT). Validation for these extraction methods was carried out using 2 types

of amino acid mixture prepared according to the procedure described in section 2.2: standard amino acids mixture (STD stock solution), and an acidified standard amino acid mixture (acidified STD stock solution).

Investigating the best extraction method required examination for the chromatographic and mass spectrometric conditions specified in section 2.5.4.

The mass spectrometric results for the amino acids standards revealed a number of facts. Firstly, different amino acids had different retention times on the ZIC-HILIC column due to differences in the physicochemical properties of these molecules. The elution of amino acids using ZIC-HILIC is divided into 2 areas: area 1 & 2 (Figure 4.1).

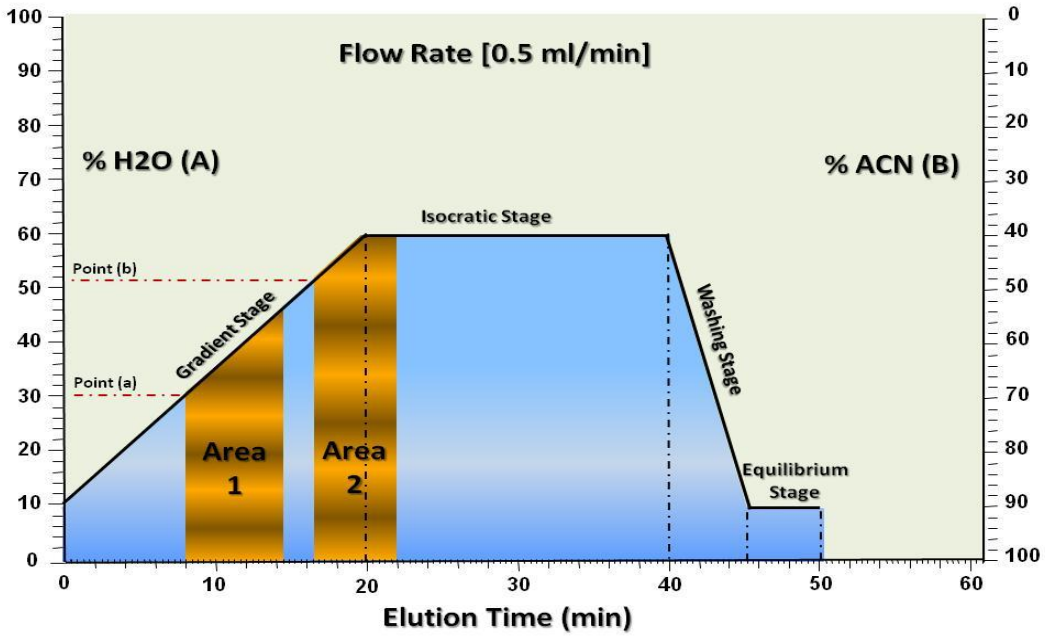

Figure 4.1: Amino acids elution ranges on a ZIC-HILIC column according to the specified chromatographic conditions in section 2.5.4.

Area 1, starts from 8 min and finishes at about 12 min, and consists of the following amino acids, arranged according to their elution time: homo-phenylalanine (I.S), phenylalanine, leucine & iso-leucine, tryptophan, methionine, methionine-d3 (I.S), valine, tyrosine, proline, alanine, glutamic acid, 4-hydroxy-proline, threonine, asparatic acid, glycine, and serine. Area 2 starts at about 17 min and finishes at about 21 min, and

consists of the following amino acids, arranged according to their elution time: cystine, histidine, homo-arginine (I.S), arginine, lysine, and hydroxy-lysine.

For validation purposes, the internal standard (MET-d3) was used as a reference to obtain response factor for the amino acids in area 1, whereas the internal standard (HARG) used for the amino acids in area 2.

Early trials on the ZIC-HILIC column using amino acids mixtures revealed the second fact related to amino acids separation and detection by LC-MS. Long isocratic stage (ca. 20 min) of the elution program is a key factor in removing any remaining compounds in ZIC-HILIC column. A carry over test for amino acids standards analysed on ZIC-HILIC column without the isocratic stage shows trace amounts of a certain amino acids after 3 subsequent injections. To solve this problem, a blank sample was run in-between runs in addition to a long isocratic time (ca. 20 min).

Different mechanisms have been proposed for amino acid retention on the ZIC-HILIC column. A partitioning mechanism is the first proposed mechanism for amino acids separation according to their solubility within the aqueous layer generated around the matrix of ZIC-HILIC column, leading to different retention times for different polar compounds according to their partition coefficient between water and acetonitrile. Due to the slightly acidic conditions of the STD amino acid stock solutions, most of the amino acids were present as zwitterions. So, their retention times could be attributed to electrostatic interaction with negatively charged sulfonate or positively charged quaternary amine groups of the ZIC-HILIC column surface ligand, in addition to the partitioning mechanism.

It is quite difficult to predict the behaviour of the molecules (regarding separation and retention) on the ZIC-HILIC column. However, certain factors can be used to predict the behaviour of these molecules such as hydrophilicity & polarity of the compounds, the acidity and basicity of the compounds, the number of ionising groups, solvent system and solvent strength.

The partitioning mechanism of the column depends on an initial column conditioning with enough water containing mobile phase to generate the aqueous layer within ZIC-HILIC matrix. Partitioning coefficient (log P) gives an indication about the hydrophilicity of the compounds, as the hydrophilicity of the compounds increases as the Log P decreases. Table 4-1 shows the retention time for amino acids arranged according to their elution from a ZIC-HILIC column, together with different experimental and theoretical log P values obtained from different sources.

Table 4-1: Retention times for different amino acids on the ZIC-HILIC column coupled to ESI-FTMS. Different experimental and theoretical log P values have been included for comparison[162].

results obtained from http://www.hmdb.ca/						**Experimental**	**Predicted by ALOGPS**	**Predicted by PubChem via XLOGP**
Amino acids	***3 letter Code***	***One-Letter Code***	***R_t control (min)***	***Side Chain Polarity***	***Side Chain Acidity or Basicity***	***Log P***	***Log P***	***Log P***
Phenylalanine	**Phe**	**F**	**8.68**	**nonpolar**	**neutral**	**-1.38**	**-1.35**	**-1.4**
Leucine	**Leu**	**L**	**8.98**	**nonpolar**	**neutral**	**-1.52**	**-1.82**	**-1.4**
Iso-leucine	**Ile**	**I**	**9.31**	**nonpolar**	**neutral**	**-1.7**	**-1.73**	**-1.6**
Tryptophan	**Trp**	**W**	**9.25**	**nonpolar**	**neutral**	**-1.06**	**-1.1**	**-1.3**
Methionine	**Met**	**M**	**10.01**	**nonpolar**	**neutral**	**-1.87**	**-1.85**	**-1.9**
Valine	**Val**	**V**	**10.58**	**nonpolar**	**neutral**	**-2.26**	**-2.29**	**-2.2**
Tyrosine	**Tyr**	**Y**	**10.79**	**polar**	**neutral**	**-2.26**	**-2.39**	**-1.8**
Proline	**Pro**	**P**	**11.77**	**nonpolar**	**neutral**	**-2.54**	**-2.71**	**-2.4**
Alanine	**Ala**	**A**	**12.25**	**nonpolar**	**neutral**	**-2.85**	**-3.05**	**-2.8**
Glutamic acid	**Glu**	**E**	**12.55**	**polar**	**acidic**	**-3.69**	**-3.54**	**-3.3**
4-hydroxyproline			**12.70**	**polar**	**neutral**	**-3.17**	**-3.31**	**-3.4**
Threonine	**Thr**	**T**	**13.07**	**polar**	**neutral**	**-2.94**	**-3.01**	**-3.5**
Aspartic acid	**Asp**	**D**	**13.42**	**polar**	**acidic**	**-3.89**	**-3.52**	**-3.7**
Glycine	**Gly**	**G**	**13.86**	**nonpolar**	**neutral**	**N/A**	**N/A**	**N/A**
Serine	**Ser**	**S**	**14.01**	**polar**	**neutral**	**-3.07**	**-3.42**	**-4**
Cystine			**17.47**	**polar**	**basic**	**-5.08**	**-3.16**	**-5.5**
Histidine	**His**	**H**	**18.77**	**polar**	**basic**	**-3.32**	**-2.67**	**-3.4**
Arginine	**Arg**	**R**	**19.41**	**polar**	**basic**	**-4.2**	**-3.6**	**-3.87**
Lysine	**Lys**	**K**	**19.69**	**polar**	**basic**	**-3.05**	**-3.76**	**-2.9**
Hydroxylysine			**20.34**	**polar**	**basic**	**N/A**	**-4**	**-3.77**
Cysteine	**Cys**	**C**	**N/A**	**polar**	**neutral**	**-2.49**	**-2.57**	**-2.6**
Asparagine	**Asn**	**N**	**N/A**	**polar**	**neutral**	**-3.82**	**-3.36**	**-4.4**
Glutamine	**Gln**	**Q**	**N/A**	**polar**	**neutral**	**-3.64**	**-3.32**	**-4.1**

The separation of the amino acids on ZIC-HILIC column may be influenced by the side chain of the amino acids. Ionised amino acids, which carry a net positive or negative charge, may undergo electrostatic interaction with ionised groups (sulfonate or quaternary amine group) of ZIC-HILIC column. The electrostatic interaction between the negatively charged sulfonate group of the ZIC-HILIC matrix and the positively charged amino acids, which contain additional basic groups in the side chain, is much stronger than the interaction of the quaternary amine group of the ZIC-HILIC matrix with the negatively charged amino acids which contain additional acidic groups in the side chain as indicated by their relative retention time on ZIC-HILIC column. Neutral amino acids which are in their zwitterions form still subject to a partitioning mechanism rather than electrostatic interaction.

A critical solvent combination is required for the mobile phase system to produce solvent strength enough to initiate amino acids elution in areas 1 and 2 (Figure 4.1); point (a) represents a mobile phase combination of 30% H_2O: 70% ACN which produces enough strength to elute amino acids in area 1 out of the aqueous layer of ZIC-HILIC column. Whereas, point (b) represents a mobile phase combination of 51% H_2O: 49% ACN which produces enough solvent strength to elute amino acids in area 2 out of ZIC-HILIC column. The separation of the amino acids in area 1 seems to be as a result of partitioning mechanism, as the elution of the amino acids is according to the increase in the hydrophilicity of the compounds (Table 4-1). Furthermore, there is no specific pattern for the separation of these amino acids according to their side chains (Figure 4.2).

In general, most of amino acids in eluted in area 1 have a neutral side chain, with the exception of glutamic and aspartic acid which have acidic side chains (see the physico-chemical properties of amino acids in Table 4-1. The elution of amino acids in area 2 is at a much longer retention time compared to the elution of the amino acids in area 1. This suggests that these amino acids (cystine, histidine, arginine, lysine and hydroxylysine) undergo a different separation mechanism on ZIC-HILIC column other than the partitioning mechanism. All the amino acids in area 2 (with the exception of

cystine which is formed from two cysteine molecules and thus has two amine groups and two carboxyl groups) have basic group in their side chains (Figure 4.2 & Table 4-1). This confirms the ability of these amino acids to interact with the sulfonate group of ZIC-HILIC matrix through electro-static interaction rather than a partitioning mechanism, leading to a longer retention time for these amino acids in comparison to the amino acids in area 1.

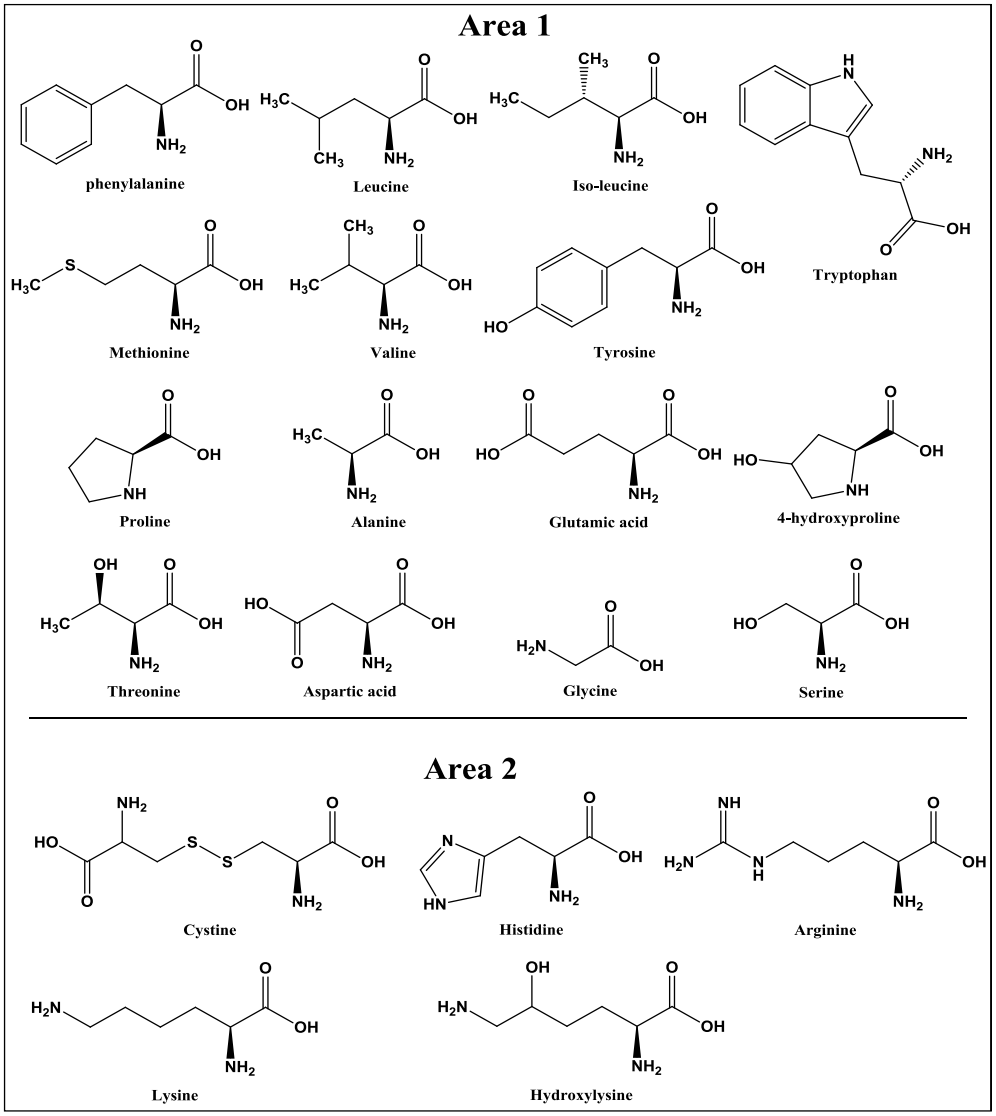

Figure 4.2: Amino acids listed according to their elution time from ZIC-HILIC column into area 1 and area 2.

Table 4-2: Average peak area for amino acids using different extraction methods. The results obtained by using ZIC-HILIC coupled to ESI-FTMS. Number of samples=3

	STD	*PPT-ACN*	*LIQ-LIQ-Chloroform*	*LIQ-LIQ-Heptane*	*SPE*	*STD 0.1% HCl*	*Isolute SAX*	*Isolute SCX*	*Strata SCX*
Amino acids	*Mean Peak Area*	*Mean Peak Area*	*Mean Peak Area*	*Mean Peak Area*	_	*Mean Peak Area*	*Mean Peak Area*	*Mean Peak Area*	*Mean Peak Area*
Phenylalanine	1.50E+09	2.08E+09	1.20E+08	1.84E+09	_	1.91E+09	1.21E+09	1.96E+09	1.13E+09
LEU, ILE	3.50E+09	4.63E+09	1.61E+09	4.06E+09	_	4.42E+09	2.81E+09	4.64E+09	1.30E+09
Tryptophan	1.03E+09	1.02E+09	0.00E+00	1.15E+09	_	1.22E+09	7.49E+08	1.25E+09	1.18E+09
Methionine	8.22E+08	1.03E+09	0.00E+00	9.70E+08	_	1.00E+09	6.54E+08	1.06E+09	1.31E+08
Valine	9.32E+08	1.19E+09	3.16E+08	1.05E+09	_	1.10E+09	6.99E+08	9.51E+08	2.07E+08
Tyrosine	6.95E+08	9.21E+08	0.00E+00	7.86E+08	_	8.39E+08	5.23E+08	6.98E+08	2.39E+08
Proline	4.56E+08	4.56E+08	4.12E+08	4.42E+08	_	4.41E+08	2.63E+08	4.03E+08	6.25E+07
Alanine	8.94E+07	8.43E+07	4.64E+07	9.66E+07	_	9.25E+07	6.09E+07	1.53E+08	2.38E+07
Glutamic acid	1.58E+08	1.71E+08	1.07E+07	1.64E+08	_	1.75E+08	1.24E+08	2.61E+08	4.91E+07
4-hydroxyproline	1.41E+08	1.40E+08	8.51E+07	1.42E+08	_	1.44E+08	1.11E+08	2.74E+08	4.58E+07
Threonine	7.73E+07	6.91E+07	0.00E+00	7.28E+07	_	7.55E+07	5.91E+07	1.82E+08	3.23E+07
Aspartic acid	4.91E+07	1.28E+08	0.00E+00	4.70E+07	_	4.34E+07	1.85E+07	1.16E+07	8.43E+06
Serine	3.81E+07	3.63E+07	4.20E+06	4.49E+07	_	3.74E+07	4.46E+07	1.54E+06	2.27E+05
Glycine	1.44E+07	2.38E+07	0.00E+00	1.45E+07	_	1.42E+07	4.10E+06	1.05E+06	7.59E+05
Cystine	1.83E+08	2.08E+08	3.85E+05	1.88E+08	_	1.91E+08	1.17E+08	1.51E+08	1.36E+07
Histidine	2.78E+08	2.76E+08	5.04E+05	2.84E+08	_	2.96E+08	1.71E+08	2.16E+08	3.50E+07
Arginine	2.72E+08	3.14E+08	1.44E+07	2.82E+08	_	2.88E+08	1.79E+08	1.25E+07	3.79E+07
Lysine	1.42E+08	1.76E+08	2.01E+07	1.62E+08	_	1.52E+08	1.07E+08	9.66E+07	2.03E+07
Hydroxylysine	2.09E+08	2.39E+08	1.45E+07	2.36E+08	_	2.44E+08	1.42E+08	1.59E+08	2.78E+07
Total Summation	1.06E+10	1.32E+10	2.65E+09	1.20E+10	_	1.27E+10	8.04E+09	1.25E+10	4.55E+09

Investigation of different extraction methods described in section 2.5 was carried out. Table 4-2 shows the average peak area for amino acids extracted by the different extraction methods, protein precipitation technique (PPT-ACN), liquid-liquid extraction (LIQ-LIQ), and solid phase extraction (SPE). The results represent the average for 3 samples prepared by each extraction method using the STD amino acid solution prepared according to the procedure described in section 2.2. Exploring the best extraction method for amino acids requires exploring the affinity of each extraction method for individual amino acid extraction. A comparison between different extraction methods was carried by considering the total peak area summation for the total amino acids (listed in Table 4-2 and Figure 4.3).

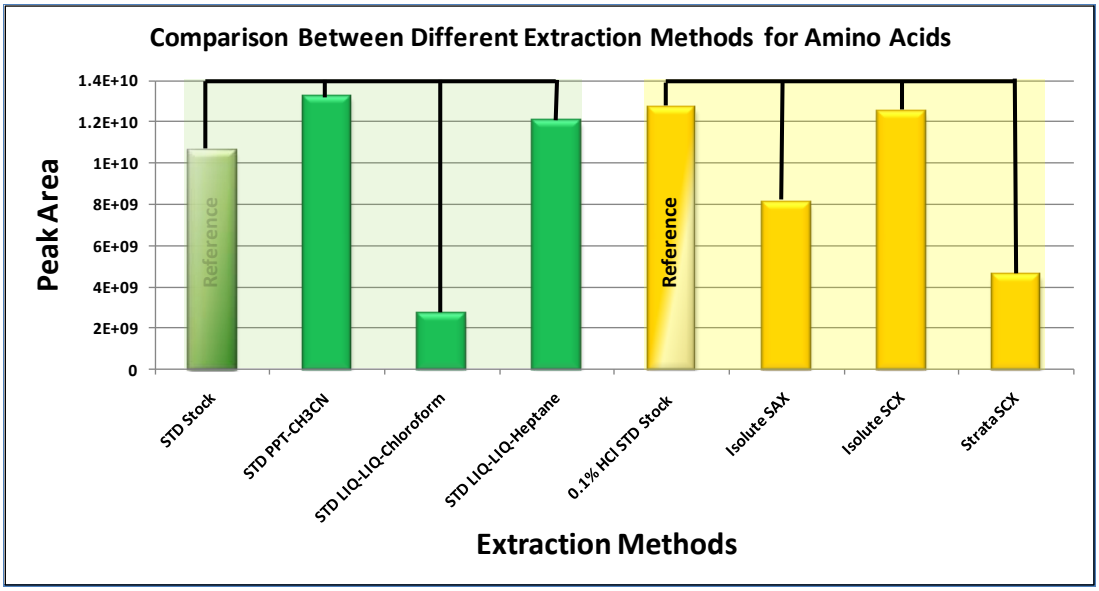

Figure 4.3: Average peak area summation for the total amino acids extracted by different extraction methods. The results obtained by using ZIC-HILIC coupled to ESI-FTMS. Number of samples=3.

By comparing the results obtained in Table 4-2 & Figure 4.3, protein precipitation technique (PPT-ACN) and LIQ-LIQ extraction with heptane show high recovery for the amino acids extraction. Whereas, solid phase extraction (SPE) using an Isolute-SCX cartridge shows good recovery for the amino acids extraction as compared to other SPE cartridges from different sources. Other extraction methods show very high percentages of amino acid loss during the extraction process. Since the research project is focused on the extraction and detection of ALEs and AGEs which are modified amino acids (mainly

lysine, arginine, and histidine amino acids), then validating the affinity of these extraction methods to extract these 3 amino acids was a crucial point in this project. Figure 4.4 shows the extraction of lysine, arginine, and histidine using PPT-ACN, LIQ-LIQ heptane, and the Isolute-SCX method, as compared to standards, using 3 repeated samples for each extraction method. Isolute-SCX shows a maximum loss of arginine amino acid and thus was excluded from validation, whereas PPT-ACN and LIQ-LIQ heptane methods show the optimum conditions for these amino acids extraction.

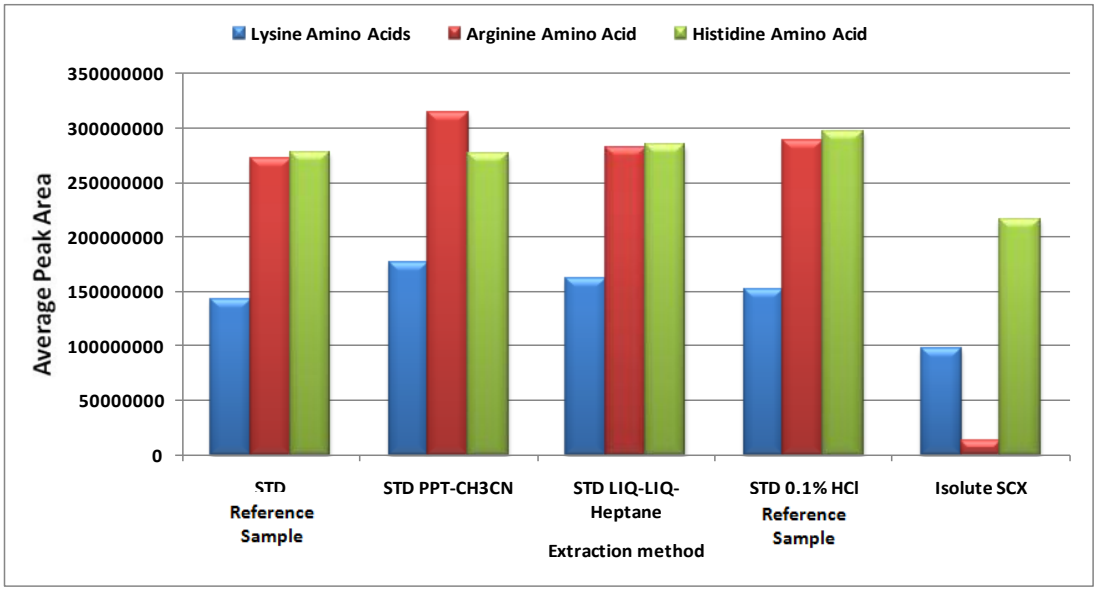

Figure 4.4: Best extraction methods for lysine, arginine, and histidine as compared to standard solutions. The results obtained by using ZIC-HILIC coupled to ESI-FTMS. Number of samples=3.

The next step was to validate these methods for ALEs product extraction. Figure 4.5 shows the affinity of different extraction methods for ALEs extraction using protein samples (HSA) incubated with 2-hexenal aldehyde. Production and hydrolysis of ALEs samples was carried out according to the procedure described in section 2.3 and the analysis was repeated 3 times. PPT-ACN shows the highest percentage of ALEs recovery as compared to the other methods, while LIQ-LIQ heptane shows the lowest recovery for such modified amino acids. Examination of different protein samples which had been incubated with different aldehydes (acrolein, crotanaldehyde, 2-pentenal, 2-heptenal, 2-nonenal, and HNE) showed the same behaviour for the extraction of the amino acids which had been modified with 2-hexenal aldehyde when LIQ-LIQ

extraction with heptane was used as an extraction method. Hence, LIQ-LIQ heptane was also excluded from validation process. Further validation focused on PPT-ACN as the best extraction method for both amino acids and the modified amino acids.

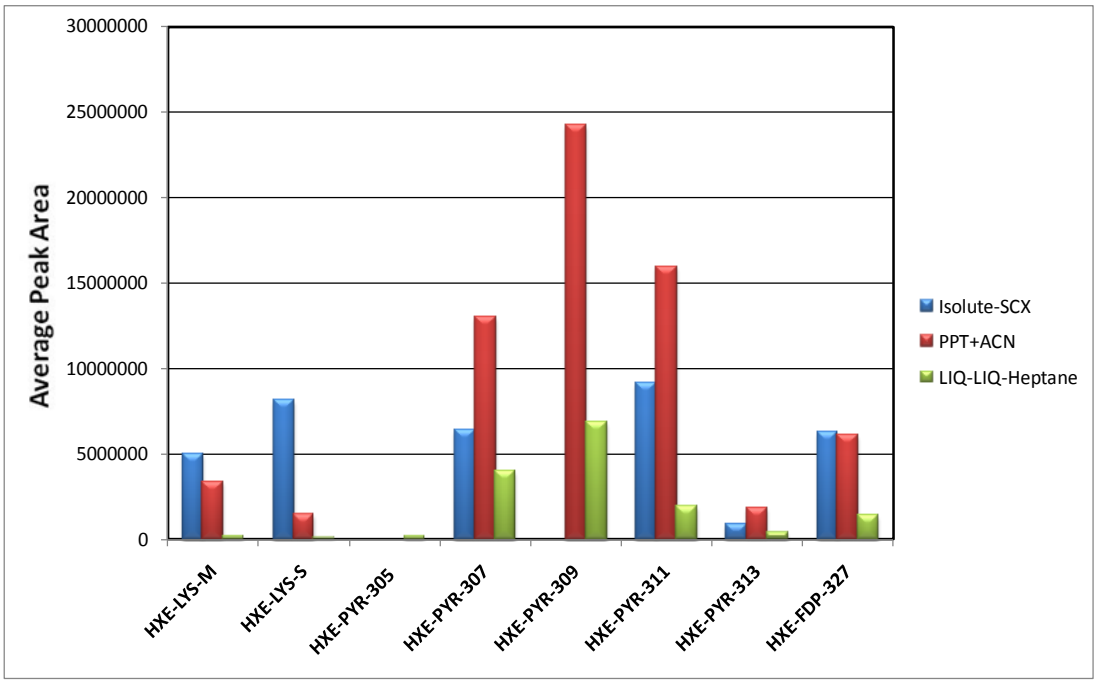

Figure 4.5: Recovery of ALEs products using different extraction methods (PPT-ACN, LIQ-LIQ heptane, and Isolute-SCX). The results obtained by using ZIC-HILIC coupled to ESI-FTMS. Number of samples=3.

Table 4.3 shows the response factors for individual amino acids relative to the internal standard amino acids (MET-d3 & HARG) following different extraction procedures. The extraction method using Isolute-SCX shows a huge difference in the total response factor summation for the total amino acids that results from poor recovery for the internal standard (HARG) leading to a theoretical high response factor as compared to standard amino acids solution without extraction.

Table 4-3: Comparison between different extraction methods according to the average response factor for each amino acid. Response factor= peak area for amino acid/ peak area for internal standard). Amino acids with green color are from the same chromatographic area (area1) and have been compared to MET-d3 as internal standard, while amino acids in red color are from he same chromatographic area (area 2) and have been comapred to HARG as internal standard. The results obtained by using ZIC-HILIC coupled to ESI-FTMS. Number of samples=3.

	STD Stock	*PPT-ACN*	*LIQ-LIQ-Chloroform*	*LIQ-LIQ-Heptane*	*SPE*	*STD 0.1% HCl*	*Isolute SAX*	*Isolute SCX*	*Strata SCX*
Amino acids	***Mean***	***Mean***	***Mean***	***Mean***	_	***Mean***	***Mean***	***Mean***	***Mean***
Phenylalanine	**1.870**	**2.004**	**0.000**	**1.912**	_	**1.871**	**1.885**	**1.855**	**8.832**
LEU, ILE	**4.307**	**4.458**	**0.000**	**4.222**	_	**4.339**	**4.367**	**4.401**	**10.147**
Tryptophan	**1.284**	**0.992**	**0.000**	**1.207**	_	**1.195**	**1.164**	**1.186**	**9.246**
Methionine	**1.008**	**0.996**	**0.000**	**1.006**	_	**0.982**	**1.018**	**1.013**	**1.023**
Valine	**1.167**	**1.164**	**0.000**	**1.104**	_	**1.079**	**1.087**	**0.917**	**1.616**
Tyrosine	**0.862**	**0.900**	**0.000**	**0.824**	_	**0.823**	**0.815**	**0.674**	**1.869**
Proline	**0.582**	**0.460**	**0.000**	**0.477**	_	**0.434**	**0.408**	**0.375**	**0.490**
Alanine	**0.113**	**0.074**	**0.000**	**0.104**	_	**0.091**	**0.095**	**0.146**	**0.185**
Glutamic acid	**0.197**	**0.169**	**0.000**	**0.173**	_	**0.172**	**0.193**	**0.253**	**0.383**
4-hydroxyproline	**0.177**	**0.142**	**0.000**	**0.151**	_	**0.142**	**0.173**	**0.261**	**0.358**
Threonine	**0.097**	**0.070**	**0.000**	**0.078**	_	**0.074**	**0.092**	**0.175**	**0.252**
Aspartic acid	**0.061**	**0.128**	**0.000**	**0.050**	_	**0.043**	**0.029**	**0.012**	**0.065**
Serine	**0.050**	**0.037**	**0.000**	**0.050**	_	**0.037**	**0.070**	**0.001**	**0.002**
Glycine	**0.019**	**0.025**	**0.000**	**0.016**	_	**0.014**	**0.006**	**0.001**	**0.006**
Cystine	**0.752**	**0.790**	**0.011**	**0.766**	_	**0.752**	**0.828**	**25.014**	**0.469**
Histidine	**1.115**	**1.050**	**0.014**	**1.138**	_	**1.167**	**1.197**	**35.928**	**1.113**
Arginine	**1.093**	**1.165**	**0.412**	**1.130**	_	**1.139**	**1.268**	**2.009**	**1.197**
Lysine	**0.581**	**0.650**	**0.574**	**0.649**	_	**0.602**	**0.757**	**15.983**	**0.650**
Hydroxylysine	**0.839**	**0.874**	**0.413**	**0.940**	_	**0.965**	**1.005**	**26.446**	**0.889**
Total Summation	**16.173**	**16.147**	**1.425**	**15.998**	_	**15.921**	**16.456**	**116.650**	**38.792**

4.4 Validation of the Extraction and Detection Methods for Amio Acids Using HILIC-FTMS

The next step in this project was to validate the extraction method using a ZIC-HILIC column interfaced with high resolution mass spectrometer according to the parameters specified in section 2.5.4. The validation process examined the specificity, precision, linearity & range for amino acids extraction using the PPT-ACN method, and detected using ZIC-HILIC-FTMS. Validation for the analytical method was carried in

accordance with the ICH protocols [127-129], which involve specificity, repeatability, linearity and range.

4.4.1 Specificity of the ZIC-HILIC Column for Amino Acids Separation

Maria *et al.* [130] have defined specificity as the ability of the detection method to detect compound (s) of interest in the presence of other components in the mixture. Maria *et al.* considered retention time stability between an amino acid standard mixture and BSA hydrolysate as an indicator for the specificity of the analytical method. A relative standard deviation within 3% was acceptable [130].

ZIC-HILIC column showed good stability for amino acid retention and good selectivity as indicated by the ability of the column to separate the amino acids isomers leucine and isoleucine which were 85% resolved (Figure 4.6).

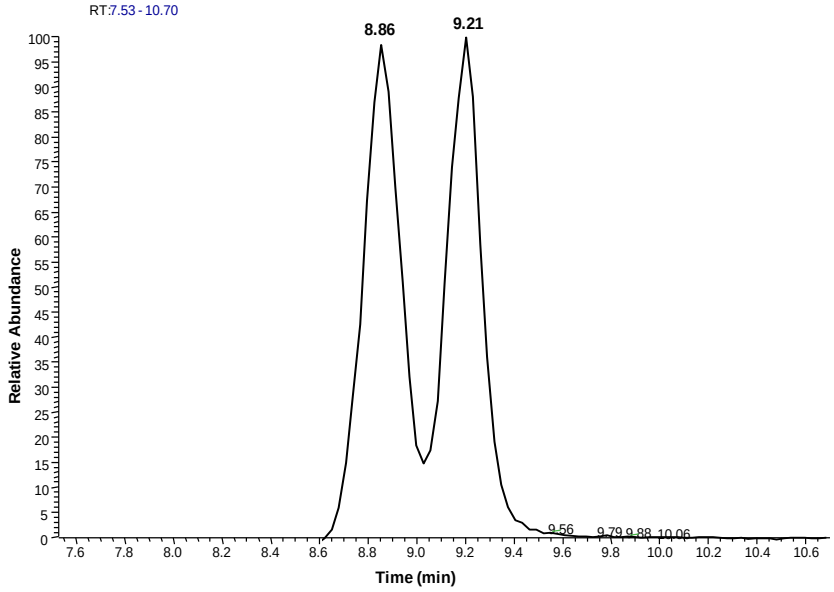

Figure 4.6: Leucine and isoleucine amino acids isomers separation on ZIC-HILIC column and detected by ESI-FTMS.

Table 4-4 shows an evaluation of the ability of the ZIC-HILIC column to retain and separate amino acids in the presence of impurities that may result from HSA protein

hydrolysis. These impurities could be peptides, proteins, lipids & phospholipids' molecules.

Table 4-4: Evaluation of ZIC-HILIC specificity by comparing retention time for different amino acids between amino acids standards mixture and HSA hydrolysate. The results obtained by using ZIC-HILIC coupled to ESI-FTMS. Number of samples=6 for each.

	AA standard, n=6		*HSA hydrolysate, n=6*				
Amino Acids	***Mean R_t (min)***	***STDEVA (min)***	***Mean R_t (min)***	***STDEVA (min)***	***Average R_t (min)***	***STDEVA (min)***	***% RSD***
Phenylalanine	**8.61**	**0.03**	**8.70**	**0.03**	**8.66**	**0.06**	**0.70**
Leucine, Iso-leucine	**8.90**	**0.02**	**9.00**	**0.01**	**8.95**	**0.07**	**0.75**
	9.23	**0.01**	**9.32**	**0.01**	**9.28**	**0.06**	**0.65**
Tryptophan	**9.20**	**0.04**	**9.29**	**0.04**	**9.24**	**0.07**	**0.72**
Methionine	**9.95**	**0.01**	**10.03**	**0.02**	**9.99**	**0.05**	**0.55**
Valine	**10.51**	**0.01**	**10.58**	**0.03**	**10.55**	**0.05**	**0.51**
Tyrosine	**10.75**	**0.01**	**10.83**	**0.01**	**10.79**	**0.06**	**0.55**
Proline	**11.71**	**0.01**	**11.79**	**0.04**	**11.75**	**0.06**	**0.49**
Alanine	**12.20**	**0.04**	**12.28**	**0.01**	**12.24**	**0.05**	**0.44**
Glutamic acid	**12.48**	**0.15**	**12.60**	**0.13**	**12.54**	**0.08**	**0.65**
4-hydroxyproline	**12.61**	**0.09**	**12.69**	**0.09**	**12.65**	**0.05**	**0.43**
Threonine	**13.02**	**0.03**	**13.10**	**0.02**	**13.06**	**0.06**	**0.43**
Aspartic acid	**13.38**	**0.03**	**13.48**	**0.04**	**13.43**	**0.07**	**0.51**
Glycine	**13.79**	**0.02**	**13.88**	**0.02**	**13.84**	**0.06**	**0.45**
Serine	**13.97**	**0.01**	**14.06**	**0.01**	**14.01**	**0.06**	**0.46**
Cystine	**17.42**	**0.03**	**17.51**	**0.03**	**17.47**	**0.06**	**0.36**
Histidine	**18.70**	**0.03**	**18.78**	**0.04**	**18.74**	**0.06**	**0.31**
Arginine	**19.33**	**0.03**	**19.41**	**0.04**	**19.37**	**0.06**	**0.30**
Lysine	**19.60**	**0.02**	**19.71**	**0.02**	**19.65**	**0.07**	**0.37**
Hydroxylysine	**20.29**	**0.03**	**20.37**	**0.03**	**20.33**	**0.06**	**0.28**
Homoarginine	**18.70**	**0.03**	**18.81**	**0.03**	**18.76**	**0.08**	**0.41**
Methionine D3	**9.95**	**0.01**	**10.04**	**0.01**	**9.99**	**0.06**	**0.61**
Homophenylalanine	**7.82**	**0.03**	**7.89**	**0.00**	**7.86**	**0.05**	**0.65**

Samples for amino acids standard solution was prepared according to the procedure for the STD stock solution described in section 2.2. Preparation and hydrolysis of HSA protein samples was done according to the procedure mentioned in 0 2.3 and then subject to the PPT procedure [section 2.5.3]. Detection of the amino acids was carried using a ZIC-HILIC column interfaced to ESI-FTMS according to the conditions specified in section 2.5.4. The ZIC-HILIC column shows high specificity for amino acids in the presence of other impurities as indicated by retention time stability for

amino acids between amino acids standard solution and the HSA hydrolysate (RSD% less than 0.75%). The sample analyses were repeated 6 times for each amino acid standard solution and HSA hydrolysate.

Also the stability of the retention times of the amino acids on the ZIC-HILIC column was examined by continuous running of amino acids standard sample over 45 hrs. The RSD was less than 0.87% (Table 4-5).

Table 4-5: Retention time stability for amino acids on a ZIC-HILIC column over 45 hrs of continuous running for the amino acids standard mixture. The results obtained by using ZIC-HILIC coupled to ESI-FTMS.

Amino acid	*Mean (min)*	*STDEVA (min)*	*% RSD*	*Amino acid*	*Mean (min)*	*STDEVA (min)*	*% RSD*
Phenylalanine	8.68	0.06	0.69	Aspartic acid	13.42	0.05	0.38
Leucine, Iso-leucine	8.98	0.06	0.72	Glycine	13.86	0.05	0.38
	9.31	0.08	0.86	Serine	14.01	0.05	0.33
Tryptophan	9.25	0.05	0.51	Cystine	17.47	0.04	0.25
Methionine	10.01	0.06	0.55	Histidine	18.77	0.06	0.33
Valine	10.58	0.07	0.64	Arginine	19.41	0.08	0.41
Tyrosine	10.79	0.04	0.39	Lysine	19.69	0.08	0.39
Proline	11.77	0.06	0.48	Hydroxylysine	20.34	0.05	0.25
Alanine	12.25	0.05	0.37	Homophenylalanine	7.87	0.05	0.62
Glutamic acid	12.55	0.06	0.47	Methionine-d3	10.02	0.06	0.57
4-hydroxyproline	12.7	0.09	0.73	Homoarginine	18.8	0.1	0.51
Threonine	13.07	0.05	0.38				

4.4.2 Linearity and Range for PPT Method

According to the ICH guidelines [127], linearity and range should be investigated by running 5 concentration points with a minimum of 3 replicates for each concentration. The linearity of the test is indicated by an R^2 value which should be greater than 0.985 [127, 130]. Since the research project was focused on detecting ALEs compounds which have very low concentrations in the biological systems, the range to examine the linearity of this method was chosen to be within the nmol range for all the amino acids.

A dilution series for amino acids mixture was prepared to examine the linearity of the method over a concentration of 7-30 nmol/ml (equivalent to 11- 40 ng on column). Five calibration levels have been examined across the specified range with each calibration level being repeated 3 times. A solution of 40 nmol/ml was prepared by diluting 800 µl of amino acids STD from the EZ:faast kit (contains 200 nmol/ml of each amino acid) to 4 ml with HPLC grade water. The solution was assigned as the STD stock solution.

A series of diluted standard samples were prepared for filtration using the PPT method. 1ml of ACN was added to 9 PPT filters and labels them as 50, 75, 80, 100, 120, 125, 150, 175, and 200%. Leave for about 5 min and then spike 75, 112.5, 120, 150, 180, 187.5, 225, 262.5, and 300 µl of the STD stock solution to the 50, 75, 80, 100, 120, 125, 150, 175, and 200% PPT array cartridges, respectively (Table 4-6). Finally, add 100 µl of I.S (reagent 1 from the EZ:faast kit) to each PPT array cartridge in order to use it as a reference compounds to obtain the response factor for each amino acid.

Vacuum manifold operating at 10mmHg was used to start the process of filtration. Collect the eluant and evaporate till dryness using dry-block at 50°c and slight nitrogen stream. Re-dissolve again in 400 µl of HPLC grade water. A concentration of 7.5, 11.25, 12, 15, 18, 18.75, 22.5, 26.25, and 30 nmol/ml of each amino acid would be expected for 50, 75, 80, 100, 120, 125, 150, 175, and 200%, respectively, after filtration process with PPT method.

The ZIC-HILIC column coupled to FTMS was used as the separation and detection method according to the conditions and parameters specified in section 2.5.4. The large amount of data generated by mass spectrometry was analysed using the SIEVE 1.2 software which is a multi-variants analysis tool for processing the data obtained from mass spectrometry [section 1.7]. The SIEVE 1.2 software provided retention time and intensity for all the amino acids.

Homoarginine with the mass of 189.13 amu was used as the IS for lysine, arginine, and histidine amino acids, these amino acids represent the main target for amino acids

modification when incubated with 2-alkenal aldehydes. Table 4-7 shows the average response factor of lysine, arginine, and histidine amino acids obtained from 3 replicates for each calibration level.

Table 4-6: Preparation of a dilution series to investigate linearity and range for the PPT method followed by detection with ZIC-HILIC-FTMS.

Dilution Step	*Conc. of amino acids (nmol/ml)*	*Vol. (µl) from the 200% STD to be spiked into PPT*	*Vol (µl)of I.S with a conc of 200 nmol/ml*
50%	**7.5**	**75**	**100**
75%	**11.25**	**112.5**	
80%	**12**	**120**	
100%	**15**	**150**	
120%	**18**	**180**	
125%	**18.75**	**187.5**	
150%	**22.5**	**225**	
175%	**26.25**	**262.5**	
200%	**30**	**300**	

Calibration curves were constructed for different amino acids according to the average response factor for each amino acid obtained by the SIEVE software for each calibration point. Figure 4.7 shows the calibration curves for lysine, arginine and histidine amino acids which all have R^2 values >0.985. The other amino acids showed a sufficient linearity indicated by R^2 values ranging between 0.9900 and 0.9994 (Table 4-8).

Thus, the PPT method was suitable for precise and accurate detection of amino acids, in the specified range. Furthermore, the high specificity and selectivity of this method suggest a promising application of this method for modified amino acids even at very low concentrations.

Table 4-7: Average response factors for Lys, His, and Arg amino acids obtained by ZIC-HILIC coupled to ESI-FTMS detection. Response factor = AA intensity / IS intensity (homoarginine has been used as internal standard to obtain the response factor for Lys, His, and Arg amino acids as it has the same retention time). Number of samples=3 repeated samples with a RSD < 6%. Concentration of IS added= 200 nmol/ml.

AA	Conc. (nmol/ml)	7.5	11.25	15	18.75	22.5	26.25
Lysine	Response Factor	0.04	0.06	0.08	0.10	0.13	0.14
Histidine	Response Factor	0.06	0.09	0.12	0.17	0.20	0.23
Arginine	Response Factor	0.13	0.18	0.25	0.32	0.37	0.42

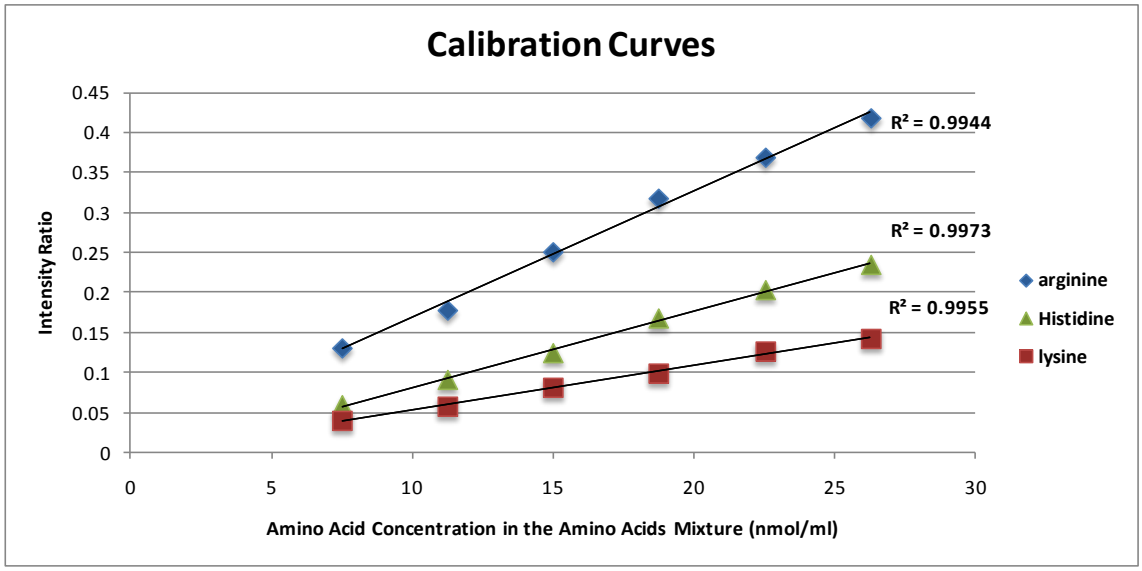

Figure 4.7: Calibration curves for lysine, arginine and histidine amino acids constructed over 6 calibration points at 7.5, 11.25, 15, 18.75, 22.5, and 26.25 nmol/ml. The results obtained by using ZIC-HILIC coupled to ESI-FTMS.

Table 4-8: R^2 values for different amino acids according to the response (peak area dor amino acid/peak area for the I.S) over the range 7.5-26.25 nmol/ml. The results obtained by using ZIC-HILIC coupled to ESI-FTMS and the data analysed by the SIEVE software.

Amino acids	*R2*	*Amino acids*	*R2*
Phenylalanine	0.9953	Glutamic acid	0.9982
Leucine, Iso-leucine	0.9976	4-hydroxyproline	0.99
Tryptophan	0.9958	Aspartic acid	0.9982
Methionine	0.9987	Glycine	0.9976
Valine	0.9951	Serine	0.9981
Tyrosine	0.9975	Cystine	0.9994
Proline	0.9973	Hydroxylysine	0.9988
Alanine	0.9985		

4.5 Structure Elucidation for Amino Acids

MS^2 fragmentation in mass spectrometry is a potential feature that can be used for structure elucidation, or to confirm the identity of the compounds in more complex matrices, according to the information gathered from the resulting fragment ions. MS^2 spectra generated by an Orbitrap are cleaner than those obtained by low resolution mass spectrometry due to high resolution, accurate mass measurement, and the powerful image current detector of the Orbitrap [121]. The amino acids STD stock solution was used to explore fragmentation pathways for amino acids using the ZIC-HILIC column coupled to FTMS. Separation and detection of amino acids were carried out according to the conditions and parameter specified in section 2.5.4, with the exception of the mass range which had been reduced to 50-400 m/z . Such narrow mass range can help in excluding interfering compounds leading to better full scan MS and MS/MS detection. Data dependent acquisition fragmentation was operated simultaneously with full scan mass spectrometry (both of them are operating in the positive mode). Hence, full scan and MS^2 data can be obtained for any single injection at the same time [section 2.5.4.1].

MS^2 spectrometry in the positive polarity mode was used for each individual amino acid with a mass window (1 amu) in order to remove any interfering compounds. CID energy of 35% was used as fragmentation energy, and the mass range for the product ion was automatically assigned by the Q value for MS/MS parameter, which was set at 0.250 which means that product ions till ¼ of mass of the precursor ion could be detected. The MS^2 results for amino acid fragmentation obtained by the Orbitrap using data dependent acquisition mode are shown inTable 6-16. Different fragments could be observed for each amino acid, and the most abundant fragment was reported in the same table. The difference between the mass for the precursor ion and the produced fragment had been assigned as “Mass Loss”. All the fragments were within 2 ppm deviation from the expected masses.

Some of the amino acids show extensive fragmentation such as phenylalanine, tryptophan, arginine, and hydroxyl-lysine, whereas other amino acids failed to show any

fragmentation e.g. alanine. Little fragmentation data can be explained by low intensity of the amino acid that may result from ionic suppression due to co-eluted compounds, such as electrolytes and charged molecules, which compete for the charge in the droplets during ESI step [163]; ion suppression phenomenon plays a negative role in the ionisation state of the molecule. By correlating mass loss with the changes in the elemental formulas of the precursor and fragment ions, 2 pathways could be predicted for amino acids fragmentation: a general pathway and a specific pathway.

4.5.1 General Pathways

According to the MS^2 data shown inTable 6-16, general pathways involve the loss of a specific mass which is common to all amino acids. An amino acid may eliminate a single group from its structure such as ammonia (NH_3, 17 amu), water (H_2O, 18 amu), formic acid (HCOOH, 46 amu), carbon or dioxide (CO_2, 44 amu) molecule, or it may eliminate a combination of more than one group such as loss of 64 amu that results from consecutive loss of H_2O and HCOOH molecules from the molecular ion (Table 4-9). Many studies confirm elimination of NH_3, H_2O [113, 146, 164-167], HCOOH [146, 165], and CO_2 [146, 166, 168-170] molecules from the precursor ion during MS^2 fragmentation. Mechanistic pathways have been proposed in Scheme 4-1 to explain the generation of different fragmentation patterns of amino acids during ESI-MS/MS. For example, lysine shows 3 main fragments at 130, 129, and 84 m/z which represent elimination of NH_3 (17 amu), H_2O (18 amu), or a consecutive elimination of NH_3 and HCOOH (63 amu) groups from the molecular ion (Figure 4.8).

Table 4-9: Fixed mass losses from amino acid precursorions during MS^2 fragmentation using data dependent acquisition mode with ESI-CID-FTMS/MS.

Mass Loss (m/z)	*Represent*	*Amino Acid*
17 m/z	**Loss of NH_3**	**All Amino Acids**
18 m/z	**Loss of H_2O**	
35 m/z	**Loss of NH_3 and H_2O**	
46 m/z	**Loss of HCOOH**	
61 m/z	**Loss of NH_3 and CO_2**	
63 m/z	**Loss of NH_3 and HCOOH**	
64 m/z	**Loss of H_2O and HCOOH**	
Note: Usually a combination of 2 or 3 fragments can be observed		

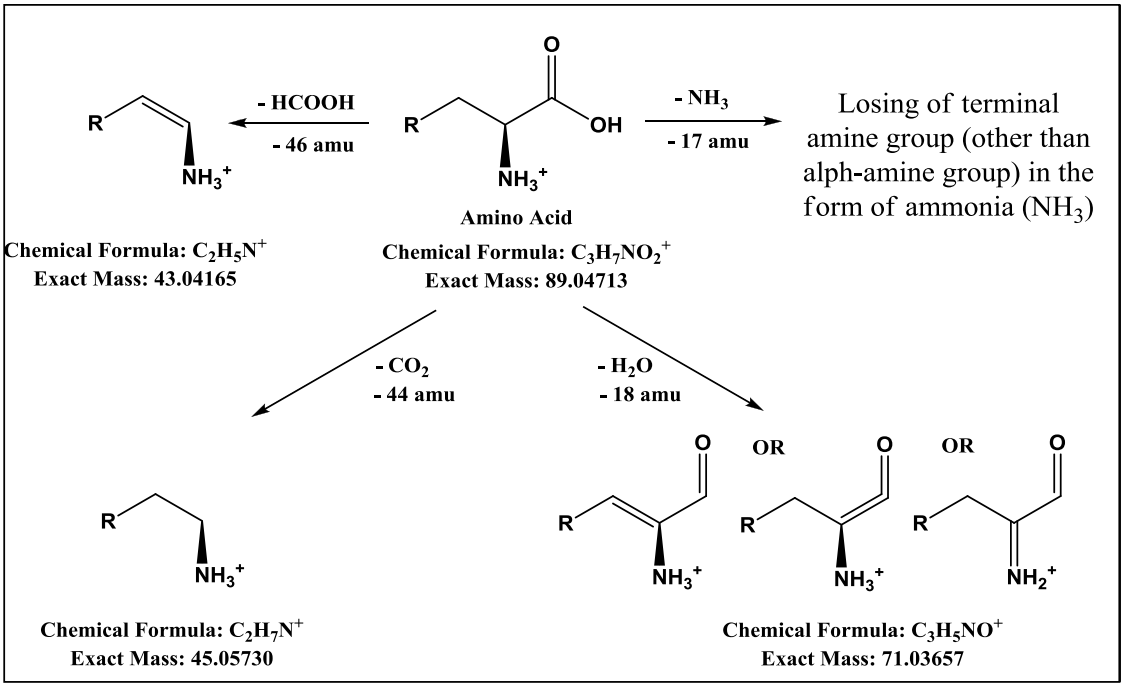

Scheme 4-1: Possible fragmentation pattern for amino acids in MS^2 spectrometry using data dependent acquisition mode with ESI-CID-FTMS/MS.

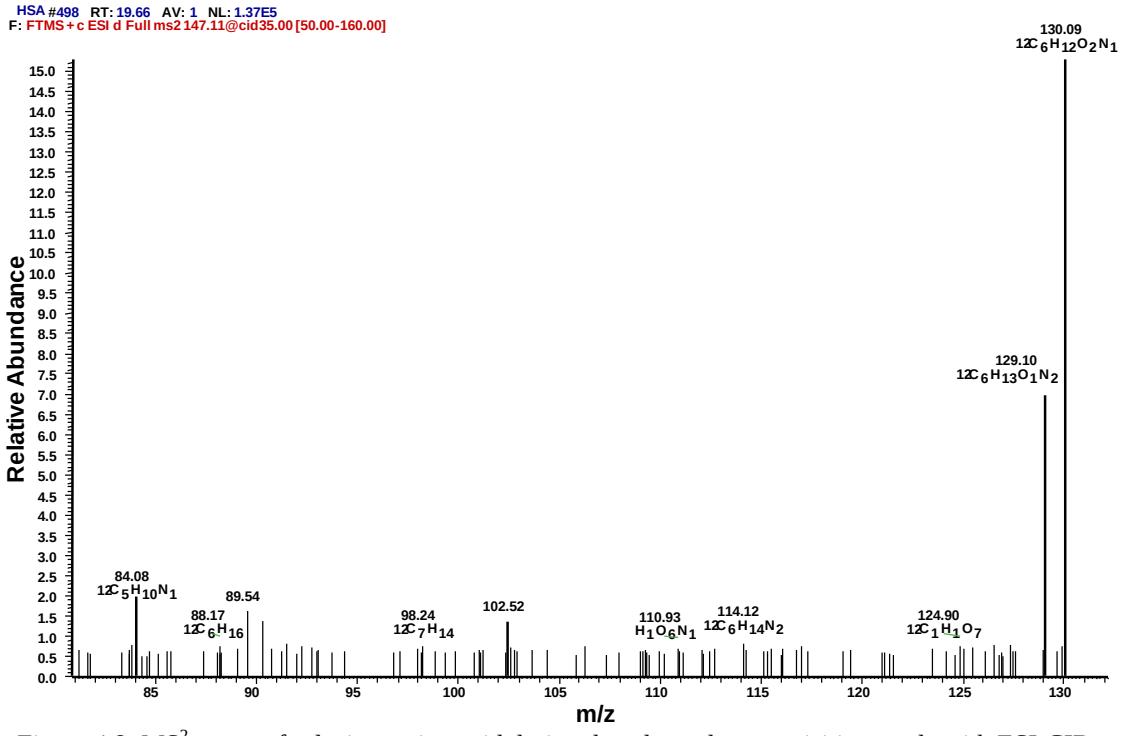

Figure 4.8: MS^2 spectra for lysine amino acid during data dependent acquisition mode with ESI-CID-FTMS/MS.

4.5.2 Specific Pathways

Amino acids may undergo normal fragmentation according to the general pathways by eliminating certain groups from the main precursor ions leading to the formation of specific fragments such as carbocation or sulphonium ion. In addition to the general fragment losses from amino acids there are a number of specific types of fragmentation occurring with certain amino acids. These include α,β- cleavage, various re-arrangements, hydroxylation, and oxidative deamination reactions. Table 4-10 shows some examples of specific fragmentation pathways.

Table 4-10: Specific fragmentation pathways for amino acids obtained by using data dependent acquisition fragmentation with ESI-CID-FTMS/MS.

Fragmentation	*Represent*	*Amino Acid*	*Mass Losing (m/z)*
Carbocation Formation	By losing the only ionisable amine group	Valine, leucine, and isoleucine	17 m/z
		Methionine	48 m/z
Alpha-Beta Cleavage	Normal Alpha-Beta Cleavage	Tryptophan	59 m/z
	Alpha-Beta Cleavage with loss of CH3COOH	Aspartic Acid	60 m/z
	Alpha-Beta Cleavage leading to ionised imidazole group only	Histidine	73 m/z
Tropylium Ion Formation	Hydroxylation and re-arrangement	Phenylalanine and Tyrosine	59 m/z
Specific Arginine Fragments	Losing of HCOOH followed by oxidative deamination reaction	Arginine	45 m/z
	Losing of the guanidine group	Arginine	59 m/z
	Formation of ionised guanidine group	Arginine	115 m/z

4.5.2.1 Carbocation Formation

Fragmentation patterns for amino acids which follow the general pathways may lead to the loss of the only ionisable group in the molecule, such as N, S, or O leaving the positive charge on the carbon atom. For example, MS^2 fragmentation for valine amino acid shows a fragment at m/z 72 and a minor fragment at m/z 55 (Figure 4.9). A

possible fragmentation pathway is shown in Scheme 4-2 which is consistent with the elemental composition for the fragments obtained by high resolution MS. Fragment at m/z 72 results from elimination of HCOOH from the main structure as a neutral loss. The fragment at m/z 72 undergoes a further elimination of NH_3 from its structure by heterolytic cleavage of C-N bond and positive charge migration from N to C leading to formation of stable and detectable carbocation fragment at m/z 55.

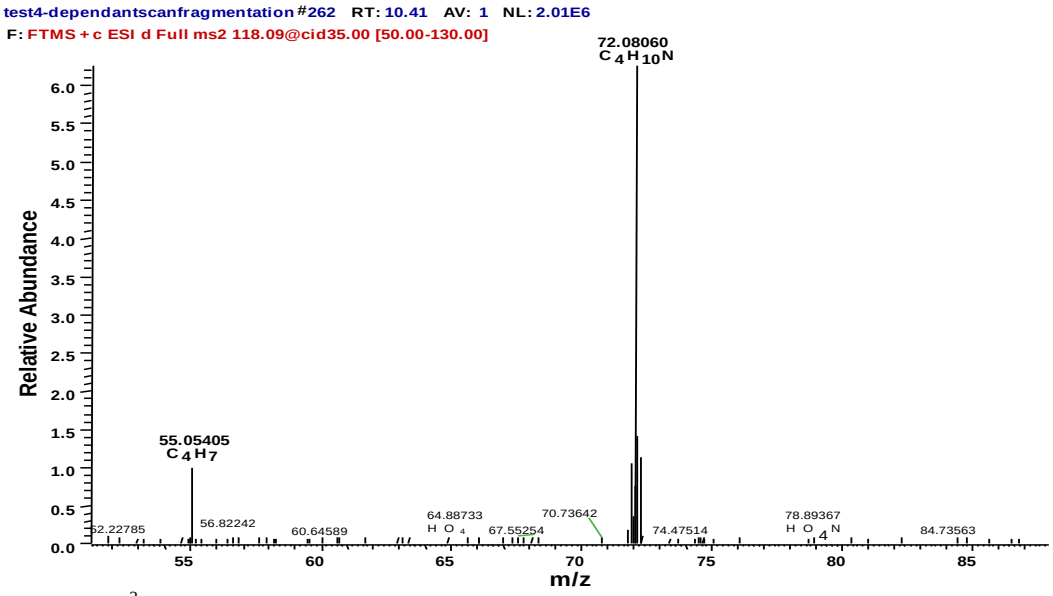

Figure 4.9: MS^2 spectrum for valine amino acid during data dependent acquisition mode with ESI-CID-FTMS/MS.

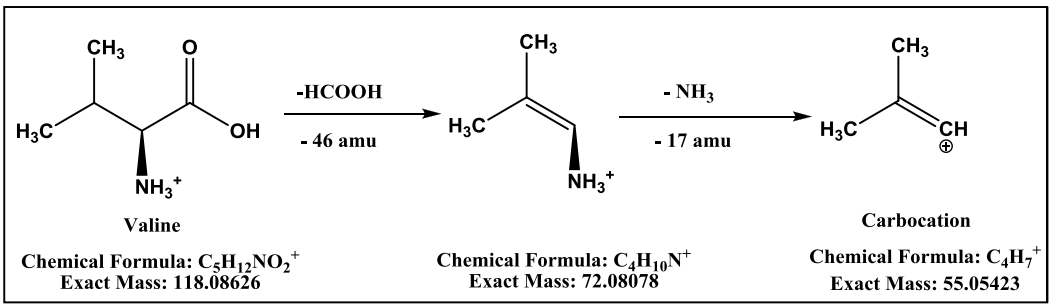

Scheme 4-2: Possible mechanistic pathways for valine amino acid fragmentation during data dependent acquisition mode with ESI-CID-FTMS/MS.

The MS^2 result for methionine shows the normal fragmentation pathways as for other amino acids with the exception of low intensity fragment at m/z 87 (Figure 4.10). This fragment can be explained by loss the ionisable groups in the main structure of the

amino acid and the formation of a fragment which consists of carbocation (Scheme 4-3). The generation of the carbocation ion from methionine is quite similar to the formation of the carbocation from valine by of 2 consecutive eliminations of HCOOH and NH_3 from the main structure of the amino acid with an additional fragmentation involving neutral loss of CH_3SH (Scheme 4-3).

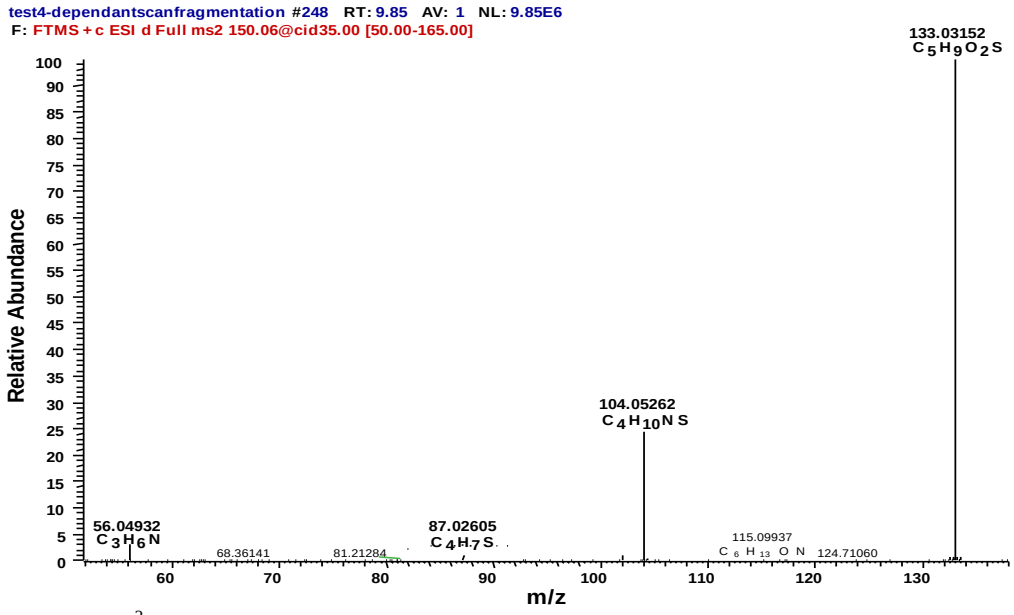

Figure 4.10: MS^2 spectra for methionine amino acid during data dependent acquisition with ESI-CID-FTMS/MS.

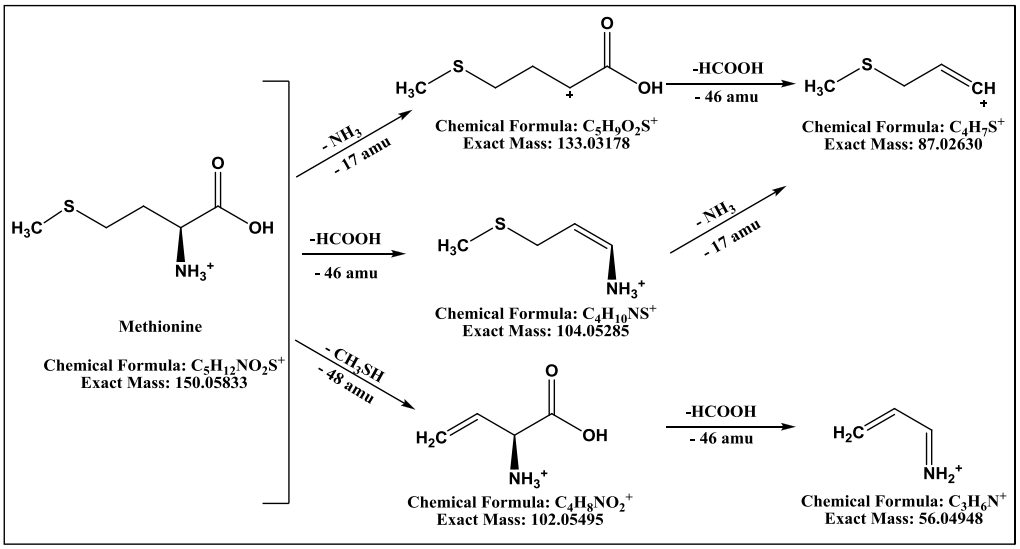

Scheme 4-3: Possible fragmentation pathways for methionine amino acid during data dependent acquisition mode with ESI-CID-FTMS/MS.

4.5.2.2 Alpha-Beta Cleavage (α,β- Cleavage)

The α,β- cleavage includes the fragmentation of the covalent bond between α,β-carbon atoms with H-shift. Fragmentation pathways following such cleavage will result in a variety of specific fragments. Although α-β cleavage is not the dominant pathway for amino acid fragmentation, the MS^2 results for some amino acids: tryptophan, aspartic acid, and histidine show specific fragments with low abundance as a result of such fragmentation pathways.

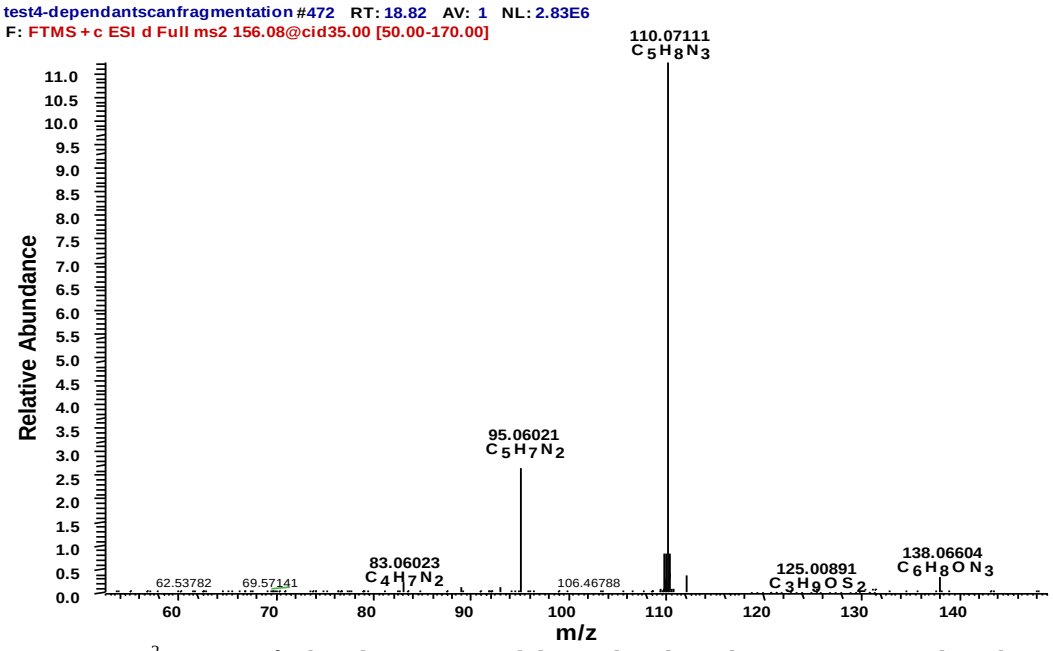

Figure 4.11: MS^2 spectrum for histidine amino acid during data dependent acquisition mode with ESI-CID-FTMS/MS.

The MS^2 spectrum for histidine amino acid (Figure 4.11) shows, in addition to the main fragments at m/z 110 (loss of HCOOH, 46 amu) and 95 (loss of NH_3 and CO_2, 61 amu), a minor fragment at m/z 83. This fragment can only be explained by the α-β cleavage of the histidine amino acid as shown in Scheme 4-4.

According to the formula for the product ion, such fragment can be explained by assuming that the positive charge will be retained by the imidazole ring rather than the α-amine group. The α-β cleavage of the histidine amino acid occurs via the elimination

of the iminoacetic acid moiety (73 amu) from the histidine amino acid leading to the formation of the methyl-imidazolium ion at m/z 83 and a neutral iminoacetic acid fragment. Such fragmentation pathway involves H-shift in order to form a cationic fragment.

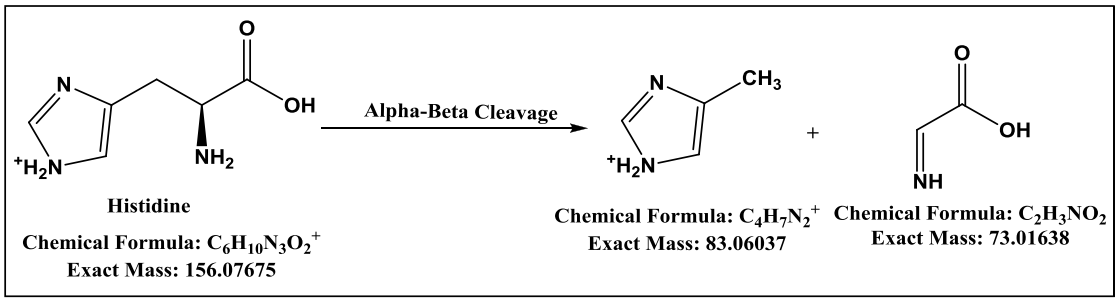

Scheme 4-4: Possible fragmentation pathway for histidine amino acid during data dependent acquisition mode with ESI-CID-FTMS/MS.

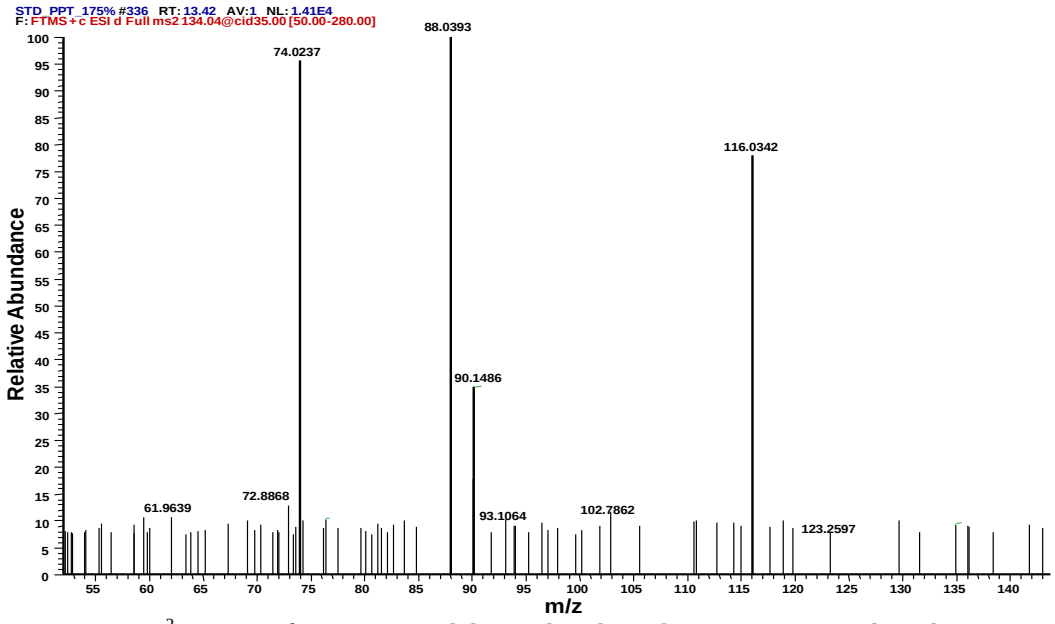

Figure 4.12: MS^2 spectrum for aspartic acid during data dependent acquisition mode with ESI-CID-FTMS/MS.

The MS^2 spectrum for aspartic acid fragmentation showed a minor fragment at m/z 74 (Figure 4.12). Unlike histidine, α-β cleavage of the aspartic acid eliminates an acetic acid moiety as a neutral fragment from the main structure of the amino acid and the possible iminoacetic acid cation formation at m/z 74.

Scheme 4-5 shows the mechanistic pathway for aspartic acid fragmentation through α-β cleavage with H-shift from the cation to the neutral fragment. Such fragmentation pathway is quite similar to α-β cleavage of histidine amino acid except that the positive charge is retained by the iminoacetic acid fragment.

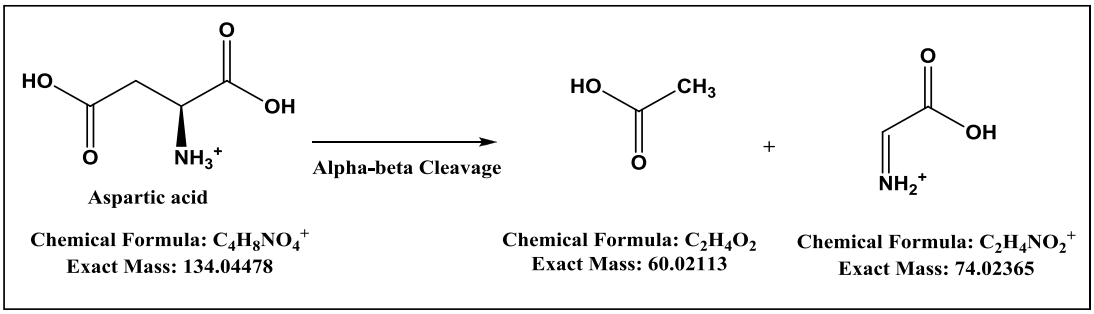

Scheme 4-5: Possible fragmentation pathway for aspartic acid during data dependent acquisition mode with ESI-CID-FTMS/MS.

The MS^2 spectrum for tryptophan (Figure 4.13) contains a minor fragment at m/z 130. Tryptophan amino acid will eliminates an aminoacetic acid moiety as a neutral fragment with H-shift from the cationic fragment to the neutral fragment.

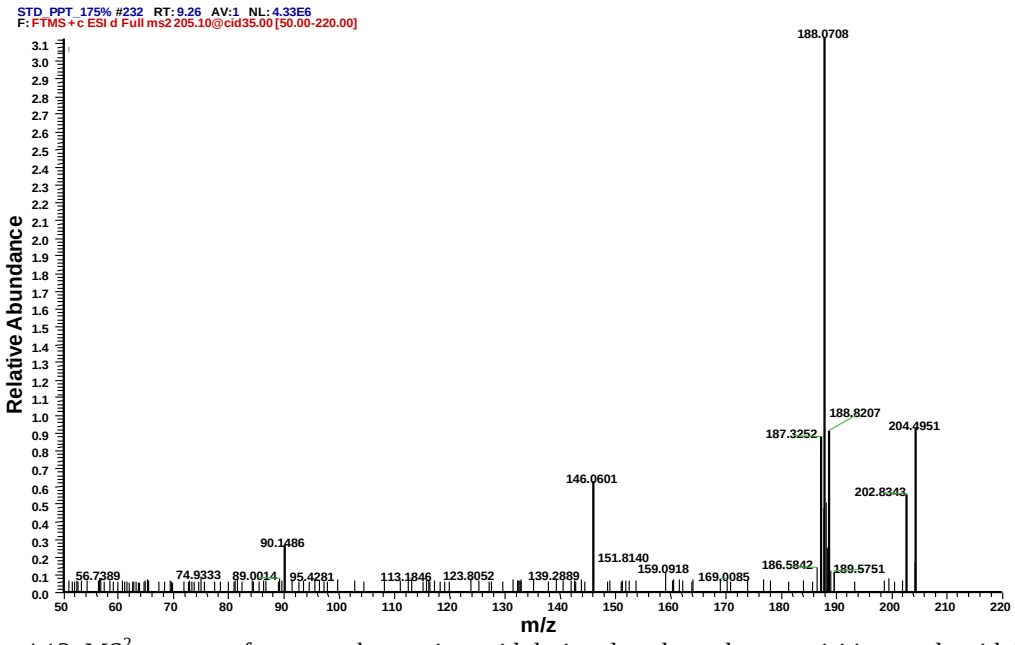

Figure 4.13: MS^2 spectrum for tryptophan amino acid during data dependent acquisition mode with ESI-CID-FTMS/MS.

Surprisingly, another fragment at m/z 146 could be detected; the formula for this fragment suggested that this fragment is different from the fragment m/z 130 by one O atom. Thus, a hydroxylation process may have occurred during MS^2 fragmentation (Scheme 4-6).

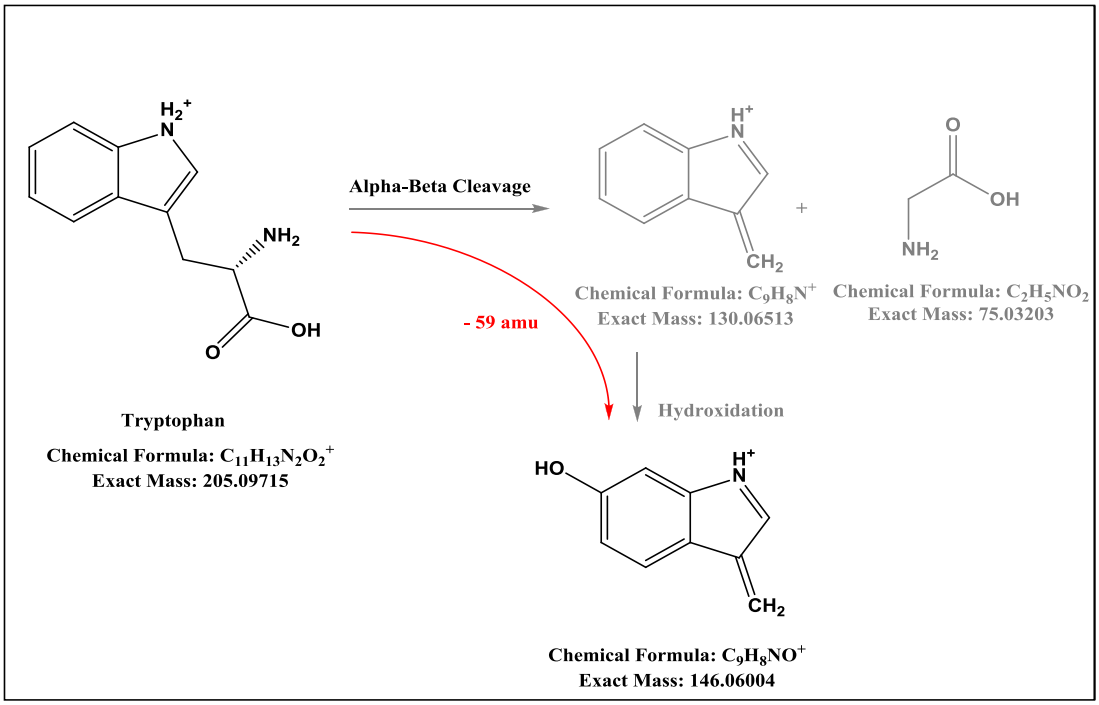

Scheme 4-6: Possible fragmentation pathways for tryptophan amino acid during data dependent acquisition mode with ESI-CID-FTMS/MS.

The process of hydroxylation can be explained by the following: tryptophan eluted at 9.25 min with high water content in the mobile phase at this moment. Thus, the iontrap (fragmentation compartment) during DDA is not 100% free of water at this moment. The CID energy will cause a water molecule to split into $H^{\bullet}$ & $OH^{\bullet}$ radicals and this explains the hydroxylation of the aromatic ring of tryptophan; this process is more likely to occur in an iontrap than a triple quadrupole instrument since all ions are held together in the trap until ejection. Formation of fragment at m/z 130 during fragmentation of tryptophan was reported by Domingues *et al.* [165] but the formation of the fragment at m/z 146 was not reported by, however he confirms the ability of tryptophan to undergo hydroxylation via the Fenton reaction. If we consider Fenton reaction as a step to bring $OH^{\bullet}$ radical into contact with tryptophan amino acid, then the same situation is occurring

inside the iontrap compartment where $OH^{\bullet}$ radical is formed during water fragmentation. Aromatic nucleus of tryptophan amino acid as well as position 2 & 3 of the pyrrole ring represent the main reaction sites for the $OH^{\bullet}$ radical [171].

4.5.2.3 Tropylium Ion Formation

The tropylium ion is a very stable cation as the charge trans-located from one site to another forming a resonance stabilised cation (Figure 4.14). Sometimes, the formation of the tropylium ion is the final product of the fragmentation process for the compound, and sometimes it can be a transitional state for the formation of another fragment[113].

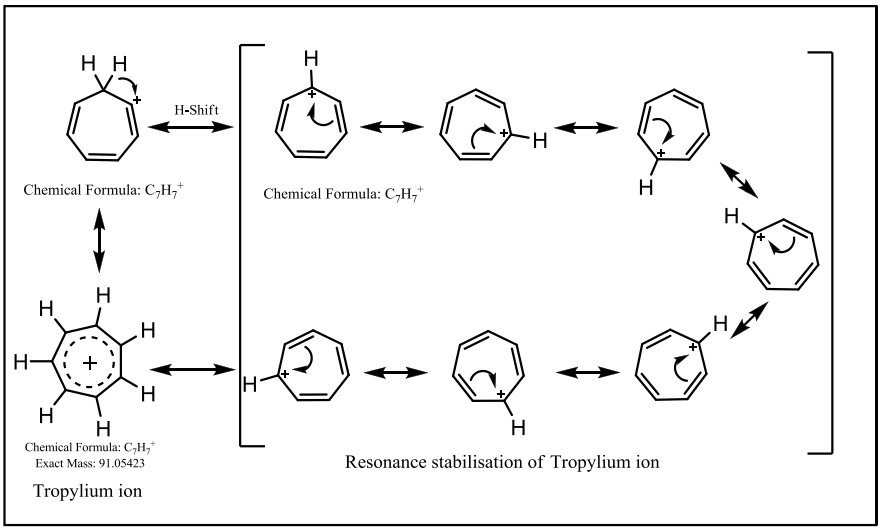

Figure 4.14: Resonance stabilisation of the tropylium ion by charge delocalisation [172].

MS^2 spectrum for tyrosine (Figure 4.15) shows abundant fragments at m/z 165 & 136 that result from loss of NH_3 (17 amu) and HCOOH (46 amu) from the precursor ion. Minor fragments could be detected at m/z 147, 123, and 107. The fragment m/z 147 is a result of a consecutive loss of water and NH_3 groups from tyrosine amino acid, whereas the fragment m/z 107 is a result of α-β cleavage and carbocation formation. Carbocation will undergo further re-arrangements to produce a tropylium ion at m/z 107 (Scheme 4-7). However, the fragment m/z 123 can only be explained by further hydroxylation of the tropylium ion, according to the chemical formula generated for this fragment and could occur as described previously for tryptophan.

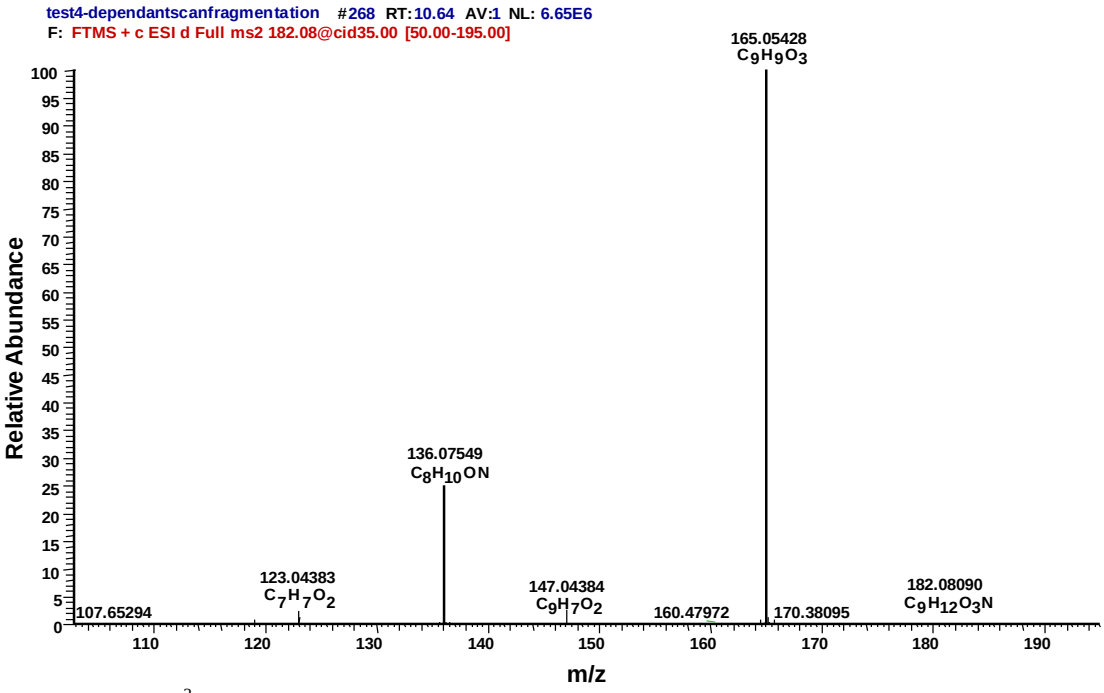

Figure 4.15: MS^2 spectrum for tyrosine amino acid during data-dependent acquisition with ESI-CID-FTMS/MS.

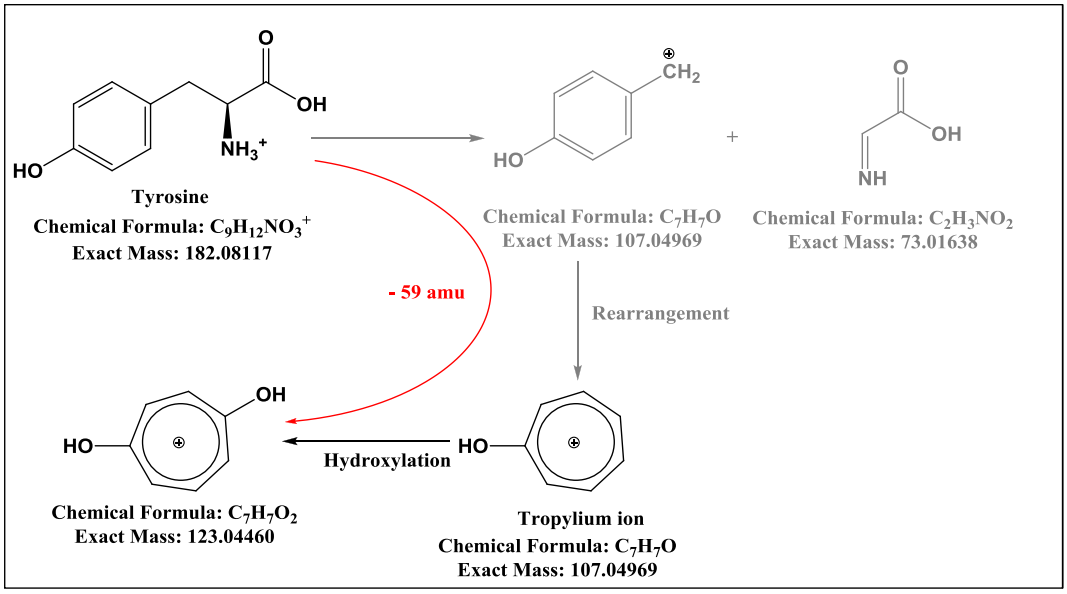

Scheme 4-7: Possible fragmentation pathways for tyrosine amino acid during data dependent acquisition mode with ESI-CID-FTMS/MS.

4.5.2.4 Specific Arginine Fragments

The MS^2 spectrum for arginine shows 2 main fragments at m/z 158 and 157 which result from the general fragmentation pathways by eliminating NH_3 (17 amu), and H_20 (18 amu) from the precursor ion (Figure 4.16).

In addition to the 2 main fragments, another 3 minor fragments could be detected at m/z 130, 116, and 60. Loss of guanidine group of arginine as neutral molecule will result in a fragment at m/z 116, whereas retention of the positive charge by the guanidine group will result in a fragment at m/z 60 (Scheme 4-8).

However, the third fragment that could be detected with enough intensity at m/z 130 which could be explained by subsequent elimination of HCOOH molecule from the main structure of the amino acid followed by oxidative deamination of the imine group, as explained in the Scheme 4-8.

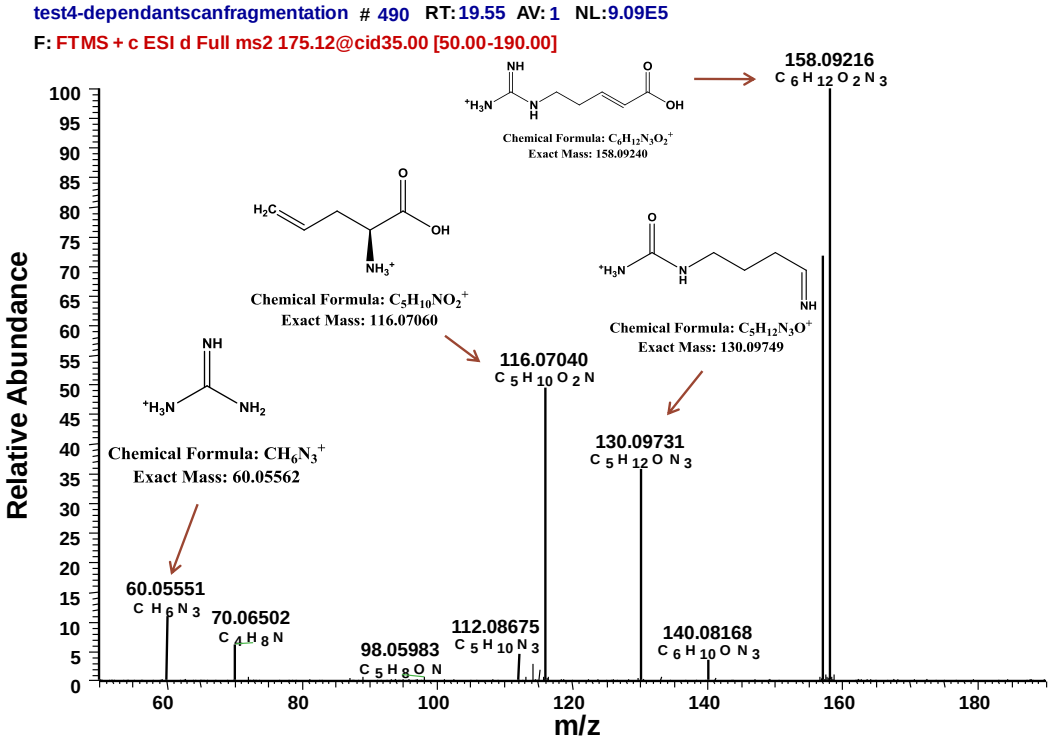

Figure 4.16: MS^2 spectrum for arginine amino acid during data dependent acquisition mode with ESI-CID-FTMS/MS.

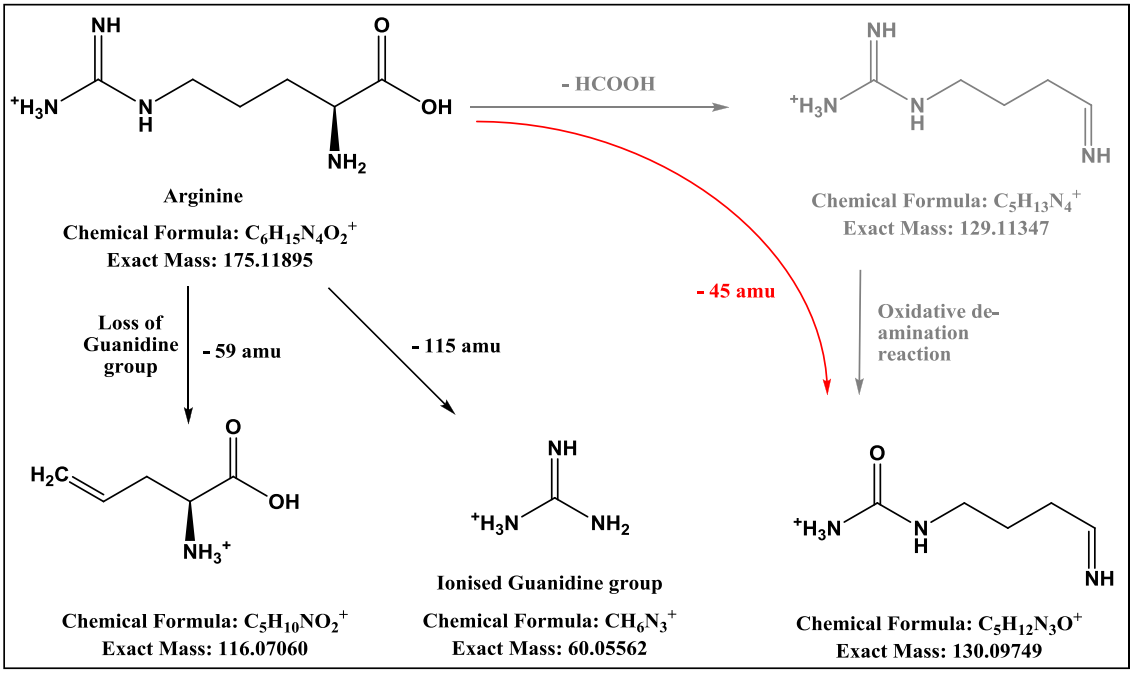

Scheme 4-8: Possible mechanistic pathway for arginine amino acid fragmentation during data dependent acquisition mode with ESI-CID-FTMS/MS.

4.6 Analysis of 2-Alkenal Adducts Using a ZIC-HILIC Column in Combination with FTMS

After finishing validation for the best method for amino acids extraction and FTMS detection, the next step was to investigate the capacity of the methods for 2-alkenal adducts detection in standard and biological samples. Production and preparation of ALEs compounds was done according to the procedure described in section 2.3. Extraction of the desired compounds from the protein hydrolysate was carried using PPT method according to procedure described in section 2.5.3.

Finally, in order to investigate the source of different 2-alkenal adducts which were generated as a result of different degrees of reduction in the reduction step with $NaBH_4$, non-reduced samples were used to indicate the sources of different forms of 2-alkenal adducts that were generated as a result of different degrees of reduction in the reduction step with $NaBH_4$.

4.6.1 Reactions of 2-Alkenals with Lysine

4.6.1.1 Schiff Base and Michael-Like Addition Reactions

A single step reaction of 2-alkenals with lysine amino acid residues in protein molecule can result in a set of compounds known as Schiff bases and Michael adducts (Figure 4.17).

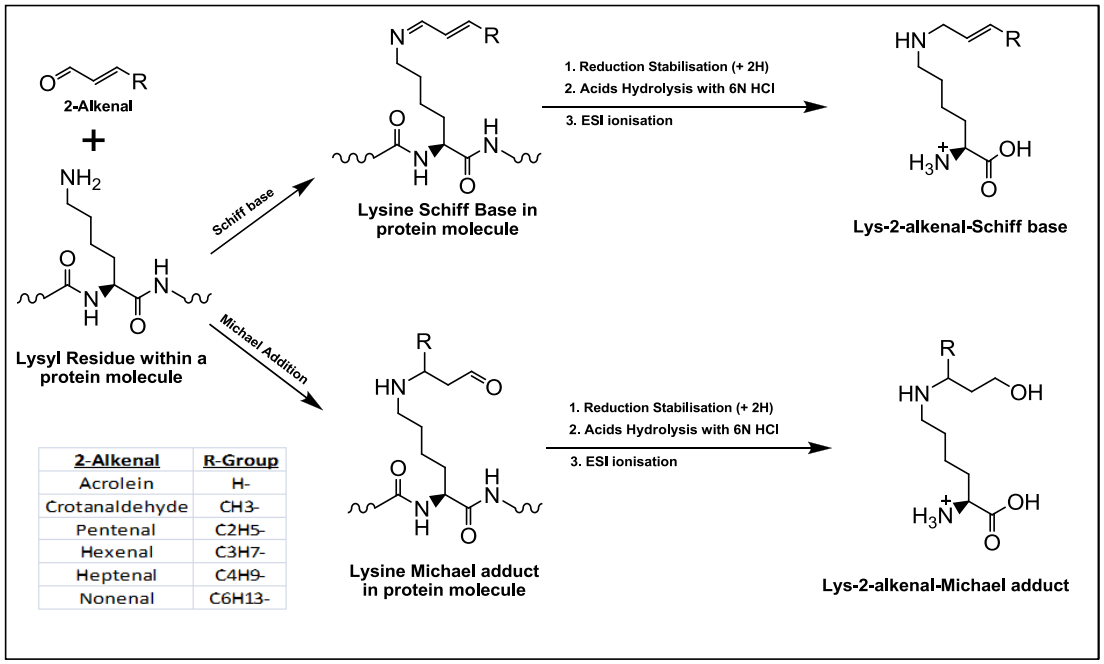

Figure 4.17: Reaction of 2-alkenal aldehydes with lysyl residue within a protein molecule through Schiff base and Michael addition reactions. Reduction stabilisation and acid hydrolysis with 6N HCl steps is essential for individual adduct detection.

Table 4-11 & Table 4-12 show the mass spectrometric results for non-derivatised Schiff base and Michael adducts that could be detected in the protein hydrolysate modified with different 2-alkenal adducts. Most of these adducts were detected within 1 ppm deviation from the theoretical masses for these adducts.

Table 4-11: Mass spectrometry results for Lys-Schiff bases modified with different 2-alkenals using ESI-FTMS.

Type of adduct	*Elemental formulae*	*RDB*	*R_t Control (min)*	*Observed m/z*	*Delta ppm*
lysine	$C_6H_{15}N_2O_2$	**0.5**	**19.47**	**147.11249**	**-1.07**
Acr-Lys-S	$C_9H_{19}N_2O_2$	**1.5**	**14.31**	**187.14410**	**0.38**
Cro-Lys-S	$C_{10}H_{21}N_2O_2$	**1.5**	**15.85**	**201.15975**	**-0.88**
Pne-Lys-S	$C_{11}H_{23}N_2O_2$	**1.5**	**12.51**	**215.17540**	**-1.26**
Hxe-Lys-S	$C_{12}H_{25}N_2O_2$	**1.5**	**12.48**	**229.19105**	**-0.78**
Hpe-Lys-S	$C_{13}H_{27}N_2O_2$	**1.5**	**11.84**	**243.20670**	**-1.06**
Nne-Lys-S	$C_{15}H_{31}N_2O_2$	**1.5**	**10.96**	**271.23800**	**-1.10**

Table 4-12: Mass spectrometric results for Lys-Michael adducts modified with different 2- alkenals using ESI-FTMS.

Type of adduct	*Elemental formulae*	*RDB*	*R_t Control (min)*	*Observed m/z*	*Delta ppm*
lysine	$C_6H_{15}N_2O_2$	**0.5**	**19.47**	**147.11249**	**-1.07**
Acr-Lys-M	$C_9H_{21}N_2O_3$	**0.5**	**18.67**	**205.15467**	**-0.89**
Cro-Lys-M	$C_{10}H_{23}N_2O_3$	**0.5**	**17.95**	**219.17032**	**-1.08**
Pne-Lys-M	$C_{11}H_{25}N_2O_3$	**0.5**	**16.67, 17.07, 17.49**	**233.18597**	**0.42**
Hxe-Lys-M	$C_{12}H_{27}N_2O_3$	**0.5**	**15.62, 16.19, 16.67**	**247.20162**	**-1.37**
Hpe-Lys-M	$C_{13}H_{29}N_2O_3$	**0.5**	**12.46**	**261.21727**	**-0.98**
Nne-Lys-M	$C_{15}H_{33}N_2O_3$	**0.5**	**11.68**	**289.24857**	**-1.10**

The elution of the compounds on the ZIC-HILIC compounds is greatly influenced by the hydrophilicity of the compounds, as the hydrophilicity the compound increases the elution time increases. The retention time for the Lys-Schiff bases range between 14.30 min (Acr-Lys-S) and 10.91 min (Nne-Lys-S adduct), whereas the retention time for Lys-Michael adducts range between 18.67 min (Acr-Lys-M adduct) and 11.68 min (Nne-Lys-M adduct). It is noticeable that the retention times for these adducts are significantly different from retention time of the lysine as a result of the reduction in hydrophilicity due to reaction with 2-alkenal aldehydes. In addition, the hydrophilicity of the adduct decreases as the length of the side chain of 2-alkenal aldehydes increases.

Multiple peaks pattern could be detected for some Michael adducts, such as Pne-Lys-M and Hxe-Lys-M. This is expected (apart from in the case of acrolein) as an additional chiral centre is being introduced during adduct formation making the possibility of two diastereoisomers is possible; the difference in the chromatographic properties for the

diastereoisomers may be related to the size of the R-group in the adduct (Figure 4.17). The second peak shows an identical fragmentation pattern to the first peak, which confirms that the second peak is related to isomeric form for that adduct. The presence of a third isomer in some cases is more difficult to explain and suggests that the amino acid may also react at different positions with aldehydes.

Michael adducts for Hpe and Nne failed to show a multiple peak pattern and this can be attributed to 3 possible reasons. The first reason for the disappearance of the multiple peaks can be attributed to very low concentration of the secondary isomers insufficient for MS detection (below the detection threshold). For example: Hpe-Lys-M shows a very low abundance (just above 0% as reported in section 4.8) amongst the different Hpe-Lys adducts. The second reason for the disappearance of the multiple peaks pattern can be attributed to peaks overlapping and peaks broadening that may result from high concentration of these adducts as compared to the concentration of Pne & Hxe Michel adducts. For example, Nne-Lys-M adduct shows a high abundance (3.78% as reported in section 4.8) amongst the different Nne-Lys adducts. The third explanation for the disappearance of the multiple peaks pattern can be attributed to an early elution time for these adducts; multiple peaks for different isomers will elute at the same time due to insufficient retention of these adducts on the ZIC-HILIC column.

Non reduced samples were used to investigate the importance of the reduction stabilisation step with 5 M $NaBH_4$ on the stability of Schiff base and Michael adducts against acid hydrolysis step with 6N HCl (Table 4-13 & Table 4-14).

With the exception of Acr-Lys-S & M and to a very low extent Hxe-Lys-S base, most of the Lys-Schiff bases and Lys-Michael adducts could not be detected in non-reduced samples as a result of their instability to acid hydrolysis.

Table 4-13: MS results for non reduced Lys-Schiff Base adducts in non reduced protein samples. All the results were within 2 ppm. N=4.

Adduct	*Type of Adduct*	*Elemental formula*	*RDB*	*R_t control (min) for the reduced adducts*	*R_t (min)*	*Observed m/z*	*Average Peak Area*
Lysine	*Amino acid*	$C_6H_{15}N_2O_2$	0.5	19.47	19.53	147.11249	27870336
Acr-Lys	*Lys-Schiff Base*	$C_9H_{17}N_2O_2$	2.5	14.31	18.69	185.12845	138748
Cro-Lys	*Lys-Schiff Base*	$C_{10}H_{19}N_2O_2$	2.5	15.85	N/A	199.1441	N/A
Pne-Lys	*Lys-Schiff Base*	$C_{11}H_{21}N_2O_2$	2.5	12.51	N/A	213.15975	N/A
Hxe-Lys	*Lys-Schiff Base*	$C_{12}H_{23}N_2O_2$	2.5	12.48	12.35	227.1754	87660.5
Hpe-Lys	*Lys-Schiff Base*	$C_{13}H_{25}N_2O_2$	2.5	11.84	N/A	241.19105	N/A
Nne-Lys	*Lys-Schiff Base*	$C_{15}H_{29}N_2O_2$	2.5	10.96	N/A	269.22235	N/A

Table 4-14: MS results for non reduced Arg-Michael adducts in non reduced protein samples. All the results were within 2 ppm. N=4.

Adduct	*Type of Adduct*	*Elemental formula*	*RDB*	*R_t control (min) for the reduced adducts*	*R_t (min)*	*Observed m/z*	*Average Peak area*
Lysine	*Amino acid*	$C_6H_{15}N_2O_2$	0.5	19.47	19.57	147.11249	27870336
Acr-Lys	*Lys-Michael Adduct*	$C_9H_{19}N_2O_3$	1.5	18.67	19.39	203.13902	31743
Cro-Lys	*Lys-Michael Adduct*	$C_{10}H_{21}N_2O_3$	1.5	17.95	N/A	217.15467	N/A
Pne-Lys	*Lys-Michael Adduct*	$C_{11}H_{23}N_2O_3$	1.5	16.67, 17.07, 17.49	N/A	231.17032	N/A
Hxe-Lys	*Lys-Michael Adduct*	$C_{12}H_{25}N_2O_3$	1.5	15.62, 16.19, 16.67	N/A	245.18597	N/A
Hpe-Lys	*Lys-Michael Adduct*	$C_{13}H_{27}N_2O_3$	1.5	12.46	N/A	259.20162	N/A
Nne-Lys	*Lys-Michael Adduct*	$C_{15}H_{31}N_2O_3$	1.5	11.68	N/A	287.23292	N/A

4.6.1.2 Lysine-Pyridinium Adduct Formation

Lysine pyridinium adducts can result from 2 subsequent reactions of 2 aldehyde molecules from 2-alkenals with lysine amino acid residues in protein molecule (Figure 1.4 in section 1.2.1.3). Reduction stabilisation of the modified protein samples with 5M $NaBH_4$ can result in different reduction levels for the same adduct and 5 different reduced and non-reduced forms could be detected (Figure 6.7).

Figure 4.18 shows the possible chemical structure for different 2-alkenal-pyridinium adducts that may result from different reduction levels during reduction step with $NaBH_4$, whereas Table 4-15 shows the expected masses for Lys-pyridinium adduct when incubated with different 2-alkenal aldehydes.

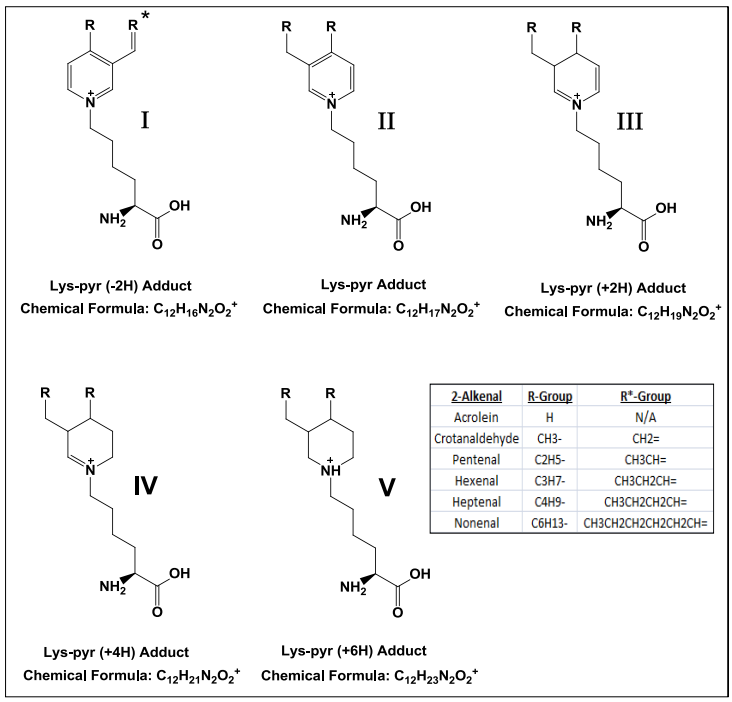

2-Alkenal	R-Group	R^+-Group
Acrolein	H	N/A
Crotanaldehyde	CH3-	CH2=
Pentenal	C2H5-	CH3CH=
Hexenal	C3H7-	CH3CH2CH=
Heptenal	C4H9-	CH3CH2CH2CH=
Nonenal	C6H13-	CH3CH2CH2CH2CH2CH=

Figure 4.18: The possible chemical structures for different reduced form for non-derivatised lysine-pyridinium adducts.

Table 6-17 to Table 6-22 show the mass spectrometric results for non-derivatised lysine-pyridinium adducts. The observed masses were within 2 ppm deviation from the theoretical masses for these adducts. A marked reduction in the retention time is obvious throughout the series of 2-alkenal adducts due to a gradual decrease in the hydrophilicity of the 2-alkenal-pyridinium compounds. Acrolein-pyridinium adducts show a minimum shift in the retention time (18.83-16.57 min) in comparison to lysine amino acid (19.47 min), whereas nonenal-pyridinium adducts shows the maximum shift in retention time (9.97-9.57 min) as compared to lysine amino acid. Acrolein aldehyde will add little lipophilicity to lysine amino acid due to the small side chain of the acrolein. Whereas 2-nonenal aldehyde adds a large degree of lipophilicity to lysine amino acid due the long side chain of the 2-nonenal aldehyde moiety.

Again, multiple peaks for isomers of the early eluting adducts, such as Hxe, Hpe, and Nne pyridinium adducts, are absent, while it is quite obvious for late eluting adducts such Acr, Cro, and Pne pyridinium adducts. Both geometrical isomers and diastereoisomers can contribute to the multiple peaks.

Analysis of non-reduced protein samples confirms Baker's assumption [section 1.2.1.3] which proposed that Lys-pyridinium adducts [Lys-pyr and Lys-pyr (-2H)] are the main pyridinium adducts that would result from the reaction between lysine amino acid with 2-alkenal aldehydes. Other Lys-pyridinium adducts [Lys-pyr (+2H), Lys-pyr (+4H), and Lys-pyr (+6H)] is a matter of reduced forms that may result from different reduction levels during reduction step with $NaBH_4$ (Table 6-23). In most of non reduced protein samples, Lys-pyr (-2H) has higher intensity than Lys-pyr adduct. This confirms that Lys-pyr (-2H) is the main final product compound for the reaction of the 2-alkenals with lysine amino acid.

Table 4-15: Expected chemical masses for the ionised Ly-pyridinium adducts that should be detected by ESI-FTMS.

2-ALKENAL	*Lys-Pyr (-2H)*	*Lys-Pyr*	*Lys-Pyr (+2H)*	*Lys-Pyr (+4H)*	*Lys-Pyr (+6H)*
ACROLEIN	**N/A**	**223**	**225**	**227**	**229**
CROTANALDEHYDE	**249**	**251**	**253**	**255**	**257**
2-PENTENAL	**277**	**279**	**281**	**283**	**285**
2-HEXENAL	**305**	**307**	**309**	**311**	**311**
2-HEPTENAL	**333**	**335**	**337**	**339**	**341**
2-NONENAL	**389**	**391**	**393**	**395**	**397**

4.6.1.3 Formyl-Dehydro-Piperidino (FDP) Lysine Adducts Formation

Formed by a similar reaction to lysine pyridinium adducts, lysine-FDP adducts also result from 2 subsequent reactions of 2 aldehyde molecules with lysine residues in protein molecules (Figure 1.5 in section 1.2.1.3). Reduction stabilisation of the modified protein samples with 5M $NaBH_4$ can result in different reduction levels for the Lys-FDP adducts and different reduced forms could be detected (Figure 3.5 in section 3.2.3). On contrast to pyridinium adducts, only 3 reduction levels would be expected for Lys-FDP adducts including reduced and non reduced forms.

Figure 4.19 shows the possible chemical structure for different 2-alkenal-Lys-FDP adducts that may result from different reduction levels during reduction step with

$NaBH_4$, whereas Table 4-16 shows the expected masses for the different Lys-FDP adducts; none of the Lys-FDP (+4H) could be deteceted with this method and could be justified by low recovery for these adducts.

2-Alkenal	R-Group
Acrolein	H-
Crotanaldehyde	CH3-
Pentenal	C2H5-
Hexenal	C3H7-
Heptenal	C4H9-
Nonenal	C6H13-

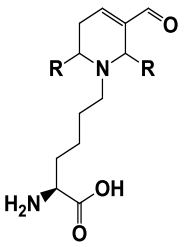

Derivatised lys-FDP adduct

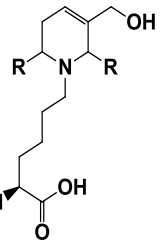

Derivatised lys-FDP (+2H) adduct

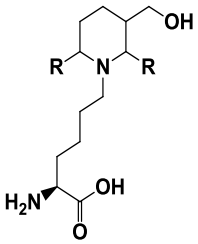

Derivatised lys-FDP (+4H) adduct

Figure 4.19: Possible chemical structures for different reduced forms of Lys-FDP adduct.

Mass spectrometry results for different reduced forms of Lys-FDP have been included in Table 4-17. The observed masses are within 1.5 ppm deviation from the theoretical masses for these adducts. With Lys-pyridinium adducts a great reduction in the retention time had been explained by the possible decrease in the hydrophilicity of the 2-alkenal-pyridinium compounds. A similar explanation for retention time can be used for Lys-FDP adducts where a decrease in the retention time of the Lys-FDP adduct can be observed as the length of the side chain of the 2-alkenal aldehyde increases.

Mass spectrometry detection of the Lys-FDP adducts using the PPT method and a ZIC-HILIC column is quite different from the situation where the EZ:faast method and a C-18 column was used. FDP adducts -2, -4, or -6H could be detected when the EZ:faast method and C-18 column were used, whereas using PPT method and ZIC-HILIC column failed to show such adducts. Since these adducts showed a very low detectability with the EZ:faast method and C-18 column, then failure to detect these adducts with HILIC suggesting that adducts may become chemically modified by the derivatisation conditions used in the EZ:faast method.

Table 4-16: Expected chemical masses for the ionised Lys-FDP adducts.

2-ALKENAL	*Ionised Lys-FDP adduct*	*Ionised Lys-FDP (+2H) Adduct*	*Ionised Lys-FDP (+4H) Adduct*
ACROLEIN	**241**	**243**	**245**
CROTANALDEHYDE	**269**	**271**	**273**
2-PENTENAL	**297**	**299**	**301**
2-HEXENAL	**325**	**327**	**329**
2-HEPTENAL	**353**	**355**	**357**
2-NONENAL	**409**	**411**	**413**

Table 4-17: Mass spectrometry results for ionised lysine-FDP (+2H) adducts.

Adduct	*Type of Adduct*	*Elemental formula*	*RDB*	*R_t control (min)*	*m/z*	*Delta ppm*
lysine	***Lysine a.a.***	$C_6H_{15}N_2O_2$	**0.5**	**19.47**	**147.11249**	**-1.40**
Acr-FDP-243	***Lys-FDP (+2H)***	$C_{12}H_{23}O_3N_2$	**2.5**	**18.18**	**243.17032**	**1.25**
Cro-FDP-271	***Lys-FDP (+2H)***	$C_{14}H_{27}O_3N_2$	**2.5**	**16.9**	**271.20162**	**-0.90**
Pne-FDP-299	***Lys-FDP (+2H)***	$C_{16}H_{31}O_3N_2$	**2.5**	**12.51**	**299.23292**	**-1.04**
Hxe-FDP-327	***Lys-FDP (+2H)***	$C_{18}H_{35}O_3N_2$	**2.5**	**12.08**	**327.26422**	**-1.25**
Hpe-FDP-355	***Lys-FDP (+2H)***	$C_{20}H39O_3N_2$	**2.5**	**10.48, 11.20**	**355.29552**	**0.49**
Non-FDP-411	***Lys-FDP (+2H)***	$C_{24}H_{47}O_3N_2$	**2.5**	**10.23**	**411.35812**	**-1.58**

4.6.2 Reaction of 2-Alkenals with Arginine

Reactions of arginine residues in protein molecules with 2-alkenals have been extensively discussed in section 3.3, where the EZ:faast method and RPLC-FTMS revealed the ability of the arginine to react with 2-alkenals through Schiff base and Michael addition reactions. Detection of non-derivatised Arg-Schiff base and Arg-Michael adducts (Figure 4.20) using the PPT method and the ZIC-HILIC column confirmed the results obtained by the earlier method.

Table 4-18 & Table 4-19 show the mass spectrometry results for non derivatised Arg-Schiff base and Michael adducts. The masses for the observed adducts were within 1 ppm deviation of the theoretical masses for the expected adducts. The retention times for Arg-Schiff base & Arg-Michael adducts range between 10 and 17 min, with significantly earlier elution of the Schiff bases as compared to Michael adducts. This can be attributed to the low hydrophilicity of the Schiff bases due to the elimination of the aldehyde group of the 2-alkenal during reaction with arginine amino acid.

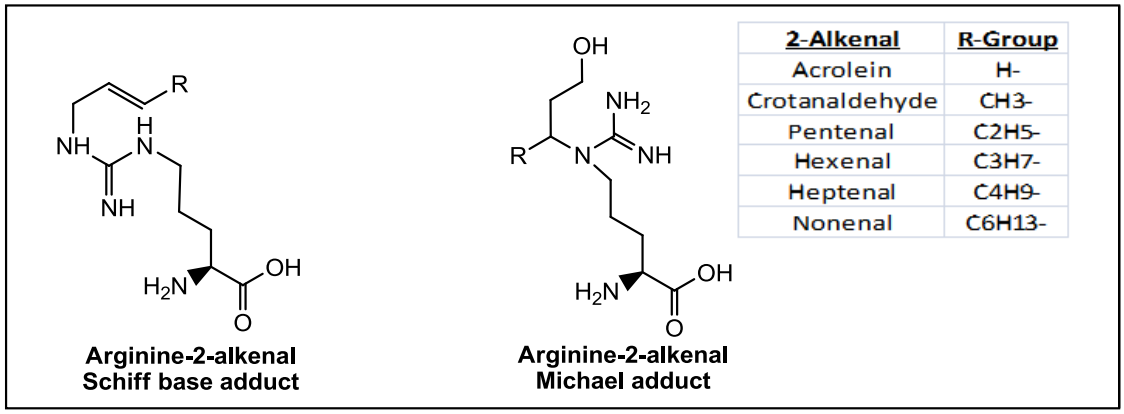

Figure 4.20: Individual arginine Schiff base and Michael adducts released from protein molecule after reduction and acid hydrolysis steps.

Table 4-18: Chemical formulas and mass spectrometry results for Schiff base formation between arginine and the 2-alkenal series.

Adduct	*Type of Adduct*	*Elemental formula*	*RDB*	*R_t control (min)*	*m/z*	*Delta ppm*
Arginine	***Amino Acid***	$C_6H_{15}N_4O_2$	**1.5**	**19.15**	**175.11861**	**-1.19**
Acr-Arg	***Arg-Schiff Base***	$C_9H_{19}N_4O_2$	**2.5**	**N/A**	**215.15025**	**-0.46**
Cro-Arg	***Arg-Schiff Base***	$C_{10}H_{21}N_4O_2$	**2.5**	**15.32, 17.09**	**229.16590**	**-1.48**
Pne-Arg	***Arg-Schiff Base***	$C_{11}H_{23}N_4O_2$	**2.5**	**N/A**	**243.18155**	**-0.04**
Hxe-Arg	***Arg-Schiff Base***	$C_{12}H_{25}N_4O_2$	**2.5**	**12.8**	**257.19720**	**-1.22**
Hpe-Arg	***Arg-Schiff Base***	$C_{13}H_{27}N_4O_2$	**2.5**	**11.92**	**271.21285**	**0.34**
Nne-Arg	***Arg-Schiff Base***	$C_{15}H_{31}N_4O_2$	**2.5**	**10.88**	**299.24415**	**-0.77**

Table 4-19: Chemical formulas and mass spectrometry results for Michael addition reaction between arginine and the 2-alkenal series.

Adduct	*Type of Adduct*	*Elemental formula*	*RDB*	*R_t control (min)*	*m/z*	*Delta ppm*
Arginine	***Amino Acid***	$C_6H_{15}N_4O_2$	**1.5**	**19.15**	**175.11861**	**-1.19**
Acr-Arg	***Arg-Michael Adduct***	$C_9H_{21}N_4O_3$	**1.5**	**N/A**	**233.16082**	**0.01**
Cro-Arg	***Arg-Michael Adduct***	$C_{10}H_{23}N_4O_3$	**1.5**	**17.06**	**247.17647**	**-0.78**
Pne-Arg	***Arg-Michael Adduct***	$C_{11}H_{25}N_4O_3$	**1.5**	**16.02**	**261.19212**	**-1.11**
Hxe-Arg	***Arg-Michael Adduct***	$C_{12}H_{27}N_4O_3$	**1.5**	**14.38**	**275.20777**	**-0.69**
Hpe-Arg	***Arg-Michael Adduct***	$C_{13}H_{29}N_4O_3$	**1.5**	**12.57**	**289.22342**	**-0.93**
Nne-Arg	***Arg-Michael Adduct***	$C_{15}H_{33}N_4O_3$	**1.5**	**11.44**	**317.25472**	**-0.79**

The extracted ion current for Cro-Arg-S at m/z 229.16 shows a major peak (at 15.32 min) overlapped with minor peak (at 17.09 min) that may result from multiple isomers for the same adduct as a consequence of cyclisation process discussed in section 3.3. However, low availability of such isomers below the detection threshold for mass spectrometry instrument can justify the inability of the current method for isomers detection.

MS^2 applications were unsuccessful in confirming the identity of multiple peaks for arginine adducts as they failed to trigger MS^2 during data dependent acquisition mode due to low intensity of the arginine adducts as compared to more intense co-eluted compounds. Manipulating the parameters for MS^2 fragmentation during data dependent acquisition mode failed to exclude the more intense co-eluted peaks from detection.

Previously in section 3.3, where the EZ:faast method had been used as an extraction and derivatisation method, the acrolein-arginine adducts (Schiff base or Michael adduct) could not be detected in some samples, and a possible justifications have been proposed. The current method, using PPT as an extraction method and ZIC-HILIC column coupled to ESI-FTMS as separation and detection method, confirms these findings as none of these adducts could be detected. However, MS detection of Acr-Arg adducts in non-reduced protein samples reveals significant levels of such adducts.

Table 4-20: MS results for non-reduced Arg-Schiff base adducts in non reduced protein samples. All the results were within 1.5 ppm. N=4.

Adduct	*Type of Adduct*	*Elemental formula*	*RDB*	*R_t control (min) for the reduced adducts*	*R_t (min)*	*Observed m/z*	*Average Peak Area*
Arginine	***Amino acid***	$C_6H_{15}N_4O_2$	**1.5**	**19.15**	**19.17**	**175.11861**	**132051648.5**
Acr-Arg	***Arg-Schiff Base***	$C_9H_{17}N_4O_2$	**3.5**	**N/A**	**18.33**	**213.1346**	**2183228**
Cro-Arg	***Arg-Schiff Base***	$C_{10}H_{19}N_4O_2$	**3.5**	**15.32, 17.09**	**17.12**	**227.15025**	**31953.5**
Pne-Arg	***Arg-Schiff Base***	$C_{11}H_{21}N_4O_2$	**3.5**	**N/A**	**N/A**	**241.1659**	**N/A**
Hxe-Arg	***Arg-Schiff Base***	$C_{12}H_{23}N_4O_2$	**3.5**	**12.8**	**N/A**	**255.18155**	**N/A**
Hpe-Arg	***Arg-Schiff Base***	$C_{13}H_{25}N_4O_2$	**3.5**	**11.92**	**N/A**	**269.1972**	**N/A**
Nne-Arg	***Arg-Schiff Base***	$C_{15}H_{29}N_4O_2$	**3.5**	**10.88**	**N/A**	**297.2285**	**N/A**

Table 4-21: MS results for non reduced Arg-Michael adducts in non reduced protein samples. All the results were within 1.5 ppm. N=4.

Adduct	*Type of Adduct*	*Elemental formula*	*RDB*	*R_t control (min) for the reduced adducts*	*R_t (min)*	*Observed m/z*	*Average Peak area*
Arginine	***Amino acid***	$C_6H_{15}N_4O_2$	**1.5**	**19.15**	**19.20**	**175.11861**	**132051648.5**
Acr-Arg	***Arg-Michael Adduct***	$C_9H_{19}N_4O_3$	**2.5**	**N/A**	**18.33**	**231.14517**	**39568412**
Cro-Arg	***Arg-Michael Adduct***	$C_{10}H_{21}N_4O_3$	**2.5**	**17.06**	**17.12**	**245.16082**	**3915299**
Pne-Arg	***Arg-Michael Adduct***	$C_{11}H_{23}N_4O_3$	**2.5**	**16.02**	**16.05**	**259.17647**	**946124.5**
Hxe-Arg	***Arg-Michael Adduct***	$C_{12}H_{25}N_4O_3$	**2.5**	**14.38**	**14.53**	**273.19212**	**40653.5**
Hpe-Arg	***Arg-Michael Adduct***	$C_{13}H_{27}N_4O_3$	**2.5**	**12.57**	**12.51**	**287.20777**	**167870**
Nne-Arg	***Arg-Michael Adduct***	$C_{15}H_{31}N_4O_3$	**2.5**	**11.44**	**11.48**	**315.23907**	**38676**

Table 4-20 & Table 4-21 show the expected chemical formula for non reduced arginine Schiff base and Michael adducts, observed masses, retention time (R_t), retention time for the corresponding reduced adducts (R_t control), and the average peak area for these adducts (n=4).

Excluding reduction step with $NaBH_4$ greatly influenced the stability of the arginine-Schiff base adducts against acid hydrolysis (with the exception of Acr-Arg-S & Cro-Arg-S). whereas arginine-Michael suffer from minor stability issue as reflected by very small peak area for the non reduced adducts as compared to the reduced form of the correspondent adducts. The debate here is to confirm whether arginine modifications have occurred during incubation with acrolein aldehydes or not? If a reduction step is essential to stabilise Schiff base and Michael adducts against the acid hydrolysis step, why can Acr-Arg Schiff base and Michael adducts be detected with non-reduced protein samples while it is not possible with reduced protein samples? Although the elemental composition of Acr-Arg adducts (Schiff and Michael adducts) in the non-reduced samples could be confirmed by: (1) accurate mass measurements (less than 1.5 ppm) and a relative retention time. Confirmation is still required to indicate if modification has occurred or not. This can be done by comparing the intensity (or peak area) of the arginine between a standard HSA sample and a modified HSA sample (which had been incubated with acrolein aldehyde). The 2 samples were subjected to reduction step with $NaBH_4$ prior acid hydrolysis step, and were also hydrolysed without a reduction step. Lysine used as a reference in both samples.

Figure 4.21 shows the retention time, chromatographic peak, and the peak area (as an indicator for concentration) for lysine and arginine between the 4 types of protein hydrolysate samples: reduced HSA (sample #1), reduced HSA modified with acrolein aldehyde (sample #2), non-reduced HSA (sample #3), and non-reduced HSA modified with acrolein aldehyde (sample #4).

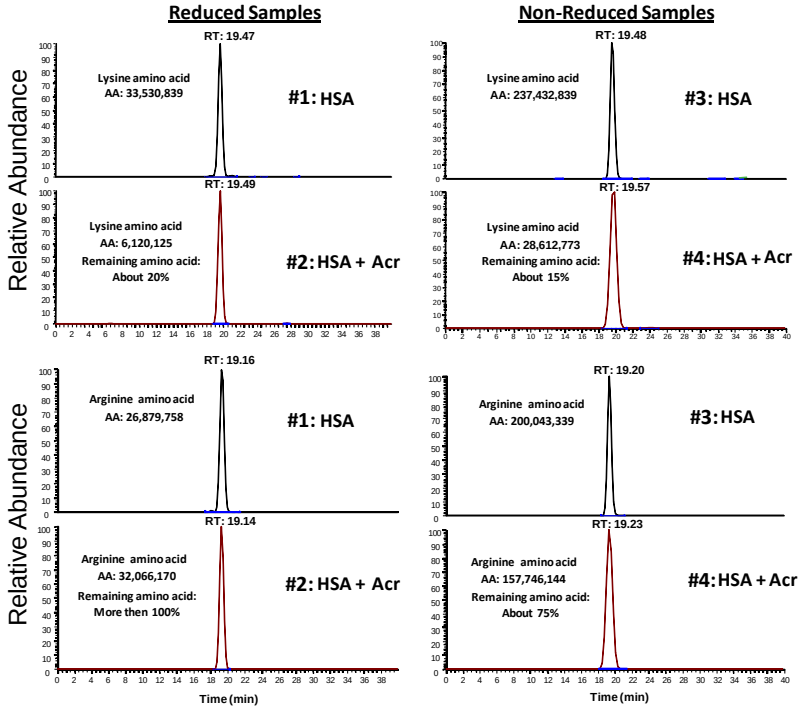

Figure 4.21: Comparison of lysine and arginine between standard HSA hydrolysate and modified HSA (modified with acrolein aldehydes) hydrolysate. Sample (#1) reduced HSA, sample (#2) reduced HSA+Acrolein, sample (#3) non- reduced HSA, and sample (#4) non- reduced HSA+Acrolein. 5 M $NaBH_4$ was used as reducing agent prior to acid hydrolysis with 6N HCl at 145°C for 4 hrs.

The percentage of the remaining lysine in reduced HSA protein samples which have been incubated with acrolein aldehyde should be around 15% (section 4.8). Arginine showed no modification at all, when HSA was incubated with acrolein aldehyde. Results obtained from non reduced protein samples (sample #1 and #2) show no modifications for arginine when HSA had been incubated with acrolein aldehyde. The peak area for arginine is almost the same between sample #1 and sample #2 if we consider the variation that may results from different arginine concentration between the 2 samples. However, non reduced protein samples (sample #3 and #4) showed arginine modification by around 25% (Figure 4.21). These arginine modifications, when HSA was incubated with acrolein aldehyde and hydrolysed without reduction step, could be recovered as Acr-Arg-Schiff base and Acr-Arg-Michael adduct. More complex modifications might be expected, however insufficient information about these modifications leaves us with the assumption that Acr-Arg Schiff base and Michael adducts are the main adducts. This gives enough indication that there was no

modification for arginine amino acid in the reduced sample, while arginine modification could be detected in non-reduced samples as Acr-Arg adducts. This raises the argument: does reduction with $NaBH_4$ affect the stability of Acrolein-Arginine adducts? Why we could see these adducts in the case when HSA was incubated with other 2-alkenals such as hexenal, heptenal, nonenal, etc.? Such questions need more investigation.

4.6.3 Reaction of 2-Alkenals with Histidine

Histidine amino acid residues in protein molecules can react with 2-alkenal aldehydes through a single step Michael addition reaction resulting in a set of compounds known as His-Michael adducts (Figure 4.22). The reaction involves the reaction between the double bond of the 2-alkenal with the imidazole ring [173]. Reduction of His-Michael adducts results in the reduction of the peripheral aldehyde group to the corresponding primary alcohol group. Table 4-22 shows the mass spectrometry results for non derivatised His-Michael adducts, and the generated formulas for the observed adducts were within 1 ppm deviation from the theoretical masses for these adducts.

The retention time for His-Michael adducts ranged between 11 and 18 min, with significant decrease in the retention time of the 2-alkenal adduct as the side chain of the 2-alkenal moiety increased. Most of these adducts could be detected as single peak, with the exception of Hpe-His Michael adducts which could be detected at m/z 270.18112 with multiple peak pattern. The MS^2 spectrum could confirm the identity of the 2 peaks as both of them show the same fragmentation pattern. Hpe-His Michael adduct showed fragments at m/z 226, 224, 209 which may resulted from the loss of CO_2 (44 amu), HCOOH (46 amu), CO_2+NH_3 (61 amu) from the parent compound (Figure 4.23). The fragment at m/z 156 represents histidine after losing the 2-heptene moiety, whereas fragments at m/z 112, 110, and 95 result from subsequent loss of CO_2, HCOOH, CO_2+NH_3 from the histidine fragment at m/z 156.

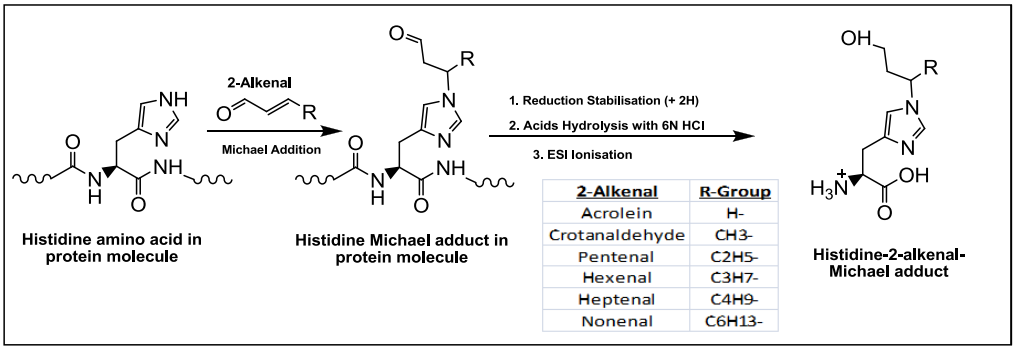

Figure 4.22: Reaction of 2-alkenal aldehydes with histidine amino acid residue in protein molecule through Schiff base and Michael addition reactions.

Table 4-22: Chemical formulas and mass spectrometry results for Michael addition reaction between histidine and the 2-alkenal series**.**

Adduct	*Type of Adduct*	*Elemental formula*	*RDB*	*R_t control (min)*	*m/z*	*Delta ppm*
Histidine	***Amino Acid***	$C_6H_{10}N_3O_2$	**3.5**	**18.5**	**156.07637**	**-1.28**
Acr-His	***His-Michael adduct***	$C_9H_{16}N_3O_3$	**3.5**	**18.02**	**214.11862**	**0.23**
Cro-His	***His-Michael adduct***	$C_{10}H_{18}N_3O_3$	**3.5**	**17.28**	**228.13427**	**-0.49**
Pne-His	***His-Michael adduct***	$C_{11}H_{20}N_3O_3$	**3.5**	**16.51**	**242.14992**	**-0.68**
Hxe-His	***His-Michael adduct***	$C_{12}H_{22}N_3O_3$	**3.5**	**14.98**	**256.16557**	**0.34**
Hpe-His	***His-Michael adduct***	$C_{13}H_{24}N_3O_3$	**3.5**	**12.57, 13.12**	**270.18122**	**-0.95**
Nne-His	***His-Michael adduct***	$C_{15}H_{28}N_3O_3$	**3.5**	**11.28**	**298.21252**	**-1.03**

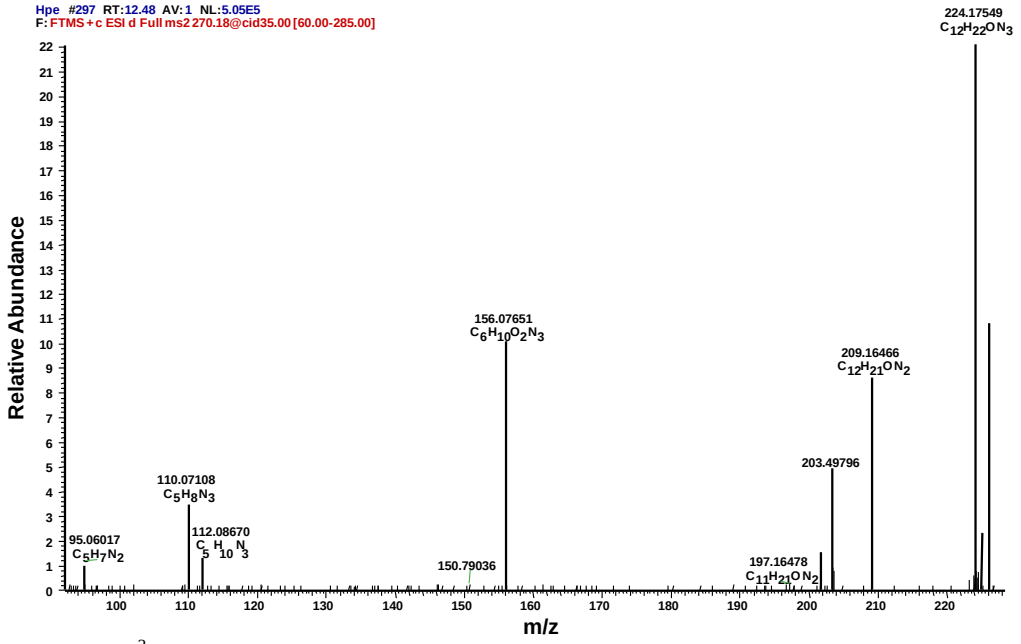

Figure 4.23: MS^2 spectrum for Hpe-His-M adducts during dependent acquisition mode with ESI-CID-FTMS/MS.

Mass spectrometry results for non reduced protein samples confirm inability of His-2-alkenal adducts (with the exception of Acr-His-M, Cro-His-M adducts which show a significant average peak area) to withstand the harsh conditions during the acid hydrolysis step. Table 4-23 shows the expected chemical formula for non reduced histidine Michael adducts, observed masses, retention time (R_t), retention time for the correspondent reduced adducts (R_t control), and the average peak area for these adducts over 4 samples.

Table 4-23: MS results for non reduced His-Michael adducts in non reduced protein samples. All the results were within 2 ppm. N=4.

Adduct	*Type of Adduct*	*Elemental formula*	*RDB*	*R_t control (min) for the reduced adducts*	*R_t (min)*	*Observed m/z*	*Average peak area*
Histidine	***Amino acid***	**$C_6H_{10}N_3O_2$**	**3.5**	**18.50**	**18.47**	**156.07637**	**20057105**
Acr-His	***His-Michael Adduct***	**$C_9H_{14}N_3O_3$**	**4.5**	**18.02**	**18.51**	**212.10297**	**9043270**
Cro-His	***His-Michael Adduct***	**$C_{10}H_{16}N_3O_3$**	**4.5**	**17.28**	**17.42**	**226.11862**	**269982.5**
Pne-His	***His-Michael Adduct***	**$C_{11}H_{18}N_3O_3$**	**4.5**	**16.51**	**N/A**	**240.13427**	**N/A**
Hxe-His	***His-Michael Adduct***	**$C_{12}H_{20}N_3O_3$**	**4.5**	**14.98**	**N/A**	**254.14992**	**N/A**
Hpe-His	***His-Michael Adduct***	**$C_{13}H_{22}N_3O_3$**	**4.5**	**12.57, 13.12**	**N/A**	**268.16557**	**N/A**
Nne-His	***His-Michael Adduct***	**$C_{15}H_{26}N_3O_3$**	**4.5**	**11.28**	**10.95**	**296.19687**	**22901**

4.6.4 Reaction of 4-Hydroxynonenal (HNE) with Amino Acids

The ability of HNE to react with different amino acids: lysine, arginine, histidine, and cysteine residues in protein molecule through Schiff base and Michael addition reactions has been discussed in detail in section 1.2.2. Furthermore, HNE shows the ability to react with 2 amino acids lysine-lysine or histidine-lysine through Michael addition reactions followed by a Schiff base reaction for the same molecule (Figure 1.10 & Figure 1.11 in section 1.2.2.5). Table 4-24 & Table 4-25 shows the mass spectrometry results for the non-derivatised HNE adducts for lysine, arginine, and histidine amino acids, respectively. All the observed adducts were within 1ppm deviation from the theoretical masses. The average peak area has been included in these tables in order to indicate the level of these adducts in the protein hydrolysate samples.

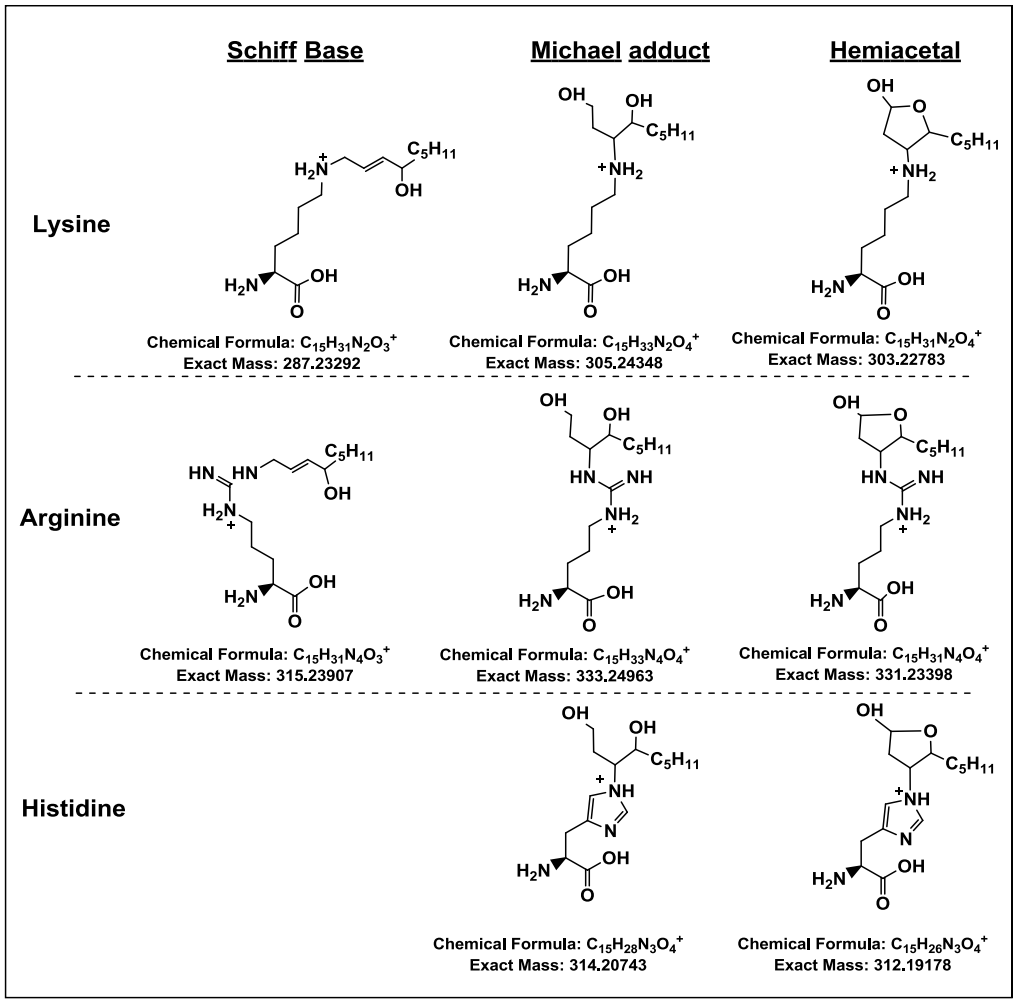

Figure 4.24: The expected chemical structure, formula, and theoretical mass for HNE adducts for lysine, arginine, and histidine amino acids.

Table 4-24: Mass spectrometry results for different HNE adducts**.**

Adduct	*Type of Adduct*	*Elemental Formula*	*R_t (min)*	*Observed mass (m/z)*	*RDB*	*ppm*	*Average peak area*
Lysine	***Amino Acid***	$C_6H_{15}N_2O_2$	**19.47**	**147.11278**	**0.5**	**-0.165**	**31513669.5**
Lys-HNE	***Schiff Base***	$C_{15}H_{31}N_2O_3$	**11.78**	**287.23309**	**1.5**	**0.594**	**26221913**
	Michael Adduct	$C_{15}H_{33}N_2O_4$	**12.15**	**305.24368**	**0.5**	**0.642**	**3463186.333**
Arginine	***Amino Acid***	$C_6H_{15}N_4O_2$	**19.20**	**175.11894**	**1.5**	**-0.07**	**37032041.83**
Arg-HNE	***Schiff Base***	$C_{15}H_{31}N_4O_3$	**11.60**	**315.23895**	**2.5**	**-0.372**	**982517.6667**
	Michael Adduct	$C_{15}H_{33}N_4O_4$	**N/A**	**N/A**	**N/A**	**N/A**	**N/A**
Histidine	***Amino Acid***	$C_6H_{10}N_3O_2$	**18.50**	**156.07674**	**3.5**	**-0.084**	**3230716.5**
His-HNE	***Michael Adduct***	$C_{15}H_{28}N_3O_4$	**11.91**	**314.2077**	**3.5**	**0.85**	**24629400.67**

Table 4-25 Accurate masses for HNE adducts formed by reaction with 2 amino acid residues HNE double adducts). N=6.

Type of Adduct	*Elemental Formula*	*R_t (min)*	*Observed mass (m/z)*	*RDB*	*Ppm*	*Average peak area*
Lys-HNE-Lys	**$C_{21}H_{45}N_4O_5$**	**24.48**	**433.33826**	**1.5**	**-0.431**	**406906.6667**
His-HNE-Lys	**$C_{21}H_{40}N_5O_5$**	**23.66**	**442.30194**	**4.5**	**-1.031**	**927023**

The retention time for HNE adducts (Schiff base & Michael adducts) range between 11 and 12 min for adducts generated by the reaction of HNE with single amino acid. Whereas, the retention time of the HNE adducts which had been generated upon reaction of HNE with 2 amino acids (HNE double adducts) have a very late elution time as compared to the amino acids and other HNE adducts. This can be explained by higher hydrophilicity of such adducts due to the availability of 2 amine groups and 2 carboxyl groups in the same molecule, compared to 1 amine group and 1 carboxyl group for other HNE adducts. All of HNE adducts show significant levels when compared to their related amino acid, and could be recovered as single peak. Inability to detect any of the hemiacetal adducts or Arg-HNE Michael adducts confirm the earlier results obtained by the EZ:faast method (Chapter 3), where none of the hemiacetal adducts could be detected. This lead to the 2 assumptions: (1) either these adducts undergo further chemical re-arrangements leading to the formation of compounds with the same chemical mass and retention time as other adducts, or (2) the formation of these adducts is not possible. Cysteine-HNE adducts could not be detected, and this can be attributed for the inability to recover the cysteine amino acids after acid hydrolysis. HNE adducts were not recovered in non-reduced samples.

4.7 Structure Elucidation for ALEs Using HILIC-FTMS/MS and PPT Method

The identity of 2-alkenal adducts was confirmed by using full scan MS, whereas MS^2 fragmentation was carried out using the data dependent acquisition mode according to the conditions and parameters specified in section 2.5.4. The MS^2 results for 2-alkenal adducts obtained by Orbitrap using data dependent acquisition mode are shown in Table 6-24. Different types of fragment could be observed for each individual adduct, and the most abundant fragment has been highlighted with red colour in the table. The detected masses for these fragments were within 2.5 ppm deviation from the assigned molecular formula.

In this section, the fragmentation pattern for 2-alkenal adducts can be related to the information and results obtained in section 4.5 for amino acids fragmentations. In general, 2-alkenal adducts will show the same fragmentation behaviour as standard amino acids when subject to the same fragmentation conditions. None of the specific fragmentation pathways [section 4.5.2] for amino acids could be detected with 2-alkenal adducts, with the exception of α,β-cleavage which could be detected with histidine adducts only.

4.7.1 Fixed Mass Loss Fragments

According to the MS/MS data shown in Table 6-24, a set of fragments which show the same behaviour by losing a specific moiety from the main structure of the 2-alkenal adduct could be detected. Mainly, fragmentation of 2-alkenal adducts occurs by the loss of a specific group from the precursor ion, such as ammonia (NH_3, 17 amu), water (H_2O, 18 amu), formic acid (HCOOH, 46 amu) or carbon dioxide (CO_2, 44amu) molecule. A combination of more than one group could be eliminated from the parent adducts, such as mass loss of 64 amu that may result from the consecutive loss of H_2O and HCOOH from the structure of the precursor ion. Fragmentation pathways for 2-alkenal adducts produced by specific mass loss from their structure are quite similar to the general fragmentation pathways for amino acids [section 4.5.1].

In the following sections only the fragmentation of lysine and histidine adducts will be discussed in details, since arginine adducts failed to trigger the MS^2 fragmentation during data dependent acquisition due to their low abundance in comparison with co-eluted compounds [section 4.6.2].

4.7.1.1 Lysine fragmentation: Fixed Mass Loss

Using high resolution mass spectrometry for accurate mass measurements for the product and precursor ions enabled us to precisely determine the chemical nature of these fragmentations. Different lysine adducts, such as Schiff base, Michael adduct, pyridinium and FDP adducts, show a similar fragmentation pathway by the loss of NH_3 (17 amu), H_2O (18 amu), CO_2 (44 amu), and HCOOH (46 amu). Losing of more than one group could be detected as the cases with mass loss of 61 amu (CO_2+NH_3) and 63 amu (HCOOH+NH_3) from the parent compounds. Other fragments could be detected resulting from the loss of most of a lysine moiety (129 amu). Finally, oxidative deamination could be detected with lysine adducts which lost 45 amu from the parent adducts. This has been explained for amino acids fragmentation in section 4.5.2.4) by losing CO_2 followed by oxidative deamination.

Table 4-26 shows the exact masses lost from the molecular ions (2-alkenal adducts) and the possible chemical nature the mass loss. Lysine adducts show a similar fragmentation for to the parent amino acid by losing of 17 amu from the molecular ion due to NH_3 elimination. For example, Nne-Lys-S base (m/z 271) shows a fragment that could be detected at m/z 254 at very low intensity as compared to other fragments (Figure 4.25). This fragment formed due to the elimination of NH_3 from the main structure of Nne-Lys-S base. Another fragment could be detected at m/z 226 which results from loss of 45 amu from the parent adduct and could be explained by oxidative deamination (Scheme 4-9). The MS^2 spectrum for the same adduct shows common ions at m/z 147, 130, and 84 with a significant intensity and will be discussed later.

Table 4-26: Fixed mass losses from Lys-2-alkenal adducts (precursor ions) during data dependent acquisition mode using ESI-CID-FTMS/MS.

Mass Loss	*Represent*	*Examples*	*Mass Loss*	*Represent*	*Examples*
17.02696	Loss of NH_3	Hxe-Lys-S	61.01663	Loss of CO_2 followed by NH_3	Hxe-pyr-305
		Acr-Lys-M			Hpe-pyr-333
		Nne-Lys-S			Nne-pyr-389
		Nne-His-M	63.03217	Loss of HCOOH+NH_3	Acr-FDP-243
18.01076	Loss of H_2O	Acr-FDP-243			Cro-Lys-M
		Acr-FDP-245			Hpe-FDP-355
		Hxe-FDP-327	129.07914	Loss of most of lysine moiety. $C_6H_{11}O_2N_1$	Acr-pyr-223
		Hpe-FDP-355			Acr-pyr-227
45.02153	Loss of CO_2 followed by oxidative deamination	Acr-Lys-M			Acr-pyr-229
		Acr-pyr-223			Acr-FDP-243
		Acr-pyr-227			Acr-FDP-245
		Acr-pyr-229			Cro-Lys-M
		Acr-FDP-243			Cro-pyr-251
		Cro-Lys-M			Pne-Lys-M
		Cro-pyr-251			Pne-pyr-277
		Pne-Lys-M			Pne-pyr-279
		Pne-pyr-277			Hxe-pyr-305
		Pne-pyr-279			Hxe-pyr-307
		Hxe-Lys-S			Hxe-FDP-327
		Hxe-pyr-307			Hpe-FDP-355
		Hxe-FDP-327			Hpe-pyr-339
		Hpe-Lys-S			Hpe-pyr-333
		Hpe-FDP-355			Nne-pyr-389
		Hpe-pyr-339	147.0897	Loss of lysine amino acid moiety followed by losing H_2O.	Acr-FDP-243
		Nne-His-M			Acr-FDP-245
		Nne-pyr-389			Hxe-FDP-327
		Nne-Lys-S			Hpe-FDP-355

Other fragmentation pathways could be detected for different lysine adducts (Schiff base, Michael adducts, pyridinium and FDP adducts) by losing 18, 63, 129, and 147 amu. For example, the MS^2 spectrum of Hpe-Lys-FDP (Figure 4.26) showed the product ions at m/z 337, 292, 226, and 208. Other fragments could be detected at m/z 310 which result from oxidative deamination pathway (loss of 45 amu), in addition to a fixed fragment which could be detected at m/z 130.

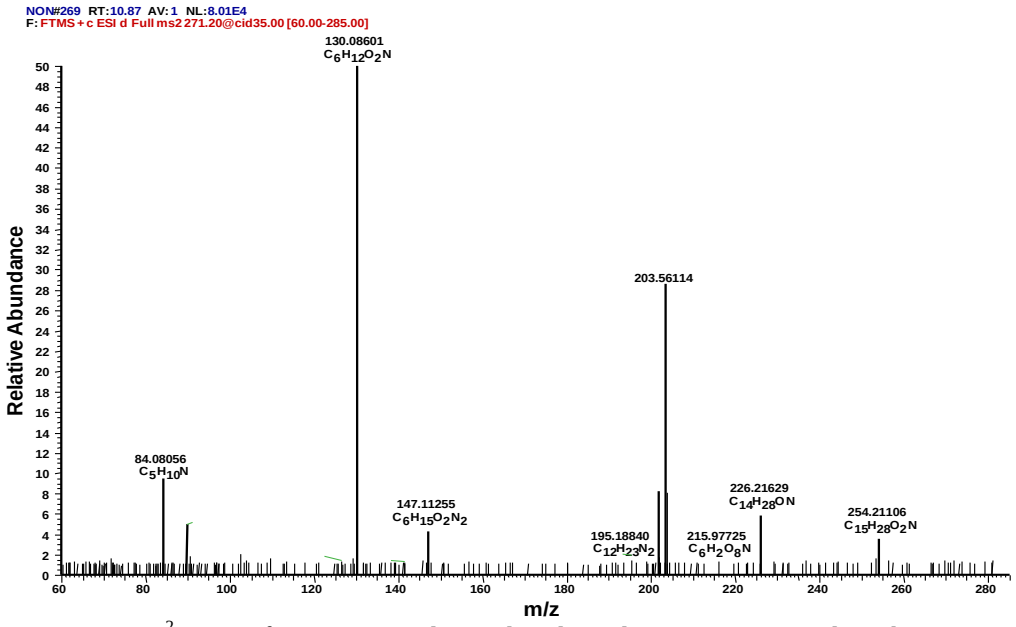

Figure 4.25: MS^2 spectra for Nne-Lys-S during data dependent acquisition mode with ESI-CID-FTMS/MS.

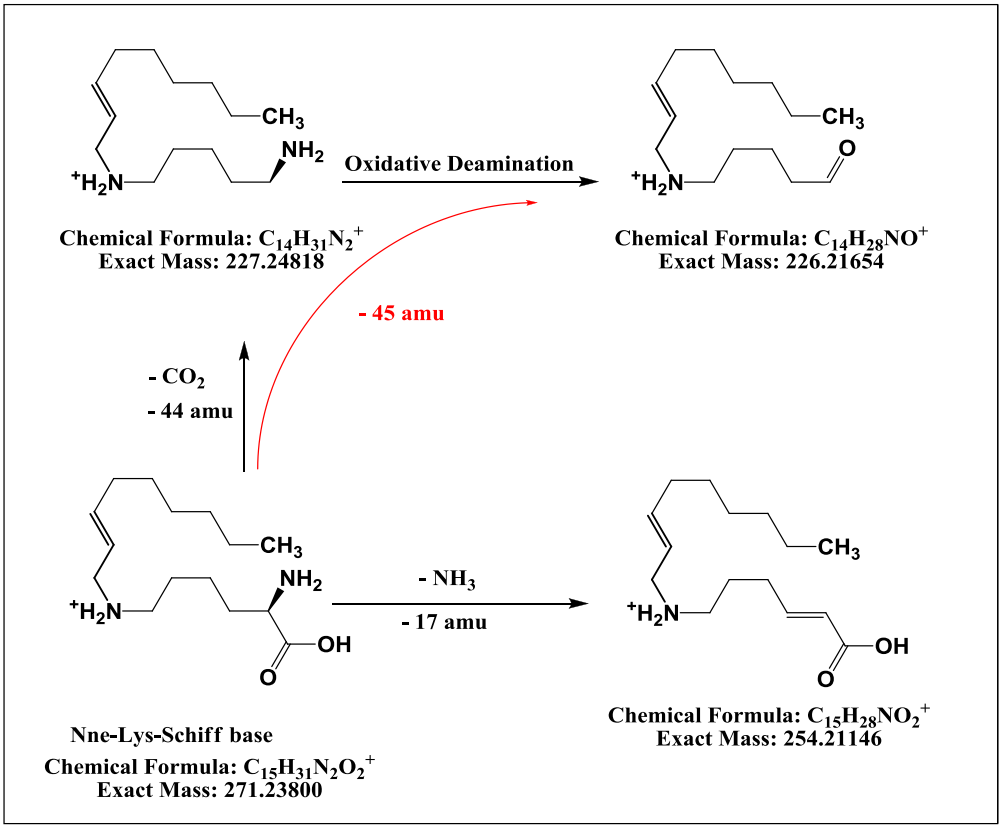

Scheme 4-9: Possible fragmentation pathways for Nne-Lys-S adduct during data dependent acquisition mode with ESI-CID-FTMS/MS.

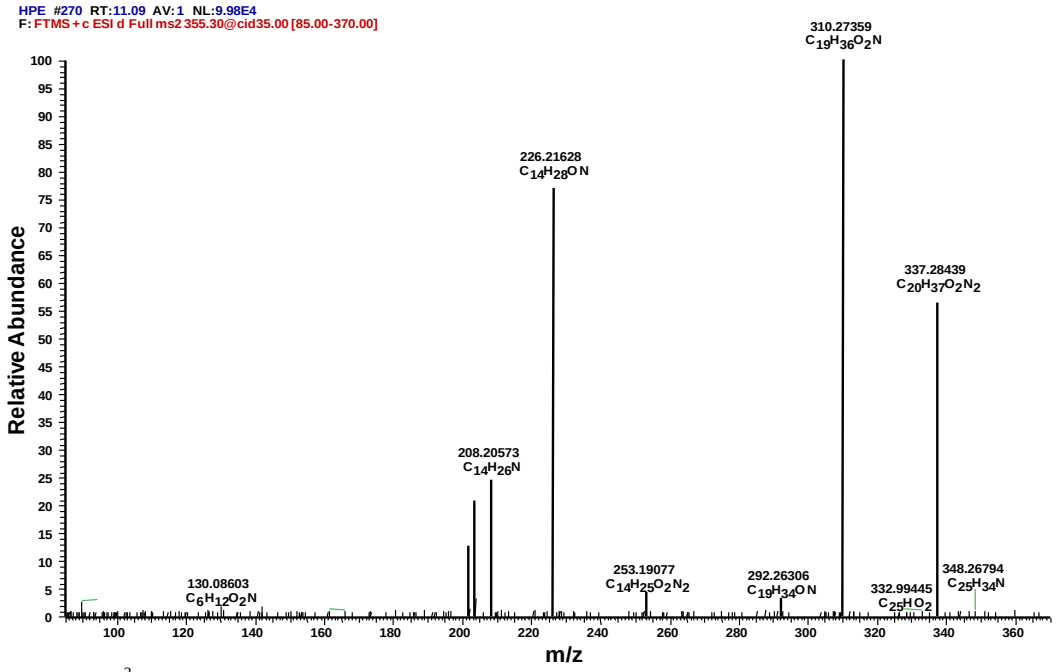

Figure 4.26: MS^2 spectra for Hpe-FDP-355 adduct during data dependent acquisition with ESI-CID-FTMS/MS.

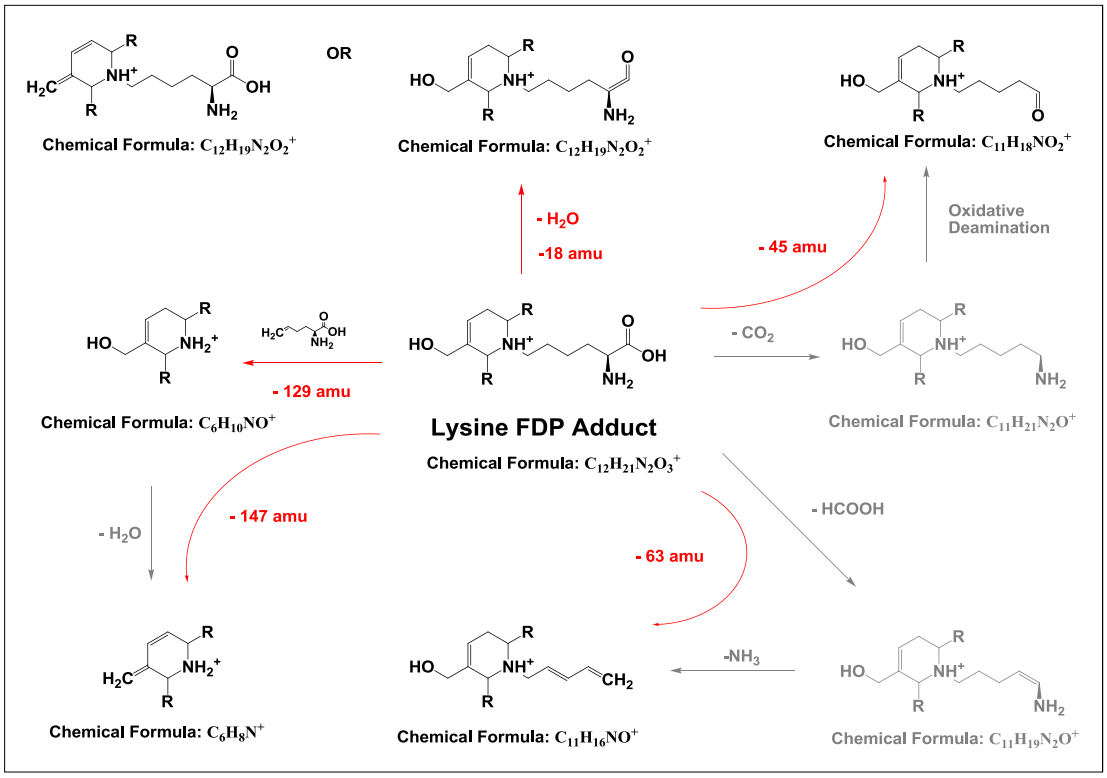

Scheme 4-10: Possible fragmentation pathways for Lys-FDP adduct during data dependent acquisition mode with ESI-CID-FTMS/MS. Acrolein (R=H), Crotanaldehyde (R=CH_3), 2-pentenal (R=CH_3CH_2-), 2-hexenal (R=$CH_3CH_2CH_2$-), 2-heptenal (R=$CH_3CH_2CH_2CH_2$-), and 2-Nonenal (R=$CH_3CH_2CH_2CH_2CH_2CH_2$-).

The sources of these fragments can be explained by the loss of H_2O (18 amu), with subsequent loss of HCOOH followed by further loss of NH_3 (63 amu), or by the loss of most of the lysine moiety (129 amu). Scheme 4-10 shows the possible pathways for Lys-FDP adduct fragmentation.

The fragment ion at m/z 310 may result from loss of CO_2 (44 amu) followed by oxidative deamination for the terminal amine group with overall loss of 45 amu. Oxidative deamination can be a dominant pathway, as the case with Hpe-Lys-FDP-355 adduct, or could be a minor pathway, as the case with Nne-Lys-Schiff base.

Finally, most of the pyridinium adducts show a fragment with minor intensity by losing of 61 amu from the parent compounds. This fragment can be attributed for the subsequent elimination of CO_2 molecule (44 amu) followed by further elimination of NH_3 group (17 amu), as explained in Scheme 4-11.

Figure 4.27 shows the MS^2 spectrum for Hpe-pyr-333 adduct with a dominant fragment peak at m/z 204 which results from the elimination of most of a lysine moiety (-129 amu), in addition to a minor fragment peak could be detected at m/z 272, which results from subsequent elimination of CO_2 and NH_3 (-61 amu) from the parent Hpe-pyr-333 adduct.

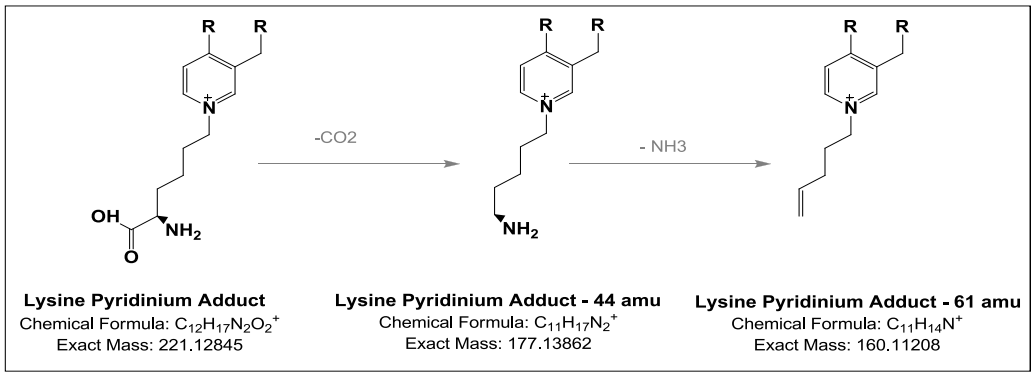

Scheme 4-11: Elimination of 61 amu from Lys-pyridinium adducts during data dependent acquisition mode with ESI-CID-FTMS/MS. Acrolein (R=H), Crotanaldehyde ($R=CH_3$), 2-pentenal ($R=CH_3CH_2$-), 2-hexenal ($R=CH_3CH_2CH_2$-), 2-heptenal ($R=CH_3CH_2CH_2CH_2$-), and 2-Nonenal ($R=CH_3CH_2CH_2CH_2CH_2CH_2$-).

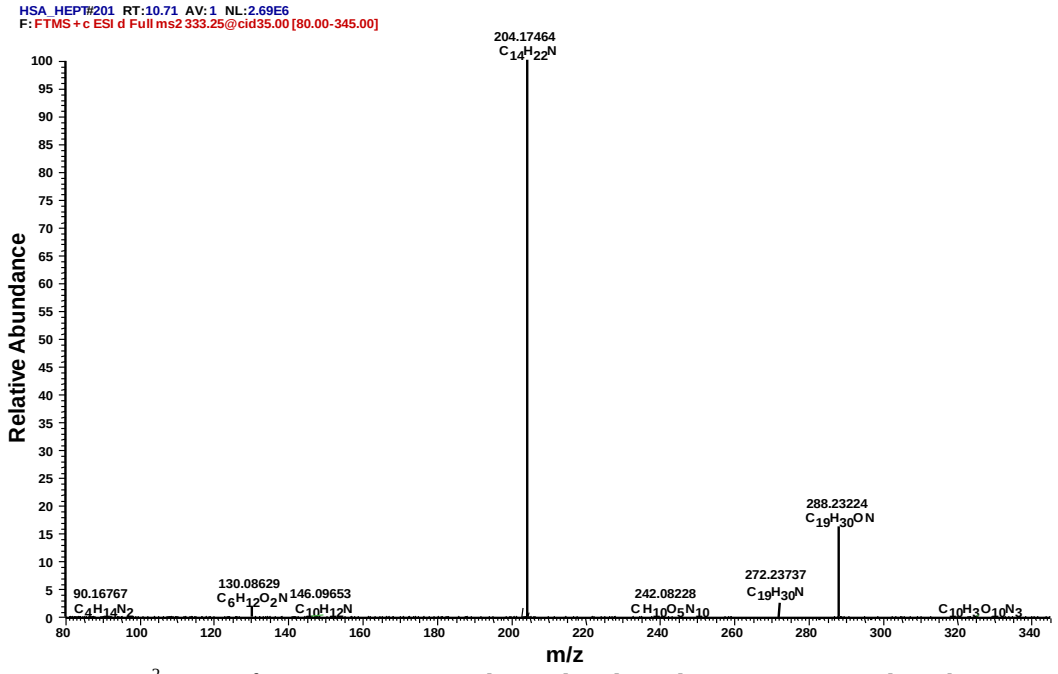

Figure 4.27: MS^2 spectra for Hpe-Lys-pyr-333 during data dependent acquisition mode with ESI-CID-FTMS/MS.

4.7.1.2 Histidine Fragmentation: Fixed Mass Loss

Histidine adducts show the same fragmentation pathways as for lysine adducts losing NH_3 (17 amu), CO_2 (44 amu), and HCOOH (64 amu) groups from the parent histidine 2-alkenal adducts; a combinations of these fragments is also possible. The α-β bond cleavage resulting in the loss of an iminoacetic acid moiety (73 amu) from the histidine [section 4.5.2.2] is also predictable for His-2-alkenal adducts.

Table 4-27 shows the exact mass loss from the parent compounds, the chemical nature of such a mass loss, and examples for the histidine adducts where these mass losses occurred in MS^2 mode. For example, MS^2 fragmentation for Pne-His-Michael adducts shows a major fragment peak at m/z 196 which results from the loss of HCOOH (46 amu) from the structure of the Pne-His-M adduct. Fragments at m/z 198 and 181, with an average intensity, result from CO_2 (44 amu) elimination and subsequent elimination of CO_2 and NH_3 (61 amu), respectively. A low intensity fragment detected at m/z 169 results from α-β cleavage of histidine with the expected elimination of an iminoacetic

acid moiety (73 amu) from the main structure of Pne-His-M adduct (Figure 4.28). The fragment peak at m/z 156 belongs to the histidine moiety after losing the modifying groups. Scheme 4-12 shows the fragmentation pathways for 2-alkenal-His-M adducts with possible loss of specific masses, such as 44, 46, 61, and 73 amu which results from elimination of CO_2, HCOOH, CO_2+NH_3, and α,β-cleavage pathways, respectively.

Table 4-27: Fixed mass losses from His-2-alkenal Michael adducts (precursor ions) during data dependent acquisition mode.

Mass Loss	***Represent***	***examples***
43.99011	Losing CO2	Acr-His-M
		Pne-His-M
		Hpe-His-M
		Nne-His-M
46.0058	Losing HCOOH	Acr-His-M
		Cro-His-M
		Cro-His-M
		Pne-His-M
		Hpe-His-M
		Nne-His-M
61.01663	Losing CO_2+NH_3	Acr-His-M
		Cro-His-M
		Cro-His-M
		Pne-His-M
		Hpe-His-M
		Nne-His-M
73.01661	α,β-cleavage: Lose of α-carbon group with its attached carboxyl and amine group with formation of double bond between α-carbon and α-amine group. As occurs in the fragmentation of histidine	Acr-His-M
		Pne-His-M

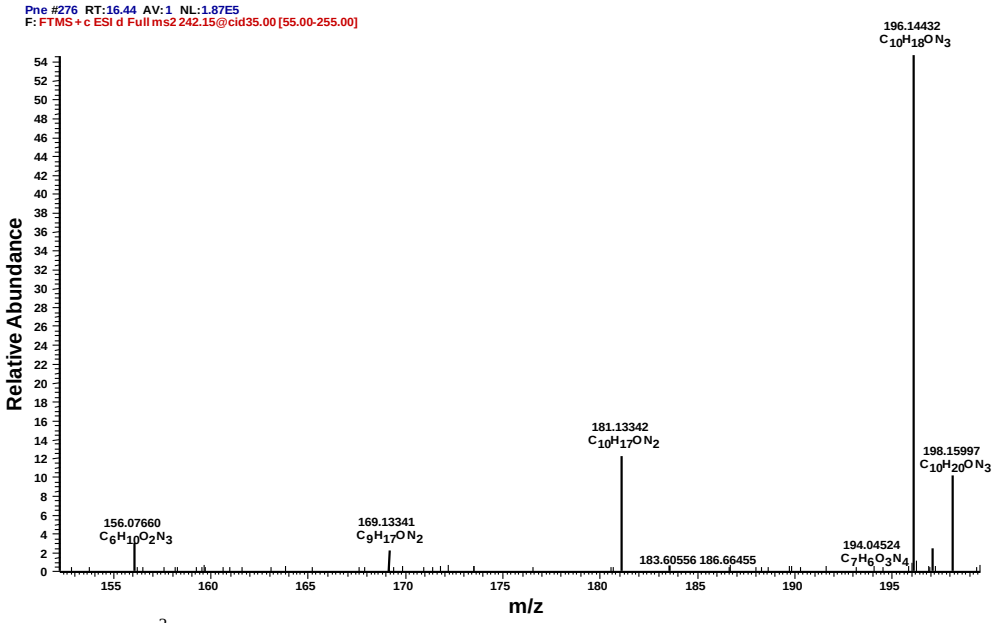

Figure 4.28: MS^2 spectra for Pne-His-M during data dependent acquisition mode with ESI-CID-FTMS/MS.

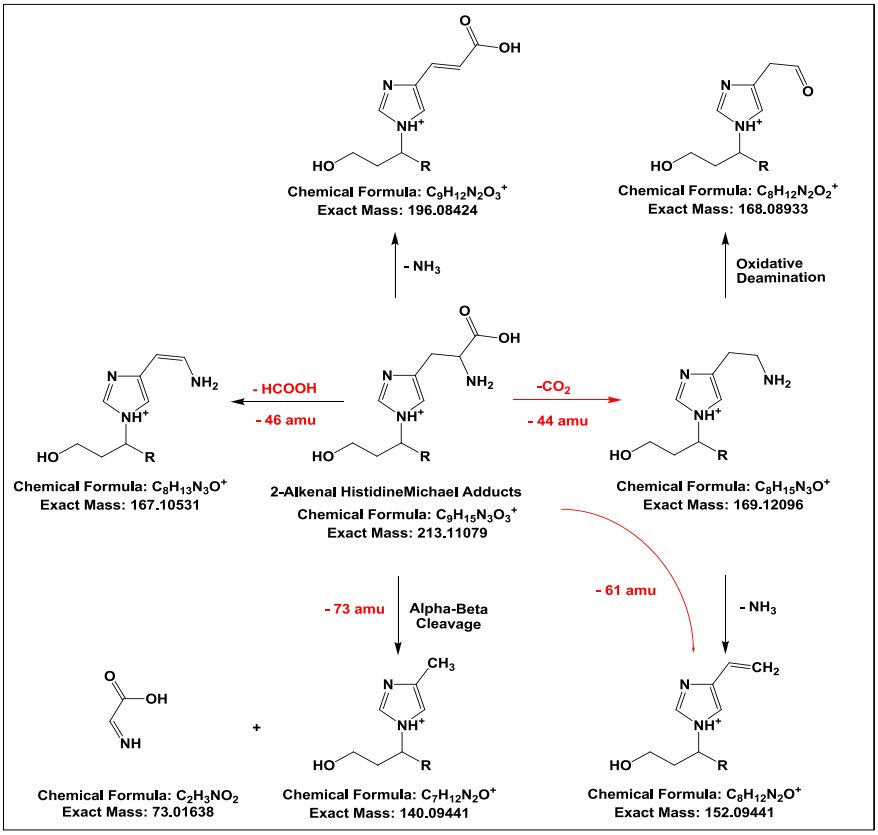

Scheme 4-12: Possible fragmentation pathways for His-Michael adducts during data dependent acquisition mode with ESI-CID-FTMS/MS. Acrolein (R=H), Crotanaldehyde (R=CH_3), 2-pentenal (R=CH_3CH_2-), 2-hexenal (R=$CH_3CH_2CH_2$-), 2-heptenal (R=$CH_3CH_2CH_2CH_2$-), and 2-Nonenal (R=$CH_3CH_2CH_2CH_2CH_2CH_2$-).

4.7.2 Common Ions Fragments

Common ion fragments appear in different 2-alkenal adducts due to the elimination of the modifying moiety from the original structure of the amino acid. Most of these fragments represent lysine, arginine, or histidine moieties which represents the backbone for such adducts. Some of these fragments then undergo further fragmentation by losing NH_3, CO_2, or HCOOH.

4.7.2.1 Common Ions Fragments for Different Lysine Adducts

Common ion fragments could be detected in different Lys-2-alkenal adducts Schiff base, Michael-like adduct, pyridinium and FDP adducts. The availability and intensity of these fragments differ from one compound to another.

Table 4-28 shows the exact mass for the common ion fragments, the possible chemical nature of such fragments, and examples for the lysine adducts where these common ion fragments could be detected during MS^2 spectrometry. For example, common ion fragments at m/z 159, 142, 130, 98, and 84 could be detected in enough intensity with MS^2 fragmentation for Acr-FDP-243 lysine adduct (Figure 4.29**)**.

Lysine adducts can follow 2 pathways for common ion fragments formation. Pathway (I) includes unsaturated ring opening through retro-Diels Alder reaction leading to common ion fragment formation at m/z 159. The retro-Diels-Alder reaction may affect unsaturated ring of the reduced pyridinium or the Lys-FDP adduct [172, 174]. Other fragments at m/z 142 and 98 are a consequence of further elimination of NH_3 and CO_2 molecules from the main structure of the product ion at m/z 159 (Scheme 4-13). Pathway (II) includes the loss of the modifying groups (2-alkenal moieties) together with the terminal amine group of the lysine amino acid leading to common ion fragments at m/z 130 and 84.

It should be mentioned that pathway (I) is specifically noticed for Lys-pyridinium and FDP adducts only, while pathway (II) is a general fragmentation pathway for all lysine

adducts. Another fragment with very low intensity could be detected at m/z 147 which show the exact chemical mass and formula for lysine amino acid (Figure 4.30). This type of common ion fragment could only be detected with lysine Schiff bases (Hpe-Lys-S and Nne-Lys-S adducts), and can be attributed to the elimination of the 1,3-diene moiety from the parent lysine Schiff base (Scheme 4-14).

Table 4-28: Common ion fragments for Lys-2-alkenal adducts (precursor ions) during data dependent acquisition mode.

Common ion	*Represent*	*Examples*	*Common ion*	*Represent*	*Examples*
84.08057	Lysine amino acid - (NH_3)- (HCOOH)	Acr-Lys-M	**130.08606**	Lysine amino acid-NH_3	Acr-Lys-M
		Acr-pyr-223			Acr-pyr-223
		Acr-pyr-227			Acr-pyr-227
		Acr-pyr-229			Acr-pyr-229
		Acr-FDP-243			Acr-pyr-243
		Cro-Lys-M			Cro-Lys-M
		Cro-pyr-251			Cro-Lys-S
		Pne-Lys-M			Cro-pyr-251
		Pne-pyr-277			Pne-Lys-M
		Hxe-Lys-S			Pne-pyr-277
		Nne-Lys-S			Pne-pyr-279
98.09618	opening of the unsaturated ring followed by NH_3 then CO_2 losing	Acr-pyr-227			Hxe-Lys-S
		Acr-FDP-243			Hxe-pyr-305
142.08609	opening of the unsaturated ring followed by NH_3 losing	Acr-pyr-227			Hxe-pyr-307
		Acr-FDP-243			Hxe-FDP-327
		Hxe-FDP-327			Hpe-Lys-S
		Hpe-FDP-355			Hpe-FDP-355
		Hpe-pyr-339			Hpe-pyr-333
147.11301	Losing of 2-alkenal moiety leaving lysine amino acid	Hpe-Lys-S			Nne-pyr-389
		Nne-Lys-S			Nne-Lys-S
159.11261	opening of the unsaturated ring	Acr-pyr-227			
		Acr-FDP-243			

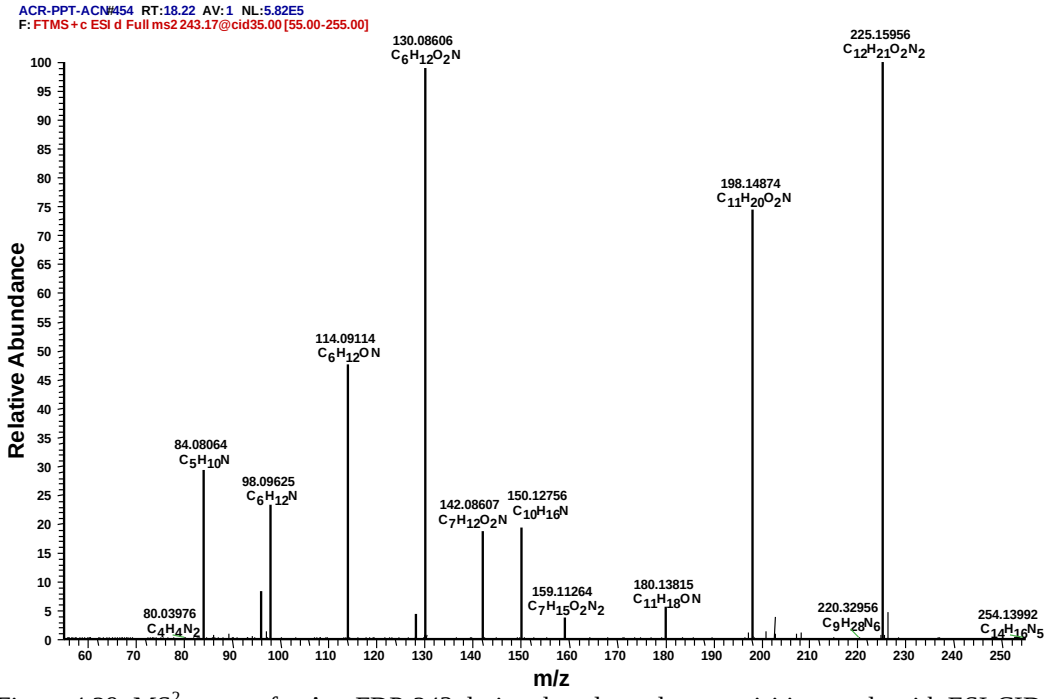

Figure 4.29: MS^2 spectra for Acr-FDP-243 during data dependent acquisition mode with ESI-CID-FTMS/MS.

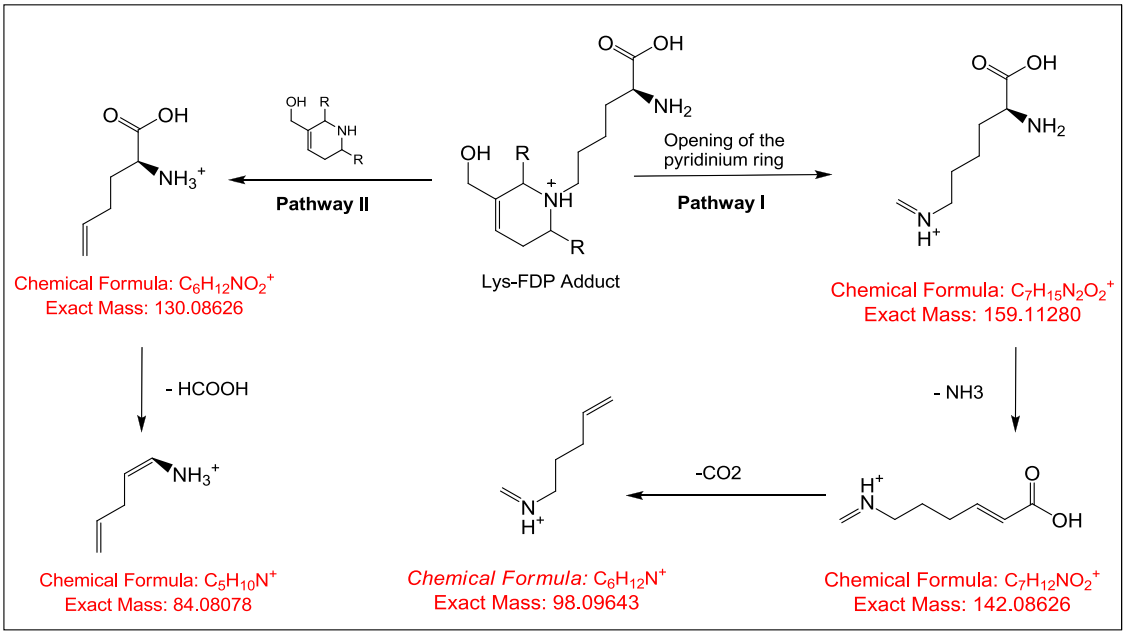

Scheme 4-13: Common ion fragments generation for Lys-pyridinium adduct fragmentation during data dependent acquisition mode with ESI-CID-FTMS/MS. Acrolein (R=H), Crotanaldehyde ($R=CH_3$), 2-pentenal ($R=CH_3CH_2$-), 2-hexenal ($R=CH_3CH_2CH_2$-), 2-heptenal ($R=CH_3CH_2CH_2CH_2$-), or 2-Nonenal ($R=CH_3CH_2CH_2CH_2CH_2CH_2$-).

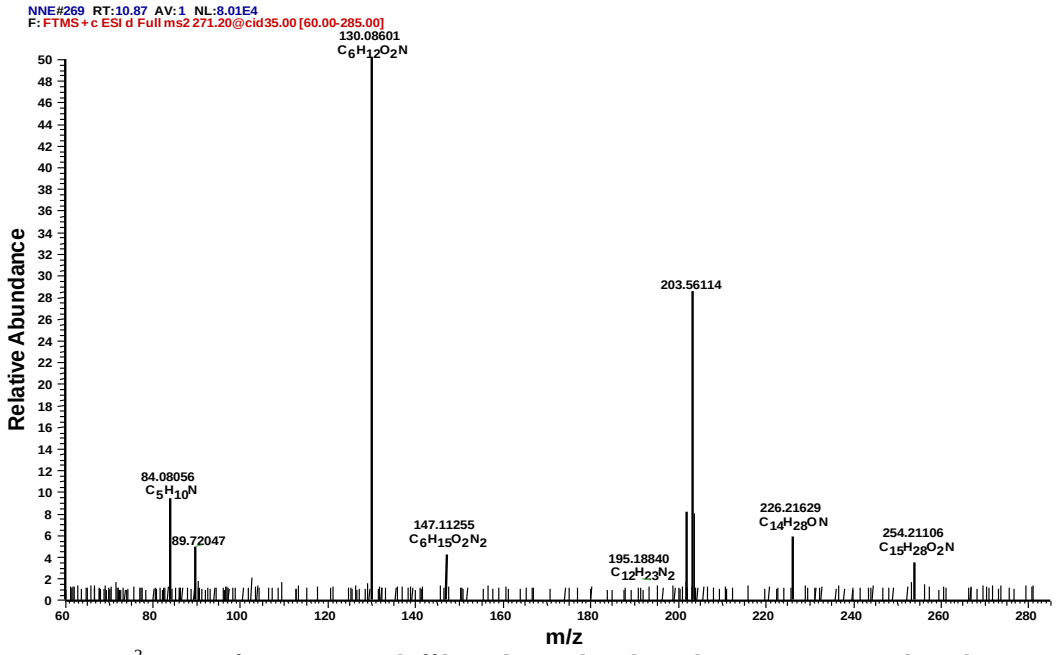

Figure 4.30: MS^2 spectra for Nne-Lys-Schiff base during data dependent acquisition mode with ESI-CID-FTMS/MS.

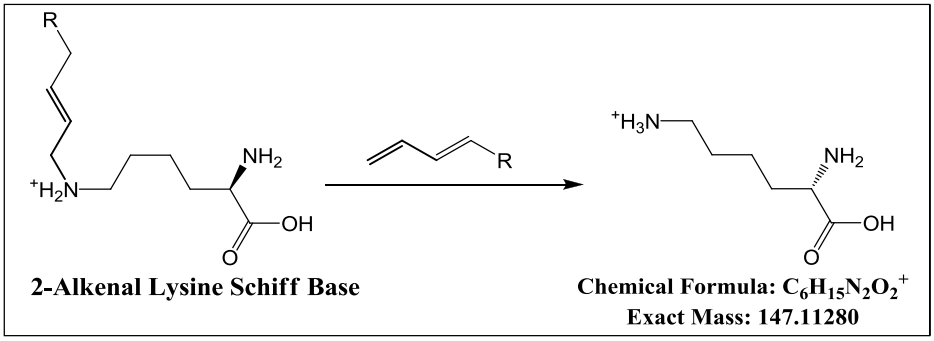

Scheme 4-14: Fixed fragment ions generation for Lys-Schiff base fragmentation during data dependent acquisition mode with ESI-CID-FTMS/MS. Acrolein (R=H), Crotanaldehyde ($R=CH_3$), 2-pentenal ($R=CH_3CH_2$-), 2-hexenal ($R=CH_3CH_2CH_2$-), 2-heptenal ($R=CH_3CH_2CH_2CH_2$-), or 2-Nonenal ($R=CH_3CH_2CH_2CH_2CH_2CH_2$-).

4.7.2.2 Common Ion Fragments for Different Histidine Adducts

Histidine 2-alkenal adducts show the same fragmentation pathways as lysine 2-alkenal adducts where common ion fragments are generated due to the elimination of the modifying moiety from the parent His-2-alkenal-Michael adducts. However, common ion fragments for His are different from the common ion fragments for Lys due to the difference in the backbone structure for the amino acid that composes the 2-alkenal adducts. Histidine adducts show common ion fragments at m/z 95, 110, 112, 156.

Table 4-29 shows the exact mass for the common ion fragments, the possible chemical nature of such fragments, and examples for the histidine adducts where these common ions could be detected during MS^2 fragmentation. For example, MS^2 spectra for Hpe-His-M adduct show common ion fragments at m/z 95, 110, 112, and 156 (Figure 4.31). The formation of these fragments could be explained by loss of the 2-alkenal moiety leaving the histidine fragment that could be detected at m/z 156. Subsequent loss of HCOOH (46 amu) leads to a common ion fragment at m/z 110. Whereas, elimination of CO_2 (44 amu) from the common ion m/z 156 leads to the formation of another common ion at m/z 112. Further elimination of NH_3 from the common ion fragment at m/z 112 leads to the formation of low intensity common ion fragment at m/z 95 (Scheme 4-15).

Table 4-29: Common ion fragments for His-2-alkenal Michael adducts (precursor ions) during data dependent acquisition mode.

Common ion	***Represent***	***examples***
95.0602	His-NH_3-CO_2	Pne-His-M
		Hpe-His-M
		Nne-His-M
110.07106	His-HCOOH	Pne-His-M
		Hpe-His-M
		Nne-His-M
112.08671	His-CO_2	Pne-His-M
		Hpe-His-M
		Nne-His-M
156.07655	Leaving histidine amino acid only	Pne-His-M
		Hpe-His-M
		Nne-His-M

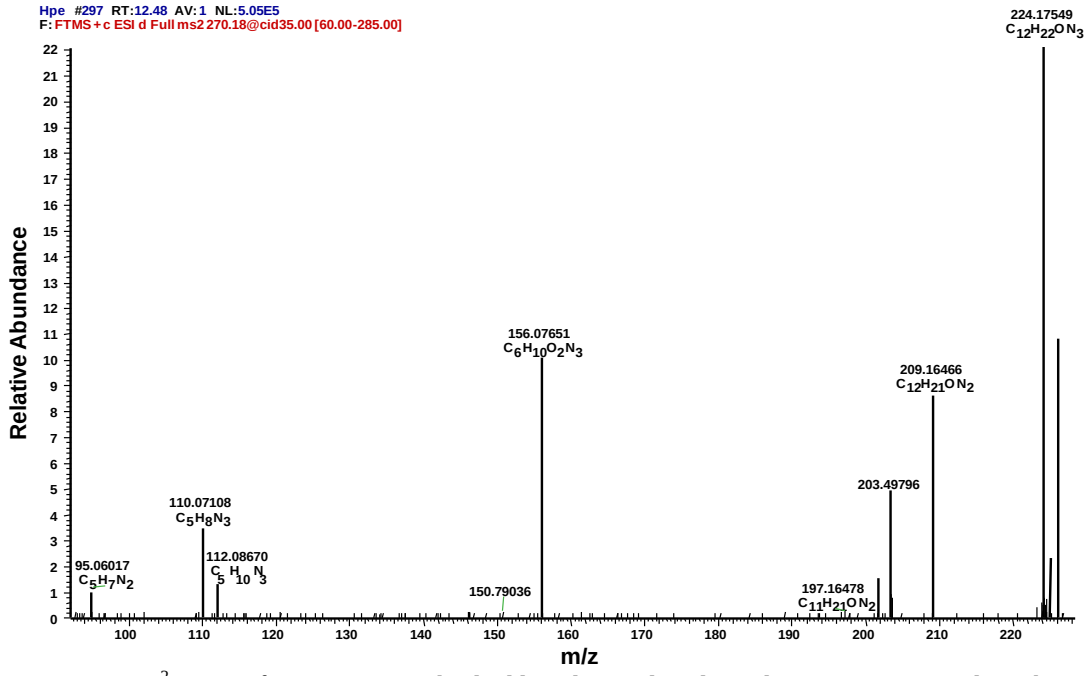

Figure 4.31: MS^2 spectra for Hpe-His-Michael adduct during data dependent acquisition mode with ESI-CID-FTMS/MS.

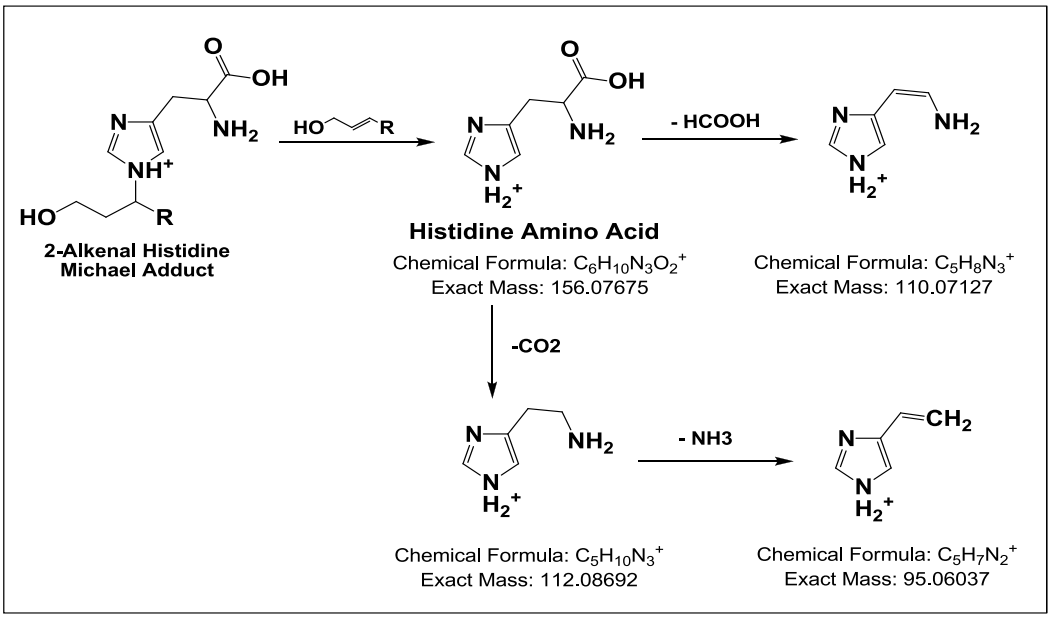

Scheme 4-15: Common ion generation for His-Michael adducts fragmentation during data dependent acquisition mode with ESI-CID-FTMS/MS. Acrolein (R=H), Crotanaldehyde ($R=CH_3$), 2-pentenal ($R=CH_3CH_2$-), 2-hexenal ($R=CH_3CH_2CH_2$-), 2-heptenal ($R=CH_3CH_2CH_2CH_2$-), or 2-Nonenal ($R=CH_3CH_2CH_2CH_2CH_2CH_2$-).

4.7.3 Structure Elucidation for HNE Adducts Using Mass Spectrometry

MS^2 results for HNE adducts show the same fragmentation pathways as other 2-alkenal adducts (Table 4-30). All the observed masses for fragments were within 1.5 ppm deviation from the theoretical mass.

Table 4-30: MS/MS results for HNE adducts with different amino acids.

Type of Adduct	*Elemental Formula*	*R_t control (min)*	*R_t (min) MS^2*	*Precursor ion*	*Mass lose*	*Product ion*	*Elemental Formula*	*Delta ppm*
Lys-HNE-Schiff	$C_{15}H_{31}N_2O_3$	11.78	11.85	287.23	18.01	269.22	$C_{15}H_{29}O_2N_2$	-0.79
					45.02	242.21	$C_{14}H_{28}O_2N$	-0.24
					63.03	224.20	$C_{14}H_{26}ON$	-0.65
					102.10	185.13	$C_9H_{17}O_2N_2$	-0.38
					129.08	158.15	$C_9H_{20}ON$	-0.94
					145.07	142.16	$C_9H_{20}N$	-1.11
					157.15	130.09	$C_6H_{12}O_2N$	-1.12
					203.15	84.08	$C_5H_{10}N$	-1.28
Lys-HNE-Michael and Hemiacetal adduct	$C_{15}H_{33}N_2O_4$	12.15	12.21	305.24	18.01	287.23	$C_{15}H_{31}O_3N_2$	-0.51
					45.02	260.22	$C_{14}H_{30}O_3N$	-0.77
					129.08	176.16	$C_9H_{22}O_2N$	-0.46
					147.09	158.15	$C_9H_{20}ON$	-1.13
					175.16	130.09	$C_6H_{12}O_2N$	-0.89
Arg-HNE-Schiff Base	$C_{15}H_{31}N_4O_3$	11.6	11.61	315.24	17.03	298.21	$C_{15}H_{28}O_3N_3$	-1.20
					45.02	270.22	$C_{14}H_{28}O_2N_3$	-0.72
					157.09	158.15	$C_9H_{20}ON$	-1.45
His-HNE Michael	$C_{15}H_{28}N_3O_4$	11.91	11.97	314.21	17.03	297.18	$C_{15}H_{25}O_4N_2$	-0.71
					43.99	270.22	$C_{14}H_{28}O_2N_3$	-1.05
					46.01	268.20	$C_{14}H_{26}O_2N_3$	-0.94
					61.02	253.19	$C_{14}H_{25}O_2N_2$	-0.62
					158.13	156.08	$C_6H_{10}O_2N_3$	-1.08
					204.14	110.07	$C_5H_8N_3$	-1.22

Data dependent acquisition for the HNE double adducts (Lys-HNE-Lys & His-HNE-Lys adducts) failed to trigger the MS^2 fragmentation during data dependent acquisition due to their low intensity (Table 4-25 in section 4.6.4). Nevertheless, fragmentation of 1 hit HNE adducts give full information about the behaviour of these adducts under MS^2 conditions.

HNE adducts can eliminate 17 amu (NH_3), 18 amu (H_2O), 45 amu (CO_2 elimination followed by oxidative deamination), 46 amu (HCOOH) 61 amu (CO_2+NH_3), 63 amu (HCOOH+NH_3), 129 amu (elimination of lysine moiety), or 147 amu (elimination of lysine moiety followed by H_2O elimination). Furthermore, common ion fragments could be detected for lysine-HNE adducts at m/z 84 & 130, whereas common ion fragments at m/z 110 & 156 could be detected for histidine-HNE adducts. MS^2 spectra for Lys-HNE-S base (Figure 4.32) show different fragments at m/z 84 (common ion), 130 (common ion), 142, 158 (- 129 amu), 185, 224 (-63 amu), 242 (-45 amu), and 269 (- 18 amu). All these fragments have been explained earlier with the exception of fragment at m/z 142 & 185.

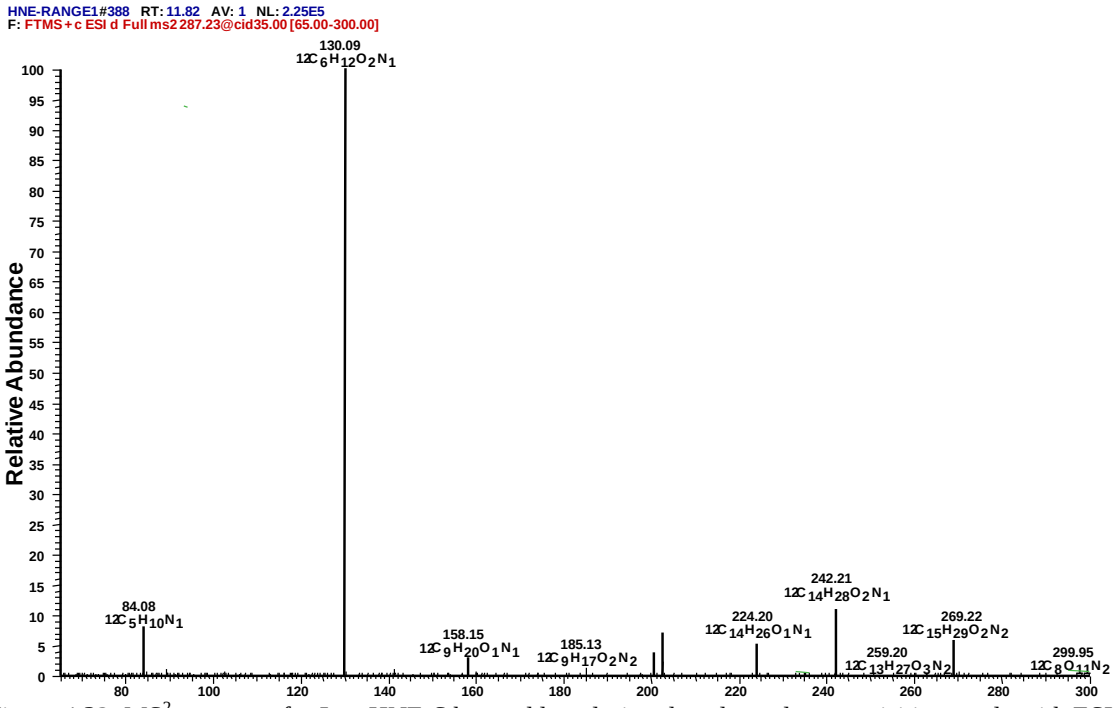

Figure 4.32: MS^2 spectrum for Lys-HNE-S base adduct during data dependent acquisition mode with ESI-CID-FTMS/MS.

Mass loss of 102 amu from Lys-HNE-S adduct can be justified by losing part of the modifying group (HNE) from the parent compound in the form of hexanol moiety, and could be detected at m/z 185. However, a fragment at m/z 142 with a chemical formula of ($C_9H_{20}N^+$) could be detected. Elimination of lysine moiety (mass loss of 129 amu) followed by de-hydroxylation process (replacement of OH group with H atom) could be

a possible explanation for the formation of such fragment although is not a well-known mass spectrometric fragmentation pathway.

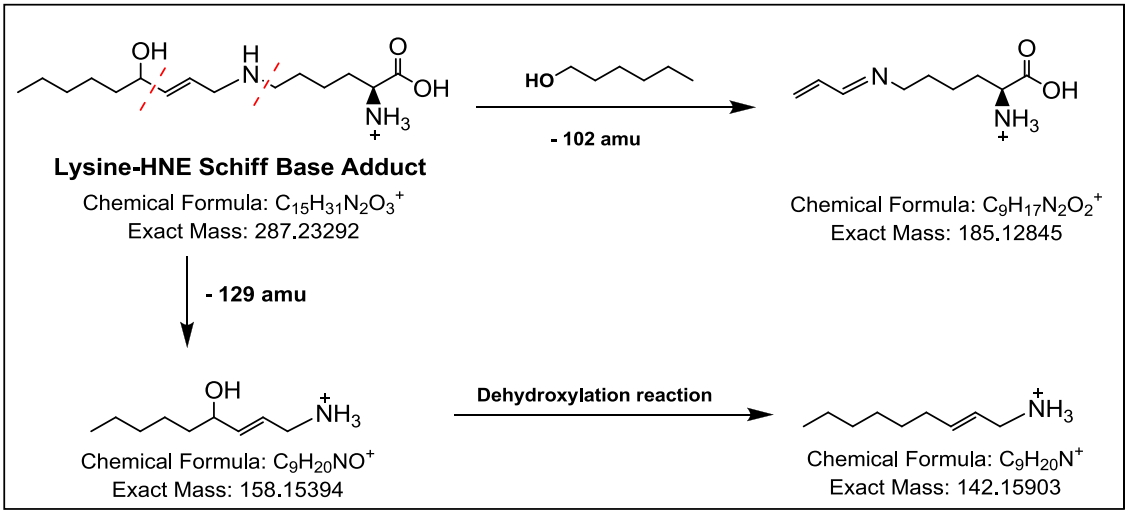

Scheme 4-16: Fragmentation pathways for Lys-HNE-S base adduct that lead to the formation of fragments at m/z 185, 158 & 142 during data dependent acquisition mode with ESI-CID-FTMS/MS.

The dehydroxylation process can be explained by the formation of $H^{\bullet}$ and $OH^{\bullet}$ radical during data dependent acquisition mode, due to the availability of high water (H_2O) content in the mobile phase at such retention time (see tryptophan fragmentation in section 4.5.2.2 for more details). Loss of the OH group from Lys-HNE-S adduct as $OH^{\bullet}$ radical gives high opportunity for exchange with $H^{\bullet}$ radical available in the atmosphere of the iontrap during MS^2 process. The exact chemical mass and formula for such adduct corresponds with such assumption.

Surprisingly, the MS^2 spectra for Lys-HNE-Michael adduct and Arg-HNE-Schiff base shows the same fragment at m/z 158. In the case of the Lys-HNE-M adduct, this fragment can be explained by elimination of the lysine moiety (- 147 amu), whereas in the case of Arg-HNE-S base, it can be explained by elimination of the arginine moiety (- 157 amu) from the Arg-HNE-Schiff base (Scheme 4-17).

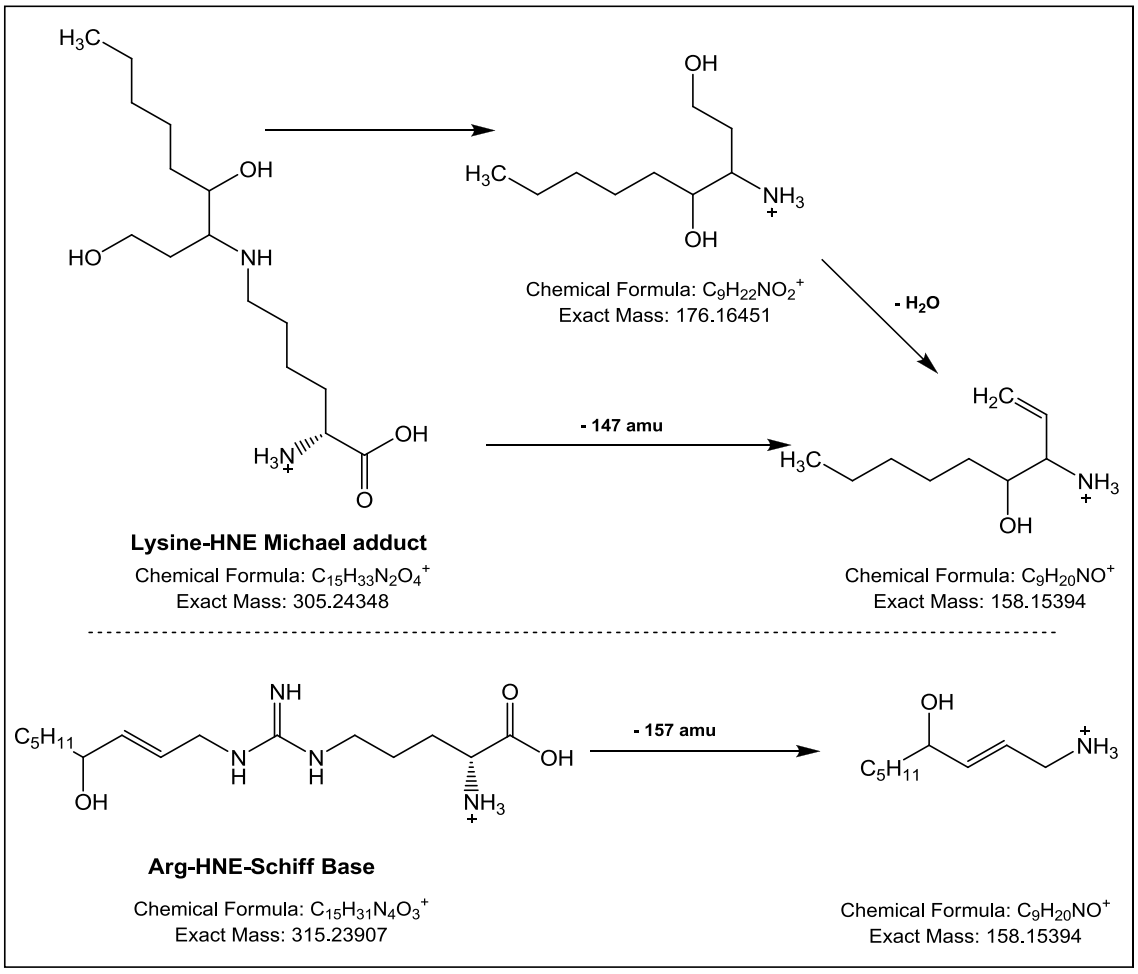

Scheme 4-17: Pathways for the formation of the fragment at m/z 158.15 for Lys-HNE-M & Arg-HNE-S base adducts during data dependent acquisition with ESI-CID-FTMS/MS.

4.8 Percentages of 2-Alkenal Adducts in HSA Hydrolysate Samples

Determining the percentage of each adduct is required for LOD and LOQ calculation for each adduct. A high protein concentration is required as some of the 2-alkenal adducts could only be detected at high protein concentration. The percentages for each 2-alkenal adduct was calculated by the same procedure described in Table 3-22 [section 3.9]. The average peak area for the detected 2-alkenal adducts is divided by the average total peak area for remaining amino acid (lysine, arginine, or histidine) together with its related adduct over repeated inections of 2 samples. Thus, it was possible to estimate the % of the different aldehyde modified amino acids which were formed upon reaction of HSA with the 2-alkenals. In the unmodified HSA, lysine gave 100%

recovery with none of Lys-2-alkenal adducts being detectable. In Table 4-31, it can be seen that the peak area obtained for the remaining lysine after reaction of HSA with acrolein gave a normalised response of 15.3%.

In the case of the acrolein-lysine reaction products the most abundant adduct formed was the lysine-FDP adduct which gave a normalised response of (47.3%). Certainly, in the absence of pure standards such estimates are only very approximate since the response factors are not known, but none-the-less the approach gives an impression of how favourable the formation of the different adducts is. Formation of the different pyridinium adducts between lysine and acrolein was quite favourable, however only small amounts of the Michael adduct and Schiff's base adduct could be detected at the end of the incubation. The Schiff base adduct represents an intermediate which reacts further to yield the more stable FDP and pyridinium adducts.

The same procedure could be adopted for histidine and arginine. After hydrolysis of the acrolein modified HSA, histidine gave a normalised peak area of (21.3%) and the Michael adduct had a normalised peak area of (78.7%). The arginine remaining after reaction of HSA with acrolein was (100%) for the reduced sample. These findings were in agreement with the previous results achieved by the EZ:faast method in section 3.9 where acrolein aldehyde showed the maximum activity with lysine amino acid and the minimum activity against arginine amino acid. However, when the reduction step was omitted, the percentage of the remaining arginine was (75%), and a percentages of (22.7%) and (1.3%) for Acr-Arg-Michael adduct and Acr-Arg-Schiff base, respectively. This suggests that reduction or reduction followed by hydrolysis in some way reverses the formation of adducts with arginine.

Pentenal is much less reactive than acrolein, and in contrast to acrolein it was mainly the Michael adduct of histidine which was formed with a normalised peak area of (46.7%). The lysine remaining after reaction of HSA with pentenal had a normalised peak area of (87.9%); only a small amount of Pne-Lys Michael adduct and pyridinium adducts were formed, whereas Lys- FDP adduct was not detectable in most of the samples.

Table 4-31: Percentages for non-derivatised 2-Alkenal Adducts in relation to its corresponding amino acid. N=4

Acrolein		*Crotanaldehyde*		*2-Pentenal*	
Type of adduct	*Average %*	*Type of adduct*	*Average %*	*Type of adduct*	*Average %*
Remaining Lysine	15.302	*Remaining Lysine*	90.197	*Remaining Lysine*	87.940
Acr-Lys-M	2.291	*Cro-Lys-M*	5.560	*Pne-Lys-M*	2.142
Acr-Lys-S	0.312	*Cro-Lys-S*	0.834	*Pne-Lys-S*	N/A
Acr-pyr-221	N/A	*Cro-pyr-249*	N/A	*Pne-pyr-277*	N/A
Acr-pyr-223	8.785	*Cro-pyr-251*	1.461	*Pne-pyr-279*	3.414
Acr-pyr-225	13.675	*Cro-pyr-253*	0.760	*Pne-pyr-281*	2.904
Acr-pyr-227	8.418	*Cro-pyr-255*	0.509	*Pne-pyr-283*	3.235
Acr-pyr-229	3.629	*Cro-pyr-257*	0.547	*Pne-pyr-285*	0.364
Acr-FDP-243	47.588	*Cro-FDP-271*	0.133	*Pne-FDP-299*	N/A
Total %	100.000	*Total %*	100.000	*Total %*	100.000
Remaining Arginine	100.000	*Remaining Arginine*	98.814	*Remaining Arginine*	99.252
Acr-Arg-M	N/A	*Cro-Arg-M*	1.094	*Pne-Arg-M*	0.748
Acr-Arg-S	N/A	*Cro-Arg-S*	0.092	*Pne-Arg-S*	N/A
Total %	100.000	*Total %*	100.000	*Total %*	100.000
Remaining Histidine	21.329	*Remaining Histidine*	63.165	*Remaining Histidine*	53.273
Acr-His-M	78.671	*Cro-His-M*	36.835	*Pne-His-M*	46.727
Total %	100.000	*Total %*	100.000	*Total %*	100.000
2-Hexenal		*2-Heptenal*		*2-Nonenal*	
Type of adduct	*Average %*	*Type of adduct*	*Average %*	*Type of adduct*	*Average %*
Remaining Lysine	76.515	*Remaining Lysine*	52.774	*Remaining Lysine*	83.904
Hxe-Lys-M	1.191	*Hpe-Lys-M*	N/A	*Nne-Lys-M*	3.779
Hxe-Lys-S	0.509	*Hpe-Lys-S*	3.248	*Nne-Lys-S*	2.044
Hxe-pyr-305	N/A	*Hpe-pyr-333*	N/A	*Nne-pyr-389*	N/A
Hxe-pyr-307	4.621	*Hpe-pyr-335*	18.015	*Nne-pyr-391*	3.797
Hxe-pyr-309	8.632	*Hpe-pyr-337*	6.777	*Nne-pyr-393*	1.150
Hxe-pyr-311	5.689	*Hpe-pyr-339*	9.100	*Nne-pyr-395*	1.866
Hxe-pyr-313	0.665	*Hpe-pyr-341*	0.680	*Nne-pyr-397*	0.055
Hxe-FDP-327	2.179	*Hpe-FDP-355*	9.406	*Nne-FDP-311*	3.404
Total %	100.000	*Total %*	100.000	*Total %*	100.000
Remaining Arginine	99.763	*Remaining Arginine*	98.848	*Remaining Arginine*	96.086
Hxe-Arg-M	0.237	*Hpe-Arg-M*	0.672	*Nne-Arg-M*	3.669
Hxe-Arg-S	N/A	*Hpe-Arg-S*	0.480	*Nne-Arg-S*	0.246
Total %	100.000	*Total %*	100.000	*Total %*	100.000
Remaining Histidine	85.847	*Remaining Histidine*	65.682	*Remaining Histidine*	16.214
Hxe-His-M	14.153	*Hpe-His-M*	34.318	*Nne-His-M*	83.786
Total %	100.000	*Total %*	100.000	*Total %*	100.000

Nonenal is also less reactive than acrolein and the remaining lysine had a normalised peak area of 83.9%. Small amounts of Nne-Lys Michael and pyridinium adducts were formed; the level of Nne-Lys Schiff base was a little higher than that for Acr-Lys Schiff base which indicates that the rearrangement of this intermediate into the pyridinium and FDP adducts is slower when nonenal is used as the reactant. However, the reaction between histidine and nonenal appears to be as extensive as in the case of acrolein with 83.8% of the histidine in HSA being converted into the Michael adduct which appears to be more favourable than in the case of pentenal.

In general, lysine amino acid residues in protein molecules are subject to more modifications than arginine and histidine, whereas arginine shows the lowest modifications as compared to the other two amino acids (the total percentages of arginine amino acid modification range between 0 and 4%). Lys-Michael adducts show higher percentages as compared to Lys-Schiff bases confirming that Michael adducts are more stable than Schiff base in withstanding the acid hydrolysis.

4.9 Determination of Limit of Detection (LOD) and Limit of Quantification (LOQ) for 2-Alkenals Adducts Using HILIC-FTMS

On the Orbitrap instrument it is difficult to define LOD and LOQ in a conventional way, since there is often no noise when the extracted ion current is entered in a narrow window (±5ppm). Furthermore, as the LOD is approached the peak for the compound of interest simply gets narrower until it disappears. In simple terms what is happening is that the trap fill parameters are discarding some of the ions due to the analyte which fall below a certain threshold in order to avoid overfilling the trap with background ions and as a peak gets lower in intensity some of its base is lost along with the discarded background ions. Thus, determination of the LOD and LOQ for any compound requires visual examination for the availability of the compounds in a serial dilution for an initial concentration of that compound.

LOD is easy to define in a serial dilution as the last concentration which could be detected before the signal disappeared, this can sometimes be the same as the LOQ. The determination of LOQ has been defined as the last concentration where the peak can be observed with an intensity > 1.50 E+4 with at least 3 scans across the peak [section 3.10]. Some might like to set it higher, however detection of minor compounds with very low intensity requires careful adjustemts for this parameter to avoid false nrgative results.

Preparation of the dilution series of 2-alkenal adducts was carried out using protein hydrolysate with a concentration of 0.3929 mg/ml which had been prepared according to the procedure described in section 2.5.3. A total of 8 dilution points (0.1, 0.05, 0.02, 0.01, 0.005, 0.002, and 0.001 mg/ml) were prepared for PPT extraction by diluting protein solutions with HPLC grade water. Table 4-32 shows the preparation of the dilution series from an initial protein concentration of 0.3929 mg/ml of protein hydrolysate. For example, the preparation of the 0.1 mg/ml of protein samples required dilution of 254.55 µl of 0.3929 mg/ml of protein hydrolysate up to 1 ml using HPLC grade water, whereas preparation of 0.05 mg/ml of protein sample required the dilution of 500 µl of 0.1 mg/ml of protein hydrolysate up to 1 ml with HPLC grade water. The samples then extracted using PPT method described in section 2.5.3

Table 4-32: Preparation of the dilution series for LOD and LOQ determination using PPT and HILIC-FTMS methods.

C1 (mg/ml)	*V1 (µl)*	*C2 (mg/ml)*	*V2 (ml)*	*Vol of HPLC grade water (µl) should be added*
0.3929	254.55	0.1	1	745.4499
0.1	500	0.05	1	500
0.05	400	0.02	1	600
0.02	500	0.01	1	500
0.01	500	0.005	1	500
0.005	400	0.002	1	600
0.002	500	0.001	1	500
0.001	500	0.0005	1	500

Preparation of the PPT cartridges was carried out by the addition of 1 ml of ACN to 9 PPT cartridges; lable them as 0.39, 0.1, 0.05, 0.02, 0.01, 0.005, 0.002, and 0.001. Aliquot of 300 µl of the correspondent protein concentration was loaded on the labelled PPT cartridges, followed by the addition of 100 µl of I.S (reagent 1 from the EZ:faast

kit). Allow the mixture to stand for 10 min then the filtration process is accomplished by using vacuum manifold operating at 10 mmHg. A set of dry and clean 4 ml vials labelled as 0.39, 0.1, 0.05, 0.02, 0.01, 0.005, 0.002, and 0.001 were used to collect the filtrate from the correspondent PPT cartridge. The filtrates were subjected to evaporation till dryness using dryblock operating at 50°C and a slight nitrogen stream, and then redissolved in 600 µl HPLC grade water.

Determination of LOD and LOQ was carried using ZIC-HILIC column coupled to ESI-FTMS mass spectrometry operating in the positive mode according to the conditions specified in section 2.5.4. Table 4-33 shows that the amount of lysine injected into the instrument in this dilution series ranges between 0.25ng and 193.5ng, calculated according the percentage of the lysine amino acid residue (9.85%) in the HSA molecule (Table 6-9).

Table 4-33: The expected amount of lysine amino acid (ng) injected in 10 µl of extracted protein hydrolysate.

Initial conc. (mg/ml)	*Amount of albumin in 300µl of hydrolysate that are subjected to PPT filtration (mg)*	*Conc. (µg/ml) after re-dissolution in 600µl*	*Amount of albumin (ng) in 10µl injected into LC-MS*	*Amount of lysine (ng)*
0.39285	0.11786	196.425	1964.25	193.4786
0.1	0.03000	50	500	49.25
0.05	0.01500	25	250	24.625
0.02	0.00600	10	100	9.85
0.01	0.00300	5	50	4.925
0.005	0.00150	2.5	25	2.4625
0.002	0.00060	1	10	0.985
0.001	0.00030	0.5	5	0.4925
0.0005	0.00015	0.25	2.5	0.24625

Since a goal of the research was to apply the methodology in an attempt to observe these adducts in tissues a method was developed for estimating an approximate LOQ for the adducts. The LOQ was estimated by diluting the hydrolysate of the aldehyde modified HSA in two fold steps until the signal could no longer be observed. Table 6-25 to Table 6-30 show the LOQs in terms of estimated amount of amino acid or adduct injected on column (oc). Thus, LOQ for lysine in the HSA could be estimated to be 0.04 ng oc. The LOQs for most of these adducts were below 1ng oc.

The figures for LOQ can only be very approximate since neither recoveries nor response factors are known. However, it is possible to get some idea of at what level the protein modifications could be observed. For example, if the LOQ for a specific adduct was around 2 ng oc in a 10 µl injection aliquot, thus equating to 200 ng/ml. That would mean for 2 mg of protein hydrolysed and then reconstituted in 1 ml according to the current method it should be possible to observe adduct formation at about 0.01% (w/w) or 100 ppm relative to the weight of the protein.

5 CHAPTER FIVE: General Conclusion and Future Work

5.1 General Conclusions

Most studies of the reactions between proteins and aldehydes have focused on examining modified peptides rather than looking at the individual adducts following complete hydrolysis of the protein. In the current study the goal was to determine whether or not amino acid modification of plasma proteins could be detected and thus potentially be used as a marker for specific disease process, much like non-enzymatic glycation is used to monitor long-term glucose levels in diabetes [175]. The current study identified unequivocally the elemental composition of a wide range of adducts which could be formed by reaction between the model protein (HSA or BSA) and 2-alkenals. Many of these adducts have been reported before and most commonly the Schiff base and Michael-like adducts have been reported. The pyridinium and FDP adducts were previously reported by workers who used NMR to elucidate their structures following reaction of amino acids (with protected α-amine group) with acrolein and crotonaldehyde [30, 51]. The current study confirmed their findings by using a protein as the reactant and extended the reactions to a broader range of aldehydes.

Adduct formation with arginine has only been recently reported [46] where the arginine adduct could be detected as pentapyrrole adduct upon reaction of arginine residue in protein molecule with HNE. In the current work the Schiff base and Michael-like adducts of HNE were observed although it was surprising that nitrogen double bond in guanidine group of arginine was not reduced upon $NaBH_4$ treatment used to stabilise these adducts prior to hydrolysis of the protein. Moreover, it was not possible to observe adducts formed between cysteine residues and the reactive aldehydes and this is probably because these adducts would be likely to be acid liable [176]. The detection of Michael adducts formed between HNE and histidine has been reported with a model peptide such as oxidised insulin B chain [111].

There are no reports of detection of aldehyde modified proteins or amino acids in plasma samples from human subjects, apart from the well established screens for glucose

modification of haemoglobin [175, 177]. However, the vast majority of research into aldehyde modification of proteins has focused on *in vitro* interactions although clearly there is a great deal of interest in extrapolating the information obtained in these experiments into biological systems, particularly into human subjects. In this study, we have developed a method for the analysis of a wide range of aldehyde-amino acid adducts and extended this work to examine human plasma in which we were able to consistently identify a pyridinium adduct formed between lysine and 2-pentenal aldehyde. It is not possible to rule out that this compound could be formed during storage, but it was the only modified residue consistently detected; a general oxidation of plasma lipids would be expected to give rise to a wide range of adducts. Indeed, we have observed such a phenomenon when commercial BSA was incubated in PBS without addition of a particular aldehyde. Many of the 2-alkenal adducts described in this work could be observed in low abundance. This is probably because BSA is a lipophilic protein and presumably carried over traces of plasma lipids during its preparation into the final product which become oxidised either prior to or during the incubation.

Assessment of the reactivity of 2-alkenals suggest that acrolein is the most reactive aldehyde in 2-alkenal series as indicated by the percentages of the remaining amount of the amino acid after incubation of protein samples with 2-alkenal aldehydes; this was in agreement with other study which confirm the same achievement [51].

5.2 Mass Spectrometric Considerations

It was important to maintain good mass spectrometry performance in order to provide definitive characterisation of adducts. Mass spectrometry with high analytical performance and accurate mass measurement, such as that provided by the Orbitrap, is an essential tool for metabolomic and proteomic studies [178].

False positive peaks can be detected in mass spectrometry as a result of inaccurate mass detection, multiple charges, insufficient separation, insufficient resolution, chemical

impurities, molecular fragmentation and hydrolysis by heat. Different parts of the mass spectrometer such as power supply, vacuum pumps, ion gauges and RF oscillators could be a source of artefact peaks that may result from radio-frequency interference [179]. Therefore, tuning and calibration processes of the mass spectrometer prior to each study are essential to achieve high mass accuracy and avoid instrument drift [121, 180].

Application of MS^2 fragmentation using the linear iontrap coupled to Orbitrap mass spectrometer illustrated the fragmentation behaviour of these adducts. These adducts underwent a simple heterolytic or homolytic fragmentation leading to the loss of a neutral molecule from their structure. Different chemical compounds –including amino acids and 2-alkenal adducts- show specific fragmentation patterns by losing specific neutral moieties from their structure such as H_2O, NH_3, HCOOH, CO, CO_2, and propanol.

A hydroxylation and dehydroxylation process could be noticed for tryptophan amino acid and HNE-adducts fragmentation process, this could be attributed to the reaction of the resulting fragments with $OH^{\bullet}$ and $H^{\bullet}$ radicals inside the fragmentation compartment. Formation of free radicals from the ionised precursor ion during ESI-CID-MS/MS has been indicated by many studies [165, 181, 182]. Oxidative de-amination of the arginine amino acid during MS^2 fragmentation could be attributed to the same principle as hydroxylation process where the availability of oxygen molecules in the fragmentation chamber can replace NH_3 from the structure of the arginine amino acid.

In addition the MS^2 results indicated that the retro-Diels-Alder fragmentation could be detected for some 2-alkenal adducts which contained rings in their structure [see common ion fragments for different lysine adducts, section 4.7.2.1] leading to ring opening. Opening of rings (saturated and unsaturated) via this mechanism was proposed by ES-Safi *et al.* [181] and Dörr *et al.* [105] when ESI was used as ionisation source during a MS^2 procedure with an iontrap mass spectrometer.

5.3 Sample Preparation: Reduction with $NaBH_4$

It was confirmed that the reduction step with $NaBH_4$ was an essential process for stabilising Schiff base and Michael adducts against acid hydrolysis. However, multiple isomers for pyridinium and FDP adducts could be detected in protein samples which had been incubated with 2-alkenals as a result of different levels of reduction with $NaBH_4$ for each adduct. Searching for different isomers of the same adduct was a time consuming-process and reduction may increase the probability of the formation of more complex compounds. The summation for the total peak areas for different lysine adducts showed a significant increase in the intensity of the total recovered adducts in reduced protein samples as compared to non reduced protein samples (Figure 5.1). This confirmed that reduction step was essential for optimal recovery of the different 2-alkenal adducts although pyridinium and FDP adducts could be detected in non-reduced samples.

Modification of arginine and histidine with acrolein or crotanaldehyde can result in a stable adducts which can withstand acidic conditions during acid digestion of the protein sample without reduction with $NaBH_4$. The stability of the 2-alkenal adducts of arginine and histidine decreased as the side chain of 2-alkenal increased from crotanaldehyde to 2-nonenal. In the case of lysine, only the Acr-lysine Schiff base and Michael adducts could withstand acid digestion without reduction with $NaBH_4$, while Schiff base and Michael adducts for other Lys-2-alkenal aldehydes could not. In general, pyridinium and FDP adducts showed the highest abundance amongst different 2-alkenal adducts as confirmed by this study. These observations with similar to those of Shao *et al.* [34] even though they used different extraction and detection methods. This can be attributed in part to the high chemical stability of these adducts as compared to Schiff bases and Michael adducts (which are acid liable), but may also be due to thermodynamic stability.

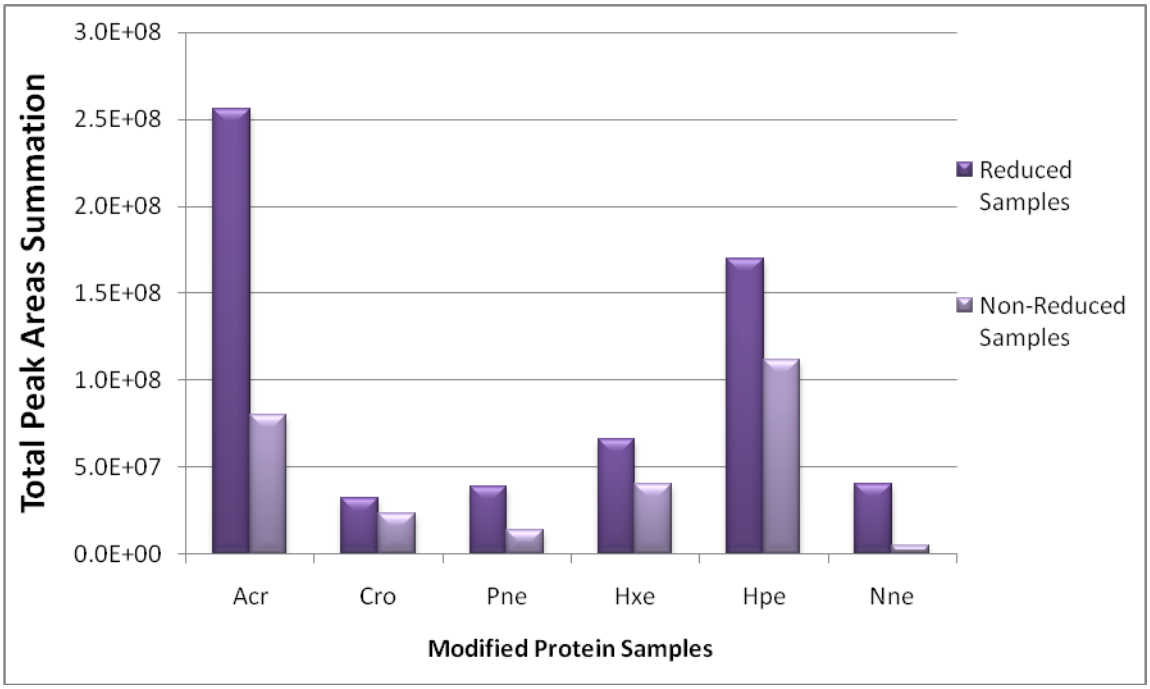

Figure 5.1: Total peak areas summation for all the recovered lysine adducts (Schiff base, Michael Adducts, Pyridinium and FDP adducts) when protein samples were incubated with different 2-alkenals.

5.4 Comparison of the EZ:faast and HILIC methods for analysis of the adducts

The EZ:faast method could achieve higher recovery for amino acids and 2-alkenal adducts as compared to the PPT+HILIC method, as it can be seen from the LOD and LOQ for these 2 methods (see section 3.10.2 and section 4.9). However, the HILIC method is more convenient for metabolomic studies due to the availability of the data bases for the non-derivatised metabolites such as Metlin, HMDB and KEGG which provide the full database for non-derivatised biological compounds and also because it involves less sample preparation.

Fluctuation in the retention times of amino acids and 2-alkenal adducts during separation and detection by HILIC-FTMS might result from the analysis conditions including the mobile phase pH, column temperature, post-run equilibration time, column aging and

some possible contaminants. It was observed that the more hydrophilic the 2-alkenal adduct the greater was its retention on the ZIC-HILIC column (Figure 5.2).

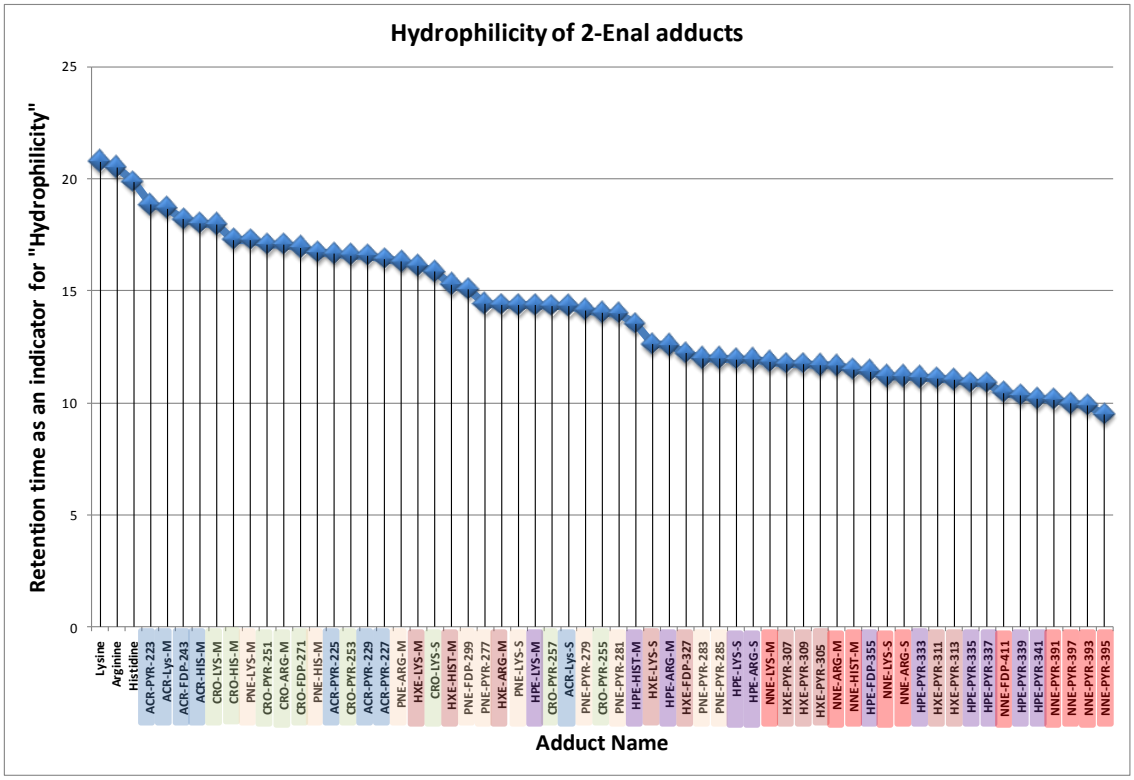

Figure 5.2: Hydrophilicity of amino acids and 2-alkenal adducts indicated by retention on a ZIC-HILIC column. The compound with high hydrophilicity had the greatest retention time on the ZIC-HILIC column.

5.5 Future Work

The obvious extension of the current work would be examine more biological samples for the presence of the alkenal adducts characterised in the current study. The detection of adducts in human plasma was not entirely consistent in the current study. In order to obtain greater sensitivity it might be necessary to switch to a high sensitivity tandem MS system using the same chromatographic conditions as those on the Orbitrap. Dedicated tandem MS systems can offer about two orders of magnitude greater sensitivity than the Orbitrap. In addition a goal that was not achieved during the current

work was to characterise advanced glycation products produced by the reaction of glucose with proteins. This could also form the basis of further work.

5.6 Published Papers

- "Development of a derivatisation method for the analysis of aldehyde modified amino acid residues in proteins by Fourier transform mass spectrometry" Mostafa Pournamdari, Ahmed Saadi, Elizabeth Ellis , Ruth Andrew, Brian Walker, David G.Watson. Analytica Chimica Acta, Volume 633, Issue 2, 9 February 2009, Pages 216-222.
- A contributor author in Pharmaceutical Chemistry: Chapter 11. Drugs exerting non-adrenergic effect on cardiac output and vascular tone. A text book by Dr. D. G. Watson. Churchill Livingstone, Elsevier Ltd. In press.
- “Mass spectrometric studies of the reaction products formed between 2-alkenals and proteins by hydrophilic interaction chromatography in combination with Fourier transform mass spectrometry. Submitted waiting for a reply.
- “Best Acid Hydrolysis Time for Biological Proteins, Using 6N HCl at 145°C”. To be submitted.

6 Appendix

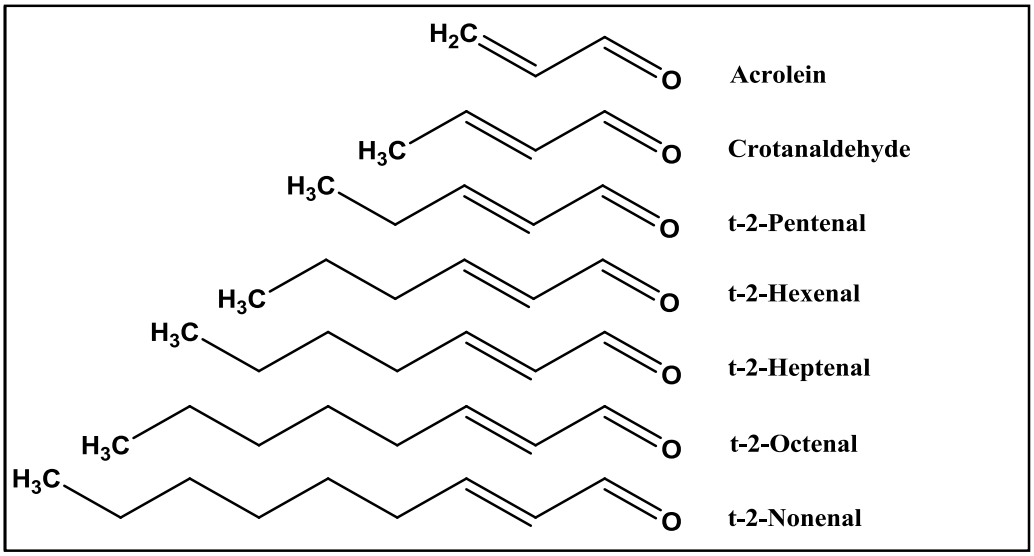

Figure 6.1: Highly reactive aldehydes that belong to trans-2-alkenal series and are generated inside biological systems as a result of the lipid peroxidation processes [30].

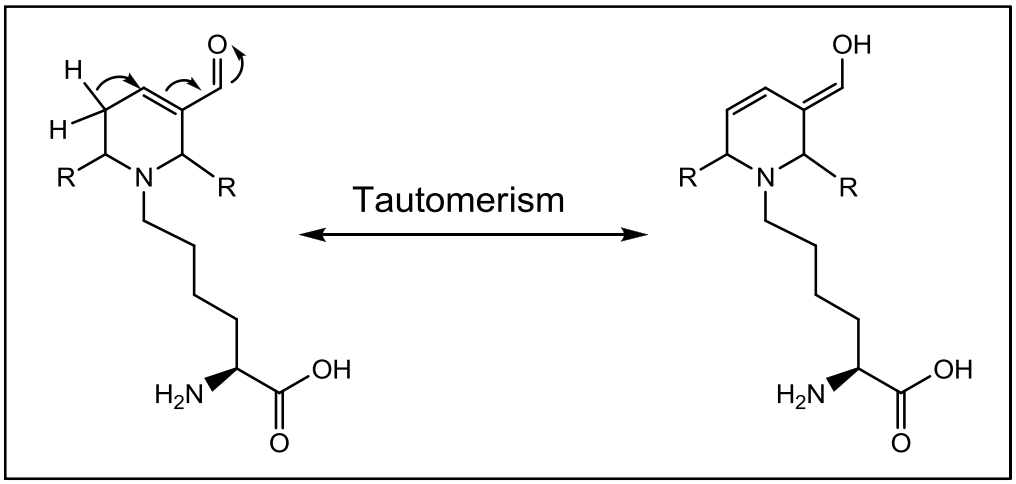

Figure 6.2: Stabilisation mechanism for a FDP-lysine adduct in acidic conditions through enal-dienol tautomerism [61].

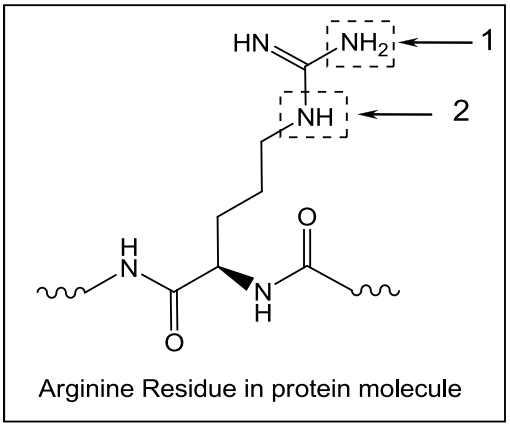

Figure 6.3: The possible locations for the reaction of HNE with arginine through the Michael addition reaction.

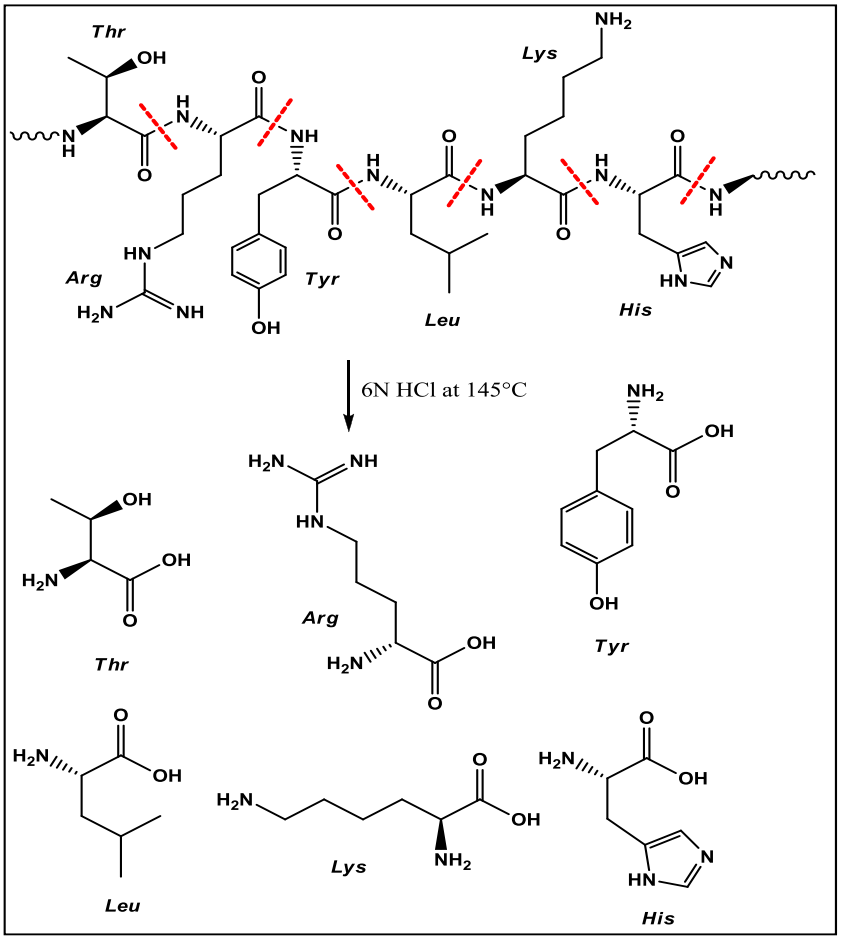

Figure 6.4: Acid hydrolysis for protein sample with 6N HCl.

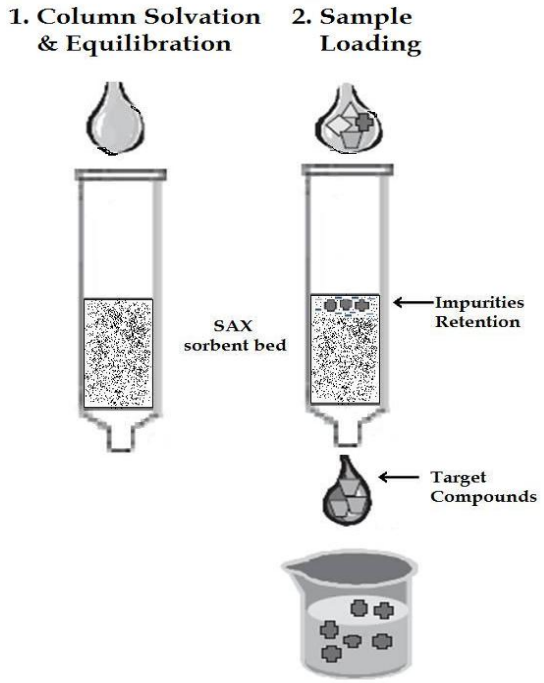

Figure 6.5: Scavenger SPE technique [83].

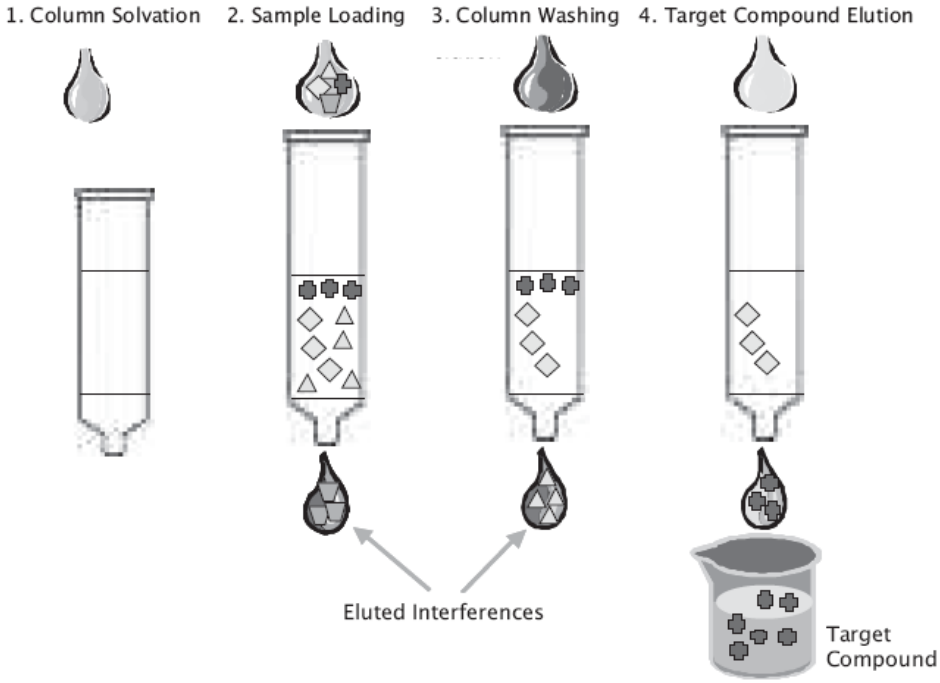

Figure 6.6: Catch & release SPE technique [83].

Table 6-1: The EZ:faast kit reagents [133].

Reagent number	Reagent name	Content
Reagent 1	Internal standard solution	Homoarginine 0.2 mM Methionine-d3 0.2 mM Homophenylalanine 0.2 mM
Reagent 2	Sodium carbonate solution	1M Na_2CO_3
Reagent 3A	Eluting medium component I	0.2M Sodium hydroxide
Reagent 3B	Eluting medium component II	N-propanol
Reagent 4	Organic solution I	Propyl chloroformate in chloroform
Reagent 5	Organic solution II	Iso-octane

Table 6-2: Mass spectrometry results for derivatised acrolein-lysine-pyridinium adducts using EZ:faast method and RPLC-FTMS.

Adduct	*Type of Adduct*	*Elemental formula*	*RDB*	*R_t (min)*	*Observed m/z*	*Delta ppm*
lysine	***Lysine a.a.***	$C_{17}H_{33}O_6N_2$	***2.5***	**7.89 min**	**361.2324**	**-1.557**
Acr-pyr-349	***Lys-pyr (-2H)***	$C_{19}H_{29}O_4N_2$	**6.5**	**N/A**	**N/A**	**N/A**
Acr-pyr-351	***Lys-pyr***	$C_{19}H_{31}O_4N_2$	**5.5**	**2.77 min**	**351.22894**	**2.149**
Acr-pyr-353	***Lys-pyr (+2H)***	$C_{19}H_{33}O_4N_2$	**4.5**	**2.82 min**	**353.24301**	**-1.342**
Acr-pyr-355	***Lys-pyr (+4H)***	$C_{19}H_{35}O_4N_2$	**3.5**	**2.94 min**	**355.25885**	**-0.799**
Acr-pyr-357	***Lys-pyr (+6H)***	$C_{19}H_{37}O_4N_2$	**2.5**	**3.00 min**	**357.27444**	**-0.966**

Table 6-3: Mass spectrometry results for derivatised crotanaldehyde-lysine-pyridinium adducts using EZ:faast method and RPLC-FTMS.

Adduct	*Type of Adduct*	*Elemental formula*	*RDB*	*R_t (min)*	*Observed m/z*	*Delta ppm*
lysine	***Lysine a.a.***	$C_{17}H_{33}O_6N_2$	***2.5***	**7.89 min**	**361.2324**	**-1557**
Cro-pyr-377	***Lys-pyr (-2H)***	$C_{21}H_{33}O_4N_2$	**6.5**	**N/A**	**N/A**	**N/A**
Cro-pyr-379	***Lys-pyr***	$C_{21}H_{35}O_4N_2$	**5.5**	**3.08 min**	**379.25967**	**1.413**
Cro-pyr-381	***Lys-pyr (+2H)***	$C_{21}H_{37}O_4N_2$	**4.5**	**3.40 min**	**381.27496**	**0.459**
Cro-pyr-383	***Lys-pyr (+4H)***	$C_{21}H_{39}O_4N_2$	**3.5**	**3.56 min**	**383.29056**	**0.326**
Cro-pyr-385	***Lys-pyr (+6H)***	$C_{21}H_{41}O_4N_2$	**2.5**	**3.60 min**	**385.30612**	**0.091**

Table 6-4: Mass spectrometry results for derivatised pentenal lysine-pyridinium adducts using EZ:faast method and RPLC-FTMS.

Adduct	*Type of Adduct*	*Elemental formula*	*RDB*	*R_t (min)*	*Observed m/z*	*Delta ppm*
lysine	***Lysine a.a.***	$C_{17}H_{33}O_6N_2$	***2.5***	**7.89 min**	**361.2324**	**-1557**
Pne-pyr-405	***Lys-pyr (-2H)***	$C_{23}H_{37}O_4N_2$	**6.5**	**3.41 min**	**405.27409**	**0.284**
Pne-pyr-407	***Lys-pyr***	$C_{23}H_{39}O_4N_2$	**5.5**	**3.56 min**	**407.29019**	**-0.602**
Pne-pyr-409	***Lys-pyr (+2H)***	$C_{23}H_{41}O_4N_2$	**4.5**	**3.69 min**	**409.30569**	**-0.965**
Pne-pyr-411	***Lys-pyr (+4H)***	$C_{23}H_{43}O_4N_2$	**3.5**	**4.41 min**	**411.32169**	**-0.109**
Pne-pyr-413	***Lys-pyr (+6H)***	$C_{23}H_{45}O_4N_2$	**2.5**	**4.71 min**	**413.3307**	**-0.937**

Table 6-5: Mass spectrometry results for derivatised hexenal lysine-pyridinium adducts using EZ:faast method and RPLC-FTMS.

Adduct	*Type of Adduct*	*Elemental formula*	*RDB*	*R_t (min)*	*Observed m/z*	*Delta ppm*
lysine	***Lysine a.a.***	$C_{17}H_{33}O_6N_2$	***2.5***	**7.89 min**	**361.2324**	**-1557**
Hxe-pyr-433	***Lys-pyr (-2H)***	$C_{25}H_{41}O_4N_2$	**6.5**	**4.14, 4.75, 5.17 min**	**433.306**	**-0.196**
Hxe-pyr-435	***Lys-pyr***	$C_{25}H_{43}O_4N_2$	**5.5**	**4.40, 5.35 min**	**435.32117**	**-1.298**
Hxe-pyr-437	***Lys-pyr (+2H)***	$C_{25}H_{45}O_4N_2$	**4.5**	**4.67, 5.63 min**	**437.33704**	**-0.789**
Hxe-pyr-439	***Lys-pyr (+4H)***	$C_{25}H_{47}O_4N_2$	**3.5**	**5.43, 6.02, 6.60, 7.36min**	**439.35242**	**-1.400**
Hxe-pyr-441	***Lys-pyr (+6H)***	$C_{25}H_{49}O_4N_2$	**2.5**	**6.47, 6.92, 7.76 min**	**441.36807**	**-1.393**

Table 6-6: Mass spectrometry results for derivatised heptenal lysine-pyridinium adducts using EZ:faast method and RPLC-FTMS.

Adduct	*Type of Adduct*	*Elemental formula*	*RDB*	*R_t (min)*	*Observed m/z*	*Delta ppm*
lysine	***Lysine a.a.***	$C_{17}H_{33}O_6N_2$	***2.5***	**7.89 min**	**361.2324**	**-1.557**
Hpe-pyr-461	***Lys-pyr (-2H)***	$C_{27}H_{45}O_4N_2$	**6.5**	**5.38, 6.19, 7.28, 8.06 min**	**461.33795**	**1.225**
Hpe-pyr-463	***Lys-pyr***	$C_{27}H_{47}O_4N_2$	**5.5**	**6.53, 8.40 min**	**463.35236**	**-1.457**
Hpe-pyr-465	***Lys-pyr (+2H)***	$C_{27}H_{49}O_4N_2$	**4.5**	**7.15, 7.64, 8.38, 8.74min**	**465.36816**	**-1.128**
Hpe-pyr-467	***Lys-pyr (+4H)***	$C_{27}H_{51}O_4N_2$	**3.5**	**8.35, 8.84, 9.64, 10.65min**	**465.36795**	**-1.579**
Hpe-pyr-469	***Lys-pyr (+6H)***	$C_{27}H_{53}O_4N_2$	**2.5**	**9.33, 10.09, 11.25min**	**469.39996**	**-1.417**

Table 6-7: Mass spectrometry results for derivatised nonenal lysine-pyridinium adducts using EZ:faast method and RPLC-FTMS.

Adduct	*Type of Adduct*	*Elemental formula*	*RDB*	*R_t (min)*	*Observed m/z*	*Delta ppm*
lysine	***Lysine a.a.***	$C_{17}H_{33}O_6N_2$	***2.5***	**7.89 min**	**361.2324**	**-1557**
Non-pyr-517	***Lys-pyr (-2H)***	$C_{31}H_{53}O_4N_2$	**6.5**	**10.55, 11.22, 12.94, 13.78min**	**517.40015**	**-0.976**
Non-pyr-519	***Lys-pyr***	$C_{31}H_{55}O_4N_2$	**5.5**	**14.14 min**	**519.41522**	**-0.799**
Non-pyr-521	***Lys-pyr (+2H)***	$C_{31}H_{57}O_4N_2$	**4.5**	**12.81, 14.00, 14.44, 15.80min**	**521.43201**	**1.390**
Non-pyr-523	***Lys-pyr (+4H)***	$C_{31}H_{59}O_4N_2$	**3.5**	**13.46, 14.15, 15.06, 16.21min**	**523.44702**	**0.162**
Non-pyr-525	***Lys-pyr (+6H)***	$C_{31}H_{61}O_4N_2$	**2.5**	**14.46, 15.57 min**	**525.46295**	**0.695**

Table 6-8: Full scan mass spectrometry results for the derivatised Lys-2-alkenal adducts in the non reduced protein samples using EZ:faast method and RPLC-FTMS.

Adduct	*Type of Adduct*	*Elemental formula*	*RDB*	*R_t Control (min)*	*R_t (min)*	*Observed m/z*	*Delta ppm*
Acr-pyr-349	*Lys-pyr (-2H)*	$C_{19}H_{29}O_4N_2$	6.5	N/A	N/A	N/A	N/A
Acr-pyr-351	*Lys-pyr*	$C_{19}H_{31}O_4N_2$	5.5	2.77 min	N/A	N/A	N/A
Adduct	*Type of Adduct*	*Elemental formula*	*RDB*	*R_t Control (min)*	*R_t (min)*	*Observed m/z*	*Delta ppm*
Cro-pyr-377	*Lys-pyr (-2H)*	$C_{21}H_{33}O_4N_2$	6.5	N/A	N/A	N/A	N/A
Cro-pyr-379	*Lys-pyr*	$C_{21}H_{35}O_4N_2$	5.5	3.08 min	2.94 min	379.2587	-1.146
Adduct	*Type of Adduct*	*Elemental formula*	*RDB*	*R_t Control (min)*	*R_t (min)*	*Observed m/z*	*Delta ppm*
Pne-pyr-405	*Lys-pyr (-2H)*	$C_{23}H_{37}O_4N_2$	6.5	3.41 min	3.43 min	405.27444	-0.85
Pne-pyr-407	*Lys-pyr*	$C_{23}H_{39}O_4N_2$	5.5	3.56 min	3.32 min	407.29007	-0.895
Adduct	*Type of Adduct*	*Elemental formula*	*RDB*	*R_t Control (min)*	*R_t (min)*	*Observed m/z*	*Delta ppm*
Hxe-pyr-433	*Lys-pyr (-2H)*	$C_{25}H_{41}O_4N_2$	6.5	4.14 min	4.01 min	433.3053	-1.811
				4.75 min	4.48 min	433.30521	-2.019
				5.17 min	4.83 min	433.3053	-1.811
Hxe-pyr-435	*Lys-pyr*	$C_{25}H_{43}O_4N_2$	5.5	4.40 min	4.16 min	435.32077	-2.216
				5.35 min	5.03 min	435.32053	-2.768
Adduct	*Type of Adduct*	*Elemental formula*	*RDB*	*R_t Control (min)*	*R_t (min)*	*Observed m/z*	*Delta ppm*
Hpe-pyr-461	*Lys-pyr (-2H)*	$C_{27}H_{45}O_4N_2$	6.5	5.38 min	5.60 min	461.33624	-2.482
				6.19 min	6.66 min	461.33636	-2.221
				7.28 min	7.33 min	461.33633	-2.286
				8.06 min	N/A	N/A	N/A
Hpe-pyr-463	*Lys-pyr*	$C_{27}H_{47}O_4N_2$	5.5	6.53 min	5.86 min	463.35178	-2.708
				8.40 min	7.62 min	463.35181	-2.644
Adduct	*Type of Adduct*	*Elemental formula*	*RDB*	*R_t Control (min)*	*R_t (min)*	*Observed m/z*	*Delta ppm*
Nne-pyr-517	*Lys-pyr (-2H)*	$C_{31}H_{53}O_4N_2$	6.5	10.55 min	10.63 min	517.39856	-2.754
				11.22 min	12.34 min	517.39874	-2.407
				12.94 min	13.20 min	517.39856	-2.754
				13.78 min	N/A	N/A	N/A
Nne-pyr-519	*Lys-pyr*	$C_{31}H_{55}O_4N_2$	5.5	14.14 min	10.98	519.41418	-2.802

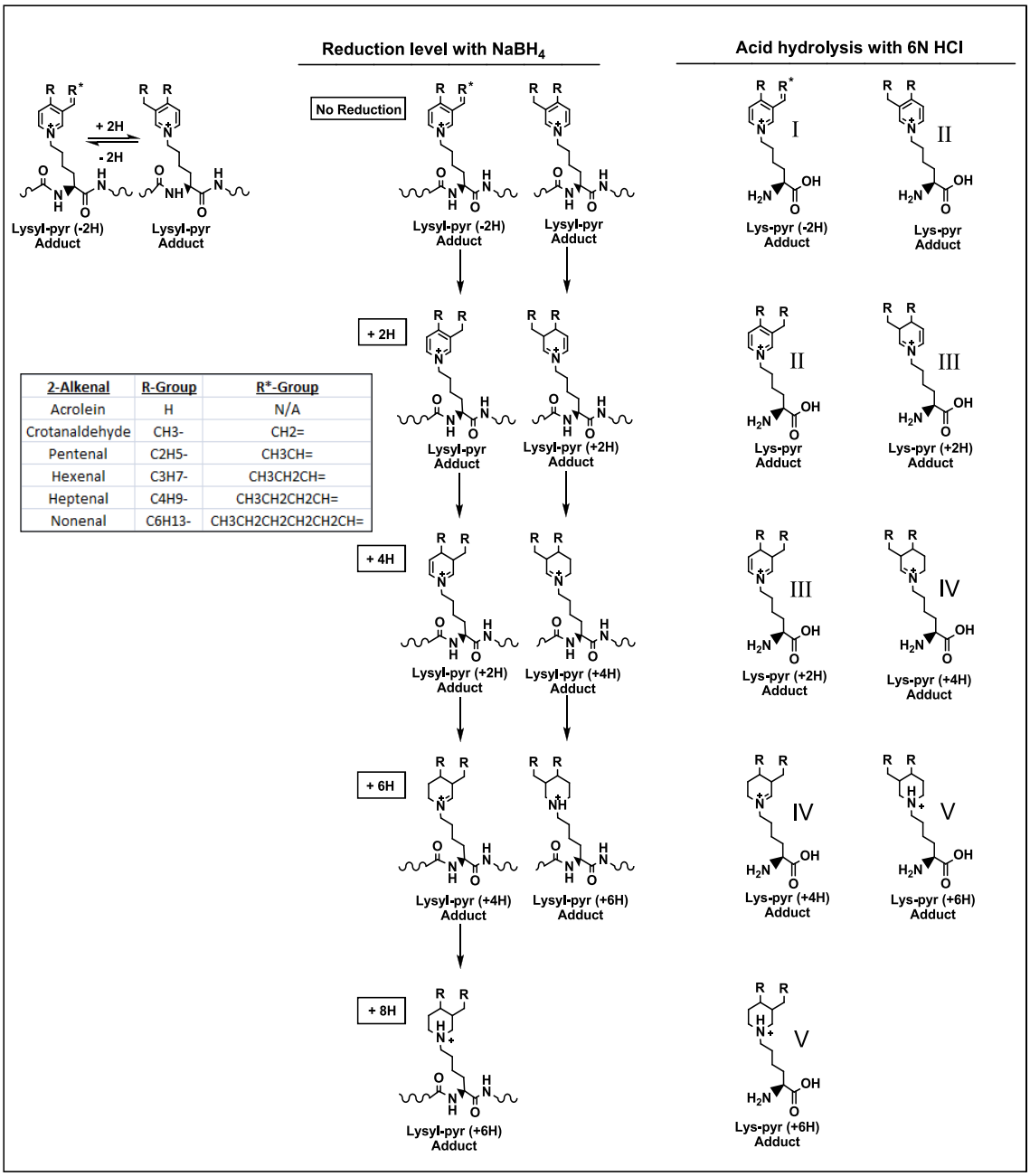

2-Alkenal	R-Group	R*-Group
Acrolein	H	N/A
Crotanaldehyde	CH3-	CH2=
Pentenal	C2H5-	CH3CH=
Hexenal	C3H7-	CH3CH2CH=
Heptenal	C4H9-	CH3CH2CH2CH=
Nonenal	C6H13-	CH3CH2CH2CH2CH=

Figure 6.7: Reduction steps for the pyridinium adduct followed by acid hydrolysis with 6N HCl. Different possible isomers and reduction levels have been suggested.

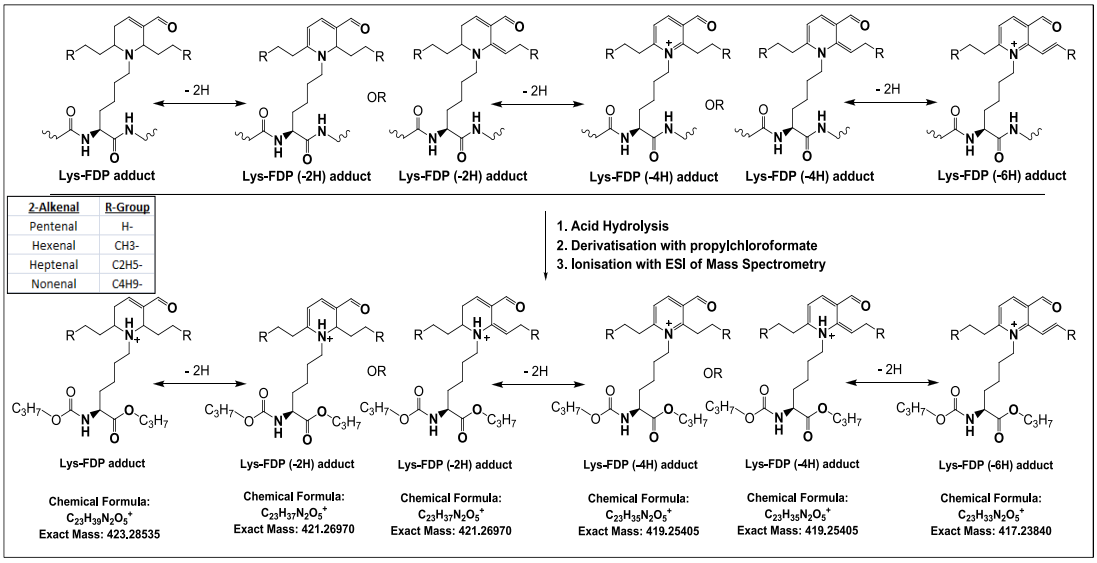

Figure 6.8: Multiple dehydrogenation processes for Lys-FDP adduct followed by acid hydrolysis with 6N HCl, then derivatised with propylchloroformate.

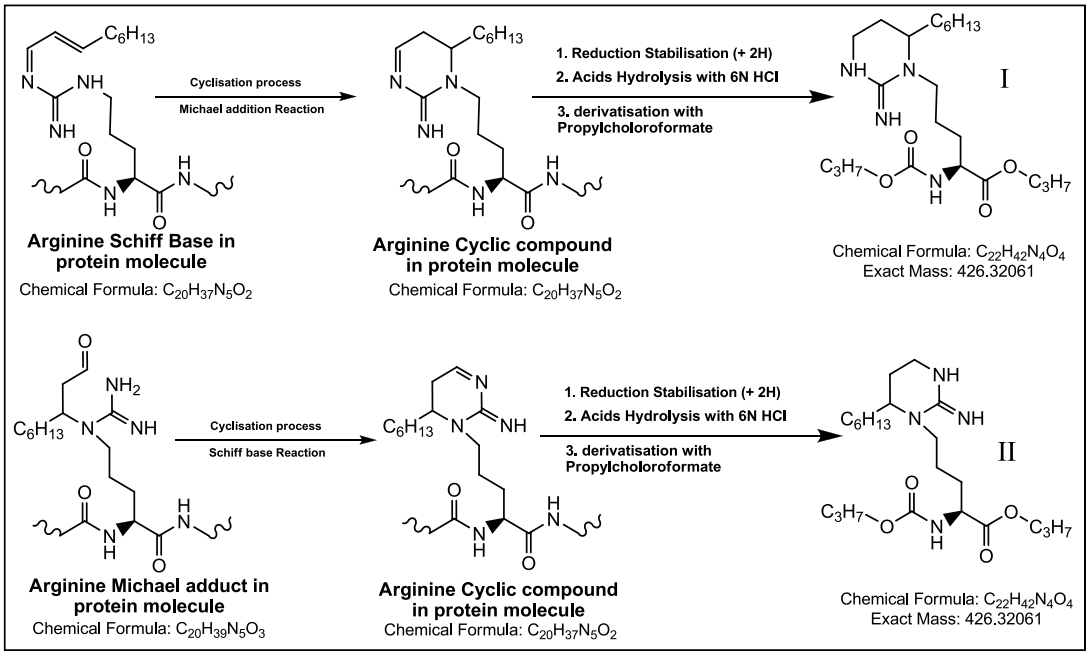

Figure 6.9: Proposed cyclisation process for arginine adducts within the protein molecule which result in the formation of cyclic arginine adduct with m/z 426 after reduction, acid hydrolysis and derivatisation with propylchloroformate.

Table 6-9: Percentage of Amino Acids in Human Serum Albumin.

HUMAN SERUM ALBUMIN sequence 1-609, mwt=69366 [88]

Amino Acids	*Triple-Code*	*One-Code*	*No. Of Residues*	*Mwt*	*Side Chain*		*% in total albumin molecule*
					Polarity	*Acidity*	
Lysine	LYS	K	60	146.1	polar	basic	9.85
Arginine	ARG	R	27	174.2	polar	basic (strongly)	4.43
Histidine	HIS	H	16	155.1	polar	basic (weakly)	2.63
Alanine	ALA	A	63	89.1	nonpolar	neutral	10.34
Aspartic acid	ASP	D	36	133.1	polar	acidic	5.91
Glutamic acid	GLU	E	62	147.1	polar	acidic	10.18
Glycine	GLY	G	13	75.1	nonpolar	neutral	2.13
Methionine	MET	M	7	149.2	nonpolar	neutral	1.15
Tryptophan	TRP	W	2	204.2	nonpolar	neutral	0.33
Valine	VAL	V	43	117.1	nonpolar	neutral	7.06
Threonine	THR	T	29	119.1	polar	neutral	4.76
Phenylalanine	PHE	F	35	165.2	nonpolar	neutral	5.75
Iso-leucine	ILE	I	9	131.2	nonpolar	neutral	1.48
Serine	SER	S	28	105.1	polar	neutral	4.60
Leucine	LEU	L	64	131.2	nonpolar	neutral	10.51
Tyrosine	TYR	Y	19	181.2	polar	neutral	3.12
Asparagine	ASN	N	17	132.1	polar	neutral	2.79
Glutamine	GLN	Q	20	146.2	polar	neutral	3.28
Cysteine	CYS	C	35	121.2	polar	neutral	5.75
Proline	PRO	P	24	115.1	nonpolar	neutral	3.94
Total amino acid residues =			609		69366 Da		

Table 6-10: Estimated LOD and LOQ for the derivatised acrolein adducts using EZ:faast method and RPLC-FTMS.

			LOD			LOQ		
Adduct	***% of amino acid in HSA***	***% of adduct to amino acid***	*Initial conc. mg/ml*	*amount of albmuin in 10 µl into LC-MS (ng)*	***LOD (ng)***	*Initial conc. mg/ml*	*amount of protein in 10 µl into LC-MS (ng)*	***LOQ (ng)***
lysine	9.850	**x**	0.050	13.095	**1.290**	0.050	13.095	**1.290**
Acr-Lys-M	9.850	**0.249**	1.000	261.900	**0.064**	1.000	261.900	**0.064**
Acr-Lys-S	9.850	**0.015**	2.000	548.000	**0.008**	2.500	654.750	**0.010**
Acr-pyr-349	9.850	**2.096**	N/A	N/A	**N/A**	N/A	N/A	**N/A**
Acr-pyr-351	9.850	**4.407**	0.100	26.190	**0.114**	0.250	65.475	**0.284**
Acr-pyr-353	9.850	**3.322**	0.100	26.190	**0.086**	0.250	65.475	**0.214**
Acr-pyr-355	9.850	**10.732**	0.050	13.095	**0.138**	0.100	26.190	**0.277**
Acr-pyr-357	9.850	**5.552**	0.050	13.095	**0.072**	0.100	26.190	**0.143**
Acr-FDP-371	9.850	**9.193**	0.050	13.095	**0.119**	0.250	65.475	**0.593**
Arginine	4.430	**x**	0.050	13.095	**0.580**	0.050	13.095	**0.580**
Acr-Arg-M	4.430	**0.081**	2.000	523.800	**0.019**	2.000	523.800	**0.019**
Acr-Arg-S	4.430	**0.028**	2.000	523.800	**0.006**	2.500	654.750	**0.008**
Histidine	2.627	**x**	0.050	13.095	**0.344**	0.050	13.095	**0.344**
Acr-His-M	2.627	**37.000**	0.250	65.475	**0.636**	0.500	130.950	**1.273**

Table 6-11: Estimated LOD and LOQ for the derivatised crotanaldehyde using EZ:faast method and RPLC-FTMS.

			LOD			LOQ		
Adduct	***% of amino acid in HSA***	***% of adduct to amino acid***	*Initial conc. mg/ml*	*amount of albmuin in 10 µl into LC-MS (ng)*	***LOD (ng)***	*Initial conc. mg/ml*	*amount of protein in 10 µl into LC-MS (ng)*	***LOQ (ng)***
lysine	9.850	**x**	0.050	13.095	**1.290**	0.050	13.095	**1.290**
Cro-Lys-M	9.850	**0.513**	0.100	26.190	**0.013**	0.250	65.475	**0.033**
Cro-Lys-S	9.850	**0.081**	0.100	26.190	**0.002**	0.250	65.475	**0.005**
Cro-pyr-377	9.850	**0.001**	N/A	N/A	**N/A**	N/A	N/A	**N/A**
Cro-pyr-379	9.850	**0.260**	0.100	26.190	**0.007**	0.500	130.950	**0.034**
Cro-pyr-381	9.850	**1.235**	0.050	13.095	**0.016**	0.100	26.190	**0.032**
Cro-pyr-383	9.850	**3.258**	0.050	13.095	**0.042**	0.100	26.190	**0.084**
Cro-pyr-385	9.850	**1.421**	0.050	13.095	**0.018**	0.100	26.190	**0.037**
Cro-FDP-399	9.850	**0.113**	0.500	130.950	**0.015**	1.000	261.900	**0.029**
Arginine	4.430	**x**	0.050	13.095	**0.580**	0.050	13.095	**0.580**
Cro-Arg-M	4.430	**1.833**	0.250	65.475	**0.053**	0.500	130.950	**0.106**
Cro-Arg-S	4.430	**2.200**	0.500	130.950	**0.128**	1.000	261.900	**0.255**
Histidine	2.627	**x**	0.050	13.095	**0.344**	0.050	13.095	**0.344**
Cro-His-M	2.627	**19.420**	0.100	26.190	**0.134**	0.250	65.475	**0.334**

Table 6-12: Estimated LOD and LOQ for the derivatised 2-pentenal adducts using EZ:faast method and RPLC-FTMS.

			LOD			LOQ		
Adduct	***% of amino acid in HSA***	***% of adduct to amino acid***	*Initial conc. mg/ml*	*amount of albmuin in 10 µl into LC-MS (ng)*	***LOD (ng)***	*Initial conc. mg/ml*	*amount of protein in 10 µl into LC-MS (ng)*	***LOQ (ng)***
lysine	9.850	**x**	0.050	13.095	**1.290**	0.050	13.095	**1.290**
Pne-Lys-M	9.850	**0.666**	0.250	65.475	**0.043**	0.500	130.950	**0.086**
Pne-Lys-S	9.850	**0.133**	0.100	26.190	**0.003**	0.500	130.950	**0.017**
Pne-pyr-405	9.850	**0.077**	0.500	130.950	**0.010**	1.000	261.900	**0.020**
Pne-pyr-407	9.850	**2.242**	0.050	13.095	**0.029**	0.100	26.190	**0.058**
Pne-pyr-409	9.850	**0.196**	2.000	523.800	**0.101**	2.000	523.800	**0.101**
Pne-pyr-411	9.850	**2.122**	0.050	13.095	**0.027**	0.250	65.475	**0.137**
Pne-pyr-413	9.850	**0.424**	0.100	26.190	**0.011**	0.250	65.475	**0.027**
Pne-FDP-427	9.850	**1.956**	0.050	13.095	**0.025**	0.100	26.190	**0.050**
Arginine	4.430	**x**	0.050	13.095	**0.580**	0.050	13.095	**0.580**
Pne-Arg-M	4.430	**3.342**	0.250	65.475	**0.097**	0.500	130.950	**0.194**
Pne-Arg-S	4.430	**3.354**	0.250	65.475	**0.097**	0.500	130.950	**0.195**
Histidine	2.627	**x**	0.050	13.095	**0.344**	0.050	13.095	**0.344**
Pne-His-M	2.627	**36.150**	0.050	13.095	**0.124**	0.250	65.475	**0.622**

Table 6-13: Estimated LOD and LOQ for the derivatised 2-hexenal adducts using EZ:faast method and RPLC-FTMS.

			LOD			LOQ		
Adduct	***% of amino acid in HSA***	***% of adduct to amino acid***	*Initial conc. mg/ml*	*amount of albmuin in 10 µl into LC-MS (ng)*	***LOD (ng)***	*Initial conc. mg/ml*	*amount of protein in 10 µl into LC-MS (ng)*	***LOQ (ng)***
lysine	9.850	**x**	0.050	13.095	**1.290**	0.050	13.095	**1.290**
Hxe-Lys-M	9.850	**0.905**	0.050	13.095	**0.012**	0.100	26.190	**0.023**
Hxe-Lys-S	9.850	**0.286**	0.100	26.190	**0.007**	0.250	65.475	**0.018**
Hxe-pyr-433	9.850	**0.012**	0.500	130.950	**0.002**	1.000	261.900	**0.003**
Hxe-pyr-435	9.850	**1.802**	0.050	13.095	**0.023**	0.100	26.190	**0.046**
Hxe-pyr-437	9.850	**2.600**	0.050	13.095	**0.034**	0.250	65.475	**0.168**
Hxe-pyr-439	9.850	**3.036**	0.050	13.095	**0.039**	0.100	26.190	**0.078**
Hxe-pyr-441	9.850	**0.230**	0.100	26.190	**0.006**	0.500	130.950	**0.030**
Hxe-FDP-455	9.850	**0.889**	1.000	261.900	**0.229**	2.000	523.800	**0.459**
Arginine	4.430	**x**	0.050	13.095	**0.580**	0.050	13.095	**0.580**
Hxe-Arg-M	4.430	**6.606**	0.050	13.095	**0.038**	0.250	65.475	**0.192**
Hxe-Arg-S	4.430	**2.036**	0.050	13.095	**0.012**	0.250	65.475	**0.059**
Histidine	2.627	**x**	0.050	13.095	**0.344**	0.050	13.095	**0.344**
Hxe-His-M	2.627	**43.858**	0.050	13.095	**0.151**	0.100	26.190	**0.302**

Table 6-14: Estimated LOD and LOQ for the derivatised 2-heptenal adducts using EZ:faast method and RPLC-FTMS.

			LOD			LOQ		
Adduct	***% of amino acid in HSA***	***% of adduct to amino acid***	*Initial conc. mg/ml*	*amount of albmuin in 10 µl into LC-MS (ng)*	***LOD (ng)***	*Initial conc. mg/ml*	*amount of protein in 10 µl into LC-MS (ng)*	***LOQ (ng)***
lysine	9.850	**x**	0.050	13.095	**1.290**	0.050	13.095	**1.290**
Hpe-Lys-M	9.850	**0.874**	0.250	65.475	**0.056**	0.500	130.950	**0.113**
Hpe-Lys-S	9.850	**0.172**	0.100	26.190	**0.004**	0.500	130.950	**0.022**
Hpe-pyr-461	9.850	**0.239**	0.500	130.950	**0.031**	1.000	261.900	**0.062**
Hpe-pyr-463	9.850	**6.222**	0.050	13.095	**0.080**	0.050	13.095	**0.080**
Hpe-pyr-465	9.850	**1.851**	0.250	65.475	**0.119**	0.500	130.950	**0.239**
Hpe-pyr-467	9.850	**3.902**	0.050	13.095	**0.050**	0.250	65.475	**0.252**
Hpe-pyr-469	9.850	**0.558**	0.250	65.475	**0.036**	0.500	130.950	**0.072**
Hpe-FDP-483	9.850	**3.419**	0.100	26.190	**0.088**	0.250	65.475	**0.221**
Arginine	4.430	**x**	0.050	13.095	**0.580**	0.050	13.095	**0.580**
Hpe-Arg-M	4.430	**12.179**	0.100	26.190	**0.141**	0.250	65.475	**0.353**
Hpe-Arg-S	4.430	**0.001**	N/A	N/A	**N/A**	N/A	N/A	**N/A**
Histidine	2.627	**x**	0.050	13.095	**0.344**	0.050	13.095	**0.344**
Hpe-His-M	2.627	**88.000**	0.050	13.095	**0.303**	0.050	13.095	**0.303**

Table 6-15: Estimated LOD and LOQ for the derivatised 2-nonenal adducts using EZ:faast method and RPLC-FTMS.

			LOD			LOQ		
Adduct	***% of amino acid in HSA***	***% of adduct to amino acid***	*Initial conc. mg/ml*	*amount of albmuin in 10 µl into LC-MS (ng)*	***LOD (ng)***	*Initial conc. mg/ml*	*amount of protein in 10 µl into LC-MS (ng)*	***LOQ (ng)***
lysine	9.850	**x**	0.050	13.095	**1.290**	0.050	13.095	**1.290**
Nne-Lys-M	9.850	**0.480**	0.250	65.475	**0.031**	0.500	130.950	**0.062**
Nne-Lys-S	9.850	**0.099**	0.500	130.950	**0.013**	2.000	523.800	**0.051**
Nne-pyr-517	9.850	**0.121**	1.000	261.900	**0.031**	2.000	523.800	**0.062**
Nne-pyr-519	9.850	**2.577**	0.100	26.190	**0.066**	0.250	65.475	**0.166**
Nne-pyr-521	9.850	**0.806**	0.250	65.475	**0.052**	1.000	261.900	**0.208**
Nne-pyr-523	9.850	**1.003**	0.500	130.950	**0.129**	1.000	261.900	**0.259**
Nne-pyr-525	9.850	**0.164**	1.000	261.900	**0.042**	2.000	523.800	**0.085**
Nne-FDP-539	9.850	**1.426**	0.250	65.475	**0.092**	0.500	130.950	**0.184**
Arginine	4.430	**x**	0.050	13.095	**0.580**	0.050	13.095	**0.580**
Nne-Arg-M	4.430	**8.000**	0.100	26.190	**0.093**	0.500	130.950	**0.464**
Nne-Arg-S	4.430	**1.590**	0.250	65.475	**0.046**	1.000	261.900	**0.184**
Histidine	2.627	**x**	0.050	13.095	**0.344**	0.050	13.095	**0.344**
Nne-His-M	2.627	**54.000**	0.050	13.095	**0.186**	0.050	13.095	**0.186**

Table 6-16: MS^2 results for different amino acids obtained using data dependent acquisition operating in the positive mode with ESI-CID-FTMS/MS. The most dominant fragment is highlighted in red.

Amino Acids	*Elemental Formula+1H⁺*	*Observed Mass (m/z)*	*R_t (min)*	*Fragment (m/z)*	*Chemical Formula*	*Delta ppm*	*Intensity*	*Mass Loss*
Phenylalanine	C9H12NO2	166.086	8.57	149.059	C9 H9 O2	-1.518	6.92E+05	17.027
				131.049	C9 H7 O1	-1.614	7.10E+05	35.037
				120.080	C8 H10 N1	-2.382	2.68E+07	46.006
				107.049	C7 H7 O1	-1.976	3.53E+04	59.037
Leucine, Iso-leucine	C6H14NO2	132.102	8.95, 9.26	86.096	C5 H12 N1	-2.509	1.34E+07	46.006
				69.070	C5 H9	-2.272	2.21E+05	-69.070
Tryptophan	C11H13N2O2	205.097	9.11	188.070	C11 H10 O2 N	-1.782	6.99E+06	17.026
				159.091	C10 H11 N2	-1.225	8.28E+03	46.005
				146.060	C9 H8 O N	-1.578	4.33E+04	59.037
Methionine	C5H12NO2S	150.058	9.90	133.032	C5 H9 O2S1	-1.939	9.85E+06	17.026
				115.099	C6 H13 O1 N1	-1.456	6.82E+05	34.959
				104.053	C4 H10 N1S1	-2.189	2.40E+06	46.005
				102.055	C4 H8 O2 N	-2.205	9.38E+04	48.003
				87.026	C4 H7S1	-2.857	1.78E+04	63.032
				56.049	C3 H6 N1	-2.780	2.86E+05	94.009
Valine	C5H12NO2	118.086	10.46	72.081	C4 H10 N1	-2.580	4.62E+06	46.005
				55.054	C4 H7	-3.031	3.58E+04	63.032
Tyrosine	C9H12NO3	182.081	10.50	165.054	C9 H9 O3	-2.065	1.86E+07	17.027
				147.044	C9 H7 O2	-1.402	5.41E+05	35.037
				136.075	C8 H10 O1 N1	-1.474	4.69E+06	46.006
				123.044	C7 H7 O2	-1.675	1.82E+05	59.037
Proline	C5H10NO2	116.071	11.49	70.065	C4 H8 N1	-2.796	9.21E+05	46.006
Alanine	C3H8NO2	90.055	11.89	x	x	x	x	x
Glutamic acid	C5H10NO4	148.060	12.05	130.050	C5 H8 O3 N1	-1.921	3.44E+06	18.011
				102.055	C4 H8 O2 N1	-2.207	5.24E+05	46.006
				84.044	C4 H6 O1 N1	-1.909	2.04E+05	64.016
4-hydroxyproline	C5H10NO3	132.066	12.13	114.055	C5 H8 O2 N1	-2.413	5.43E+04	18.011
				86.060	C4 H8 O1 N1	-2.679	9.77E+05	46.006
				68.049	C4 H6 N1	-2.731	2.70E+04	64.016
Threonine	C4H10NO3	120.066	12.60	102.055	C4 H8 O2 N1	-2.598	8.27E+05	18.011
				84.044	C4 H6 O1 N1	-2.861	1.24E+04	36.021
				74.060	C3 H8 O1 N1	-2.573	4.52E+05	46.006
				56.049	C3 H6 N1	-2.959	2.00E+04	64.016
Aspartic acid	C4H8NO4	134.045	12.91	116.034	C4 H6 O3 N1	-2.325	8.15E+05	18.011
				88.039	C3 H6 O2 N1	-2.443	7.08E+05	46.006
				74.023	C2 H4 O2 N1	-2.365	3.12E+05	60.021
				70.029	C3 H4 O1 N1	-2.290	1.13E+04	64.016
Serine	C3H8NO3	106.050	13.70	88.039	C3 H6 O2 N1	-2.443	4.60E+04	18.011

				60.044	C2 H6 O1 N1	-2.339	8.13E+04	46.006
Histidine	C6H10N3O2	156.077	18.87	138.066	C6 H8 O1 N3	-1.076	9.33E+03	18.011
				110.071	C5 H8 N3	-1.489	2.83E+06	46.006
				95.060	C5 H7 N2	-1.734	7.46E+04	61.017
				83.060	C4 H7 N2	-1.744	6.19E+03	73.017
Arginine	C6H15N4O2	175.119	19.59	158.092	C6 H12 O2 N3	-1.729	9.60E+05	17.027
				157.108	C6H13O1N4	-1.004	4.30E+05	18.011
				140.082	C6 H10 O1 N3	-1.204	3.08E+04	35.037
				130.097	C5 H12 O1 N3	-1.527	3.27E+05	45.022
				116.070	C5 H10 O2 N1	-1.855	4.69E+05	59.049
				112.087	C5 H10 N3	-1.820	3.51E+04	63.032
				98.060	C5 H8 O1 N1	-2.045	4.79E+03	77.059
				70.065	C4 H8 N1	-1.797	5.10E+04	105.054
				60.056	C1 H6 N3	-2.062	1.10E+05	115.063
Lysine	C6H15N2O2	147.113	19.90	130.086	C6 H12 O2 N1	-1.502	3.03E+06	17.027
				129.102	C6H13N2O1	-1.237	3.57E+05	18.011
				84.081	C5 H10 N1	-1.617	7.86E+04	63.032
Hydroxylysine	C6H15N2O3	163.108	20.50	145.097	C6 H13 O2 N2	-1.202	1.74E+06	18.011
				132.081	C9 H10 N1	-2.014	1.71E+03	31.027
				128.070	C6 H10 O2 N1	-1.447	7.56E+05	35.037
				117.102	C5 H13 O1 N2	-1.706	3.63E+03	46.006
				100.076	C5 H10 O1 N1	-1.805	1.07E+04	63.032
				82.065	C5 H8 N1	-1.534	2.82E+03	81.043

Table 6-17: Mass spectrometric results for Acr-Lys-pyridinium adducts using HILIC-FTMS.

Adduct	*Type of Adduct*	*Elemental formula*	*RDB*	*R_t control (min)*	*Observed m/z*	*Delta ppm*
Lysine	***Lysine a.a.***	**$C_6H_{15}N_2O_2$**	**0.5**	**19.47**	**147.11249**	**-1.04**
Acr-pyr-221	***Lys-pyr (-2H)***	**N/A**	**N/A**	**N/A**	**N/A**	**0.37**
Acr-pyr-223	***Lys-pyr***	**$C_{12}H_{19}O_2N_2$**	**4.5**	**18.83**	**223.14410**	**-0.85**
Acr-pyr-225	***Lys-pyr (+2H)***	**$C_{12}H_{21}O_2N_2$**	**3.5**	**16.65, 18.91**	**225.15975**	**-2.27**
Acr-pyr-227	***Lys-pyr (+4H)***	**$C_{12}H_{23}O_2N_2$**	**2.5**	**16.41**	**227.17540**	**-0.76**
Acr-pyr-229	***Lys-pyr (+6H)***	**$C_{12}H_{25}O_2N_2$**	**1.5**	**16.57**	**229.19105**	**-1.02**

Table 6-18: Mass spectrometric results for Cro-Lys-pyridinium adducts using HILIC-FTMS.

Adduct	*Type of Adduct*	*Elemental formula*	*RDB*	*R_t control (min)*	*Observed m/z*	*Delta ppm*
Lysine	***Lysine a.a.***	**$C_6H_{15}N_2O_2$**	**0.5**	**19.47**	**147.11249**	**-0.82**
Cro-pyr-249	***Lys-pyr (-2H)***	**$C_{14}H_{21}O_2N_2$**	**5.5**	**17.78**	**249.15975**	**-0.90**
Cro-pyr-251	***Lys-pyr***	**$C_{14}H_{23}O_2N_2$**	**4.5**	**17.6**	**251.17540**	**0.98**
Cro-pyr-253	***Lys-pyr (+2H)***	**$C_{14}H_{25}O_2N_2$**	**3.5**	**16.58, 17.46**	**253.19105**	**-1.07**
Cro-pyr-255	***Lys-pyr (+4H)***	**$C_{14}H_{27}O_2N_2$**	**2.5**	**13.52,14.00**	**255.20670**	**-1.15**
Cro-pyr-257	***Lys-pyr (+6H)***	**$C_{14}H_{29}O_2N_2$**	**1.5**	**14.32**	**257.22235**	**-1.23**

Table 6-19: Mass spectrometric results for Pne-Lys-pyridinium adducts using HILIC-FTMS.

Adduct	*Type of Adduct*	*Elemental formula*	*RDB*	*R_t control (min)*	*Observed m/z*	*Delta ppm*
Lysine	*Lysine a.a.*	$C_6H_{15}N_2O_2$	0.5	19.47	147.11249	1.03
Pne-pyr-277	*Lys-pyr (-2H)*	$C_{16}H_{25}O_2N_2$	5.5	13.67, 14.57	277.19105	-1.59
Pne-pyr-279	*Lys-pyr*	$C_{16}H27O_2N_2$	4.5	13.85, 14.57	279.20670	-1.30
Pne-pyr-281	*Lys-pyr (+2H)*	$C_{16}H29O_2N_2$	3.5	12.16, 13.69, 14.89	281.22235	0.66
Pne-pyr-283	*Lys-pyr (+4H)*	$C_{16}H31O_2N_2$	2.5	11.84	283.23800	-1.63
Pne-pyr-285	*Lys-pyr (+6H)*	$C_{16}H_{33}O_2N_2$	1.5	11.91	285.25365	-1.81

Table 6-20: Mass spectrometric results for Hxe-Lys-pyridinium adducts using HILIC-FTMS.

Adduct	*Type of Adduct*	*Elemental formula*	*RDB*	*R_t control (min)*	*Observed m/z*	*Delta ppm*
Lysine	*Lysine a.a.*	$C_6H_{15}N_2O_2$	0.5	19.47	147.11249	0.73
Hxe-pyr-305	*Lys-pyr (-2H)*	$C_{18}H_{29}O_2N_2$	5.5	11.65	305.22235	-1.45
Hxe-pyr-307	*Lys-pyr*	$C_{18}H_{31}O_2N_2$	4.5	11.6	307.23800	-0.86
Hxe-pyr-309	*Lys-pyr (+2H)*	$C_{18}H_{33}O_2N_2$	3.5	11.6	309.25365	-1.04
Hxe-pyr-311	*Lys-pyr (+4H)*	$C_{18}H_{35}O_2N_2$	2.5	10.95	311.26930	0.41
Hxe-pyr-313	*Lys-pyr (+6H)*	$C_{18}H_{37}O_2N_2$	1.5	10.87	313.28495	-1.32

Table 6-21: Mass spectrometric results for Hpe-Lys-pyridinium adducts using HILIC-FTMS.

Adduct	*Type of Adduct*	*Elemental formula*	*RDB*	*R_t control (min)*	*Observed m/z*	*Delta ppm*
Lysine	*Lysine a.a.*	$C_6H_{15}N_2O_2$	0.5	19.47	147.11249	-1.66
Hpe-pyr-333	*Lys-pyr (-2H)*	$C_{20}H_{33}O_2N_2$	5.5	10.6	333.25365	2.10
Hpe-pyr-335	*Lys-pyr*	$C_{20}H_{35}O_2N_2$	4.5	10.52	335.26930	0.78
Hpe-pyr-337	*Lys-pyr (+2H)*	$C_{20}H_{37}O_2N_2$	3.5	10.64	337.28495	0.55
Hpe-pyr-339	*Lys-pyr (+4H)*	$C_{20}H_{39}O_2N_2$	2.5	10.24	339.30060	1.51
Hpe-pyr-341	*Lys-pyr (+6H)*	$C_{20}H_{41}O_2N_2$	1.5	9.99	341.31626	1.06

Table 6-22: Mass spectrometric results for Nne-Lys-pyridinium adducts using HILIC-FTMS.

Adduct	*Type of Adduct*	*Elemental formula*	*RDB*	*R_t control (min)*	*Observed m/z*	*Delta ppm*
Lysine	*Lysine a.a.*	$C_6H_{15}N_2O_2$	0.5	19.47	147.11249	-1.40
Nne-pyr-389	*Lys-pyr (-2H)*	$C_{24}H4_1O_2N_2$	5.5	9.97	389.31626	0.26
Nne-pyr-391	*Lys-pyr*	$C_{24}H_{43}O_2N_2$	4.5	9.83	391.33191	-0.54
Nne-pyr-393	*Lys-pyr (+2H)*	$C_{24}H_{45}O_2N_2$	3.5	9.67	393.34756	-0.87
Nne-pyr-395	*Lys-pyr (+4H)*	$C_{24}H_{47}O_2N_2$	2.5	9.26	395.36321	-1.10
Nne-pyr-397	*Lys-pyr (+6H)*	$C_{24}H_{49}O_2N_2$	1.5	N/A	N/A	N/A

Table 6-23: MS results for different Lys-pyridinium adducts in non reduced protein samples using HILIC-FTMS. All the results were within 1.5 ppm of the theoretical masses. N=4.

Adduct	*Type of Adduct*	*Elemental formula*	*RDB*	*R_t control (min)*	*R_t (min)*	*Observed m/z*	*Average Peak area*
Acr-pyr-221	*Lys-pyr (-2H)*	N/A	N/A	N/A	N/A	N/A	N/A
Acr-pyr-223	*Lys-pyr*	$C_{12}H_{19}O_2N_2$	4.5	18.83	18.89	223.14410	79799347
Cro-pyr-249	*Lys-pyr (-2H)*	$C_{14}H_{21}O_2N_2$	5.5	17.78	17.39	249.15975	378831
Cro-pyr-251	*Lys-pyr*	$C_{14}H_{23}O_2N_2$	4.5	17.6	17.3	251.17540	22892827
Pne-pyr-277	*Lys-pyr (-2H)*	$C_{16}H_{25}O_2N_2$	5.5	13.67, 14.57	14.46	277.19105	10667562
Pne-pyr-279	*Lys-pyr*	$C_{16}H_{27}O_2N_2$	4.5	13.85, 14.57	14.41	279.20670	3591891
Hxe-pyr-305	*Lys-pyr (-2H)*	$C_{18}H_{29}O_2N_2$	5.5	11.65	11.8	305.22235	31274628
Hxe-pyr-307	*Lys-pyr*	$C_{18}H_{31}O_2N_2$	4.5	11.6	11.8	307.23800	8959161
Hpe-pyr-333	*Lys-pyr (-2H)*	$C_{20}H_{33}O_2N_2$	5.5	10.6	10.95	333.25365	96612805
Hpe-pyr-335	*Lys-pyr*	$C_{20}H_{35}O_2N_2$	4.5	10.52	10.77	335.26930	14853961
Non-pyr-389	*Lys-pyr (-2H)*	$C_{24}H_{41}O_2N_2$	5.5	9.97	9.9	389.31626	4034860
Non-pyr-391	*Lys-pyr*	$C_{24}H_{43}O_2N_2$	4.5	9.83	9.54	391.33191	712219

Table 6-24: MS^2 for different 2-alkenal adducts using ZIC-HILIC column coupled to ESI-CID-FTMS/MS. The results obtained using data dependent acquisition mode.

Adduct	*Elemental formula*	*Observed (m/z)*	*R_t control (min)*	*Fragment (m/z)*	*Chemical formula*	*Delta ppm*	*Mass loss*
Acr-Lys-M	$C_9H_{21}N_2O_3$	205.15467	18.67	160.13295	$C_8H_{18}O_2N_1$	-1.595	45.02172
		205.15467		130.08606	$C_6H_{12}O_2N_1$	-1.5	75.06861
		205.15467		188.12788	$C_9H_{18}O_3N_1$	-1.275	17.02679
		205.15467		84.08057	$C_5H_{10}N_1$	-2.449	121.0741
Acr-pyr-223	$C_{12}H_{19}O_2N_2$	223.1441	19.6	130.08607	$C_6H_{12}O_2N_1$	-1.423	93.05803
		223.1441		94.06496	$C_6H_8N_1$	-1.763	129.07914
		223.1441		84.08065	$C_5H_{10}N_1$	-1.497	139.06345
		223.1441		178.12257	$C_{11}H_{16}O_1N_1$	-0.397	45.02153
Acr-pyr-227	$C_{12}H_{23}O_2N_2$	227.1754	16.41	182.15372	$C11H20O_1N1$	-1.212	45.02168
		227.1754		159.11261	$C_7H_{15}O_2N_2$	-1.221	68.06279
		227.1754		142.08609	$C_7H_{12}O_2N_1$	-1.162	85.08931
		227.1754		130.08601	$C_6H_{12}O_2N_1$	-1.885	97.08939
		227.1754		98.09618	$C_6H_{12}N_1$	-2.507	129.07922
		227.1754		84.08058	$C_5H_{10}N_1$	-2.33	143.09482
Acr-pyr-229	$C_{12}H_{25}O_2N_2$	229.19105	16.57	184.16948	$C_{11}H_{22}O_1N_1$	-0.602	45.02157
		229.19105		130.08609	$C_6H_{12}O_2N_1$	-1.27	99.10496
		229.19105		100.11192	$C_6H_{14}N_1$	-1.558	129.07913
		229.19105		84.0806	$C_5H_{10}N_1$	-2.092	145.11045
Acr-FDP-243	$C_{12}H_{23}O_3N_2$	243.17032	18.18	225.15956	$C_{12}H_{21}O_2N_2$	-0.864	18.01076
		243.17032		198.14874	$C_{11}H_{20}O_2N_1$	-0.582	45.02158
		243.17032		180.13815	$C_{11}H_{18}O_1N_1$	-0.781	63.03217

		243.17032		159.11264	$C_7H_{15}O_2N_2$	-1.032	84.05768
		243.17032		150.12756	$C_{10}H_{16}N_1$	-1.106	93.04276
		243.17032		142.08611	$C_7H_{12}O_2N_1$	-1.022	101.08421
		243.17032		130.08606	$C_6H_{12}O_2N_1$	-1.5	113.08426
		243.17032		114.09114	$C_6H_{12}O_1N_1$	-1.758	129.07918
		243.17032		98.09625	$C_6H_{12}N_1$	-1.794	145.07407
		243.17032		96.08062	$C_6H_{10}N_1$	-1.623	147.0897
		243.17032		84.08064	$C_5H_{10}N_1$	-1.616	159.08968
Acr-FDP-245	$C_{12}H_{25}O_3N_2$	245.18568	18.72	227.17537	$C_{12}H_{23}O_2N_2$	-0.152	18.01031
		245.18568		200.16435	$C_{11}H_{22}O_2N_1$	-0.777	45.02133
		245.18568		130.08615	$C_6H_{12}O_2N_1$	-0.808	115.09953
		245.18568		116.10686	$C_6H_{14}O_1N_1$	-1.125	129.07882
		245.18568		98.09626	$C_6H_{12}N_1$	-1.692	147.08942
Acr-His-M	$C_9H_{16}N_3O_3$	214.11862	18.02	170.12851	$C_8H_{16}O_1N_3$	-1.638	43.99011
		214.11862		168.11282	$C_8H_{14}O_1N_3$	-1.895	46.0058
		214.11862		153.10199	$C_8H_{13}O_1N_2$	-1.63	61.01663
		214.11862		141.10201	$C_7H_{13}O_1N_2$	-1.627	73.01661
Cro-Lys-M	$C_{10}H_{23}N_2O_3$	219.17032	17.95	174.14861	$C_9H_{20}O_2N_1$	-1.409	45.02171
		219.17032		156.138	$C_9H_{18}O_1N_1$	-1.862	63.03232
		219.17032		130.08598	$C_6H_{12}O_2N_1$	-2.115	89.08434
		219.17032		90.09113	$C_4H_{12}O_1N_1$	-2.337	129.07919
		219.17032		84.08056	$C_5H_{10}N_1$	-2.568	135.08976
Cro-Lys-S	$C_{10}H_{21}N_2O_2$	201.15975	15.85	130.086	$C_6H_{12}O_2N_1$	-1.961	71.07375
Cro-pyr-251	$C_{14}H_{23}O_2N_2$	251.1754	17.06	206.15396	$C_{13}H_{20}O_1N_1$	0.093	45.02144
		251.1754		130.08618	$C_6H_{12}O_2N_1$	-0.578	121.08922
		251.1754		122.09632	$C_8H_{12}N_1$	-0.868	129.07908
		251.1754		84.08069	$C_5H_{10}N_1$	-1.022	167.09471
Cro-His-M	$C_{10}H_{18}N_3O_3$	228.13427	17.28	182.12869	$C_9H1_6ON_3$	-0.542	46.00558
		228.13427		167.1178	$C_9H_{15}O_1N_2$	-0.536	61.01647
Pne-Lys-M	$C_{11}H_{25}N_2O_3$	233.18597	16.67, 17.07, 17.49	188.16428	$C_{10}H_{22}O_2N_1$	-1.198	45.02169
		233.18597		130.08601	$C_6H_{12}O_2N_1$	-1.885	103.09996
		233.18597		104.10681	$C_5H_{14}O_1N_1$	-1.735	129.07916
		233.18597		84.0806	$C_5H_{10}N_1$	-2.092	149.10537
Pne-His-M	$C_{11}H_{20}N_3O_3$	242.14992	16.71	198.15987	$C_{10}H_{20}O_1N_3$	-1.104	43.99005
		242.14992		196.14423	$C_{10}H_{18}O_1N_3$	-1.064	46.00569
		242.14992		181.13335	$C_{10}H1_7O_1N_2$	-1.047	61.01657
		242.14992		169.13335	$C_9H1_7O_1N_2$	-1.122	73.01657
		242.14992		156.07655	$C_6H_{10}O_2N_3$	-1.301	86.07337
		242.14992		112.08671	$C_5H_{10}N_3$	-1.908	130.06321
		242.14992		110.07106	$C_5H_8N_3$	-1.943	132.07886

		242.14992		**95.0602**	**$C_5H_7N_2$**	**-1.839**	**147.08972**
Pnr-pyr-277	**$C_{16}H_{25}O_2N_2$**	**277.19105**	**13.57, 14.57**	**232.16965**	**$C_{15}H_{22}O_1N_1$**	**0.255**	**45.0214**
		277.19105		**148.11195**	**$C_{10}H_{14}N_1$**	**-0.851**	**129.0791**
		277.19105		**130.0862**	**$C_6H_{12}O_2N_1$**	**-0.424**	**147.10485**
		277.19105		**84.08071**	**$C_5H_{10}N_1$**	**-0.784**	**193.11034**
Pnr-pyr-279	**$C_{16}H27O_2N_2$**	**279.2067**	**13.85, 14.57**	**234.18529**	**$C_{15}H_{24}O_1N_1$**	**0.21**	**45.02141**
		279.2067		**150.12759**	**$C_{10}H_{16}N_1$**	**-0.906**	**129.07911**
		279.2067		**130.08621**	**$C_6H_{12}O_2N_1$**	**-0.347**	**149.12049**
		279.2067		**166.08626**	**$C_9H_{12}O_2N_1$**	**0.029**	**113.12044**
		279.2067		**120.08068**	**$C_8H_{10}N_1$**	**-0.799**	**159.12602**
Hxe-Lys-S	**$C_{12}H_{25}N_2O_2$**	**229.19105**	**12.48**	**212.16409**	**$C_{12}H_{22}O_2N_1$**	**-1.958**	**17.02696**
		229.19105		**184.16943**	**$C_{11}H_{22}O_1N_1$**	**-0.873**	**45.02162**
		229.19105		**130.08606**	**$C_6H_{12}O_2N_1$**	**-1.5**	**99.10499**
		229.19105		**84.0806**	**$C_5H_{10}N_1$**	**-2.092**	**145.11045**
Hxe-pyr-305	**$C_{18}H_{29}O_2N_2$**	**305.22235**	**11.6**	**260.20087**	**$C_{17}H_{26}O_1N_1$**	**-0.081**	**45.02148**
		305.22235		**244.20607**	**$C_{17}H_{26}N_1$**	**0.383**	**61.01628**
		305.22235		**189.18419**	**$C_{11}H_{25}O_2$**	**-3.788**	**116.03816**
		305.22235		**176.14328**	**$C_{12}H_{18}N_1$**	**-0.546**	**129.07907**
		305.22235		**130.08621**	**$C_6H_{12}O_2N_1$**	**-0.347**	**175.13614**
Hxe-pyr-307	**$C_{18}H_{31}O_2N_2$**	**307.238**	**11.6**	**262.21622**	**$C_{17}H_{28}O_1N_1$**	**-1.224**	**45.02178**
		307.238		**178.15874**	**$C_{12}H_{20}N_1$**	**-1.606**	**129.07926**
		307.238		**130.08604**	**$C_6H_{12}O_2N_1$**	**-1.654**	**177.15196**
Hxe-FDP-327	**$C_{18}H_{35}O_3N_2$**	**327.26422**	**12.08**	**309.25336**	**$C_{18}H_{33}O_2N_2$**	**-0.953**	**18.01086**
		327.26422		**282.24255**	**$C_{17}H_{32}O_2N_1$**	**-0.729**	**45.02167**
		327.26422		**198.18515**	**$C_{12}H_{24}O_1N_1$**	**-0.459**	**129.07907**
		327.26422		**180.17458**	**$C_{12}H_{22}N_1$**	**-0.534**	**147.08964**
		327.26422		**142.08611**	**$C_7H_{12}O_2N_1$**	**-1.022**	**185.17811**
		327.26422		**130.08614**	**$C_6H_{12}O_2N_1$**	**-0.885**	**197.17808**
Hpe-Lys-S	**$C_{13}H_{27}N_2O_2$**	**243.2067**	**11.84**	**198.18565**	**$C_{12}H_{24}O_1N_1$**	**2.064**	**45.02105**
		243.2067		**147.11301**	**$C_6H_{15}O_2N_2$**	**1.399**	**96.09369**
		243.2067		**130.08638**	**$C_6H_{12}O_2N_1$**	**0.96**	**113.12032**
Hpe-pyr-333	**$C_{20}H_{33}O_2N_2$**	**333.25365**	**10.6**	**288.23221**	**$C_{19}H_{30}O_1N_1$**	**0.066**	**45.02144**
		333.25365		**272.23721**	**$C_{19}H_{30}N_1$**	**-0.244**	**61.01644**
		333.25365		**204.17462**	**$C_{14}H_{22}N_1$**	**-0.276**	**129.07903**
		333.25365		**130.08623**	**$C_6H_{12}O_2N_1$**	**-0.193**	**203.16742**
Hpe-FDP-355	**$C_{20}H_{39}O_3N_2$**	**355.29552**	**10.48, 11.20**	**337.28552**	**$C_{20}H_{37}O_2N_2$**	**1.675**	**18.01**
		355.29552		**310.27463**	**$C_{19}H_{36}O_2N_1$**	**1.85**	**45.02089**
		355.29552		**292.26306**	**$C_{19}H_{34}O_1N_1$**	**-1.475**	**63.03246**
		355.29552		**253.19077**	**$C_{14}H_{25}O_2N_2$**	**-1.124**	**102.10475**
		355.29552		**226.21693**	**$C_{14}H_{28}O_1N_1$**	**1.719**	**129.07859**

		355.29552		208.20638	$C_{14}H_{26}N_1$	1.939	147.08914
		355.29552		130.08603	$C_6H_{12}O_2N_1$	-1.731	225.20949
		355.29552		142.08604	$C_7H_{12}O_2N_1$	-1.514	213.20948
Hpe-pyr-339	$C_{20}H_{39}O_2N_2$	339.3006	10.24	294.27994	$C_{19}H_{36}O_1N_1$	2.714	45.02066
		339.3006		215.17592	$C_{11}H_{23}O_2N_2$	2.396	124.12468
		339.3006		210.22215	$C_{14}H_{28}N_1$	2.491	129.07845
		339.3006		142.08601	$C_7H_{12}O_2N_1$	-1.725	197.21459
Hpe-His-M	$C_{13}H_{24}N_3O_3$	270.18122	12.71, 13.52	226.19131	$C_{12}H_{24}O_1N_3$	-0.349	43.98991
		270.18122		224.17564	$C_{12}H_{22}O_1N_3$	-0.441	46.00558
		270.18122		209.16481	$C_{12}H_{21}O_1N_2$	-0.143	61.01641
		270.18122		156.07668	$C_6H_{10}O_2N_3$	-0.468	114.10454
		270.18122		112.08678	$C_5H_{10}N_3$	-1.284	158.09444
		270.18122		110.07115	$C_5H_8N_3$	-1.125	160.11007
		270.18122		95.06026	$C_5H_7N_2$	-1.208	175.12096
Nne-Lys-S	$C_{15}H_{31}N_2O_2$	271.238	10.96	254.21106	$C_{15}H_{28}O_2N_1$	-1.556	17.02694
		271.238		226.21629	$C_{14}H_{28}O_1N_1$	-1.11	45.02171
		271.238		147.11255	$C_6H_{15}O_2N_2$	-1.728	124.12545
		271.238		84.08056	$C_5H_{10}N_1$	-2.568	187.15744
		271.238		130.08601	$C_6H_{12}O_2N_1$	-1.885	141.15199
Nne-pyr-389	$C_{24}H_{41}O_2N_2$	389.31626	9.7	344.29453	$C_{23}H_{38}O_1N_1$	-0.759	45.02173
		389.31626		328.29977	$C_{23}H_{38}N_1$	-0.325	61.01649
		389.31626		307.27518	$C_{19}H_{35}O_1N_2$	2.57	82.04108
		389.31626		260.23697	$C_{18}H_{30}N_1$	-1.178	129.07929
		389.31626		130.08612	$C_6H_{12}O_2N_1$	-1.039	259.23014
Nne-His-M	$C_{15}H_{28}N_3O_3$	298.21252	11.49	254.22256	$C_{14}H_{28}O_1N_3$	-0.508	43.98996
		298.21252		252.20694	$C_{14}H_{26}O_1N_3$	-0.392	46.00558
		298.21252		237.19609	$C_{14}H_{25}O_1N_2$	-0.211	61.01643
		298.21252		156.07661	$C_6H_{10}O_2N_3$	-0.917	142.13591
		298.21252		112.08675	$C_5H_{10}N_3$	-1.551	186.12577
		298.21252		110.07112	$C_5H_8N_3$	-1.398	188.1414
		298.21252		95.06024	$C_5H_7N_2$	-1.418	203.15228
		298.21252		281.18588	$C_{15}H_{25}O_3N_2$	-0.317	17.02664
		298.21252		267.07599	$C_{15}H_{11}O_3N_2$	-1.605	31.13653
		298.21252		253.19096	$C_{14}H_{25}O_2N_2$	-0.373	45.02156

Table 6-25: LOD and LOQ for acrolein adducts depending on the results obtained by using PPT method and HILIC-FTMS method.

			LOD			LOQ		
Adducts	% of amino Acid in HSA albumin	% to 100% amino acid+C74	Initial albumin conc. mg/ml	amount of albmuin in 10 µl injected on column (ng)	***LOD (ng)***	Initial albumin conc. mg/ml	amount of albmuin in 10 µl injected on column (ng)	***LOQ (ng)***
Remaining lysine	9.850	**15.302**	0.001	2.500	***0.038***	0.001	2.500	***0.038***
Acr-Lys-M	9.850	**2.291**	0.010	50.000	***0.113***	0.100	500.000	***1.128***
Acr-Lys-S	9.850	**0.312**	N/A	N/A	***N/A***	N/A	N/A	***N/A***
Acr-pyr-221	9.850	**N/A**	N/A	N/A	***N/A***	N/A	N/A	***N/A***
Acr-pyr-223	9.850	**8.785**	0.010	50.000	***0.433***	0.050	250.000	***2.163***
Acr-pyr-225	9.850	**13.675**	0.005	25.000	***0.337***	0.020	100.000	***1.347***
Acr-pyr-227	9.850	**8.418**	0.002	10.000	***0.083***	0.010	50.000	***0.415***
Acr-pyr-229	9.850	**3.629**	0.010	50.000	***0.179***	0.050	250.000	***0.894***
Acr-FDP-243	9.850	**47.588**	0.002	10.000	***0.469***	0.005	25.000	***1.172***
100 % Lysine	9.850	**100.000**	0.393	1964.250	***193.479***	0.393	1964.250	***193.479***
Remaining Arginine	4.430	**100.000**	0.001	2.500	***0.111***	0.002	10.000	***0.443***
Acr-Arg-M	4.430	**N/A**	N/A	N/A	***N/A***	N/A	N/A	***N/A***
Acr-Arg-S	4.430	**N/A**	N/A	N/A	***N/A***	N/A	N/A	***N/A***
100 % Arginine	4.430	**100.000**	0.393	1964.250	***87.016***	0.393	1964.250	***87.016***
Remaining Histidine	2.627	**21.329**	0.002	10.000	***0.056***	0.002	10.000	***0.056***
Acr-His-M	2.627	**78.671**	0.002	10.000	***0.207***	0.010	50.000	***1.033***
100% Histidine	2.627	**100.000**	0.393	1964.250	***51.601***	0.393	1964.250	***51.601***

Table 6-26: LOD and LOQ for crotanaldehdye adducts depending on the results obtained by using PPT method and HILIC-FTMS method.

			LOD			LOQ		
Adducts	% of amino Acid in HSA albumin	**% to 100% amino acid+C74**	Initial albumin conc. mg/ml	amount of albmuin in 10 µl injected on column (ng)	***LOD (ng)***	Initial albumin conc. mg/ml	amount of albmuin in 10 µl injected on column (ng)	***LOQ (ng)***
Remaining lysine	9.850	**90.197**	0.001	2.500	***0.222***	0.001	2.500	***0.222***
Cro-Lys-M	9.850	**5.560**	0.010	50.000	***0.274***	0.050	250.000	***1.369***
Cro-Lys-S	9.850	**0.834**	0.020	100.000	***0.082***	0.393	1964.250	***1.613***
Cro-pyr-249	9.850	**N/A**	N/A	N/A	***N/A***	N/A	N/A	***N/A***
Cro-pyr-251	9.850	**1.461**	0.050	250.000	***0.360***	0.393	1964.250	***2.826***
Cro-pyr-253	9.850	**0.760**	N/A	N/A	***N/A***	N/A	N/A	***N/A***
Cro-pyr-255	9.850	**0.509**	0.100	500.000	***0.250***	0.393	1964.250	***0.984***
Cro-pyr-257	9.850	**0.547**	N/A	N/A	***N/A***	N/A	N/A	***N/A***
Cro-FDP-271	9.850	**0.133**	0.100	500.000	***0.066***	0.393	1964.250	***0.258***
100 % Lysine	9.850	**100.000**	0.393	1964.250	***193.479***	0.393	1964.250	***193.479***
Remaining Arginine	4.430	**98.814**	0.001	2.500	***0.109***	0.002	10.000	***0.438***
Cro-Arg-M	4.430	**1.094**	0.050	250.000	***0.121***	0.393	1964.250	***0.952***
Cro-Arg-S	4.430	**0.092**	0.100	500.000	***0.020***	0.393	1964.250	***0.080***
100 % Arginine	4.430	**100.000**	0.393	1964.250	***87.016***	0.393	1964.250	***87.016***
Remaining Histidine	2.627	**63.165**	0.001	2.500	***0.041***	0.002	10.000	***0.166***
Cro-His-M	2.627	**36.835**	0.002	10.000	***0.097***	0.010	50.000	***0.484***
100% Histidine	2.627	**100.000**	0.393	1964.250	***51.601***	0.393	1964.250	***51.601***

Table 6-27: LOD and LOQ for 2-pentenal adducts depending on the results obtained by using PPT method and HILIC-FTMS method.

			LOD			LOQ		
Adducts	% of amino Acid in HSA albumin	**% to 100% amino acid+C74**	Initial albumin conc. mg/ml	amount of albmuin in 10 µl injected on column (ng)	***LOD (ng)***	Initial albumin conc. mg/ml	amount of albmuin in 10 µl injected on column (ng)	***LOQ (ng)***
Remaining lysine	9.850	**87.940**	0.001	2.500	***0.217***	0.001	2.500	***0.217***
Pne-Lys-M	9.850	**2.142**	0.050	250.000	***0.527***	0.100	500.000	***1.055***
Pne-Lys-S	9.850	**0.000**	0.050	250.000	***0.000***	0.393	1964.250	***0.000***
Pne-pyr-277	9.850	**N/A**	N/A	N/A	***N/A***	N/A	N/A	***N/A***
Pne-pyr-279	9.850	**3.414**	0.050	250.000	***0.841***	0.393	1964.250	***6.605***
Pne-pyr-281	9.850	**2.904**	N/A	N/A	***N/A***	N/A	N/A	***N/A***
Pne-pyr-283	9.850	**3.235**	0.020	100.000	***0.319***	0.100	500.000	***1.593***
Pne-pyr-285	9.850	**0.364**	0.100	500.000	***0.179***	0.393	1964.250	***0.704***
Pne-FDP-299	9.850	**N/A**	0.100	500.000	***N/A***	0.393	1964.250	***N/A***
100 % Lysine	9.850	**100.000**	0.393	1964.250	***193.479***	0.393	1964.250	***193.479***
Remaining Arginine	4.430	**99.252**	0.001	2.500	***0.110***	0.001	5.000	***0.220***
Pne-Arg-M	4.430	**0.748**	0.020	100.000	***0.033***	0.393	1964.250	***0.651***
Pne-Arg-S	4.430	**N/A**	N/A	N/A	***N/A***	N/A	N/A	***N/A***
100 % Arginine	4.430	**100.000**	0.393	1964.250	***87.016***	0.393	1964.250	***87.016***
Remaining Histidine	2.627	**53.273**	0.001	5.000	***0.070***	0.002	10.000	***0.140***
Pne-His-M	2.627	**46.727**	0.002	10.000	***0.123***	0.005	25.000	***0.307***
100% Histidine	2.627	**100.000**	0.393	1964.250	***51.601***	0.393	1964.250	***51.601***

Table 6-28: LOD and LOQ for 2-hexenal adducts depending on the results obtained by using PPT method and HILIC-FTMS method..

			LOD			LOQ		
Adducts	% of amino Acid in HSA albumin	**% to 100% amino acid+C74**	Initial albumin conc. mg/ml	amount of albmuin in 10 µl injected on column (ng)	***LOD (ng)***	Initial albumin conc. mg/ml	amount of albmuin in 10 µl injected on column (ng)	***LOQ (ng)***
Remaining lysine	9.850	**76.515**	0.001	2.500	***0.188***	0.001	2.500	***0.188***
Hxe-Lys-M	9.850	**1.191**	0.050	250.000	***0.293***	0.393	1964.250	***2.304***
Hxe-Lys-S	9.850	**0.509**	0.050	250.000	***0.125***	0.393	1964.250	***0.984***
Hxe-pyr-305	9.850	**N/A**	N/A	N/A	***N/A***	N/A	N/A	***N/A***
Hxe-pyr-307	9.850	**4.621**	0.050	250.000	***1.138***	0.100	500.000	***2.276***
Hxe-pyr-309	9.850	**8.632**	0.020	100.000	***0.850***	0.393	1964.250	***16.700***
Hxe-pyr-311	9.850	**5.689**	0.010	50.000	***0.280***	0.050	250.000	***1.401***
Hxe-pyr-313	9.850	**0.665**	0.100	500.000	***0.327***	0.393	1964.250	***1.286***
Hxe-FDP-327	9.850	**2.179**	0.050	250.000	***0.536***	0.100	500.000	***1.073***
100 % Lysine	9.850	**100.000**	0.393	1964.250	***193.479***	0.393	1964.250	***193.479***
Remaining Arginine	4.430	**99.763**	0.001	2.500	***0.110***	0.001	5.000	***0.221***
Hxe-Arg-M	4.430	**0.237**	0.050	250.000	***0.026***	0.393	1964.250	***0.206***
Hxe-Arg-S	4.430	**N/A**	N/A	N/A	***N/A***	N/A	N/A	***N/A***
100 % Arginine	4.430	**100.000**	0.393	1964.250	***87.016***	0.393	1964.250	***87.016***
Remaining Histidine	2.627	**85.847**	0.001	2.500	***0.056***	0.001	5.000	***0.113***
Hxe-His-M	2.627	**14.153**	0.100	500.000	***1.859***	0.393	1964.250	***7.303***
100% Histidine	2.627	**100.000**	0.393	1964.250	***51.601***	0.393	1964.250	***51.601***

Table 6-29: LOD and LOQ for 2-heptenal adducts depending on the results obtained by using PPT method and HILIC-FTMS method.

			LOD			LOQ		
Adducts	% of amino Acid in HSA albumin	**% to 100% amino acid+C74**	Initial albumin conc. mg/ml	amount of albmuin in 10 µl injected on column (ng)	***LOD (ng)***	Initial albumin conc. mg/ml	amount of albmuin in 10 µl injected on column (ng)	***LOQ (ng)***
Remaining lysine	9.850	**52.774**	0.001	2.500	***0.130***	0.001	5.000	***0.260***
Hpe-Lys-M	9.850	**0.000**	0.050	250.000	***0.000***	0.393	1964.250	***0.000***
Hpe-Lys-S	9.850	**3.248**	0.010	50.000	***0.160***	0.050	250.000	***0.800***
Hpe-pyr-333	9.850	**N/A**	N/A	N/A	***N/A***	N/A	N/A	***N/A***
Hpe-pyr-335	9.850	**18.015**	0.020	100.000	***1.774***	0.050	250.000	***4.436***
Hpe-pyr-337	9.850	**6.777**	0.005	25.000	***0.167***	0.020	100.000	***0.668***
Hpe-pyr-339	9.850	**9.100**	0.010	50.000	***0.448***	0.050	250.000	***2.241***
Hpe-pyr-341	9.850	**0.680**	0.100	500.000	***0.335***	0.393	1964.250	***1.315***
Hpe-FDP-355	9.850	**9.406**	0.010	50.000	***0.463***	0.050	250.000	***2.316***
100 % Lysine	9.850	**100.000**	0.393	1964.250	***193.479***	0.393	1964.250	***193.479***
Remaining Arginine	4.430	**98.848**	0.001	2.500	***0.109***	0.001	5.000	***0.219***
Hpe-Arg-M	4.430	**0.672**	0.050	250.000	***0.074***	0.393	1964.250	***0.585***
Hpe-Arg-S	4.430	**0.480**	0.100	500.000	***0.106***	0.393	1964.250	***0.417***
100 % Arginine	4.430	**100.000**	0.393	1964.250	***87.016***	0.393	1964.250	***87.016***
Remaining Histidine	2.627	**65.682**	0.001	2.500	***0.043***	0.001	5.000	***0.086***
Hpe-His-M	2.627	**34.318**	0.002	10.000	***0.090***	0.010	50.000	***0.451***
100% Histidine	2.627	**100.000**	0.393	1964.250	***51.601***	0.393	1964.250	***51.601***

Table 6-30: LOD and LOQ for 2-nonenal adducts depending on the results obtained by using PPT method and HILIC-FTMS method.

			LOD			LOQ		
Adducts	% of amino Acid in HSA albumin	**% to 100% amino acid+C74**	Initial albumin conc. mg/ml	amount of albmuin in 10 µl injected on column (ng)	***LOD (ng)***	Initial albumin conc. mg/ml	amount of albmuin in 10 µl injected on column (ng)	***LOQ (ng)***
Remaining lysine	9.850	**83.904**	0.001	2.500	***0.207***	0.001	2.500	***0.207***
Nne-Lys-M	9.850	**3.779**	0.005	25.000	***0.093***	0.020	100.000	***0.372***
Nne-Lys-S	9.850	**2.044**	0.010	50.000	***0.101***	0.050	250.000	***0.503***
Nne-pyr-389	9.850	**N/A**	N/A	N/A	***N/A***	N/A	N/A	***N/A***
Nne-pyr-391	9.850	**3.797**	0.050	250.000	***0.935***	0.100	500.000	***1.870***
Nne-pyr-393	9.850	**1.150**	0.100	500.000	***0.567***	0.393	1964.250	***2.226***
Nne-pyr-395	9.850	**1.866**	0.100	500.000	***0.919***	0.393	1964.250	***3.611***
Nne-pyr-397	9.850	**0.055**	N/A	N/A	***N/A***	N/A	N/A	***N/A***
Nne-FDP-411	9.850	**3.404**	0.020	100.000	***0.335***	0.100	500.000	***1.676***
100 % Lysine	9.850	**100.000**	0.393	1964.250	***193.479***	0.393	1964.250	***193.479***
Remaining Arginine	4.430	**96.086**	0.001	2.500	***0.106***	0.002	10.000	***0.426***
Nne-Arg-M	4.430	**3.669**	0.020	100.000	***0.163***	0.050	250.000	***0.406***
Nne-Arg-S	4.430	**0.246**	0.050	250.000	***0.027***	0.393	1964.250	***0.214***
100 % Arginine	4.430	**100.000**	0.393	1964.250	***87.016***	0.393	1964.250	***87.016***
Remaining Histidine	2.627	**16.214**	0.002	10.000	***0.043***	0.005	25.000	***0.106***
Nne-His-M	2.627	**83.786**	0.001	2.500	***0.055***	0.002	10.000	***0.220***
100% Histidine	2.627	**100.000**	0.393	1964.250	***51.601***	0.393	1964.250	***51.601***

References

1. C. Dominguez, E. Ruiz, M. Gussinye and A. Carrascosa, *Oxidative stress at onset and in early stages of type 1 diabetes in children and adolescents.* Diabetes Care, 1998. 21(10): p. 1736-1742.

2. Kaneto, Fujii, Myint, Miyazawa, Islam, Kawasaki, Suzuki, Nakamura, Tatsumi, Yamasaki and Taniguchi, *Reducing sugars trigger oxidative modification and apoptosis in pancreatic beta-cells by provoking oxidative stress through the glycation reaction.* Biochemical Journal, 1996. 320 (Pt 3): p. 855-63.

3. M. Eggink, S. Charret, M. Wijtmans, H. Lingeman, J. Kool, W. M. A. Niessen and H. Irth, *Development of an on-line weak-cation exchange liquid chromatography-tandem mass spectrometric method for screening aldehyde products in biological matrices*. Journal of Chromatography B, 2009. 877(31): p. 3937-3945.

4. H. McBride, M. Neuspiel and S. Wasiak. Mitochondria: *More Than Just a Powerhouse*. Current Biology, 2006. 16(14) p. R551-R560.

5. A. Jenkins, M. Hill and K. Rowley, *Diabetes and Oxidant Stress,* in *Atherosclerosis and Oxidant Stress,* Jordan L. Holtzamn, Editor. New York, USA: Springer Science+Business Media, LLC; 2008. p. 123-158.

6. H. H. F. Refsgaard, L. Tsai and E. R. Stadtman, *Modifications of proteins by polyunsaturated fatty acid peroxidation products.* Proceedings of the National Academy of Sciences of the United States of America, 2000. 97(2): p. 611-616.

7. G. Suji and S. Sivakami, *DNA damage during glycation of lysine by methylglyoxal: assessment of vitamins in preventing damage*. Amino Acids, 2007. 33(4): p. 615-621.

8. R. J. Kapphahn, B. M. Giwa, K. M. Berg, H. Roehrich, X. Feng, T. W. Olsen and D. A. Ferrington, *Retinal proteins modified by 4-hydroxynonenal: Identification of molecular targets.* Experimental Eye Research, 2006. 83(1): p. 165-175.

9. M. S. Jeong and J. H. Kang, *Acrolein, the toxic endogenous aldehyde, induces neurofilament-L aggregation*. BMB Rep, 2008. 41(9): p. 635-9.

10. B. Halliwell, and J. M. C. Gutteridge, *Free Radicals in Biology and Medicine.* 3rd Edition. Oxford, UK: Oxford University Press; 1999.

11. P. A. C. Cloos and S. Christgau, *Non-enzymatic covalent modifications of proteins: mechanisms, physiological consequences and clinical applications.* Matrix Biology, 2002. 21(1): p. 39-52.

12. G. Spiteller, *Peroxidation of linoleic acid and its relation to aging and age dependent diseases*. Mechanisms of Ageing and Development, 2001. 122(7): p. 617-657.

13. K. Uchida, *Role of reactive aldehyde in cardiovascular diseases*. Free Radical Biology and Medicine, 2000. 28(12): p. 1685-1696.

14. G. Ferretti, T. Bacchetti, A. Nègre-Salvayre, R. Salvayre, N. Dousset and G. Curatola, *Structural modifications of HDL and functional consequences*. Atherosclerosis, 2006. 184(1): p. 1-7.

15. G. D. Norata, A. Pirillo and A. L. Catapano, *Modified HDL: Biological and physiopathological consequences*. Nutrition, Metabolism and Cardiovascular Diseases, 2006. 16(5): p. 371-386.

16. M. P. Cohen, *Diabetes and protein glycation, clinical and pathophysiologic relevance*. Philadelphia, PA, USA: JC Press; 1996.

17. A. Lapolla, D. Fedele and P. Traldi, *Glyco-oxidation in diabetes and related diseases.* Clinica Chimica Acta, 2005. 357(2): p. 236-250.

18. S. Kikuchi, K. Shinpo, M. Takeuchi, S. Yamagishi, Z. Makita, N. Sasaki and K. Tashiro, *Glycation--a sweet tempter for neuronal death.* Brain Research Reviews, 2003. 41(2-3): p. 306-323.

19. L. Seon Hwa and A. B. Ian, *Oxidative DNA Damage and Cardiovascular Disease.* Trends in cardiovascular medicine, 2001. 11(3): p. 148-155.

20. O. K. Argirov, B. Lin, P. Olesen and B. J. Ortwerth, *Isolation and characterization of a new advanced glycation endproduct of dehydroascorbic acid and lysine*. Biochimica et Biophysica Acta (BBA) - General Subjects, 2003. 1620(1-3): p. 235-244.

21. R. Cheng, Q. Feng and B. J. Ortwerth, *LC-MS display of the total modified amino acids in cataract lens proteins and in lens proteins glycated by ascorbic acid in vitro.* Biochimica et Biophysica Acta (BBA) - Molecular Basis of Disease, 2006. 1762(5): p. 533-543.

22. W. R. Markesbery, *Oxidative Stress Hypothesis in Alzheimer's Disease.* Free Radical Biology and Medicine, 1997. 23(1): p. 134-147.

23. M. J. Picklo, T. J. Montine, V. Amarnath and M. D. Neely, *Carbonyl Toxicology and Alzheimer's Disease.* Toxicology and Applied Pharmacology, 2002. 184(3): p. 187-197.

24. K. Zarkovic, *4-Hydroxynonenal and neurodegenerative diseases.* Molecular Aspects of Medicine, 2003. 24(4-5): p. 293-303.

25. R. J. Castellani, G. Perry, P. L. R. Harris, M. L. Cohen, L. M. Sayre, R. G. Salomon and M. A. Smith, *Advanced lipid peroxidation end-products in Alexander's disease.* Brain Research, 1998. 787(1): p. 15-18.

26. M. Perluigi, H. Fai Poon, K. Hensley, W. M. Pierce, J. B. Klein, V. Calabrese, C. De Marco and D. A. Butterfield, *Proteomic analysis of 4-hydroxy-2-nonenal-modified proteins in G93A-SOD1 transgenic mice-A model of familial amyotrophic lateral sclerosis.* Free Radical Biology and Medicine, 2005. 38(7): p. 960-968.

27. J. J. Ou, Y. Zhang and T. J. Montine, *In Vivo Assessment of Lipid Peroxidation Products Associated with Age-Related Neurodegenerative Diseases.* Experimental Neurology, 2002. 175(2): p. 363-369.

28. A. Baker, L. Zidek, D. Wiesler, J. Chmelik, M. Pagel and M. V. Novotny, *Reaction of N-Acetylglycyllysine Methyl Ester with 2-Alkenals: An Alternative Model for Covalent Modification of Proteins.* Chemical Research in Toxicology, 1998. 11(7): p. 730-740.

29. A. G. Baker, D. Wiesler and M. V. Novotny, *Tandem mass spectrometry of model peptides modified with trans-2-hexenal, a product of lipid peroxidation.* Journal of the American Society for Mass Spectrometry, 1999. 10(7): p. 613-624.

30. K. Ichihashi, T. Osawa, S. Toyokuni and K. Uchida, *Endogenous Formation of Protein Adducts with Carcinogenic Aldehydes: implications for oxidative stress.* Journal of Biological Chemistry, 2001. 276(26): p. 23903-23913.

31. L. M. Kaminskas, S. M. Pyke and P. C. Burcham, *Michael addition of acrolein to lysinyl and N-terminal residues of a model peptide: targets for cytoprotective hydrazino drugs.* Rapid Commun Mass Spectrom, 2007. 21(7): p. 1155-64.

32. M. Orioli, G. Aldini, M. C. Benfatto, R. M. Facino and M. Carini, *HNE Michael adducts to histidine and histidine-containing peptides as biomarkers of lipid-derived carbonyl stress in urines: LC-MS/MS profiling in Zucker obese rats.* Analytical Chemistry, 2007. 79(23): p. 9174-84.

33. A. Negre-Salvayre, C. Coatrieux, C. Ingueneau and R. Salvayre, *Advanced lipid peroxidation end products in oxidative damage to proteins. Potential role in diseases and therapeutic prospects for the inhibitors.* British Journal Pharmacology, 2008. 153(1): p. 6-20.

34. B. Shao, X. Fu, T. O. McDonald, P. S. Green, K. Uchida, K. D. O'Brien, J. F. Oram and J. W. Heinecke, *Acrolein Impairs ATP Binding Cassette Transporter*

A1-dependent Cholesterol Export from Cells through Site-specific Modification of Apolipoprotein A-I. Journal of Biological Chemistry, 2005. 280(43): p. 36386-36396.

35. C. Lambert, J. McCue, M. Portas, Y. Ouyang, J. Li, T. G. Rosano, A. Lazis and B. M. Freed, *Acrolein in cigarette smoke inhibits T-cell responses.* Journal of Allergy and Clinical Immunology, 2005. 116(4): p. 916-22.

36. S. Tamamizu-Kato, J. Y. Wong, V. Jairam, K. Uchida, V. Raussens, H. Kato, J. M. Ruysschaert and V. Narayanaswami, *Modification by acrolein, a component of tobacco smoke and age-related oxidative stress, mediates functional impairment of human apolipoprotein E.* Biochemistry, 2007. 46(28): p. 8392-400.

37. K. Hamann, A. Durkes, H. Ouyang, K. Uchida, A. Pond and R. Shi, *Critical role of acrolein in secondary injury following ex vivo spinal cord trauma.* Journal of Neurochemistry, 2008. 107(3): p. 712-21.

38. C. F. Mello, R. Sultana, M. Piroddi, J. Cai, W. M. Pierce, J. B. Klein and D. A. Butterfield, *Acrolein induces selective protein carbonylation in synaptosomes.* Neuroscience, 2007. 147(3): p. 674-9.

39. T. I. Williams, B. C. Lynn, W. R. Markesbery and M. A. Lovell, *Increased levels of 4-hydroxynonenal and acrolein, neurotoxic markers of lipid peroxidation, in the brain in Mild Cognitive Impairment and early Alzheimer's disease.* Neurobiology of Aging, 2006. 27(8): p. 1094-9.

40. GW. Wang, Y. Guo, T. M. Vondriska, J. Zhang, S. Zhang, L. L. Tsai, N. C. Zong, R. Bolli, A. Bhatnagar and S. D. Prabhu, *Acrolein consumption exacerbates myocardial ischemic injury and blocks nitric oxide-induced PKC[epsilon] signaling and cardioprotection.* Journal of Molecular and Cellular Cardiology, 2008. 44(6): p. 1016-1022.

41. M. Yoshida, H. Tomitori, Y. Machi, D. Katagiri, S. Ueda, K. Horiguchi, E. Kobayashi, N. Saeki, K. Nishimura, I. Ishii, K. Kashiwagi and K. Igarashi, *Acrolein, IL-6 and CRP as markers of silent brain infarction.* Atherosclerosis, 2009. 203(2): p. 557-562.

42. B. A. Bruenner, A. D. Jones and J. B. German, *Direct Characterization of Protein Adducts of the Lipid Peroxidation Product 4-Hydroxy-2-nonenal Using Electrospray Mass Spectrometry.* Chemical Research in Toxicology, 1995. 8(4): p. 552-559.

43. M. S. Bolgar and S. J. Gaskell, *Determination of the Sites of 4-Hydroxy-2-nonenal Adduction to Protein by Electrospray Tandem Mass Spectrometry.* Analytical Chemistry, 1996. 68(14): p. 2325-2330.

44. B. A. Bruenner, A. D. Jones and J. B. German, *Maximum entropy deconvolution of heterogeneity in protein modification: Protein adducts of 4-hydroxy-2-nonenal.* Rapid Communications in Mass Spectrometry, 1994. 8(7): p. 509-512.

45. F. Magni, C. Galbusera, L. Tremolada, C. Ferrarese , M. Galli Kienle, *Characterisation of adducts of the lipid peroxidation product 4-hydroxy-2-nonenal and amyloid &bgr;-peptides by liquid chromatography/electrospray ionisation mass spectrometry.* Rapid Communications in Mass Spectrometry, 2002. 16(15): p. 1485-1493.

46. A. L. Isom, S. Barnes, L. Wilson, M. Kirk, L. Coward and V. Darley-Usmar, *Modification of Cytochrome c by 4-hydroxy- 2-nonenal: evidence for histidine, lysine, and arginine-aldehyde adducts.* Journal of the American Society for Mass Spectrometry, 2004. 15(8): p. 1136-1147.

47. W. H. Zhang, J. Liu, G. Xu, Q. Yuan and L. M. Sayre, *Model Studies on Protein Side Chain Modification by 4-Oxo-2-nonenal.* Chemical Research in Toxicology, 2003. 16(4): p. 512-523.

48. D. W. Boerth, E. Eder, S. Hussain and C. Hoffman, *Structures of Acrolein-Guanine Adducts: A Semi-Empirical Self-Consistent Field and Nuclear Magnetic Resonance Spectral Study.* Chemical Research in Toxicology, 1998. 11(4): p. 284-294.

49. E. Eder and C. Hoffman, *Identification and characterization of deoxyguanosine adducts of mutagenic .beta.-alkyl-substituted acrolein congeners.* Chemical Research in Toxicology, 1993. 6(4): p. 486-494.

50. C. Bleasdale, B. T. Golding, G. Kennedy, J. O. MacGregor and W. P. Watson, *Reactions of muconaldehyde isomers with nucleophiles including tri-O-acetylguanosine: Formation of 1,2-disubstituted pyrroles from reactions of the (Z,Z)-isomer with primary amines.* Chemical Research in Toxicology, 1993. 6(4): p. 407-412.

51. A. Furuhata, T. Ishii, S. Kumazawa, T. Yamada, T. Nakayama and K. Uchida, *N{epsilon}-(3-Methylpyridinium)lysine, a Major Antigenic Adduct Generated in Acrolein-modified Protein.* Journal of Biological Chemistry, 2003. 278(49): p. 48658-48665.

52. M. Alaiz and S. Barragá, *Reaction of a lysyl residue analogue with E-2-octenal.* Chemistry and Physics of Lipids, 1995. 75(1): p. 43-49.

53. M. Alaiz and S. Barragá, *Changes induced in bovine serum albumin following interactions with the lipid peroxidation product E-2-octenal.* Chemistry and Physics of Lipids, 1995. 77(2): p. 217-223.

54. J. Cai, A. Bhatnagar and W. M. Pierce, *Protein Modification by Acrolein: Formation and Stability of Cysteine Adducts.* Chemical Research in Toxicology, 2009. 22(4): p. 708-716.

55. J. Cai, B. G. Hill, A. Bhatnagar, W. M. Pierce and R. A. Prough, *Bioactivation and Protein Modification Reactions of Unsaturated Aldehydes,* in *Advances in Bioactivation Research,* Adnan A. Elfarra, Editor. New York, USA: Springer+American Association of Pharmaceutical Scientists; 2008. p. 233-253.

56. H. Chen and J. Rhode, *Schiff base forming drugs: mechanisms of immune potentiation and therapeutic potential.* Journal of Molecular Medicine, 1996. 74(9): p. 497-504.

57. J. L. Wautier , P. J. Guillausseau, *Advanced Glycation End Products, Their Receptors and Diabetic Angiopathy.* Diabetes and Metabolism, 2001. 27(5 pt 1): p. 535-542.

58. L. J. Litchfield J, B. Haigh,D. Guralski, AL. Carrington, S. Cannan, and J. SredySredy, *Non-Enzymatic Glycation of Plasma and Cellular Proteins in a short-term STZ-Diabetic Rat Model*. Diabetologia, 1998. 41(S1): p.A301.

59. B. D. Mather, K. Viswanathan, K. M. Miller and T. E. Long, *Michael addition reactions in macromolecular design for emerging technologies.* Progress in Polymer Science, 2006. 31(5): p. 487-531.

60. X. Zhu, X. Tang, J. Zhang, G. P. Tochtrop, V. E. Anderson and L. M. Sayre, *Mass Spectrometric Evidence for the Existence of Distinct Modifications of Different Proteins by 2(E),4(E)-Decadienal.* Chemical Research in Toxicology, 2009.

61. K. Uchida, M. Kanematsu, Y. Morimitsu, T. Osawa, N. Noguchi and E. Niki, *Acrolein is a product of lipid peroxidation reaction: Formation of free acrolein and its conjugate with lysine residues in oxidized low density lipoproteins.* Journal of Biological Chemistry, 1998. 273(26): p. 16058-66.

62. E. Rathahao, G. Peiro, N. Martins, J. Alary, F. Guéraud and L. Debrauwer, *Liquid chromatography–multistage tandem mass spectrometry for the quantification of dihydroxynonene mercapturic acid (DHN-MA), a urinary end-metabolite of 4-hydroxynonenal.* Analytical and Bioanalytical Chemistry, 2005. 381(8): p. 1532-1539.

63. J. A. Doorn and D. R. Petersen, *Covalent Modification of Amino Acid Nucleophiles by the Lipid Peroxidation Products 4-Hydroxy-2-nonenal and 4-Oxo-2-nonenal.* Chemical Research in Toxicology, 2002. 15(11): p. 1445-1450.

64. K. Uchida and E. R. Stadtman, *Modification of Histidine Residues in Proteins by Reaction with 4-Hydroxynonenal.* Proceedings of the National Academy of Sciences, 1992. 89(10): p. 4544-4548.

65. H. Esterbauer, R. J. Schaur and H. Zollner, *Chemistry and biochemistry of 4-hydroxynonenal, malonaldehyde and related aldehydes.* Free Radical Biology and Medicine, 1991. 11(1): p. 81-128.

66. N. Zarkovic, *4-Hydroxynonenal as a bioactive marker of pathophysiological processes.* Molecular Aspects of Medicine, 2003. 24(4-5): p. 281-291.

67. T. Kumagai, N. Matsukawa, Y. Kaneko, Y. Kusumi, M. Mitsumata and K. Uchida, *A lipid peroxidation-derived inflammatory mediator: Identification of 4-hydroxy-2-nonenal as a potential inducer of cyclooxygenase-2 in macrophages.* Journal of Biological Chemistry, 2004. 279(46): p. 48389-48396.

68. C. Marina, A. Giancarlo and F. Roberto Maffei, *Mass spectrometry for detection of 4-hydroxy-trans-2-nonenal (HNE) adducts with peptides and proteins.* Mass Spectrometry Reviews, 2004. 23(4): p. 281-305.

69. T. Oe, S. H. Lee, M. V. Silva Elipe, B. H. Arison and I. A. Blair, *A Novel Lipid Hydroperoxide-Derived Modification to Arginine.* Chemical Research in Toxicology, 2003. 16(12): p. 1598-1605.

70. D. A. Servetnick, D. Bryant, K. J. Wells-Knecht and P. L. Wiesenfeld, *L-Arginine inhibits in vitro nonenzymatic glycation and advanced glycosylated end product formation of human serum albumin.* Amino Acids, 1996. 11(1): p. 69-81.

71. H. H. F. Refsgaard, L. Tsai and E. R. Stadtman, *Modifications of proteins by polyunsaturated fatty acid peroxidation products.* Proceedings of the National Academy of Sciences, 2000. 97(2): p. 611-616.

72. Allen, G., *Sequencing of Proteins and Peptides*, in *Laboratory Techniques in Biochemistry and Molecular Biology*, T. S. Work and R.H. Burdon, Editors. Volume 9. Amsterdam, The Netherlands: Elsevier/North-Holland Biomedical Press; 1981. p. ii-x, 1-327.

73. *Amino Acid Analysis*, in *Stage 5-Proposal, Global Document*. Tokyo, Japan: National Institute of Health Science, 2006. Available from the URL: www.nihs.go.jp/dbcb/Bio-Topic/amino.pdf

74. R. W. Zumwalt, J. S. Absheer, F. E. Kaiser and C. W. Gehrke, *Acid hydrolsis of Proteins for Chromatographic analysis of Amino Acids.* Journal of the Association of Official Analytical Chemists, 1987. 70(1): p. 147-151.

75. K. L. Stone, M. B. LoPresti, and K. R. William, *Enzymatic Digestion of Proteins and HPLC Peptide Isolation in the Subnanomole Range*, in *Laboratory Methodology in Biochemistry,* Carlo Fini, Ardesio Floridi, Vincent N. Finelli, and B. Wittman-Liebold, Editors.. Florida, USA: CRC Press Inc; 1990. P. 181-206.

76. R. Rial-Otero, R. J. Carreira, F. M. Cordeiro, A. J. Moro, H. M. Santos, G. Vale, I. Moura and J. L. Capelo, *Ultrasonic assisted protein enzymatic digestion for fast protein identification by matrix-assisted laser desorption/ionization time-of-flight mass spectrometry: Sonoreactor versus ultrasonic probe.* Journal of Chromatography A, 2007. 1166(1-2): p. 101-107.

77. R. L. Levine, *Rapid benchtop method of alkaline hydrolysis of proteins.* Journal of Chromatography A, 1982. 236(2): p. 496-498.

78. F. E. Kaiser, C. W. Gehrke, R. W. Zumwalt and K. C. Kuo, *Amino acid analysis: Hydrolysis, ion-exchange cleanup, derivatization, and quantitation by gas-liquid chromatography.* Journal of Chromatography, 1974. 94(0): p. 113-33.

79. E. Marconi, G. Panfili, L. Bruschi, V. Vivanti and L. Pizzoferrato, *Comparative study on microwave and conventional methods for protein hydrolysis in food.* Amino Acids, 1995. 8(2): p. 201-208.

80. F. Westall and H. Hesser, *Fifteen-minute acid hydrolysis of peptides.* Analytical Biochemistry, 1974. 61(2): p. 610-613.

81. J. W. Lugg, *Problems associated with the acid hydrolysis of an impure protein preparation.* Biochemical Journal, 1946. 40(1): p. 88-96.

82. P. R. R. Charles W. Gehrke, Robert M. Schisal, Joseph S Absheer, and Robert W. Ziumlat, *Quantitative analysis of cystine, methio- nine, lysine, and nine other amino acids by a single oxidation-4 hours hydrolysis method.* Journal of the Association of Official Analytical Chemists, 1987. 70: p. 171-176.

83. Biotage-Ltd, *Synthesis & Purification Catalog*. 2008/09. Available from the URL: http://www.biotage.com/DynPage.aspx?id=21992.

84. Biotage-Ltd, *Analytical Sample Preparation Catalog*. 2006. Available from the URL: http://www.biotage.com/DynPage.aspx?id=21992

85. M. Alzweiri. *Investigations and Optimisations of Metabonomics as a Clinical Tool of Analysis*. PhD [thesis]. Glasgow,UK: University of Strathclyde; 2008.

86. M. Alzweiri, D. G. Watson, C. Robertson, G. J. Sills and J. A. Parkinson, *Comparison of different water-miscible solvents for the preparation of plasma*

and urine samples in metabolic profiling studies. Talanta, 2008. 74(4): p. 1060-1065.

87. J. C. Mathies and M. A. Austin, *Modified acetonitrile protein-precipitation method of sample preparation for drug assay by liquid chromatography.* Clinical Chemistry, 1980. 26(12): p. 1760.

88. C. A. Daykin, P. J. D. Foxall, S. C. Connor, J. C. Lindon and J. K. Nicholson, *The Comparison of Plasma Deproteinization Methods for the Detection of Low-Molecular-Weight Metabolites by 1H Nuclear Magnetic Resonance Spectroscopy.* Analytical Biochemistry, 2002. 304(2): p. 220-230.

89. SeQuant, *A Practical Guide to HILIC: A tutorial and Application book.* Umea°, Sweden: SeQuant AB, 2008.

90. N. H. Davies, M. R. Euerby and D. V. McCalley, *A study of retention and overloading of basic compounds with mixed-mode reversed-phase/cation-exchange columns in high performance liquid chromatography.* Journal of Chromatography A, 2007. 1138(1-2): p. 65-72.

91. J. W. Eschelbach and J. W. Jorgenson, *Improved Protein Recovery in Reversed-Phase Liquid Chromatography by the Use of Ultrahigh Pressures.* Analytical Chemistry, 2006. 78(5): p. 1697-1706.

92. M. A. Kamleh, J. A. T. Dow and D. G. Watson, *Applications of mass spectrometry in metabolomic studies of animal model and invertebrate systems.* Briefings in Functional Genomics and Proteomics, 2009. 8(1): p. 28-48.

93. M. R. Euerby, P. Petersson, W. Campbell and W. Roe, *Chromatographic classification and comparison of commercially available reversed-phase liquid chromatographic columns containing phenyl moieties using principal component analysis.* Journal of Chromatography A, 2007. 1154(1-2): p. 138-151.

94. P. T. Anders Nordström, Danuse Tarkowska, Karel Dolezal, Crister Åstot, Göran Sandberg, and Thomas Morit, *Derivatization for LC-Electrospray Ionization-MS: A Tool for Improving Reversed-Phase Separation and ESI Responses of Bases, Ribosides, and Intact Nucleotides.* Analytical Chemistry, 2004. 76(10): p. 2869-2877.

95. F. Gritti and G. Guiochon, *Adsorption Mechanism in RPLC: Effect of the Nature of the Organic Modifier.* Analytical Chemistry, 2005. 77(13): p. 4257-4272.

96. Wilfried M. A. Niessen, *Atmospheric-Pressure Ionization*, in *Liquid Chromatography-Mass Spectrometry, 3rd Edition*. Florida, USA: CRC Press; 2009.

97. M. R. Euerby and P. Petersson, *Chromatographic classification and comparison of commercially available reversed-phase liquid chromatographic columns using principal component analysis.* Journal of Chromatography A, 2003. 994(1-2): p. 13-36.

98. J. A. Lippert, T. M. Johnson, J. B. Lloyd, J. P. Smith, B. T. Johnson, J. Furlow, A. Proctor and S. J. Marin, *Effects of elevated temperature and mobile phase composition on a novel C18 silica column.* Journal of Separation Science, 2007. 30(8): p. 1141-9.

99. D. V. McCalley, *Effect of temperature and flow-rate on analysis of basic compounds in high-performance liquid chromatography using a reversed-phase column.* Journal of Chromatography A, 2000. 902(2): p. 311-321.

100. N. H. Davies, M. R. Euerby and D. V. McCalley, *Analysis of basic compounds by reversed-phase high-performance liquid chromatography using hybrid inorganic/organic phases at high pH.* Journal of Chromatography A, 2008. 1178(1-2): p. 71-78.

101. N. H. Davies, M. R. Euerby and D. V. McCalley, *Study of overload for basic compounds in reversed-phase high performance liquid chromatography as a function of mobile phase pH.* Journal of Chromatography A, 2006. 1119(1-2): p. 11-19.

102. M. R. Euerby, F. Scannapieco, H. J. Rieger and I. Molnar, *Retention modelling in ternary solvent-strength gradient elution reversed-phase chromatography using 30 mm columns.* Journal of Chromatography A, 2006. 1121(2): p. 219-27.

103. D. G. Watson, *The potential of mass spectrometry for the global profiling of parasite metabolomes.* Parasitology, 2009. 137(9): p. 1409-23.

104. C. Simon, A. Carla, W. Julie and T.-O. Jane, *Metabolomic applications of HILIC-LC-MS.* Mass Spectrometry Reviews, 2009. 9999(9999): p. n/a.

105. F. A. Dörr, V. Rodríguez, R. Molica, P. Henriksen, B. Krock and E. Pinto, *Methods for detection of anatoxin-a(s) by liquid chromatography coupled to electrospray ionization-tandem mass spectrometry.* Toxicon, 2010. 55(1): p. 92-99.

106. M. Liu, J. Ostovic, E. X. Chen and N. Cauchon, *Hydrophilic interaction liquid chromatography with alcohol as a weak eluent.* Journal of Chromatography A, 2009. 1216(12): p. 2362-2370.

107. RI. Chirita, C. West, A.-L. Finaru and C. Elfakir, *Approach to hydrophilic interaction chromatography column selection: Application to neurotransmitters analysis.* Journal of Chromatography A. 1217(18): p. 3091-3104.

108. B. J. Stewart, J. A. Doorn and D. R. Petersen, *Residue-Specific Adduction of Tubulin by 4-Hydroxynonenal and 4-Oxononenal Causes Cross-Linking and Inhibits Polymerization.* Chemical Research in Toxicology, 2007. 20(8): p. 1111-1119.

109. I. Dalle-Donne, M. Carini, G. Vistoli, L. Gamberoni, D. Giustarini, R. Colombo, R. Maffei Facino, R. Rossi, A. Milzani and G. Aldini, *Actin Cys374 as a nucleophilic target of [alpha],[beta]-unsaturated aldehydes.* Free Radical Biology and Medicine, 2007. 42(5): p. 583-598.

110. M. Orioli, G. Aldini, G. Beretta, R. M. Facino and M. Carini, *LC-ESI-MS/MS determination of 4-hydroxy-trans-2-nonenal Michael adducts with cysteine and histidine-containing peptides as early markers of oxidative stress in excitable tissues.* Journal of Chromatography B, 2005. 827(1): p. 109-118.

111. F. Fenaille, P. A. Guy and J.-C. Tabe, *Study of protein modification by 4-hydroxy-2-nonenal and other short chain aldehydes analyzed by electrospray ionization tandem mass spectrometry.* Journal of the American Society for Mass Spectrometry, 2003. 14(3): p. 215-226.

112. Gèrard Hopfgartner, *Mass Spectrometry in Bioanalysis-Methods, Principles and Instrumentation,* in *Mass Spectrometry in medicinal chemistry,* Klaus T. Wanner, and Georg Höfner, Editors. Volume 36. Weinheim, Germany: WILEY-VCH Verlag GmbH & Co.; 2007. p. 3-62

113. Edmond de Hoffmann, Vincent Stroobant, *Mass Spectrometry Principles and Applications*. 3rd Edition. Chichester, England: John Wiley & Sons, Ltd; 2007.

114. G. Valérie and P. Edwin De, *Internal energy and fragmentation of ions produced in electrospray sources.* Mass Spectrometry Reviews, 2005. 24(4): p. 566-587.

115. M. Dole, L. L. Mack, R. L. Hines, R. C. Mobley, L. D. Ferguson and M. B. Alice, *Molecular Beams of Macroions.* The Journal of Chemical Physics, 1968. 49(5): p. 2240-2249.

116. J. V. Iribarne, and B.A. Thomson, *On the evaporation of small ions from charged droplets.* The Journal of Chemical Physics, 1976. 64(6): p. 2287-2294.

117. Chhabil Dass, *Fundamentala of Contemporary Mass Spectrometry,* Dominic M. Desiderio and Nico M. Nibbering, Editors. New Jersey, USA: John Wiley & Sons, Inc; 2007.

118. K. P. Bateman, M. Kellmann, H. Muenster, R. Papp and L. Taylor, *Quantitative-Qualitative Data Acquisition Using a Benchtop Orbitrap Mass Spectrometer.* Journal of the American Society for Mass Spectrometry, 2009. 20(8): p. 1441-1450.

119. B. Macek, L. F. Waanders, J. V. Olsen and M. Mann, *Top-down Protein Sequencing and MS3 on a Hybrid Linear Quadrupole Ion Trap-Orbitrap Mass Spectrometer*. Molecular & Cellular Proteomics, 2006. 5(5): p. 949-958.

120. Robert K. Boyd, Cecilia Basic, Robert A. Bethem, *Trace Quantitative Analysis by Mass Spectrometry*. Chichester, England: John Wiley & Sons, Ltd; 2008.

121. J. V. Olsen, L. M. F. de Godoy, G. Li, B. Macek, P. Mortensen, R. Pesch, A. Makarov, O. Lange, S. Horning and M. Mann, *Parts per Million Mass Accuracy on an Orbitrap Mass Spectrometer via Lock Mass Injection into a C-trap.* Molecular & Cellular Proteomics, 2005. 4(12): p. 2010-2021.

122. C. C. L. Wong, D. Cociorva, J. D. Venable, T. Xu and J. R. Yates Iii, *Comparison of Different Signal Thresholds on Data Dependent Sampling in Orbitrap and LTQ Mass Spectrometry for the Identification of Peptides and Proteins in Complex Mixtures.* Journal of the American Society for Mass Spectrometry, 2009. 20(8): p. 1405-1414.

123. K. Strupat, V. Kovtoun, H. Bui, R. Viner, G. Stafford and S. Horning, *MALDI Produced Ions Inspected with a Linear Ion Trap-Orbitrap Hybrid Mass Analyzer*. Journal of the American Society for Mass Spectrometry, 2009. 20(8): p. 1451-1463.

124. W. Lu, B. D. Bennett and J. D. Rabinowitz, *Analytical strategies for LC-MS-based targeted metabolomics*. Journal of chromatography B: Analytical technologies in the biomedical and life science, 2008. 871(2): p. 236-42.

125. J. Foley and J. Dorsey, *Clarification of the limit of detection in chromatography.* Chromatographia, 1984. 18(9): p. 503-511.

126. Johannes Corley, *Best practices in establishing detection and quantification limits for pesticide residues in foods*, in *Handbook of Residue Analytical Methods for Agrochemicals*. NJ, USA: John Wiley and Sons Ltd; 2003.

127. S. Walfish, *Analytical Methods: A Statistical Perspective on the ICH Q2A and Q2B Guidelines for Validation of Analytical Methods.* BioPharm International, 2006.

128. International Conference of Harmonisation (ICH), *Harmonised Tripartite Guidline. Validation of Analytical Procedures: Text and Methodology Q2 (R1)*. November 1996. Available from the URL: http://www.ich.org/LOB/media/MEDIA417.pdf

129. *International Conference of Harmonisation (ICH) Harmonised Tripartite Guidline. Validation of analytical procedures: Methodology Q2B*. November 1996.

130. M. P. Bartolomeo, and F. Maisano, *Validation of a reversed-phase HPLC method for quantitative amino acid analysis.* Journal of Biomolecular Techniques, 2006. 17(2): p. 131-7.

131. Vast Scientific Inc. [Online]. *SIEVE Software*. 2009 [cited 2010 July 12]. Available from the URL: http://www.vastscientific.com/contact/index.html.

132. M. Pournamdari, A. Saadi, E. Ellis, R. Andrew, B. Walker and D. G. Watson, *Development of a derivatisation method for the analysis of aldehyde modified amino acid residues in proteins by Fourier transform mass spectrometry.* Analytica Chimica Acta, 2009. **633**(2): p. 216-222.

133. EZ:faast_users_manual, *"Amino Acids Analysis of Protein Hydrolysate by LC-MS, user manual"*. California, USA: Phenomenex Company, 2006.

134. M. Kinter and N. E. Sherman, *Protein Sequencing and Identification Using Tandem Mass Spectrometry*. New York, USA: John Wiley & Sons Inc; 2000. 135. K. Uchida, *Histidine and lysine as targets of oxidative modification.* Amino Acids, 2003. 25(3): p. 249-257.

136. K. Uchida, M. Kanematsu, K. Sakai, T. Matsuda, N. Hattori, Y. Mizuno, D. Suzuki, T. Miyata, N. Noguchi, E. Niki and T. Osawa, *Protein-bound acrolein: Potential markers for oxidative stress.* Proceedings of the National Academy of Sciences of the United States of America, 1998. 95(9): p. 4882-4887.

137. G. Witz, *Biological interactions of alpha,beta-unsaturated aldehydes.* Free Radical Biology and Medicine, 1989. 7(3): p. 333-49.

138. L. Yin, J. i. Mano, S. Wang, W. Tsuji and K. Tanaka, *The involvement of lipid peroxide-derived aldehydes in aluminum toxicity of tobacco roots.* Plant Physiology, 2009: p. pp.109.151449.

139. T. Sung-Chun, V. A. Thiruma, G. C. Roy, J. Dong-Gyu, M. Tim, L. C. Sic, R. M. Mohamed, S. T. Richard, N. Matthew, O. Xin, C. Andrea, R. Paolo, G. Andrea and P. M. Mark, *Neuroprotective actions of a histidine analogue in models of ischemic stroke.* Journal of Neurochemistry, 2007. 101(3): p. 729-736.

140. A. Marquez-Quinones, A. Cipak, K. Zarkovic, S. Fattel-Fazenda, S. Villa-Trevino, G. Waeg, N. Zarkovic and F. Gueraud, *HNE-protein adducts formation in different pre-carcinogenic stages of hepatitis in LEC rats.* Free Radical Research, 2010. 44(2): p. 119-127.

141. G. Barrera, O. Brossa, V. M. Fazio, M. G. Farace, L. Paradisi, E. Gravela and M. U. Dianzani, *Effects of 4-Hydroxynonenal, A Product of Lipid Peroxidation, on Cell Proliferation and Ornithine Decarboxylase Activity.* Free Radical Research, 1991. 14(2): p. 81-89.

142. A. Radu, and N. Moldovan, *4-Hydroxynonenal reduces junctional communication between endothelial cells in culture.* Experimental Cell Research, 1991. 196(1): p. 121-6.

143. L. M. Sayre, D. Lin, Q. Yuan, X. Zhu and X. Tang, *Protein Adducts Generated from Products of Lipid Oxidation: Focus on HNE and ONE.* Drug Metabolism Reviews, 2006. 38(4): p. 651-675.

144. J. Sasaki, S. M. Aschmann, E. S. C. Kwok, R. Atkinson and J. Arey, *Products of the Gas-Phase OH and NO_3 Radical-Initiated Reactions of Naphthalene.* Environmental Science & Technology, 1997. 31(11): p. 3173-3179.

145. C. Joyce, W. F. Smyth, V. N. Ramachandran, E. O'Kane and D. J. Coulter, *The characterisation of selected drugs with amine-containing side chains using electrospray ionisation and ion trap mass spectrometry and their determination by HPLC-ESI-MS.* Journal of Pharmaceutical and Biomedical Analysis, 2004. 36(3): p. 465-476.

146. W. F. Smyth, V. Ramachandran, E. O'Kane and D. Coulter, *Characterisation of selected drugs with nitrogen-containing saturated ring structures by use of electrospray ionisation with ion-trap mass spectrometry.* Analytical and Bioanalytical Chemistry, 2004. 378(5): p. 1305-1312.

147. L. J. Núñez-Vergara, P. A. Navarrete-Encina, S. Salas, B. Conde, J. Carbajo, J. A. Squella and C. Camargo, *Analyses by GC-MS and GC-MS-MS of the hantzsch synthesis products using hydroxy- and methoxy-aromatic aldehydes.* Journal of Pharmaceutical and Biomedical Analysis, 2007. 44(1): p. 236-242.

148. M. Antonio García, V. Enrique Teso, F. Amelia García, M.-Á. Roberto, C. Santiago de la Moya and M.-R. Paloma, *Electron ionization mass spectral studies of bridgehead 7,7-dimethylnorbornane-based β-amino alcohols.* Rapid Communications in Mass Spectrometry, 2005. 19(8): p. 1005-1010.

149. T. Susumu, F. Atsuyo, N. Satoshi, T. Yutaka and S. Osamu, *Metastable decompositions of gem-dialkoxyalkanes upon electron impact. III. Diethoxymethane ($CH_2(OCH_2CH_3)_2$).* Rapid Communications in Mass Spectrometry, 2000. 14(14): p. 1195-1199.

150. X. Jiaxi and Z. Gang, *Mass spectral fragmentation of (S,S)-2-substituted 4,4-diphenyl-3,1-oxazabicyclo[3.3.0]octanes: ring contraction of pyrrolidine and 1,3-oxazolidine in mass spectrometry.* Rapid Communications in Mass Spectrometry, 2003. 17(14): p. 1651-1656.

151. B. H. M. Mruthyunjayaswamy, Y. Jadegoud, O. B. Ijare, S. G. Patil and S. M. Kudari, *Synthesis, characterization and antimicrobial activity of macrocylic phenoxo-bridged di- and tetra-nuclear complexes from N,N-bis[2,6-*

diiminomethyl-4-methyl-1-hydroxyphenyl]succinoyl/sebacoyldicarboxamides. Transition Metal Chemistry, 2005. 30(2): p. 234-242.

152. ARUP-Laboratories, University of Utah [Online]. *Laboratory Reference.* [Cited 2008 Jan 09]. Available from the URL: http://library.med.utah.edu/.

153. M. S. S. Alhamdani, A. H. A. M. Al-Kassir, N. A. Jaleel, A. M. Hmood and H. M. Ali, *Elevated Levels of Alkanals, Alkenals and 4-HO-Alkenals in Plasma of Hemodialysis Patients.* American Journal of Nephrology, 2006. 26(3): p. 299-303.

154. Swiss Institute of Bioinformatics [Online], ExPASy Proteomic Server. Albu_Human (P02768). [Cited 2008 July 21]. Available from the URL: http://expasy.org/cgi-bin/sprot-ft-details.pl?P02768@SEQUENCE@25@609%20UniProtKB/Swiss-Prot%20entry%20P02768.

155. H. Iwase, S. Ozawa, M. Ikuta and I. Ono, *Determination of amino acids in human plasma by liquid chromatography with postcolumn ninhydrin derivatization using a hydroxyapatite cartridge for precolumn deproteination.* Journal of Chromatography B: Biomedical Sciences and Applications, 1995. 663(1): p. 15-24.

156. O. Boulat, D. G. McLaren, E. A. Arriaga and D. D. Y. Chen, *Separation of free amino acids in human plasma by capillary electrophoresis with laser induced fluorescence: potential for emergency diagnosis of inborn errors of metabolism.* Journal of Chromatography B: Biomedical Sciences and Applications, 2001. 754(1): p. 217-228.

157. R. Richter, P. Schulz-Knappe, M. Schrader, L. Standker, M. Jurgens, H. Tammen and W. G. Forssmann, *Composition of the peptide fraction in human blood plasma: database of circulating human peptides.* Journal of Chromatography B: Biomedical Sciences and Applications, 1999. 726: p. 25-35.

158. T. Harald, S. Imke, H. Rudiger, M. Christoph, K. Markus, M. Thomas and S.-K. Peter, *Peptidomic analysis of human blood specimens: Comparison between plasma specimens and serum by differential peptide display.* Proteomics, 2005. 5(13): p. 3414-3422.

159. A. M. Proenza, P. Roca, C. Crespí, I. Lladó and A. Palou, *Blood amino acid compartmentation in men and women with different degrees of obesity.* The Journal of Nutritional Biochemistry, 1998. 9(12): p. 697-704.

160. S. A. Adibi, *Influence of dietary deprivations on plasma concentration of free amino acids of man.* Journal of Applied Physiology, 1968. 25(1): p. 52-57.

161. V. Jirgl, *Paper Chromatography of Free Amino Acids in Human Blood Serum.* Clinical Chemistry, 1957. 3(3): p. 154-155.

162. Human Metabolite Database Bank [Online]. [cited 2009 Jun 17]. Available from the URL: http//:www.hmdb.ca.

163. B. Francis, and V. Pascal, *Electrospray ionization suppression, a physical or a chemical phenomenon?* Biomedical Chromatography, 2006. 20(2): p. 200-205.

164. A. E. M. Crotti, T. Fonseca, H. Hong, J. Staunton, S. E. Galembeck, N. P. Lopes and P. J. Gates, *The fragmentation mechanism of five-membered lactones by electrospray ionisation tandem mass spectrometry.* International Journal of Mass Spectrometry, 2004. 232(3): p. 271-276.

165. M. R. Domingues, P. Domingues, A. Reis, C. Fonseca, F. M. Amado and A. J. Ferrer-Correia, *Identification of oxidation products and free radicals of tryptophan by mass spectrometry.* Journal of the American Society for Mass Spectrometry, 2003. 14(4): p. 406-16.

166. K. Whitehead, and J.I. Hedges, *Electrospray ionization tandem mass spectrometric and electron impact mass spectrometric characterization of mycosporine-like amino acids.* Rapid Communications Mass Spectrometry, 2003. 17(18): p. 2133-8.

167. D. L. Tabb, L. L. Smith, L. A. Breci, V. H. Wysocki, D. Lin and J. R. Yates, III, *Statistical characterization of ion trap tandem mass spectra from doubly charged tryptic peptides.* Analytical Chemistry, 2003. 75(5): p. 1155-63.

168. P. R. Tiller, Z. E. Fallah, V. Wilson, J. Huysman and D. Patel, *Qualitative assessment of leachables using data-dependent liquid chromatography/mass spectrometry and liquid chromatography/tandem mass spectrometry*. Rapid Communications in Mass Spectrometry, 1997. 11(14): p. 1570-1574.

169. F. Fenaille, J. C. Tabet, and P.A. Guy, *Study of peptides containing modified lysine residues by tandem mass spectrometry: precursor ion scanning of hexanal-modified peptides.* Rapid Communications in Mass Spectrometry, 2004. 18(1): p. 67-76.

170. M. Holčapek, L. Kolářová and M. Nobilis, *High-performance liquid chromatography–tandem mass spectrometry in the identification and determination of phase I and phase II drug metabolites.* Analytical and Bioanalytical Chemistry, 2008. 391(1): p. 59-78.

171. Z. Maskos, J. D. Rush, and W. H. Koppenol, *The hydroxylation of tryptophan.* Archives of Biochemistry and Biophysics, 1992. 296(2): p. 514-520.

172. Rosaleen J. Anderson, David J.Bendell, Paul W. Groundwater, *Organic Spectroscopic Analysis*. Tutorial chemistry text 22. Cambridge, UK: Published by The Royal Society of Chemistry; 2004.

173. A. Meynier, V. Rampon, M. Dalgalarrondo and C. Genot, *Hexanal and t-2-hexenal form covalent bonds with whey proteins and sodium caseinate in aqueous solution.* International Dairy Journal, 2004. 14(8): p. 681-690.

174. Robert M. Silverstein, Francis X. Webster, David J. Kiemle, *Spectrometric Identification of Organic Compounds*. 7th Edition. New York, USA: John Wiley & Sons, Inc; 2005.

175. A. Lapolla, P. Traldi, and D. Fedele, *Importance of measuring products of non-enzymatic glycation of proteins.* Clinical Biochemistry, 2005. 38(2): p. 103-115.

176. Margaret I. Tyler, *Amino Acid Analysis*, in *Amino Acid Analysis Protocols*, Catherine Cooper, Nicolle Packer and Keith Williams, Editors. NJ, USA: Humana Press Inc; 2000.

177. R. Valdes, Jr., *Modification of human haemoglobin with glucose 6-phosphate enhances tetramer-dimer subunit dissociation.* Biochemical Journal, 1986. 239(3): p. 769-72.

178. H. Qizhi, J. N. Robert, L. Hongyan, M. Alexander, H. Mark and R. G. Cooks, *The Orbitrap: a new mass spectrometer*. Journal of Mass Spectrometry, 2005. 40(4): p. 430-443.

179. M. Raman, and B.O.C. Peter, *Artifacts in Fourier transform mass spectrometry*. Rapid Communications in Mass Spectrometry, 2009. 23(4): p. 523-529.

180. T. B Ken Webb, Mike Sargent and Bridget Stein, *Methodology for Accurate Mass Measurement of Small Molecules. Best Practice Guide*. Teddington, UK: LGC Limited, 2004. Available from the URL: www.bmss.org.uk/Docs/VIMMS_guide.pdf

181. N. E. Es-Safi, L. Kerhoas, J. Einhorn and P. H. Ducrot, *Application of ESI/MS, CID/MS and tandem MS/MS to the fragmentation study of eriodictyol 7-O-glucosyl-(1→ 2)-glucoside and luteolin 7-O-glucosyl-(1→ 2)-glucoside.* International Journal of Mass Spectrometry, 2005. 247(1-3): p. 93-100.

182. Guifen Xu, T.H., Jennifer Zhang, Thomas D. McClure, and Shichang Miao, *App. Note 406: Study of Free Radical Fragment Ions Generated from ESI-CID-MS/MS Using LTQ and LTQ Orbitrap Mass Spectrometers*. San Jose, USA: Thermo Fisher Scientific Inc, 2007. Available from the URL: *http://www.thermoscientific.com/wps/portal/ts/techresource?resourceId=89746*.